

**Developing a non-human primate model of
dendritic cell based immunotherapy in
transplantation:
Studies in the common marmoset monkey
(*Callithrix jacchus*)**

Dr Michael Gerard Collins, MBChB, FRACP

Transplantation Immunology Laboratory
The Queen Elizabeth Hospital
Discipline of Medicine, Faculty of Health Sciences
University of Adelaide

A thesis submitted in fulfilment of the requirements for the degree of
Doctor of Philosophy, University of Adelaide

July 2013

TABLE OF CONTENTS

List of Tables and Figures	viii
Thesis Abstract	xv
Declaration	xvii
Awards.....	xviii
Publications	xix
Presentations.....	xx
Acknowledgments	xxii
Abbreviations	xxiv
Chapter 1: Background and Literature Review.....	1
1.1. The context: End-stage kidney disease and transplantation	3
1.2. Transplant tolerance – a coming clinical reality?	5
1.2.1. Clinical occurrence of tolerance.....	5
1.2.2. Strategies to induce tolerance used in pre-clinical and clinical studies	6
1.3. Dendritic cells: derivation, biology and classification.....	10
1.3.1. The origins and development of DC	11
1.3.2. Classification of DC	14
1.3.3. In vitro propagated DC: models for investigating DC development and immunobiology	25
1.3.4. DC pattern recognition receptors	26
1.4. Dendritic cells and tolerance.....	32
1.4.1. Central tolerance	32
1.4.2. Peripheral tolerance.....	32
1.5. Dendritic cells in transplantation	36
1.5.1. DC and allo-recognition.....	36
1.5.2. Using DC to promote tolerance: Tolerogenic DC.....	40

1.5.3. Tolerogenic DC therapy in transplantation	44
1.5.4. Targeting DC in situ to promote transplant tolerance	48
1.6. Non human primate dendritic cells	50
1.6.1. NHP models of DC biology	50
1.6.2. In vitro propagated DC in NHP models	51
1.6.3. In vivo NHP DC	66
1.6.4. NHP DC: conclusions	72
1.7. Liposomes and nanoparticles	74
1.7.1. Liposomes	74
1.7.2. Polymeric nanoparticles	82
1.8. Developing a non-human primate model of DC immunotherapy: the common marmoset monkey	91
1.8.1. The common marmoset as a novel transplant model	91
1.8.2. Marmosets as a potential NHP model for DC immunotherapy studies	93
1.8.3. DC immunotherapy studies in marmoset monkeys	93
1.9. Literature Review: Conclusions	96
1.10. Thesis aims and hypotheses	98
Chapter 2: Materials and Methods	99
2.1. Introduction	100
2.2. Materials	100
2.2.1. Antibodies	100
2.2.2. Cytokines	101
2.2.3. Prepared buffers, media and solutions	101
2.2.4. Materials for immunoliposomes and polymeric PLGA nanoparticles	102
2.3. Animals	104
2.3.1. Animals	104
2.3.2. Marmoset colony maintenance	104
2.3.3. Ethical clearance	104

2.3.4. Peripheral blood sampling.....	105
2.3.5. Urine collection and analysis	105
2.3.6. Euthanasia	106
2.4. Cell culture protocols	107
2.4.1. Washes	107
2.4.2. Marmoset.....	107
2.4.3. Human	110
2.4.4. Cryopreservation of cells	111
2.5. Immunofluorescence and microscopy	113
2.6. Flow cytometry	114
2.7. Molecular biology techniques: cloning of marmoset and human DC-SIGN.....	115
2.7.1. Cloning of marmoset and human DC-SIGN	115
2.7.2. Transfection of CHO cell line with marmoset or human DC-SIGN	117
2.8. Manufacturers	119
Chapter 3: Establishing the basis for a marmoset renal transplant model: Characterisation of marmoset renal histology and correlation with serum and urinary findings	121
3.1. Introduction.....	123
3.2. Methods.....	125
3.2.1. Animals	125
3.2.2. Evaluation of marmoset renal tissues.....	126
3.2.3. Assessment of blood and urine parameters	127
3.2.4. Statistical analysis	128
3.3. Results.....	129
3.3.1. Animals	129
3.3.2. Histology	129
3.3.3. Immunofluorescence	130
3.3.4. Electron microscopy.....	130

3.3.5. Biochemistry parameters and urinary protein	141
3.4. Discussion	145
Chapter 4: Donor-derived dendritic cell therapy: Trafficking of allogeneic and autologous marmoset dendritic cells <i>in vivo</i>.....	149
4.1. Introduction.....	150
4.2. Methods.....	152
4.2.1. Animals	152
4.2.2. Cell culture	152
4.2.3. Fluorescent labelling of <i>in vitro</i> propagated marmoset DC	153
4.2.4. Confirmation of suitability of propagated labelled marmoset DC for DC infusion.....	154
4.2.5. Selection of donor and recipient animals for DC administration studies.....	154
4.2.6. Administration of labelled DC via subcutaneous and intravenous infusion	155
4.2.7. Collection and analysis of marmoset tissues following DC administration.....	156
4.3. Results.....	158
4.3.1. Suitability of <i>in vitro</i> propagated and fluorescently labelled marmoset DC for DC infusion studies.....	158
4.3.2. Selection of donor-recipient pairs	161
4.3.3. Yield of marmoset MoDC and HPDC following culture.....	162
4.3.4. Confirmation of allo-reactivity between donors and recipients in allogeneic mixed leucocyte reaction	165
4.3.5. Administration of allogeneic and autologous DC to marmoset recipients and collection of tissues	166
4.3.6. Trafficking of subcutaneously administered marmoset MoDC <i>in vivo</i>	166
4.3.7. Trafficking of intravenously administered marmoset HPDC <i>in vivo</i>	169
4.4. Discussion	173
Chapter 5: Development of monoclonal antibodies to target DC-SIGN on marmoset dendritic cells to facilitate targeted therapy	179
5.1. Introduction.....	180

5.2. Methods.....	182
5.2.1. Cell culture	182
5.2.2. Cloning of marmoset and human DC-SIGN	182
5.2.3. Development of monoclonal antibodies targeting marmoset DC-SIGN	183
5.2.4. Screening of monoclonal antibodies for binding to marmoset and human DC-SIGN.....	185
5.2.5. Generation of purified monoclonal antibodies against marmoset DC-SIGN	185
5.2.6. Identification of DC-SIGN positive cells in marmoset spleen and confirmation of monoclonal antibody binding.....	186
5.2.7. Confirmation of binding of purified monoclonal antibodies to marmoset and human DC- SIGN.....	187
5.3. Results.....	188
5.3.1. Cloning of human and marmoset DC-SIGN	188
5.3.2. Screening of hybridoma supernatants for binding to marmoset and human MoDC.....	199
5.3.3. Screening of hybridoma supernatants for binding to marmoset and human DC-SIGN transfected CHO cells.....	199
5.3.4. Immunofluorescence microscopy: binding of hybridoma supernatants to DC-SIGN in marmoset and human lymphoid tissues	199
5.3.5. Generation of purified monoclonal antibodies targeting marmoset DC-SIGN from hybridoma supernatants.....	206
5.3.6. Identification of DC-SIGN positive cells in marmoset spleen; lack of staining with generated monoclonal antibodies.....	206
5.3.7. Studies of binding of purified monoclonal antibodies to marmoset and human DC-SIGN	208
5.4. Discussion.....	210
Chapter 6: Development of immunoliposomes and nanoparticles targeting human and marmoset DC-SIGN to modify dendritic cell function.....	214
6.1. Introduction.....	216
6.2. Methods.....	218
6.2.1. Materials.....	218
6.2.2. Preparation and characterisation of immunoliposomes	218
6.2.3. Preparation and characterisation of PLGA nanoparticles targeting DC-SIGN.....	221

6.2.4. DC-SIGN binding assay – enzyme-linked immunosorbent assay (ELISA)	223
6.2.5. Protein quantification assay	224
6.2.6. Cell culture	225
6.2.7. Immunoliposome and PLGA nanoparticle uptake by human MoDC	225
6.2.8. PLGA nanoparticle uptake by marmoset splenocytes.....	227
6.2.9. Curcumin-containing PLGA nanoparticles – effects on human MoDC	228
6.3. Results.....	230
6.3.1. Immunoliposomes	230
6.3.2. PLGA nanoparticles	240
6.4. Discussion	253
6.4.1. Immunoliposomes targeting DC-SIGN.....	253
6.4.2. PLGA nanoparticles targeting DC-SIGN.....	257
6.4.3. Conclusions	260
Chapter 7: Conclusions and Future directions.....	261
7.1. Summary and Conclusions	262
7.2. Future directions	265
7.2.1. Proposed further studies evaluating allogeneic DC therapy in marmosets: allogeneic DC trafficking and effects on the immune response in vivo	265
7.2.2. Proposed further studies of monoclonal antibodies targeted to marmoset DC-SIGN, and the evaluation of marmoset DC-SIGN ⁺ cells identified using DCN46 monoclonal antibody...266	
7.2.3. Proposed further studies of DC-SIGN targeted immunoliposomes.....	267
7.2.4. Proposed further studies of DC-SIGN targeted PLGA nanoparticles.....	268
References	270
Appendix	332

LIST OF TABLES AND FIGURES

Figure 1.3.1. Scanning electron micrograph of a mature dendritic cell, demonstrating the presence of abundant well-developed dendrites at the cell surface.....	10
Figure 1.3.2. Dendritic cell and monocyte origin and development.	13
Table 1.3.1. Phenotypic markers of dendritic cell (DC) subsets in the mouse.....	17
Figure 1.3.3. Distribution of human DC.....	21
Figure 1.3.4. Surface markers of the major human DC populations and their murine homologues.....	24
Table 1.3.2. Toll-like receptor and C-type lectin receptor expression by human DC subtypes	27
Figure 1.3.5. Structure of human DC-SIGN.....	31
Figure 1.4.1. The interaction of DC with naïve T-cells can lead to either immune activation or tolerance.	35
Figure 1.5.1. The role of dendritic cells (DC) in peripheral tolerance and graft rejection.	39
Table 1.5.1. Efficacy of donor DC pre-treatment on allograft survival in small animal studies.....	45
Table 1.5.2. Efficacy of recipient DC pre-treatment on allograft survival in small animal studies.	46
Figure 1.6.1. Simplified phylogenetic tree demonstrating the evolutionary distances and relationships between key NHP species used for biomedical research and humans.....	52
Table 1.6.1. Surface Marker Expression and Response to Maturation Stimuli of NHP DC: Summary of Selected Studies.	53
Table 1.6.2. Functional studies of NHP DC: summary of selected studies.....	56
Figure 1.6.2. Morphology of marmoset and human MoDC differentiated from G-CSF mobilised monocytes.	61

Figure 1.6.3. Four-color gating strategy for identification of presumptive pre-DC subsets in blood of rhesus monkeys.	67
Figure 1.6.4. Morphology of flow-sorted rhesus DC subsets.....	67
Table 1.7.1. Liposome vesicle types, size and lipid layers.....	75
Figure 1.7.1. Aspects of liposomes and micelles.	75
Figure 1.7.2. Sterically stabilised PEGylated immunoliposome. This schematic representation shows antibodies coupled to the distal end of the PEG-chains.....	77
Figure 1.7.3. Evolution of liposomes.	78
Figure 1.7.4. Thiolation of antibodies using Traut's reagent and conjugation of thiolated antibody to maleimide groups on the derivatized PEG.	81
Figure 1.7.5. Cartoon depicting the combinatorial approach to the formation of ligand-targeted liposomal anticancer drugs.....	81
Figure 1.7.6. Chemical structure of polylactide-co-glycolide (PLGA), showing its degradation to lactic and glycolic acid.	82
Figure 1.7.7. Schematic representation of aspects of the design of targeted nanoparticle systems.....	83
Figure 1.7.8. Preparation of polymeric nanocarriers by nanoprecipitation.....	86
Figure 1.7.9. Chemical structure of PEG- <i>b</i> -PLGA copolymer with terminating carboxyl group.....	87
Figure 1.7.10. Schematic illustration of formation of drug containing PLGA nanoparticles using amphiphilic PLGA- <i>b</i> -PEG copolymers.....	88
Figure 1.7.11. Sulfo-NHS plus EDC (carbodiimide) crosslinking reaction scheme.....	89
Figure 1.7.12. Schematic illustration of synthesis of targeted PLGA nanoparticles utilising carbodiimide chemistry.	90
Figure 1.8.1. Marmoset recipient immune responses following the infusion of allogeneic donor-derived DC.	94
Table 2.7.1. Ligation reaction for pGEM®-T easy vector.....	116

Figure 3.3.1. Representative marmoset kidney light microscopy images showing mesangial expansion and hypercellularity.....	131
Figure 3.3.2. Representative image of the measurement method used to assess marmoset glomerular diameter in this study.	132
Table 3.3.1. Renal histology, immunofluorescence and ultrastructural analysis in 25 adult marmoset monkeys.....	133
Table 3.3.2. Summary of renal histology and ultrastructural quantitative data.	135
Figure 3.3.3. Glomerular diameter in 25 adult marmoset monkeys.....	136
Figure 3.3.4. Frequency distribution of the diameters of 333 non-sclerotic glomeruli in 25 adult marmoset monkeys aged up 14 years.....	137
Figure 3.3.5. Representative immunofluorescence microscopy images of marmoset kidneys showing mesangial immunoglobulin deposits.....	138
Figure 3.3.6. Representative electron microscopic images of marmoset kidney showing the presence of mesangial deposits.....	139
Figure 3.3.7. Ultrastructural analysis of glomerular basement membrane (GBM) thickness in 23 marmoset monkeys.....	140
Figure 3.3.8. Frequency distribution of serum creatinine ($\mu\text{mol/L}$) results from 45 peripheral blood samples taken from 34 marmoset monkeys aged up 14 years.....	141
Table 3.3.3. Serum biochemistry in adult marmoset monkeys.....	142
Figure 3.3.9. Urinary dipstick protein measurements from 84 urine samples taken from 34 marmoset monkeys aged up to 14 years.....	143
Table 3.3.4. Urine biochemistry and dipstick parameters in adult marmoset monkeys.....	144
Figure 4.3.1. Fluorescent labelling of <i>in vitro</i> propagated marmoset MoDC with CFSE or DiI does not alter stimulation potential in a xenogeneic mixed leucocyte reaction.....	159
Figure 4.3.2. Marmoset HPDC propagated <i>in vitro</i> have excellent viability, which is not altered by labelling with CFSE.....	160
Table 4.3.1. <i>Caja</i> -DRB (Class II MHC) genotyping of the marmoset donors and recipients used in studies of DC trafficking.....	161

Figure 4.3.3. Yield of marmoset peripheral blood mononuclear cells (PBMCs) and immature monocyte-derived dendritic cells (MoDC) following G-CSF mobilisation and subsequent MoDC culture.	163
Figure 4.3.4. Yield of haematopoietic progenitor (HP) culture of G-CSF mobilised marmoset PBMCs, and subsequent differentiation of haematopoietic progenitor derived dendritic cells (HPDC).	164
Figure 4.3.5. Confirmation of allo-reactivity between allogeneic marmoset donors and recipients in allogeneic mixed leucocyte reactions (MLR).	165
Figure 4.3.6. Marmoset MoDC labelled with DiI and injected subcutaneously are present at the site of injection after 48 hours but do not migrate to the draining lymph node.	167
Figure 4.3.7. DiI positive marmoset MoDC are not found in the draining lymph node at 48 hours following subcutaneous injection.	168
Figure 4.3.8. Allogeneic marmoset HPDC labelled with CFSE and injected intravenously are not detectable in tissues after 48 hours.	170
Figure 4.3.9. CFSE positive allogeneic marmoset HPDC are not found in the spleen at 48 hours following intravenous injection.	171
Figure 4.3.10. Autologous marmoset HPDC labelled with CFSE and injected intravenously are detectable in spleen and possibly liver after 48 hours.	172
Table 5.2.1. Sense and anti-sense primers used for cloning of human and marmoset DC-SIGN.	182
Figure 5.2.1. Summary of the steps in the process of generating monoclonal antibodies with the use of hybridoma technology.	184
Figure 5.2.2. Forward and side scatter plot showing representative gate used to select marmoset splenocytes in the flow cytometry studies to identify DC-SIGN positive cells.	187
Figure 5.3.1. Schematic representation of cloning of marmoset and human DC-SIGN into the pGEM®T-easy vector.	189
Figure 5.3.2. Nucleotide sequence alignment of marmoset DC-SIGN.	191
Figure 5.3.3. Nucleotide sequence alignment of human DC-SIGN.	193

Figure 5.3.4. Schematic representation of sub-cloning of marmoset and human DC-SIGN into the pCI mammalian expression vector.....	195
Figure 5.3.5. Cloned marmoset and human DC-SIGN were successfully ligated into pCI mammalian expression vector in the correct orientation.....	196
Figure 5.3.6. Comparison of the amino acid sequences of marmoset and human DC-SIGN, showing the alignment of antigens #1, #2 and #3 within the marmoset peptide.	198
Figure 5.3.7. Flow cytometry screening of binding of hybridoma supernatants to marmoset MoDC.....	200
Figure 5.3.8. Hybridoma supernatants bind to <u>marmoset</u> DC-SIGN expressed on the surface of CHO cells.	201
Figure 5.3.9. Hybridoma supernatants bind to <u>human</u> DC-SIGN expressed on the surface of CHO cells.	202
Figure 5.3.10. Hybridoma supernatants targeting marmoset DC-SIGN and anti-human DC-SIGN (DCN46) bind to cells in marmoset thymus.....	203
Figure 5.3.11. Hybridoma supernatants targeting marmoset DC-SIGN and anti-human DC-SIGN (DCN46) bind to cells in marmoset spleen.	204
Figure 5.3.12. Hybridoma supernatants targeting marmoset DC-SIGN bind to cells in <i>human</i> spleen.	205
Figure 5.3.13. Anti-human DC-SIGN (DCN46) stains a population of Lineage ⁻ Class II ⁺ Cd11c ⁺ marmoset spleen cells, but no staining is observed with generated monoclonal antibodies.....	207
Figure 5.3.14. Anti-human DC-SIGN (DCN46) – but not generated monoclonal antibody 9E6A8 – binds to CHO cells transfected with marmoset and human DC-SIGN.....	209
Figure 6.2.1. Forward and side scatter plot showing representative gate used to select DC-SIGN positive MoDC in the flow cytometry studies of immunoliposome and PLGA nanoparticle uptake.	226
Figure 6.2.2. Forward and side scatter plot showing gate used to select marmoset splenocytes in the flow cytometry studies of PLGA nanoparticle uptake.....	228
Table 6.3.1 Physicochemical characteristics of liposome preparations	230

Figure 6.3.1. Immunoliposomes conjugated to DCN46 show evidence of binding to DC-SIGN in a semi-quantitative ELISA assay.	232
Figure 6.3.2. DiI immunoliposomes targeted to DC-SIGN incubated overnight with human MoDC do not show evidence of significant uptake.	234
Figure 6.3.3. DiI immunoliposomes targeted to DC-SIGN incubated overnight with human MoDC do not show evidence of significant uptake.	235
Figure 6.3.4. Protein quantitation assay: incubation of liposome preparations with Triton X-100 or SDS to remove phospholipid contamination.	237
Figure 6.3.5. Protein quantitation assay: coumarin 6 liposome preparations with differing levels of protein conjugated to liposomes.	238
Table 6.3.2 Protein quantitation assay: Coumarin 6 liposomes spiked with known concentrations of human serum albumin (HSA) to reflect 10%, 60% and 100% conjugation of DCN46 antibody used in immunoliposome preparations.	239
Table 6.3.3 Physicochemical characteristics of PLGA nanoparticles.....	240
Figure 6.3.6. PLGA nanoparticles targeted to DC-SIGN show evidence of strong binding to DC-SIGN in a qualitative ELISA assay.....	241
Figure 6.3.7. Coumarin 6-PLGA nanoparticles targeted to DC-SIGN incubated at 4°C with human MoDC are taken up to a greater extent than non-targeted nanoparticles.....	243
Figure 6.3.8. Coumarin 6-PLGA nanoparticles incubated at 37°C with human MoDC are taken up non-specifically by cells; targeting to DC-SIGN significantly improves this uptake.....	244
Figure 6.3.9. DC-SIGN targeted PLGA nanoparticles are taken up into the cytoplasm of human MoDC to a greater extent than non-targeted nanoparticles.....	245
Figure 6.3.10 Coumarin 6-PLGA nanoparticles incubated overnight with marmoset splenocytes are taken up by a small population of Class II ⁺ CD11c ⁺ cells.....	247
Figure 6.3.11. Human MoDC treated with curcumin containing PLGA nanoparticles targeted to DC-SIGN show alterations in DC maturation markers.....	250

Figure 6.3.12. Human MoDC treated with curcumin containing PLGA nanoparticles targeted to DC-SIGN did not exhibit significant differences in allostimulatory capacity in a dendritic cell mixed leucocyte reaction (MLR).251

Figure 6.3.13. Curcumin containing PLGA nanoparticles cause dose-dependent suppression of alloproliferation in a two-way mixed leucocyte reaction (MLR).252

THESIS ABSTRACT

Kidney transplantation represents the best treatment for end-stage kidney disease, and in comparison to dialysis treatment has been shown to improve survival, quality of life, and reduce health-care costs over time. However, in order to prevent transplant failure from allograft rejection, immunosuppressive drug therapy is required.

Immunosuppression is associated with significant systemic toxicities, and continues to impair optimal patient and graft outcomes. The avoidance or minimisation of immunosuppression via the promotion of tolerance of the allograft, or the use of targeted therapeutic strategies, in clinical transplantation is therefore an important goal that could have many benefits for patients. Dendritic cells (DC) are potent antigen-presenting cells that play a pivotal role in the initiation and maintenance of immune responses, and therapies utilising or targeting DC offer the potential to manipulate immune responses towards tolerance. This thesis seeks to develop the potential of DC based immunotherapies in a small and clinically relevant non-human primate (NHP) transplant model, the common marmoset monkey, and thereby facilitate translation of these therapies towards human clinical trials.

Chapter 1 establishes the context for this thesis by outlining the background and providing a comprehensive review of relevant literature.

Chapter 2 describes the materials and methods utilised in this thesis. Additional details of methods are contained in relevant chapters.

Chapter 3 presents a comprehensive study of renal pathology in a colony of laboratory marmosets, including histology, immunofluorescence and electron microscopy, and correlates this for the first time with serum and urine biochemistry. This work demonstrates that the spontaneously observed glomerular pathology in marmosets represents a benign occurrence that would not impact on the assessment of renal function or histology in a marmoset kidney transplant model.

Chapter 4 examines the trafficking behaviour *in vivo* of intravenously and subcutaneously administered allogeneic marmoset DC propagated *in vitro* from genetically disparate marmoset donors. The findings indicate that allogeneic marmoset

DC do not necessarily exhibit normal trafficking behaviour *in vivo*, as they are not found in secondary lymphoid tissues at 48 hours, in contrast to similarly administered autologous DC. This finding lends weight to other recent studies of donor DC cellular therapy that indicate that the tolerogenic effects of this therapy are not mediated through cell to cell interactions with recipient T-cells, but rather through providing a source of donor antigen for acquisition and processing by recipient DC.

Chapter 5 describes studies to develop a monoclonal antibody to marmoset DC-specific ICAM 3-grabbing non-integrin (DC-SIGN), which is a DC-specific marker. Ultimately, a marmoset cross-reactive commercially available anti-human DC-SIGN antibody (DCN46) was identified, and found to be suitable to utilise in the development of DC-SIGN targeted cell-specific therapy. Using this antibody, marmoset DC-SIGN positive cells were identified in the Lineage⁻ CD11c⁺ Class II⁺ fraction of marmoset spleen; in contrast *in vitro* propagated marmoset monocyte-derived DC have been confirmed to lack DC-SIGN expression.

Chapter 6 describes the successful development of a novel nanocarrier targeted to DC: PLGA nanoparticles that target DC using the human and marmoset DC-SIGN cross-reactive antibody identified in Chapter 5. A series of preliminary studies have demonstrated that DC-SIGN targeted PLGA nanoparticles are taken up by Class II⁺ CD11c⁺ marmoset spleen cells, and that loading of the nanoparticles with the immunomodulatory drug curcumin shows evidence of *in vitro* immunosuppressive capacity, as shown in mixed leucocyte reaction; however the specificity for DC of immunosuppressive targeted PLGA nanoparticles remains to be demonstrated.

Chapter 7 summarises the overall findings from this thesis, and proposes a series of necessary studies to exploit the identified potentials from this work further.

Overall, the work in this thesis significantly advances the marmoset NHP model as a means to translate the potential of DC based immunotherapies towards clinical transplantation. The feasibility of DC-targeted therapy using nanoparticles has been established, and represents an opportunity to specifically target DC with immunosuppressive drugs *in vivo*, and thereby manipulate the immune response towards tolerance, while reducing the burden of non-targeted immunosuppression.

DECLARATION

I certify that this work contains no material which has been accepted for the award of any other degree or diploma in any university or other tertiary institution to Michael Gerard Collins and, to the best of my knowledge and belief, contains no material previously published or written by another person, except where due reference has been made in the text. In addition, I certify that no part of this work will, in the future, be used in a submission for any other degree or diploma in any university or other tertiary institution without the prior approval of the University of Adelaide.

I give consent to this copy of my thesis, when deposited in the University Library, being made available for loan and photocopying, subject to the provisions of the Copyright Act 1968.

I acknowledge that the copyright of any published works contained within this thesis resides with the copyright holder(s) of those works.

I also give permission for the digital version of my thesis to be made available on the web, via the University's digital research repository, the Library catalogue and also through web search engines, unless permission has been granted by the University to restrict access for a period of time.

Michael Gerard Collins

Date

AWARDS

- 2013 Transplantation Society of Australia and New Zealand
Young Investigator Award
- 2012 The Queen Elizabeth Hospital – Research Day
Winner, Best Poster Presentation
- 2011 The Queen Elizabeth Hospital – Research Day
Finalist, Best Presentation – Basic Science Higher Degree
- 2009 National Health and Medical Research Council
Medical Postgraduate Scholarship
- 2008 The University of Adelaide
Australian Postgraduate Award
- 2008 Royal Australasian College of Physicians
Jacquot Research Entry Scholarship

PUBLICATIONS

Published papers

Jesudason S, **Collins MG**, Rogers NM, Kireta S, and Coates PT. Non-human primate dendritic cells. *J Leukoc Biol* 2012; 91: 217-28.

Manuscripts in preparation

Collins MG, Rogers NM, Kireta S, Brealey J and Coates PT. Spontaneous glomerular mesangial lesions in common marmoset monkeys (*Callithrix jacchus*): a benign non-progressive glomerulopathy. [*Manuscript in preparation*]

Collins MG, Jesudason S, Kireta S, and Coates PT. Infusion of allogeneic donor derived dendritic cells in marmoset monkeys to promote tolerance: studies of recipient immune responses and trafficking of administered cells in vivo. [*Manuscript in preparation*]

Jesudason S, Kireta S, **Collins MG**, Rogers NM, and Coates PT. Blood and tissue dendritic cell subsets in common marmoset monkeys. [*Manuscript in preparation*]

Published abstracts

Collins MG, Rogers NM, Jesudason S, Kireta S, Brealey J and Coates PT. Spontaneous immune complex deposition and proteinuria in the common marmoset monkey (*Callithrix jacchus*) – a model of benign non-progressive glomerulopathy. *Nephrology* 2012; 17 Suppl 2: 43-44.

Collins MG, Rogers NM, Kireta S, Jesudason S, and Coates PT. Developing a monoclonal antibody to target DC-SIGN in non-human primates: a novel tolerogenic cell-specific therapy. *Nephrology* 2011; 16 Suppl 1: 54.

PRESENTATIONS

Invited presentations

“Targeting dendritic cells via DC-SIGN to deliver cell-specific therapy in transplantation: studies in a non-human primate model”

- Basil Hetzel Institute for Medical Research, Adelaide, SA – May 2013
- The annual *DC Down Under* Symposium 2012: Applications in Transplantation and Immunotherapy. Sydney, NSW – August 2012
- Department of Nephrology, Prince of Wales Hospital, Sydney, NSW – May 2012

“Dendritic cell research in transplantation: preclinical cellular transplantation therapy in non-human primates”

- Department of Virology and Immunology, Southwest National Primate Research Center. San Antonio, Texas, USA– November 2009

Conference Presentations

Oral Presentations

Collins MG, Kitto LJ, Jesudason S, Thierry B, Coates PT. Dendritic cell targeted therapy: polymeric nanoparticles targeting human and non-human primate DC-SIGN to inhibit dendritic cell function.

- Transplantation Society of Australia and New Zealand, Annual Scientific Meeting, Canberra ACT, June 2013

Collins MG, Rogers NM, Kireta S, Jesudason S, and Coates PT. Developing a monoclonal antibody to target DC-SIGN in non-human primates: a novel tolerogenic cell-specific therapy

- The Queen Elizabeth Hospital Research Day, Adelaide SA – October 2011

Mini-oral presentations

Collins MG, Rogers NM, Jesudason S, Kireta S, Brealey J and Coates PT. Spontaneous immune complex deposition and proteinuria in the common marmoset monkey (*Callithrix jacchus*) – a model of benign non-progressive glomerulopathy

- Australian and New Zealand Society of Nephrology, Annual Scientific Meeting, Auckland, NZ – August 2012

Collins MG, Rogers NM, Kireta S, Jesudason S, and Coates PT. Development of a novel antibody to target DC-SIGN in non-human primate models of DC immunotherapy for transplant tolerance

- Transplantation Society of Australia and New Zealand, Annual Scientific Meeting, Canberra ACT – June 2012

Poster presentations

Collins MG, Kitto LJ, Jesudason S, Barnes TJ, Thierry B, Prestidge CA, and Coates PT. Targeting dendritic cells using anti-DC-SIGN conjugated immunoliposomes: a novel approach to immunotherapy

- The Queen Elizabeth Hospital Research Day, Adelaide SA – October 2012

Collins MG, Rogers NM, Kireta S, Jesudason S, and Coates PT. Targeting dendritic cells via the dendritic cell-specific C type lectin DC-SIGN in non-human primates: towards a novel tolerogenic cell-specific therapy

- XXIV International Congress of the Transplantation Society, Berlin, Germany – July 2012

Collins MG, Rogers NM, Kireta S, Jesudason S, and Coates PT. Developing a monoclonal antibody to target DC-SIGN in non-human primates: a novel tolerogenic cell-specific therapy

- Australasian Society of Immunology, Annual Scientific Meeting, Adelaide, SA – December 2011
- Australian and New Zealand Society of Nephrology, Annual Scientific Meeting, Adelaide, SA – September 2011

ACKNOWLEDGMENTS

No PhD thesis ever occurs through individual work done solely by one's own efforts in isolation. Many people have contributed in large and small ways to this work, and all have played a vitally important role in enabling me to submit this thesis.

Firstly, I would sincerely like to thank my supervisors, Associate Professor Toby Coates, Dr Shilpa Jesudason, and Professor Graeme Russ. Toby convinced me in the first place that doing a PhD was a good idea, and has been the inspiration ever since for my (perhaps misplaced) desire to become a clinician scientist in the field of transplantation. I admire greatly his intellect, brilliance, passion and drive to not only do good science, but also his ability to balance this with his many other commitments while remaining an excellent and very much admired physician. I have been lucky to work with him on this and a number of other projects over the time I have been in Adelaide, and it has been a privilege from start to finish. I am very grateful for the considerable support he has always shown me, and the friendship we have. I look forward to our collaborations into the future.

Shilpa, through her own PhD thesis on marmoset immunobiology, laid the necessary foundations for this thesis. Many of the techniques and procedures involving marmosets that have become standard for me were established through her pioneering work, and she remains a significant world authority on marmoset DC biology. I greatly value all of the contributions she has made to this work, with her many suggestions resulting in things succeeding where they had previously failed. I thank Graeme particularly for the many opportunities he has facilitated for me (perhaps most significantly offering me a position in the first place), without which this work would never have been completed. He has always been there to provide incisive commentary on the progress (or lack thereof) of this work, and I am grateful to him for being part of the team.

In the laboratory, Svjetlana Kireta and Julie Johnston have provided endless assistance with marmoset procedures, cell culture, flow cytometry, and general laboratory skills, always without complaint or expectation. Their input has been vital. I also thank Dr Natasha Rogers for her assistance and contribution to the cloning studies, marmoset

biopsy analysis and data collection; John Brealey for the electron microscopy analysis; Chris Drogemuller for help with cloning and antibody studies; Clare Kelly (née Mee) for help with the antibody development; Dr Claire Jessup for your general good sense and advice; and the other members of our laboratory over the last 4 years who have been my friends and colleagues: Dr Shaundee Sen, Dr Amy Hughes, Dr Matthew Stephenson, Chris Hope, Dr Darling Rojas, Austin Milton, Clyde Milner, Mariea Bosco, Kisha Sivanathan, and Dr Daisy Mohansundaran. I would also like to thank the staff of TQEH Animal House, and the Research Secretariat at the Basil Hetzel Institute, for their help during the course of this work. Thanks also to the NHMRC for providing me with scholarship funding.

I would like to especially thank Associate Professor Benjamin Thierry from the Ian Wark Institute at the University of South Australia for his assistance and intellectual input to the work on liposomes and PLGA nanoparticles. This work would not have been possible without collaboration with his group. I would also like to thank Benjamin's amazing Honours student, Lisa Kitto (also supervised by Dr Tim Barnes), who assisted with many of the studies in Chapter 6, and whose help with the preparation of liposomes and nanoparticles was vital to this project.

To my parents, John and Jenny, and siblings Francis, David, and Kathryn, you have always inspired me with your commitment to excellence; Mum and Francis, your both having done this before made me think it was possible. I have also been very fortunate at all times to be strongly supported in these endeavours by my Adelaide 'family': Janet and Peter Smith, Kate, Emma, Scott and Adam. Thank you for being there and sharing good times over the last few years.

And finally, to my wife and best friend, Sarah. We weren't yet married when I started this PhD, and I'm sure you've thought at times since that it would never be completed. However, it has been your love, unwavering support and constant encouragement that have made the difference in getting this completed. I dedicate this thesis to you, and to our daughter Eliza, whose birth before I had quite finished helped spur me to get across the finish line.

ABBREVIATIONS

7AAD	7-amino-actinomycin D
AEC	animal ethics committee
ALP	alkaline phosphatase
ANOVA	analysis of variance
APC	allophycocyanin
APC	antigen presenting cell(s)
BDCA	blood dendritic cell antigen
BM	bone marrow
BSA	bovine serum albumin
C3	complement component 3
CCL	chemokine ligand
CCR	chemokine receptor
CD	cluster of differentiation
cDC	conventional dendritic cell(s)
CFSE	carboxyfluorescein diacetate succinimidyl ester
CHO	Chinese Hamster Ovary
CLEC	C-type lectin
CLR	C-type lectin (receptor)
CM	complete medium
COOH	carboxyl group
CRD	carbohydrate recognition domain
CTLA4	cytotoxic T-lymphocyte antigen 4
CTLA4-Ig	CTLA4 immunoglobulin fusion protein
DAPI	4', 6-diamidino-2-phenylindole dihydrochloride
DC	dendritic cell(s)
DC-SIGN	dendritic cell specific intercellular adhesion molecule (ICAM) 3-grabbing non-integrin
DiI	1,1'-dioctadecyl-3, 3, 3', 3'-tetramethylindocarbocyanine perchlorate
DMSO	dimethyl sulfoxide
DNA	deoxyribonucleic acid
DPPC	1,2-dipalmitoyl- <i>sn</i> -glycero-3-phosphocholine
DSA	donor specific antibody
DSPE	1,2-distearoyl-phosphatidyl ethanolamine

EDC	1-ethyl-3-(3-dimethylaminopropyl) carbodiimide hydrochloride
EDTA	ethylenediaminetetraacetic acid
ELISA	enzyme-linked immunosorbent assay
ELISPOT	enzyme-linked immunospot
EM	electron microscopy
ESKD	end-stage kidney disease
Fab	fragment antigen-binding region (of an immunoglobulin)
Fc	fragment crystallisable region (of an immunoglobulin)
FCS	fetal calf serum
FITC	fluorescein isothiocyanate
Flt3	fms-related tyrosine kinase 3
Flt3L	Flt3 ligand
FMO	fluorescence minus one
G-CSF	granulocyte-colony stimulating factor
GBM	glomerular basement membrane
GM-CSF	granulocyte macrophage-colony stimulating factor
GVHD	graft versus host disease
HEPES	4-(2-hydroxyethyl)-1-piperazineethanesulfonic acid
HIV	human immunodeficiency virus
HLA	human leukocyte antigen
HP	haematopoietic progenitor
HPDC	haematopoietic progenitor-derived dendritic cell(s)
HSA	human serum albumin
ICAM	intercellular adhesion molecule
ICOS	inducible costimulator
ICOS-L	ICOS ligand
IFN	interferon
IgA	immunoglobulin A
IgG	immunoglobulin G
IgM	immunoglobulin M
IL	interleukin
iNOS	inducible nitric oxide synthase
IPTG	isopropyl- β -D-1-thiogalactopyranoside
IQR	interquartile range
ISIS	International Species Information System
KLH	keyhole limpet haemocyanin

LB	liquid broth
LC	Langerhan cell(s)
Lin	lineage
LPS	(bacterial) lipopolysaccharide
M-CSF	macrophage colony-stimulating factor
M-CSFR	M-CSF receptor
mal	maleimide
MHC	major histocompatibility complex
MLR	mixed leukocyte reaction
MoDC	monocyte-derived dendritic cell(s)
mTOR	mammalian target of rapamycin
NF- κ B	nuclear factor of activated T-cells kappa B
NHMRC	National Health and Medical Research Council
NHP	non-human primate
NHS	<i>N</i> -hydroxysuccinimide
NK	natural killer
NWP	new world primate
NWT	nylon wool T-cells
OCT	optimal cutting temperature compound
OWP	old world primate
PAMPs	pathogen-associated molecular patterns
PAS	periodic acid-Schiff
PBMC	peripheral blood mononuclear cell(s)
PBS	phosphate buffered saline
PCR	polymerase chain reaction
pDC	plasmacytoid dendritic cell(s)
PDL	programmed death ligand
PE	phycoerythrin
PEG	polyethylene glycol
PLA	polylactic acid
PLGA	polylactic-co-glycolic acid
pre-DC	dendritic cell precursor(s)
PRRs	pattern recognition receptors
RCF	relative centrifugal force
RES	reticuloendothelial system
rh	recombinant human

RNA	ribonucleic acid
RPMI	Roswell Park Memorial Institute medium (aka RPMI-1640)
SCF	stem cell factor
SD	standard deviation
SIV	simian immunodeficiency virus
TGF β	transforming growth factor beta
Th1	T helper type 1
Th17	T helper type 17
Th2	T helper type 2
TLR	toll-like receptor
TNF	tumour necrosis factor
TPO	thrombopoietin
Tr1	T regulatory type 1 cell(s)
Treg	T regulatory cell(s)
WB	whole blood
Xgal	5-bromo-4-chloro-3-indoyl- β -D-galactopyranoside

Chapter 1: BACKGROUND AND LITERATURE REVIEW

Acknowledgment

In Chapter 1, section 1.6 (including the tables and figures therein) is a reproduction with some modifications of the following previously published article:

- Jesudason S, Collins MG, Rogers NM, Kireta S, Coates PT. Non-human primate dendritic cells. *J Leukoc Biol* 2012; 91: 217-228.

This article was co-written by Dr Shilpanjali Jesudason and the author, with contributions from the other authors as listed in the printed version of the article, which appears in full as an appendix to this thesis.

© *Society of Leukocyte Biology 2012 – used with permission.*

The rest of the writing in this chapter represents an independent review of literature by the author, except where due reference is made in the text.

1.1. The context: End-stage kidney disease and transplantation

The global incidence of End-stage Kidney Disease (ESKD) is rising, driven in large part by increasing rates of diabetes and hypertension. The availability of haemodialysis and peritoneal dialysis treatment prevents death due to terminal uraemia, but patients on dialysis have a very high rate of morbidity and mortality, in large part due to cardiovascular disease.^{1,2} The median survival for a patient commencing dialysis in Australia who does not receive a transplant is currently 5 years.¹ In addition, dialysis treatments only partially correct the chronic uraemic state, and many patients suffer significant morbidity due to bone and mineral disorder,³ malnutrition,^{4,5} psychological disturbance,⁶ and poor quality of life.⁷ Dialysis treatment is also expensive, with the average cost per patient estimated at greater than \$AUD50,000 per year.⁸

The restoration of organ function with kidney transplantation leads to improved survival,^{9,10} better quality of life,¹¹ and lower costs over time.⁸ Outcomes after kidney transplantation in Australia are excellent, with 1-year and 5-year survival of 96% and 90% respectively for recipients of deceased donor transplants, and 99% and 95% respectively for recipients of live donor transplants.¹ Currently available immunosuppressive regimes are associated with low rates of acute rejection, and very few grafts are lost from acute rejection in the current era. However, this has not been associated with a significant improvement in long term graft survival beyond that achieved after the introduction of cyclosporin in the 1980s.¹² Progressive graft loss due to chronic allograft nephropathy and patient death with graft function remain the major challenges to improving long-term patient outcomes.

Avoiding or minimising the complications of immunosuppression is increasingly the focus of strategies to improve outcomes post-transplantation. The major causes of death with graft function are now malignancy, cardiovascular disease and to a lesser extent infection¹; immunosuppression is a significant factor in the pathogenesis of each of these in transplant recipients. Of particular concern is the significantly increased incidence of many different types of cancers in transplant recipients, compared with both the general population and patients on dialysis.¹³ Cancers with a known or suspected viral aetiology, such as non-melanoma skin cancers, lip and genital cancers, lymphomas and Kaposi's sarcoma have particularly increased incidence, supporting a

strong link with post-transplant exposure to immunosuppression. There is also an increased risk of many non-virally mediated and more common solid organ tumours, underlying the case for enhanced screening of transplant recipients.¹⁴

In addition, nephrotoxicity from calcineurin inhibitors, which currently form the mainstay of most immunosuppressive regimes, is a major contributor to premature graft loss due to chronic allograft nephropathy¹⁵, and leads to chronic kidney disease and ESKD in recipients of non-renal organ transplants in a significant number of patients¹⁶.

For these reasons, considerable effort in transplantation research has focused on trying to successfully promote transplant tolerance, as a means to minimise or avoid the long-term consequences of immunosuppression in transplant recipients.¹⁷ This has been widely viewed as the ‘holy grail’ of transplantation and has “served as a focal point for achievement in the field.”¹⁸

1.2. Transplant tolerance – a coming clinical reality?

The first description of tolerance was by Medawar and colleagues who, in 1953, described acquired immunological tolerance to foreign cells in the neonate.¹⁹

Considerable effort has been expended since that time to translate this phenomenon into the clinical transplant setting. The “true” definition of transplant tolerance has been said to be “a well-functioning graft lacking histological signs of rejection, in the absence of any immunosuppressive drugs, in an immunocompetent host capable of accepting a second graft of the same donor origin while being able to reject a third-party graft.”²⁰ However, despite success with achieving this in small animal models, it has generally not been possible to induce tolerance that meets this strict definition in non-human primates (NHP) or humans.

1.2.1. Clinical occurrence of tolerance

In the clinical setting, there have been a limited number of reports of what has been described as *operational tolerance*, a state defined as stable graft function in the complete absence of immunosuppression.²¹ This has been observed more frequently in liver transplant recipients,²²⁻²⁴ which may reflect the fact that the liver is a more “tolerogenic” organ than other transplanted solid organs. Rare “spontaneous” operational tolerance has been reported in kidney transplant recipients,^{21,25-34} most commonly following patient non-compliance with immunosuppressive medications, and occasionally deliberate immunosuppression withdrawal due to intolerable or life-threatening side effects. However, these patients are rarely, if ever, biopsied and it is clear that some of these patients still experience late rejection and graft loss long after immunosuppression withdrawal, and thus it is not always possible to determine that these grafts are truly free of chronic rejection, despite what may appear to be stable graft function. Furthermore, although a number of methods have shown promise, there is currently no reliable assay for tolerance that can be used to prospectively determine which patients might be suitable to have their immunosuppression withdrawn.³⁵

A more realistic approach for the clinic might be the concept introduced by Calne and colleagues of *Prope tolerance* or ‘almost’ tolerance, where stable graft function is maintained in the presence of minimal immunosuppression.^{36,37} This approach is attractive because it would enable the minimisation of drug-related adverse effects,

although it is not clear if in fact this merely represents the minimal level of immunosuppression to maintain graft function and prevent graft rejection. In any case, given the risks of immunosuppression withdrawal, this approach may be more achievable than true tolerance and deliver comparable long-term benefits to patients.

1.2.2. Strategies to induce tolerance used in pre-clinical and clinical studies

A variety of strategies have been utilised to try and induce tolerance in pre-clinical animal models and the human clinical transplantation setting³⁸⁻⁴⁰ (and most recently reviewed by Page et al).⁴¹ The transplant literature contains many examples of tolerance induction regimens that have been developed in rodent models of transplantation. However, only a few of these tolerance induction regimes have been able to be successfully applied in NHP or to human clinical transplantation with any degree of success. Significant differences in Major Histocompatibility Complex (MHC) expression and the much less complex immune systems of rodents underlie the much more permissive nature of these models of tolerance.⁴⁰ In addition, allo-immune responses in NHP and humans are significantly influenced by these species' heterologous immunity – memory responses that develop in response to prior exposure to environmental antigens – that has proven to be significant barrier to tolerance induction.^{42,43}

Approaches that have been successfully used in pre-clinical NHP studies have focused on modification of T-cell function to induce a state of donor-specific hypo-responsiveness. *T-cell depletion* strategies, the induction of *mixed haematopoietic chimerism* with donor bone marrow or stem cell infusion, and T-cell *co-stimulation blockade* have all been shown to be promising in the induction of tolerance, but have yet to reach widespread applicability in the clinic.

Although co-stimulation blockade involving targeting of a number of molecular pathways (Cluster of differentiation (CD)80, CD86 / CD28 and the CD40 / CD154 (CD40L) pathways) has been extensively investigated in rodents, as yet this approach has not produced tolerance when used alone in NHPs in a number of studies.^{38,40} However, a new immunosuppressive drug⁴⁴ based on cytotoxic T-lymphocyte antigen 4 immunoglobulin fusion protein (CTLA4-Ig), which inhibits the ability of CD80 / CD86 to interact with CD28 in a non-antigen specific way, known as belatacept has entered

phase II and III clinical trials,⁴⁵ and has shown promise as a calcineurin-inhibitor sparing agent, albeit without inducing tolerance.

Lymphoid depletion has utilised total lymphoid irradiation and anti-lymphocyte therapy with both polyclonal (e.g. anti-thymocyte globulin, anti-lymphocyte globulin) and monoclonal antibodies (e.g. anti-CD3 immunotoxin, alemtuzumab), with or without donor bone marrow re-constitution or co-stimulation blockade.³⁸⁻⁴⁰ This strategy is one of prevention of deleterious immune effects against the allograft around the time of transplantation when “danger signals” from ischaemia-reperfusion injury, surgical trauma and inflammation are at their peak. Immune reconstitution then occurs once a steady-state immune environment has developed, and in the absence of “danger signals” a state of graft acceptance, with deviation towards regulatory rather than cytotoxic anti-donor T-cell responses, is promoted.⁴⁶ In NHP, depletion strategies have been shown to prolong allograft survival in preclinical NHP models of transplantation,³⁸⁻⁴⁰ but have been associated with significant and profound immunosuppression, and do not reliably produce a tolerant state. In human transplantation, the monoclonal anti-CD52 lymphocyte depleting antibody alemtuzumab, which depletes peripheral T and B cells, has been utilised as a potentially tolerogenic therapy alone or in combination with low dose maintenance immunosuppression, and has led to reasonable midterm graft outcomes, but high rates of (reversible) acute rejection if immunosuppression was withdrawn.^{37,47-50}

Mixed chimerism involves the co-existence of allogeneic and host haematopoietic cells in the recipient, either as micro-chimerism (detectable only at a individual cellular level within organs) or as macro-chimerism (detectable in the peripheral blood). This can be achieved with a number of total or partial myelo- and lympho-ablative strategies (chemotherapy, antibody-based depletion similar to that described above, co-stimulation, calcineurin inhibitor based-immunosuppression and/or irradiation), followed by donor bone marrow or stem cell transplantation. This state of chimerism promotes thymic deletion of both self and donor reactive T-lymphocytes during immune re-constitution, and thus leads to potentially more robust tolerance than strategies that rely on manipulation of peripheral tolerance alone.⁵¹ Although in rodent studies permanent chimerism can be induced,⁵² in most NHP models,⁵³⁻⁵⁶ and most human studies only transient chimerism has been achieved, although ‘tolerance’ can be achieved without it.^{57,58}

Three recent landmark studies of human tolerance induction clinical trials in renal transplantation highlight the potential and some of the risks for mixed chimerism as a tolerance induction strategy.

A study by Kawai et al⁵⁹ reported 4 out of 5 patients who received human leukocyte antigen (HLA; the human form of MHC) haplo-identical (i.e. mismatched at 3 HLA loci) live donor kidney transplants weaned from all immunosuppression for greater than 2 years with stable renal function and preserved histology. These patients received a conditioning regimen of cyclophosphamide, T-cell depletion with a CD2-specific monoclonal antibody MEDI 507, and thymic irradiation, followed by donor bone marrow infusion and kidney transplantation. The regimen was later modified to include rituximab. Initial cyclosporin maintenance therapy was weaned off over several months. Durable mixed chimerism was not achieved in any individual, although it was transiently seen in all patients. No patient developed graft versus host disease (GVHD). Two patients experienced humoral (antibody-mediated) rejection, and one patient who had high levels of *non*-donor specific alloantibody pre-transplant lost their graft to irreversible humoral rejection after developing a donor specific antibody (DSA); one other developed thrombotic microangiopathy and lost their graft. Another patient developed post-transplant DSA and this persisted with mild glomerulopathy (a histological finding of chronic humoral rejection) on biopsy. As the rate of humoral rejection would be expected to be relatively low with single haplotype-identical live donor transplants, this implies that the therapy did not produce adequate humoral / B-cell tolerance.¹⁸ However, at the time of reporting, the patients with surviving grafts appear grossly immunocompetent, and there was some evidence presented for the induction of T regulatory function in these patients. A further report of this study including data on a total of 10 patients, with longer follow-up showed that 5 patients remain well and off all immunosuppression.⁶⁰

A second study reported by Scandling et al⁶¹ described a case of 1 of 3 patients rendered tolerant to an HLA identical graft after induction with corticosteroids, rabbit anti-thymocyte globulin and total lymphoid irradiation followed by donor bone marrow infusion enriched for CD34+ haematopoietic progenitor cells and depleted of T cells, to reduce the risk of GVHD. Unlike the previous series, *persistent mixed chimerism* was achieved in this patient. Two other patients who underwent this induction failed to achieve tolerance – one developed recurrent primary disease, and the other had mild

rejection with loss of chimerism and was maintained on low dose maintenance cyclosporin.

In a recent phase 2 study, Leventhal and colleagues reported the results of a trial of the administration of donor granulocyte-colony stimulating factor (G-CSF)-mobilised cells enriched for haematopoietic stem cells and so-called graft ‘facilitating’ cells (predominantly plasmacytoid precursor dendritic cells – see below)⁶² along with non-myeloablative conditioning in recipients of an HLA-mismatched living donor kidney transplant.^{63,64} Tacrolimus and mycophenolate maintenance immunosuppression was weaned off over the course of the first post-transplant year. Of 15 transplant recipients, 8 (53%) exhibited enduring chimerism and immune competence, and were successfully weaned off immunosuppression by 1 year.⁶⁴ None of these patients developed GVHD or engraftment syndrome, despite significant HLA mismatch. The authors proposed that in the setting of their approach to tolerance induction, durable chimerism could be regarded as necessary prior to the withdrawal of immunosuppression. However, prior sensitisation to HLA still represents a significant barrier to the development of chimerism, and the successful withdrawal of immunosuppression.

These studies raise the possibility of further studies of tolerance induction using these protocols,^{18,41} but it should be noted that there are still quite significant drawbacks inherent in these strategies. The need for heavy initial immunosuppression, the problems with lack of humoral / B-cell tolerance and the risk of GVHD need to be weighed against the currently excellent outcomes seen with standard approaches to transplantation in low to moderate risk patients.¹ Whether these recipients are indeed fully immunocompetent (and thus truly tolerant) or whether in fact their heavy initial immunosuppression provokes long term immunodeficiency (with the risks of longer term malignancies or infection) is also unclear.⁶⁵

In view of the difficulties with these described approaches to clinical tolerance, and the lack of donor-specificity in the techniques used, opportunities to induce tolerance or reduce the need for immunosuppression using less toxic and more targeted therapies should be explored.

1.3. Dendritic cells: derivation, biology and classification

Dendritic cells (DC) were originally identified in mouse spleen in the 1970s by Steinman and Cohn,⁶⁶⁻⁶⁸ and are so named for their probing, tree-like or dendritic shapes (from the Greek *dendron*, meaning tree; see Figure 1.3.1).⁶⁹ They are a heterogeneous group of rare but potent professional antigen presenting cells (APC) that have a central role linking innate and adaptive immunity. The derivation, immunobiology, and classification of DC have been extensively reviewed.⁶⁹⁻⁸⁴

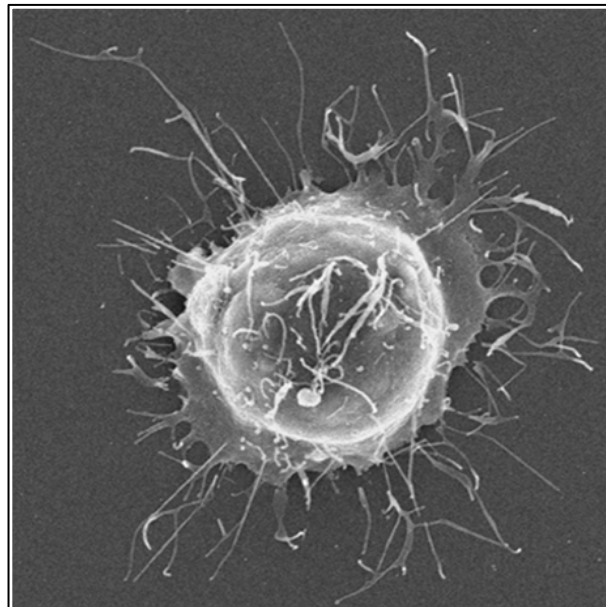


Figure 1.3.1. Scanning electron micrograph of a mature dendritic cell, demonstrating the presence of abundant well-developed dendrites at the cell surface.

Rhesus monkey CD123⁺ pre-DC were sorted using flow cytometry, and matured with human IL-3 and human CD40L for 3 days. Scanning electron micrograph; original magnification 3500x. Image courtesy of PTH Coates; part of an original figure published in Coates PT et al (2003),⁸⁵ used with permission.

The primary function of DC is the uptake, (via macropinocytosis, phagocytosis or receptor-mediated endocytosis via pattern recognition receptors; see below) and processing of exogenous and endogenous (including self) antigens, and presentation of these antigens in the context of MHC molecules to T-cells.⁷³ Like other APC, they

have the ability to upregulate T-cell co-stimulatory molecules (e.g. CD80, CD86 and CD40) onto their surface in addition to MHC class I and II. However, unlike “non-professional” APC (B-cells, monocytes, macrophages), they have the unique ability to fully activate and induce clonal expansion of both naïve and memory T-cells, can migrate from peripheral tissues to secondary lymphoid organs, and can cross-present (extracellular) antigens in the context of MHC class I to antigen specific CD8 T-cells.⁷³ They are therefore crucial to the development of primary immune responses.

DC arise from haematopoietic progenitor cells and exist as both migratory and tissue-resident cells throughout the body in the circulation and a wide variety of tissues. Although they share common features, multiple subtypes of DC with distinct life spans and immune functions have been described in mice and in humans.^{70,73,75,77,86}

1.3.1. The origins and development of DC

The understanding of the lineage origin of DC has changed in recent years.⁷⁷ Initial evidence pointed towards DC having either a myeloid or a lymphoid origin. Classical migratory DC such as conventional DC (cDC), or Langerhans cells (LC),⁸⁷ most lymphoid tissue DC,⁸⁸⁻⁹¹ and monocyte-derived DC (MoDC)⁹²⁻⁹⁴ were considered to be myeloid in origin; plasmacytoid DC (pDC),^{95,96} as well as some lymphoid tissue resident DC⁹⁷⁻⁹⁹ in thymus, spleen and lymph nodes were thought to have a lymphoid origin. However, later it was shown that both common myeloid and lymphoid progenitor populations arising from haematopoietic progenitors can give rise to all types of cDC and pDC,¹⁰⁰⁻¹⁰² and this has been confirmed with both *in vitro* cultured cells and cells derived *in vivo*.¹⁰³

It has been demonstrated that cells expressing Flt3 (fms-related tyrosine kinase 3) within common myeloid or lymphoid progenitors are the ones that can develop into DC¹⁰⁴ in the presence of Flt3-ligand (Flt3L), which is an important cytokine central to steady state DC development. It is evident that commitment to a particular DC precursor or subtype is not an all or nothing event, but rather is a sequential multistep process, and can be altered.^{75,103} However there is evidence of a common, committed clonal DC precursor arising downstream from either a myeloid or lymphoid progenitor.^{103,105} These cells are negative for lineage (Lin) markers CD14 (monocytes), CD3 (T-cells), CD19 and CD20 (B-cells) and CD56 (natural killer, NK cells), CD11c

and MHC Class II⁻, but may acquire CD11c later on, perhaps reflecting a divergence of cDC from pDC.

Although it has been known that monocytes develop many phenotypic features of DC in the presence of inflammation, such as the so-called tumour necrosis factor (TNF) and inducible nitric oxide synthase (iNOS) producing ‘DC’ (Tip-DC),¹⁰⁶ or as best characterised *in vitro* by inflammatory MoDC,⁷⁵ it is apparent that the cDC, pDC and monocyte lineages separate by the time these cells reach peripheral tissues. Moreover, in steady state conditions, neither monocytes nor pDC develop into cDC,^{79,107} although monocytes can readily differentiate into DC *in vivo* (as well as *in vitro*) in the presence of inflammatory stimuli.¹⁰⁸ It has been shown that DC development progresses from the macrophage and DC precursor to common DC precursors that give rise to pDC, and committed pre-cDC, but not monocytes, which split from the DC pathway while still in the bone marrow (see Figure 1.3.2).^{79,109} However, to add to the complexity, a recent study has shown that immunostimulatory CD11c⁺ MHC class II⁺ DC can evolve into immunosuppressive CD11c⁻ MHC class II⁻ macrophage like cells under certain conditions, suggesting an element of homeostatic regulation.¹¹⁰

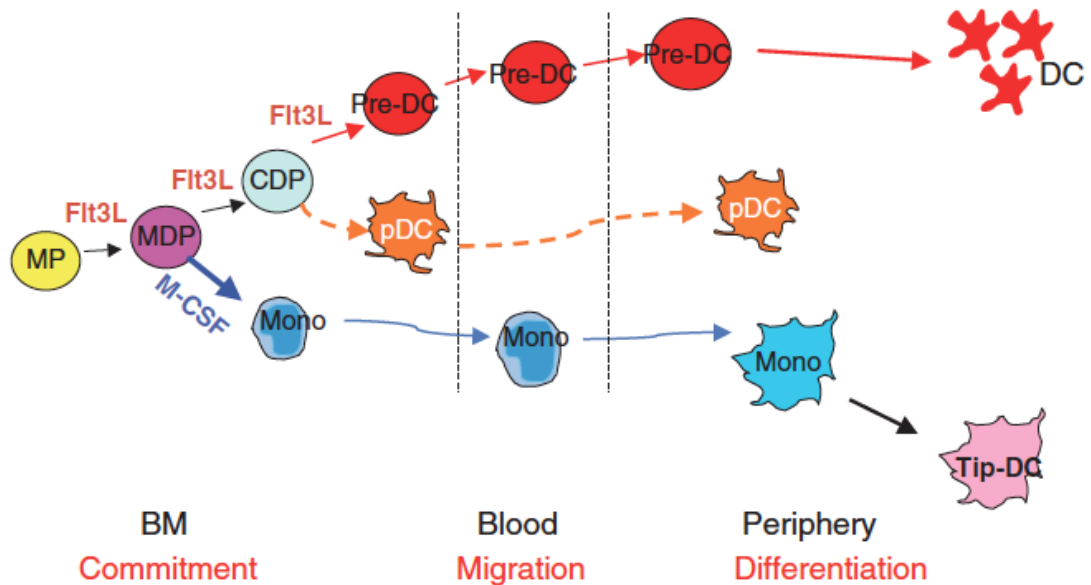


Figure 1.3.2. Dendritic cell and monocyte origin and development.

DC and monocytes arise from common myeloid precursors (MP) and macrophage-DC progenitors (MDP) in the bone marrow, but diverge to produce a common DC-progenitor (CDP) or monocytes (Mono) under the influence of Flt3L or M-CSF, respectively. Both plasmacytoid DC (pDC) and Pre-cDC (Pre-DC) arise from the CDP.

BM = bone marrow; M-CSF = macrophage-colony stimulating factor; Flt3L = fms-like tyrosine kinase 3 ligand; Tip-DC = TNF-iNOS producing DC (see text)

Reproduced from Liu K and Nussenzweig MC. *Immunol Rev* 2010; 234: 45-54.

© 2010 John Wiley & Sons A/S. Used with permission.

Further differentiation of DC subtypes is dependent on the tissue microenvironment, cytokines and transcription factors. This plasticity gives the DC system enormous flexibility and ability to respond different situations that may face the immune system.

A number of cytokines and growth factors are important for DC development, and as discussed above, Flt3L appears to be the most critical of these.^{103-105,111} Interestingly, administration of Flt3L to mice,¹¹² humans,¹¹³ and rhesus macaques⁸⁵ leads to exceptionally high levels of both cDC and pDC in the peripheral blood. In addition to Flt3, both c-kit (the receptor for stem cell factor (SCF) and granulocyte-macrophage colony stimulating factor (GM-CSF) are expressed on DC precursors, and are important cytokines in DC development. GM-CSF promotes the development of cDC from precursors over pDC or macrophages,⁷⁷ and is important (along with interleukin-4; IL-4) in the differentiation *in vitro* of DC from monocytes.⁹² Transforming growth factor beta (TGF β) is important in the development of Langerhans cells,¹¹⁴ which do not actually require GM-CSF for development. G-CSF is not required for DC development *in vivo* or *in vitro*, but when it is administered *in vivo* it can also massively expand the numbers of DC in peripheral blood (with predominance of pDC over cDC),^{115,116} along with precursors including monocytes and CD34⁺ cells.

Finally, a series of transcription factors including Spi3, nuclear factor of activated T-cells-kappa-B (NF- κ B)¹¹⁷⁻¹²⁰ (RelB protein up-regulation), Ikaros, interferon (IFN) regulatory factors (IRF-2, 4 and 8), helix-loop-helix transcription factors (ID2), STAT5 and STAT3 have been shown to be important to DC development and the determination of DC subsets. These have been reviewed in detail by Wu and Lu.⁷⁷

1.3.2. Classification of DC

The classification of DC is complex, and a number of classifications have been used in the literature. The DC system has been most extensively characterised in the laboratory mouse, and until recently most human studies were limited to DC obtainable from the peripheral blood (e.g. using monocytes as precursors for *in vitro* DC propagation), rather than lymphoid or other tissue specific DC. Until recently, presumed differences between the murine and human DC systems have limited direct comparisons.⁸⁶ However, recent work has examined the homology between human and mouse DC subsets through the use of transcriptional profiling,¹²¹⁻¹²⁸ and an organised systematic

effort to profile human and mouse leukocytes,^{129,130} has established that there are a relatively small number of distinct DC subsets that are widely distributed in all mammals.

The difficulty with studying the DC system has been apparent for many years: DC are very rare cells, and their precursors are rarer still. The DC system is constitutively in a state of flux and substantial differences exist between the steady state and during infection or inflammation.⁷⁵ For the purposes of this chapter, the classification of murine DC will first be reviewed, and this will then be compared with human DC equivalents.

1.3.2.1 Murine DC

In the mouse, there are four major categories of DC: conventional DC, which predominate in the steady state; Langerhans cells; plasmacytoid DC (pDC); and monocyte-derived DC (MoDC), which become induced in response to inflammation. A summary of the classification of these DC and their phenotypic markers is shown in Table 1.3.1.

Conventional DC (cDC), also referred to as classical or myeloid DC, have classical DC morphology, with a stellate shape and long projections (“dendrites”), and exhibit DC functions in *steady state*. They are distinct from DC precursors (pre-DC), which require further development to acquire the classical DC morphology and full DC function. Pre-DC can be considered the last precursor stage of DC development, and different pre-DC produce different types of DC. The development of pre-DC into DC frequently requires a microbial or inflammatory stimulus, but can also occur in the steady state. Murine cDC express a range of cell surface molecules that assist in their classification and phenotyping.^{75,77,86} The most important are CD11c (found on all cDC), CD11b, CD8 α , CD4 and MHC Class II.

cDC can be divided into *migratory* DC and *lymphoid-tissue-resident* DC. Migratory DC arise from peripheral precursors, are immature in steady state in peripheral tissue where they act as antigen sampling sentinels, and migrate through the lymphatics to lymph nodes in response to immune danger signals (e.g. microbial infection, tissue damage).^{75,77} This process also occurs, at a lower rate, in the steady state. During the migration process, these DC typically develop a mature phenotype with up-regulation of

surface MHC class II and co-stimulatory molecules, lose their ability to uptake antigen and upon arrival in the lymph node, present antigen to T-cells.¹³¹ Examples of migratory DC include dermal DC, and other non-lymphoid tissue resident DC such as kidney^{132,133}, lung¹³⁴ and liver DC.^{135,136} Recently, it has been possible to broadly phenotypically characterise migratory DC as either CD11b⁺ or CD11b⁻ CD103⁺ on the basis of whether they present antigen on MHC class II (major subset), or cross present antigen in the context of MHC class I (cross-presenting subset), respectively.^{79,137,138}

Lymphoid-tissue-resident DC, in contrast, do not migrate into lymphoid organs but rather originate from blood precursors, collect and present antigens in the lymphoid organ itself.^{75,139} This category includes most of the DC in the thymus and the spleen, but only around half of those found in lymph nodes, the rest being migratory DC. Lymphoid-tissue-resident DC develop from pre-DC found in lymphoid tissues themselves,¹⁴⁰ typically have an immature phenotype, and actively take up and process antigen, in contrast to classical migratory DC.¹³⁹ In mouse spleen, there are 3 distinct cDC subsets (all CD11c⁺) which can be divided on the basis of CD8 α and CD4 surface expression into CD4⁺, CD8 α ⁺, and CD4⁻CD8 α ⁻ DC (typically referred to as double-negative DC); in addition smaller numbers of pDC (see below) and a identified lineage of IFN producing killer DC have been identified.⁷⁷ CD8 α ⁺ DC cross-present antigens, and have a major role in priming cytotoxic CD8⁺ T-cell responses.^{141,142} CD4⁺ and CD4⁻ CD8 α DC are more efficient at presenting MHC class II-associated antigens to CD4⁺ T-cells.¹⁴³ Thymic DC, in contrast to other DC, arise from a local thymic precursor, do not migrate and play an important role in central tolerance through the presentation of self antigen and negative selection of T-cells.⁷⁵ Mouse (as well as human) thymus contains several subsets of CD11c⁺ DC, as well as pDC.

Table 1.3.1. Phenotypic markers of dendritic cell (DC) subsets in the mouse.

DC subset	DC type	CD8 α	CD103	CD205	EPCAM (CD326)	CD11b	B220 or CD45RA	DC-SIGN	Langerin (CD207)	Antigen presentation	Major cytokine produced
pDC	Lymphoid resident DC	+/-	-	-	-	-	+	++	-	Poor	IFN α
CD8α⁺ DC	Lymphoid resident DC	+	low	+	-	+	-	-	+/-	Cross-presentation on MHC class I; expression of cystatin C	IL-12p70, IFN λ
CD4⁺ DC	Lymphoid resident DC	-	-	-	-	+	-	-	-	Presentation on MHC class II	
DN DC	Lymphoid resident DC	-	-	-	-	+	-	-	-	Presentation on MHC class II	
CD11b⁺ DC	Migratory DC	-	+/-	+	-	+	+	ND	-	Presentation on MHC class II	
CD103⁺ DC											
- lung	Migratory DC	-	+	++	+/-	-	-	-	+	Cross presentation on MHC class I	
- intestine		-	+	-	-	+	-	-	-		
Langerhans cells	Migratory DC	-	-	++	+	+	-	-	++	Presentation of self antigens for tolerance induction	IL-10
Monocyte-derived DC	Induced by inflammation	-	-	-	-	+	-	+	-	Cross-presentation	TNF

DC-SIGN = DC-specific ICAM3-grabbing non-integrin; DN = double negative; EPCAM = epithelial cell adhesion molecule; IFN = interferon; IL = interleukin; ND = not determined; pDC = plasmacytoid DC.

Table reproduced from Belz and Nutt (2012).⁸³ Reprinted by permission from Macmillan Publishers Ltd: Nat Rev Immunol. 2012 Jan 25;12(2):101-13, © 2012

Langerhans cells (LC) are specialised self-renewing DC resident in the epidermis of the skin, and like migratory DC, migrate to lymph nodes to present antigen.^{144 145} They are distinct from other CD207/Langerin⁺ dermal cells which can be identified in skin and lymph nodes.¹⁴⁶ However, unlike cDC, they arise from local LY6C⁺ myelomonocytic precursors in the skin that are derived from macrophages present in the epidermis early in the course of embryonic development, and that undergo a proliferative burst in the first few days after birth.^{83,147}

Plasmacytoid DC (pDC), also known as the natural IFN producing cell,^{96,148,149} exist as pre-DC in steady state, and develop from bone marrow in the presence of Flt3L and G-CSF. The morphology of these cells is of a rounded cell with a similar appearance to the immunoglobulin-producing plasma cells of the B cell lineage (hence the terminology). They were previously known as plasmacytoid T-cells and plasmacytoid monocytes, before they were recognised as a DC precursor. pDC do not develop dendritic cell appearance or full function until stimulated, such as by viral or other infections, at which point they produce large amounts of Type 1 IFNs (IFN α and β) and acquire DC antigen processing and presentation properties.^{95,150} pDC are continuously produced from CD34⁺ haematopoietic stem cells in bone marrow, and migrate through the blood to lymph nodes and spleen in steady state. Under inflammatory conditions, circulating pDC preferentially accumulate in lymph nodes.^{149,151} However, they are less efficient antigen-presenting cells and T-cell stimulators than cDC, lead to deviation towards a Th2 (anti-inflammatory) immune response,⁹⁶ and require additional stimuli to reach full activation.¹⁵² Significantly (see discussion below) they have been shown to be important participants in the immune response to allografts, and can induce regulatory T-cells that can promote tolerance.¹⁵³

pDC (present as pre-DC) can be identified in mice by their expression of several characteristic markers, including sialic acid-binding immunoglobulin-like lectin H (SIGLEC-H) and bone marrow stromal antigen 2 (BST2). Murine pDC are CD11c^{low} CD45RA⁺ B220⁺ MHC Class II⁺ and express CD8 α when activated (Table 1.3.1).⁸⁶

Monocyte-derived DC (MoDC) are not present *in vivo* in the steady state, but under inflammatory conditions can be rapidly mobilised from circulating blood monocytes.^{106,140,154,155} As discussed above, MoDC possess many of the phenotypical features of DC but do not necessarily originate via the same pathway as cDC. In steady

state, monocytes express macrophage colony-stimulating factor (M-CSF) receptor (M-CSFR, or CD115), and other markers including LY6C and CX3C-chemokine receptor 1 (CX3CR1); but in response to Toll-like receptor (TLR) 4 ligands, or bacteria, fully differentiate into MoDC. A similar process occurs *in vitro* in response to growth factors such as GM-CSF – see discussion below. MoDC express CD11c, MHC class II, CD24 and SIRP α , and they upregulate the expression of DC-specific intercellular adhesion molecule (ICAM)3-grabbing non-integrin (DC-SIGN, or CD209), while losing expression of M-CSFR and LY6C.^{83,108} Through this process they develop potent antigen presentation capacity, including the ability to cross present antigens in the context of MHC class I to CD8 T-cells.¹⁰⁸

1.3.2.2 Human DC

Similar to mouse DC, human DC have been characterised according to function and anatomical location.⁸⁴ Human DC can be classified as *migratory* DC that traffic through tissues to lymph nodes, and *resident* DC that are present in lymph nodes but arise from blood. In addition, human blood DC and inflammatory DC represent important subsets. The distribution of the various human DC subsets is shown in Figure 1.3.3, and a comparison of human DC with their homologues is shown in Figure 1.3.4. The nomenclature of (blood) DC in humans has recently been standardised.⁸¹

Myeloid DC in humans express typical myeloid markers (CD11c, CD13, CD33 and CD11b), and correspond to the CD11c⁺ conventional DC in mice. They are divided into two major subsets CD1c⁺ and CD141⁺, which are homologous with mouse CD11b⁺ DC (human CD1c⁺) and CD8 α ⁺/CD103⁺ (human CD141⁺), respectively.⁸⁴

CD1c⁺ myeloid DC are the major population present in human blood, tissues and lymphoid tissues. They express myeloid antigens CD11b, CD11c, CD13, CD33, CD172 (SIRP α) and CD45RO, and represent approximately 1% of mononuclear cells in blood.⁸⁴ CD1c was previously identified as blood dendritic cell antigen (BDCA)-1, and its expression enables the differentiation of these cells from pDC.^{156,157} These cells express a wide range of lectins (CLEC7A, CLEC6A, CLEC13B or DEC205, CLEC13D or macrophage mannose receptor), TLRs (1-8) and other pattern recognition receptors (see below), and perform the classical DC functions of antigen uptake, transport and presentation.⁸⁴ Following stimulation, CD1c⁺ DC secrete TNF α , IL-8 and IL-10, and

IL-12 following the ligation of TLR7/8.¹⁵⁸ Like mouse CD4⁺ DC they can stimulate naïve CD4 T-cells, but do not effectively cross-present antigen via MHC class I to CD8 T-cells.^{123,159}

CD1c⁺ DC present in tissues (as opposed to blood) include dermal DC,¹⁶⁰⁻¹⁶² and the interdigitating cells of the T-cell areas of lymph nodes¹⁶³⁻¹⁶⁵; in both cases they are distinguishable from Langerhans cells by the lack of Langerin and EPCAM expression and the lack of Birbeck granules. They are also present in tonsil and spleen, where they are thought to originate directly from DC circulating within the blood.^{158,166}

CD141⁺ myeloid DC, originally identified with the use of BDCA-3, make up approximately 10% of human blood myeloid DC (0.1% of mononuclear cells),^{156,157} and can be found among tissue resident DC in lymph nodes, tonsil, spleen, bone marrow,^{158,165,167,168} and the non-lymphoid tissues skin, lung and liver.¹²³ In a major breakthrough for the field of DC biology, it is now established that human CD141⁺ DC are homologous to mouse CD8α⁺ spleen/lymph node DC and CD103⁺ tissue DC, and this has allowed the alignment of the classification human and mouse DC subsets in both lymphoid and non-lymphoid tissues.⁸⁴ CD141⁺ DC also have the ability to cross present antigen, and XCR1 and CLEC9A (also known as DNGR-1) have been recognised as markers of cross-presenting DC across species.^{169,170} They secrete TNFα, CXCL10 and IFNλ, although IL-12 p70 secretion is reduced compared to mouse CD8α⁺ DC, or human CD1c⁺.^{123,158}

Plasmacytoid DC (pDC) have a similar phenotype and function in mice and humans and are distinct from conventional or myeloid DC in both species.^{171,172} They lack the myeloid markers CD11b, CD11c, CD13 and CD33, are distinguishable by their expression of CD123, CD303 (CLEC4D or BDCA-2) and CD304 (neuropilin or BDCA-4), and are the most numerous blood DC.¹⁵⁶ In steady state, they are not present in quiescent tissues, but are present in lymph nodes and are recruited rapidly to both in the presence of inflammatory stimuli such as viral infection, where they produce type 1 interferons in response to ligation of TLR 7 and 9.^{84,149,173} pDC have reduced capacity to take up antigen, do not express high levels of co-stimulatory molecules,^{95,149} and appear to have an important role in the maintenance of tolerance to self and foreign antigens.¹⁷²

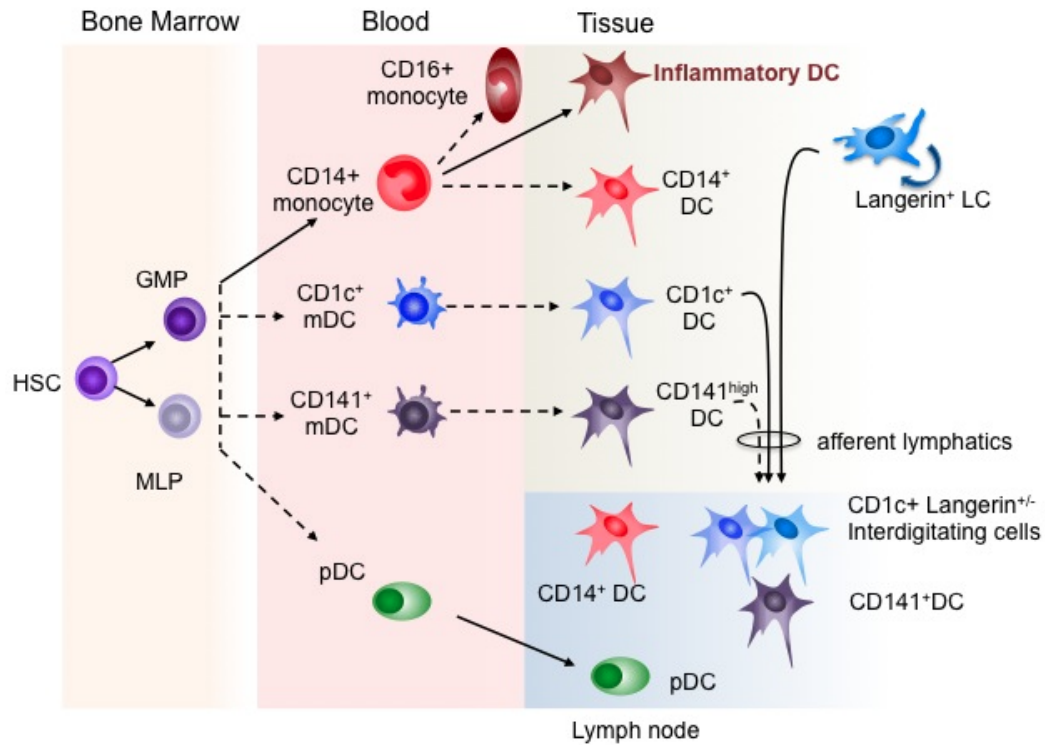


Figure 1.3.3. Distribution of human DC.

The distribution of major human DC subsets in blood, epithelial tissues and lymph nodes. Broken arrows indicate relationships that require further confirmation in humans. Human DC can be generated either from granulocyte-macrophage progenitors (GMP) or multilymphoid progenitors (MLP) both of which ultimately arise from haematopoietic stem cells (HSC). Classical monocytes, blood myeloid DC (mDC) and plasmacytoid DC (pDC) are putative precursors of tissue and lymphoid DC. Nonclassical monocytes are reported to arise by conversion of classical monocytes in the mouse. Inflammatory DC and CD14+ DC have transcriptional profiles suggesting that they arise from monocytes; likewise tissue CD1c+ DC and CD141+ DC are related to their blood counterparts. Myeloid DC and Langerhans cells (LCs) both form interdigitating cells in skin-draining lymph nodes. CD14+ DC and pDC are also found in nodes but may arise directly from the blood rather than by migration from tissues.

Reprinted from Collin M, McGovern N, Haniffa M. *Immunology* 2013; Apr 29. doi: 10.1111/imm.12117. This image is protected by copyright. All rights reserved.

© 2013 John Wiley & Sons – used with permission.

CD14⁺ DC represent a third subset of CD11c⁺ myeloid cells, previously known as interstitial DC, that are found in tissues and lymph nodes, and appear to originate from monocytes. However, they lack CD1c and CD141, and do not express co-stimulatory molecules or CCR7.^{160,174,175} CD14⁺ DC also express DC-SIGN and the macrophage markers FXIIIa and CD163,^{175,176} although it can be difficult to separate these cells from macrophages *in situ*.¹⁷⁵ Whether they are capable of migration to lymph nodes is uncertain; important functions appear to include the formation of follicular helper T-cells,¹⁷⁴ and providing B-cell help.¹⁷⁷ A mouse equivalent of CD14⁺ DC is still to be definitively identified, but a subset of the CD11b DC population has been identified as being derived from monocytes, through the use of markers including CD64,^{178,179} a finding that if further confirmed would support the presumed monocytoid origin of human CD14⁺ DC.

Langerhans cells (LC) in humans express high levels of the C-type lectin Langerin (CD207), and CD1a (non-polymorphic MHC class I), are found in the epidermis, and other stratified epithelia in the lung and oral and genital mucosae, where they form a network.¹⁸⁰⁻¹⁸² LC were the original migratory DC identified, and migrate to lymph nodes under both steady state and inflammatory conditions.¹²¹ LC contain a specialised endosomal compartment known as the Birbeck granule, which has a distinctive ‘tennis racket’ appearance on electron microscopy, is linked to Langerin (CD207) expression, and serves both antigen capture and presentation function.¹⁸³⁻¹⁸⁵ Despite long being recognised, the exact function of LC *in vivo* currently remains unclear, in part due to recent observations that other dermal DC also express Langerin/CD207 (thus confounding the interpretation of prior studies), and findings of several studies suggesting significant differences between the functions of LC *in vitro* and *in vivo*, depending on the underlying conditions (reviewed in Romani et al).¹⁸⁴

Inflammatory DC. Although DC derived from monocytes *in vitro* (MoDC, see below) have been a standard model used by DC biologists for many years,⁹² the relationship between inflammatory monocytes and DC *in vivo* has remained less well defined. Recently, transcriptional profiling of DC-like cells within human inflammatory exudates has suggested that these cells might represent a distinct DC subset that shares gene signatures with *in vitro* MoDC. These human inflammatory DC, but not inflammatory macrophages, stimulated autologous memory CD4⁺ T cells to produce IL-17, and induced naive CD4⁺ T cells to differentiate into T helper 17 (Th17) cells.¹²⁸

These inflammatory DC express CD1c, CD1a, CD206, CD11b, SIRP α , FC ϵ RI, and low levels of CD14, but do not express CD16 or DC-SIGN (CD209). Another example of inflammatory DC that has been reported include inflammatory dendritic epidermal cells, found in T helper type 2 (Th2)-mediated dermatitis.¹⁸⁶ Whether blood DC also form inflammatory DC directly, and whether inflammatory DC migrate to lymph nodes or remain as steady state resident cells after inflammation resolves remains unresolved.⁸⁴

In addition to inflammatory DC, some reports have suggested that CD16⁺ monocytes possess characteristics of DC, including higher MHC class II expression and co-stimulatory antigen expression.¹⁵⁷ In support of this, antigen 6-sulfo LacNAc (SLAN) expressing CD16⁺ monocytes (SLAN-DC) have been reported to secrete large amounts of TNF α , IL-1b and IL-12, and to respond to inflammatory stimuli.¹⁸⁷ However, whether these CD16⁺ CD14^{dim} cells, that appear homologous to GR-1/Ly6C^{low} patrolling monocytes in mice, are in fact DC remains uncertain.¹⁸⁸





	Human	Mouse
Myeloid / Classical		
Major subset 	CD1c⁺ <i>Dectin 1 (CLEC 7A)</i> <i>Dectin 2 (CLEC6A)</i>	CD11b⁺ (tissues) CD4⁺ CD11b⁺ (lymphoid)
Cross-presenting 	CD141⁺ <i>CLEC9A</i> <i>XCR1</i>	CD103⁺ (tissues) CD8⁺ (lymphoid) <i>CLEC9A</i> <i>XCR1</i> <i>Langerin</i>
Plasmacytoid 	<i>CD303 (CLEC4C)</i> <i>CD304 (neuropilin)</i> <i>CD123 (IL-3R)</i>	<i>B220</i> <i>Siglec H</i>
Monocyte-related		
	CD14⁺ DC <i>CD209 (DC-SIGN)</i> <i>Factor XIIIa</i>	CD11b⁺ CD64⁺ tissue DC <i>CX3CR1</i> <i>CD14</i>
	CD16⁺ monocyte <i>CX3CR1^{hi}</i> <i>SLAN (subset)</i>	Gr-1/Ly6C low monocyte <i>CX3CR1^{hi}</i> <i>CCR2 negative</i>
	Inflammatory DC <i>CD1c</i> <i>CD16 negative</i>	Monocyte-derived DC <i>CD209 (DC-SIGN)</i> <i>CD206</i>

Figure 1.3.4. Surface markers of the major human DC populations and their murine homologues.

Myeloid DC and mouse classical DC (also known as conventional DC) contain a major subset and a minor specialised cross-presenting subset. Plasmacytoid DC are easily recognisable in many species. Monocyte related DC include a recently recognized subset of CD11b⁺ DC that may be homologous to human CD14⁺ DC. Inflammatory monocyte-derived DC are also recognised in both species but are heterogeneous.

Modified from Collin M, McGovern N, Haniffa M. *Immunology* 2013; Apr 29. doi: 10.1111/imm.12117. This image is protected by copyright. All rights reserved.

© 2013 John Wiley & Sons – used with permission.

1.3.3. In vitro propagated DC: models for investigating DC development and immunobiology

Well-defined *in vitro* culture systems that permit the generation of large numbers of DC from mouse bone marrow or human peripheral blood monocytes have been essential tools in advancing the understanding of DC biology. *In vitro* propagated DC could be considered another major category of (human or murine) DC, and although they may not replicate exactly *in vivo* DC development, they are important not only in the study of DC biology, but also offer the most likely potential source of DC for clinical applications. The use of growth factors such as G-CSF, Flt3L and GM-CSF can significantly increase the yield of these procedures, and although there are some differences noted between G-CSF mobilised DC and DC propagated from non-mobilised blood,^{189,190} overall DC functions appear similar.¹⁹¹

MoDC can be differentiated from monocytes using *in vitro* culture of CD14⁺ cells collected from peripheral blood (with or without prior mobilisation with growth factors such as Flt3L or G-CSF). In the presence of GM-CSF and IL-4 these cells differentiate into immature DC without proliferation over 5-7 days.^{92,93} GM-CSF is critical in the development of 'myeloid' DC, and IL-4 inhibits the development of macrophages from monocytes. These immature DC have low expression of MHC Class II, co-stimulatory molecules (CD40, CD80 and CD86) and some reduction in CD14 expression.¹⁹² However, they express DC-SIGN at high levels,¹⁹³ have high migration and antigen uptake ability, and can be matured with additional stimuli in culture including TNF- α , bacterial lipopolysaccharide (LPS), IFN- γ , CD40L, prostaglandin E2, IL-6, IL-1 β , alone or in combination, and also with monocyte-conditioned medium.¹⁹² Maturation is associated (see above) with CD83 surface expression (a specific marker for DC maturation),⁹⁴ up-regulation of co-stimulatory molecules and MHC-Class II, loss of antigen uptake ability, and enhanced ability to stimulate T-cell proliferation and secretion of inflammatory cytokines (IL-12p70).^{93,192,194,195} These MoDC correspond to the dominant inflammatory DC type that is mobilised during bacterial infection *in vivo*.¹⁰⁸

DC can also be derived by *in vitro* cultures of haematopoietic progenitor cells from bone marrow, or alternatively growth factor-mobilised peripheral blood.^{196,197} These protocols expand DC precursors from progenitor cells (including CD34⁺ stem cells and

other progenitors at various developmental stages) using early acting cytokines critical to DC development such as Flt3L, SCF (the ligand for c-kit), GM-CSF, TNF- α and thrombopoietin (TPO). Further culture with GM-CSF and IL-4 and subsequent maturation stimuli produces DC that have considerable similarities with MoDC. pDC can also be specifically expanded using cultures of Flt3L and TPO alone.¹⁹⁸

1.3.4. DC pattern recognition receptors

DC recognise pathogens through shared molecular components common to many pathogens, consisting of proteins, lipids, carbohydrate or nucleic acids, which are known as pathogen-associated molecular patterns (PAMPs). This recognition is primarily achieved by pattern recognition receptors (PRRs) found on DC, both at the DC surface and intracellularly. DC PRRs that interact with PAMPs include the ubiquitous toll-like receptors (TLRs), the intracellular nucleotide-binding domain and leucine-rich-repeat-containing family (NLRs, retinoic acid-inducible gene I (RIG-I)-like receptors and the C-type lectin receptors (also known as CLR or CLECs). The expression of TLRs and CLR varies considerably between different DC subsets (see Table 1.3.2), and is linked to the downstream signalling pathways that influence DC phenotype and function.^{82,199}

In particular, CLR play an important role in shaping the immune responses to pathogens by DC, for example in the setting of human immunodeficiency virus (HIV) infection,⁸² and are unique in their DC expression profiles and contribution to DC function.

Table 1.3.2. Toll-like receptor and C-type lectin receptor expression by human DC subtypes

Receptor	Dermal DC			Blood DC		
	LC	CD14 ⁺	CD1a ⁺	Myeloid		Plasmacytoid
				CD1c ⁺	CD141 ⁺	
<i>C-type lectin receptors</i> ²⁰⁰⁻²⁰²						
CD206 (mannose)	-	+	+++	-	-	-
CD207 (langerin)	+	-	-	-	-	-
CD209 (DC-SIGN)	-	+	-	-	-	-
CD303* (BDCA2)		-	-	-	-	+
CD141 (BDCA3)		-	-	-	+	-
CD304** (BDCA4)		-	-	-	-	+
<i>Toll-like receptors</i> ²⁰³⁻²⁰⁷						

TLR1	+	+		-	-	+
TLR2	+	+		+	+	-
TLR3	+	+		+	+	-
TLR4	-	+		+	-	-
TLR5	±	-		-	-	-
TLR6	+	+		-	-	+
TLR7	-	-		+	-	++
TLR8	-	+		+	+	-
TLR9	-	-		-	-	++
TLR10	+	+		-	-	+

* CD303 is the standard name for BDCA2, also known as CLEC4A.

** CD304 is the standard name for BDCA4, also known as neuropilin.

*** CD14⁺ dermal DC have a similar profile to monocyte derived DC.²⁰⁶

Reproduced from Cunningham AL, Harman A, Kim M, Nasr N, Lai J. *Immunobiology of Dendritic Cells and the Influence of HIV infection*. In: L. Wu and O. Schwartz (editors). *HIV Interactions with Dendritic Cells: Infection and Immunity*, Advances in Experimental Medicine and Biology 2013; 762: 1-44.

© Springer Science+Business Media New York 2013

Used with kind permission of Springer Science+Business Media

1.3.4.1 C-type lectins

CLRs possess an extracellular carbohydrate recognition domain (CRD) that recognises and binds to sugar (mannose, fucose, and glucan) structures on most classes of human pathogens. CLRs are so-named because this binding occurs in a calcium dependent manner. Following recognition and binding by CLRs, pathogens are internalised, degraded and processed for antigen presentation.²⁰⁸ CLRs are critically important to DC function, are typically membrane bound but may be secreted in soluble form,²⁰⁹ and consist of several families including the CLR domain family members (CLECs), collectins and selectins. CLECs bind foreign antigen and include CLEC-1 (CLEC1A), DC-SIGN (CLEC4L; CD209), langerin (CLEC4K), DCIR (CLEC4A), BDCA2 (CLEC4C; CD303), dectins 1 and 2 (CLEC7A/6A), mannose receptor types 1 and 2 (CD206, CLEC13D/E) and DEC205 (CD205, CLEC13B).^{82,199}

Membrane-bound CLRs are classified into two groups on the basis of their molecular structure.²⁰¹ Type I CLRs, including the mannose receptor types 1 and 2, and DEC-205, have their N-terminal ends pointing outwards from the cell membrane, and contain multiple CRDs. Type II CLRs in contrast, are characterised by having their N-terminal end inside the cytoplasm, and contain only one CRD. DC-SIGN, langerin, DCIR, dectin-1 and 2, BDCA2 and CLEC-1 are all examples of Type II CLRs. The cytoplasmic domain of CLRs is responsible for mediating endocytosis, and guides the antigen-receptor complex to distinct endosomal compartments.^{199,201} Several CLRs that have been demonstrated to have important functions and are well characterised in DC biology will be discussed further below.

The mannose receptor (CD206) is an archetypal type I CLR, contains multiple domains, and is expressed on various DC subsets, but also on macrophages, astrocytes, and epithelial and liver endothelial cells. It acts as an antigen uptake and processing receptor,²¹⁰ and functions as a PRR, recognising ligands bearing mannose residues such as pituitary hormones cleared in the liver, lysosomal enzymes, and tissue plasminogen activator, which are often released in areas of inflammation or tissue damage.^{82,211}

DEC-205 (CD205) is another type I CLR that has a similar function in terms of antigen internalisation, although its specific natural ligand *in vivo* remains undetermined. A recent study has identified however that synthetic CpG oligonucleotides, which have therapeutic potential as a vaccine adjuvant, directly bind DEC-205.²¹² The cytoplasmic

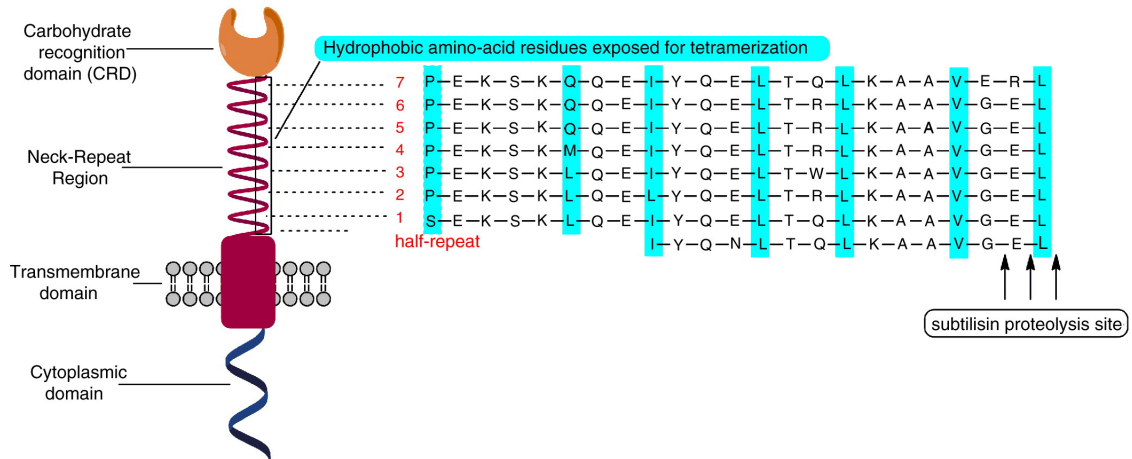
domain of DEC-205 contains protein motifs that enable direct intracellular delivery of antigen to MHC class II for presentation to T-cells, and repetitive recycling of DEC-205 to the DC surface enhances the presentation efficiency significantly in comparison to the mannose receptor.²¹³ It is expressed at different levels on DC, B cells, T cells, and thymic epithelial cells.²¹⁴ The domain structure of DEC-205 suggests the potential for recognition of multiple ligands, and it is hypothesised that DEC-205 may function as a “promiscuous” antigen receptor.^{215,216}

Langerin (CD207) is a type II CLR that is solely expressed on epidermal Langerhans cells, and some other dermal DC. It is involved in the formation of Birbeck granules (see section 1.3.2.2).¹⁸³⁻¹⁸⁵ It consists of a single C-terminal CRD, with a coiled neck domain that facilitates its oligomerization into trimers (which facilitates binding affinity), and it binds high mannose structures, fucose, GlcNAc, galactose-6-sulphated oligosaccharides and Lewis Y containing carbohydrate residues. In particular it has been shown to bind yeast mannan, β -glucans on the surface of pathogenic fungi, and high mannose residues on HIV gp120.⁸²

Of particular relevance in the context of this thesis is the type II CLR, DC-SIGN, (also known as CD209). DC-SIGN is the most important CLR expressed by CD14⁺ blood and tissue resident DC, is highly expressed on immature MoDC propagated *in vitro*, and binds to gp120 on HIV-1 and HIV-2, as well as rhesus simian immunodeficiency virus (SIV), which facilitates its transport to secondary lymphoid organs rich in CD4⁺ T cells, and leads to infection *in trans* of these target cells.^{217,218} It is structurally similar to other Type II CLRs with a single CRD at the C-terminus, a coiled neck domain that is involved in receptor oligomerization, a transmembrane domain, and a short cytoplasmic tail mediating ligand internalisation following binding (see Figure 1.3.5). DC-SIGN forms a tetramer at the cell surface, a structure that is required for HIV binding,²¹⁹ and this occurs through the structural arrangements of repeated hydrophobic amino acid residues within the neck region. DC-SIGN binds to ICAM-3 expressed by naïve CD4⁺ T-cells, and also to ICAM-2²¹⁸; binding to a wide variety of microbes and viruses has also been demonstrated.⁸² DC-SIGN plays a critical role in DC functioning, including the regulation of adhesion and trafficking, and in establishing the initial contact for the formation of DC-T-cell synapses.

Other CLRs that have particular expression profiles and importance in DC function include BDCA2 (CLEC4C) exclusively expressed on pDC and involved in TLR9 function and the production of type 1 IFN, TNF, IL-6 and IL-10; dectin 1 (CLEC7A), expressed on myeloid DC, monocytes, macrophages and B-cells and involved in the differentiation of Th1 and Th17 cells; DNGR1 (CLEC9A), expressed on CD141⁺ DC and involved in induction of TNF production and antigen cross-presentation; and BDCA4 (CD304 or neuropilin), expressed (non-exclusively) on pDC.¹⁹⁹

a) DC-SIGN schematic structure



b) DC-SIGN tetramer

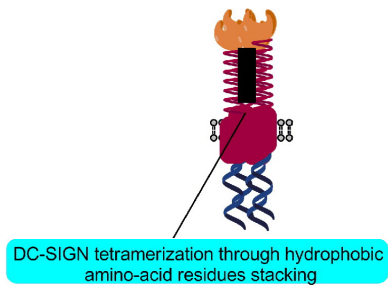


Figure 1.3.5. Structure of human DC-SIGN

(A) Schematic structure of DC-SIGN and amino-acid sequence alignment of the neck-repeat domain. The repeated hydrophobic amino-acid residues (hydrophobic heptad), crucial for tetramerization, are highlighted. Arrows point to a subtilisin site of digestion.

(B) DC-SIGN tetramerization through hydrophobic residues stacking in the neck-repeat domain.

Reprinted from Švajger U et al. *Cellular Signalling* 2010; 22 (10): 1397-1405. ²²⁰

© 2010 Elsevier; used with permission.

1.4. Dendritic cells and tolerance

DC play a critical role in the maintenance of both central and peripheral tolerance to self-antigens in the steady state.

1.4.1. Central tolerance

Central tolerance occurs prior to the entry of lymphocytes into the circulation and involves the removal of auto-reactive T-cell clones in the thymus by local or circulating DC via a process of clonal deletion and the induction of T regulatory cells (Treg).²²¹⁻²²⁴ Both (myeloid) cDC and pDC are involved in this process.^{225,226} However not all possible self antigens will have been encountered by lymphocytes prior to their exit from the thymus and mechanisms to ensure self tolerance is maintained in the periphery are vital to avoid damaging auto-immunity and maintain homeostasis.

1.4.2. Peripheral tolerance

The critical role that DC play in regulating peripheral tolerance has been demonstrated through studies showing that when all subsets of DC are absent fatal auto-immunity ensues.²²⁷ Peripheral tolerance is said to occur when auto-reactive lymphocytes encounter DC with self-antigen in the MHC in the absence of additional co-stimulatory signals that usually occur in response to tissue damage or inflammation. This interaction between so-called *immature* DC and T-cells in the absence of “danger signals” can lead to T-cell anergy (hypo-responsiveness), apoptosis, immune deviation towards anti-inflammatory Th2 responses (e.g. production of the anti-inflammatory cytokine IL-10), and the generation of Treg (including naturally occurring Treg; CD4⁺CD25⁺ T cells that constitutively express forkhead box P3 (Foxp3)), which suppress the self-reactive immune response.^{72,228-230} A number of inhibitory pathways may also be involved, including programmed death ligands (PDL)-1 and 2,^{231,232} indoleamine dioxygenase (IDO),²³³ the non-classical MHC class I molecule HLA-G,²³⁴ haem oxygenase 1 (HO-1),²³⁵ Fas (CD95) / Fas Ligand (FasL),²³⁶ and Galectin-1.²³⁷

The uptake of antigen in the steady state by immature DC with low levels of surface MHC and co-stimulatory molecules leads to anergy or apoptosis of the antigen specific T-cells,²³⁸ or to the generation of T cells with a regulatory or suppressor function.²³⁹ Alternatively, if antigens are delivered to DC under the influence of activating danger

signals then high levels of MHC and co-stimulation, as well as secretion of pro-inflammatory cytokines (e.g. IL-12p70) – so called DC maturation – lead to potent T-cell activation.²⁴⁰ This paradigm of the outcome of DC interaction with naïve T-cells is shown schematically in Figure 1.4.1. Apoptosis (programmed cell death), which occurs in response to cell damage or as part of normal cell turnover in peripheral tissues is an important source of self antigen for DC which are presented to T cells, and immature DC are able to phagocytose apoptotic cells efficiently.²⁴¹⁻²⁴³ Circulating apoptotic cells that enter lymph nodes or spleen can be captured *in situ* by the resident DC.^{244,245} Other sources of self antigen include soluble molecules captured by endocytosis and internalised plasma membrane-shed micro-vesicles,²⁴⁶ exosomes,²⁴⁷ or intracellular structures released by cells present in the DC microenvironment.²⁴⁸

After encountering self-antigen, immature DC traffic to secondary lymphoid tissue. Notably however, animal models of migratory DC have shown them to have the phenotype of *mature* DC,²⁴⁹⁻²⁵¹ with up-regulation of MHC, co-stimulatory and adhesion molecules. It is proposed that a certain degree of DC maturation is probably required to enable homeostatic migration, and indeed it is notable that these DC exhibit low levels of pro-inflammatory cytokines such as IL-12p70, and evidence of IL-10 production. The term '*semi-mature*' has been applied to these cells,²⁵² and the DC maturation status paradigm in relation to tolerance and immunity may be more complex than has been previously proposed.²⁵³ Once in the secondary lymphoid tissue, migratory DC present this self-antigen to auto-reactive CD4 and CD8 T-cells without breaching self tolerance.²⁵⁴ They may also transfer the antigen to lymphoid tissue resident DC that are inherently tolerogenic.^{242,244,255}

In mice, immature DC administered in transplant studies as tolerogenic therapy (see below) have been shown to induce anergy and apoptosis of allo-reactive T-cells.^{256,257} Human CD4 positive T-cells with regulatory characteristics (low proliferation, IL-10 secretion, and inhibition of allo-antigen specific T-cell proliferation) can be generated *in vitro* following stimulation of naive CD4 T-cells with allogeneic immature DC.²³⁹ In a seminal paper involving human volunteers, subcutaneous administration of immature autologous MoDC pulsed with HLA A*0201-restricted influenza matrix peptide (MP) led to specific inhibition of MP-specific CD8 cytotoxic T-cell responses and induced IL-10-secreting T-cells.²⁵⁸ All of these mechanisms may contribute to peripheral

tolerance; it is unclear though to what extent these models replicate the normal state of tolerance *in vivo*.

In addition to inducing T cell anergy and deletion as described previously, DC have been shown to regulate Treg expansion, differentiation and suppressive capacity *in vitro*.²⁵⁹ This has been confirmed *in vivo*, where depletion of DC leads to a loss of Treg and increases in T-cells producing the inflammatory cytokines IFN γ and IL-17²⁶⁰; these investigators proposed that DC and Treg form a feedback loop whereby reduced Treg numbers leads to an increase in DC, mediated via Flt3. Additionally, DC secreting high levels of IL-10 without IL-12, a tolerogenic phenotype of DC, induce IL-10 producing regulatory type-1 (Tr1) T-cells *in vitro*.²⁶¹ pDC, after maturation, increase the expression of inducible costimulator (ICOS) ligand (ICOS-L), which is involved in the de novo differentiation of IL-10 producing Treg²⁶²; moreover activated human pDC can also induce the generation of CD4⁺CD25⁺ Treg.²⁶³ These findings are in contrast to the more immunogenic effects of activation and maturation on cDC, and are an example of the plasticity and complexity of the DC system, and the different functional roles of the different DC subsets.

Overall, the mechanisms of DC-based tolerance that operate *in vivo* remain incompletely understood. Ongoing work being performed by many groups is slowly revealing the complexity of DC interactions with other cells and microenvironments, via multiple receptors and signalling networks, in the induction and maintenance of tolerance.^{229,254,264,265}

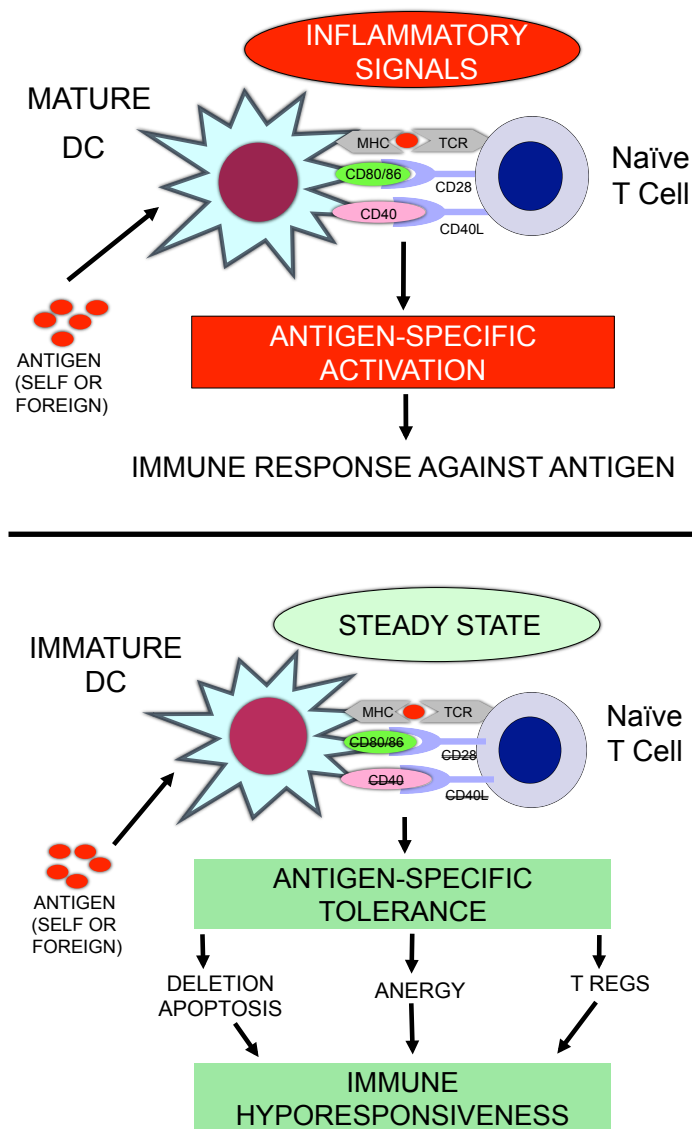


Figure 1.4.1. The interaction of DC with naïve T-cells can lead to either immune activation or tolerance.

Upper panel: In the presence of an inflammatory stimuli and danger signals, DC upregulate expression of MHC class II and associated co-stimulatory molecules such as CD80/86, CD40, and interact with T-cells via the T-cell receptor complex (CD3), and co-stimulatory ligands such as CD28 and CD40L, forming an immunological synapse. This leads to robust T-cell activation and differentiation of effector T-cells. *Lower panel:* In the absence of inflammatory stimuli, or in the steady state, DC display an immature phenotype characterised by low expression of MHC class II and co-stimulatory molecules. This leads to suboptimal T-cell priming and promotes antigen specific immune hyporesponsiveness (tolerance) via deletion/apoptosis, T-cell anergy or the induction of T-regulatory cells (T regs).

This schema represents a simplification; see the text for further discussion.

1.5. Dendritic cells in transplantation

1.5.1. DC and allo-recognition

In the setting of organ or tissue transplantation, there are multi-faceted and multi-directional interactions between the recipient immune system and the donor tissue or organ. *Allo-recognition* is the process by which the recipient immune system recognises the donor organ or tissue as foreign and initiates the immune response.

This process of initiating the immune response to an allograft occurs through several distinct but co-existent pathways of allo-recognition.^{254,266} In the *direct* pathway, DC from the allograft (so-called “passenger leukocytes”) of donor origin migrate out of the graft to recipient lymphoid tissue and present intact donor MHC molecules to allo-specific T-cells.^{131,267} The *indirect* pathway involves recipient DC that migrate into the graft in response to inflammatory stimuli, encounter and process donor tissue allo-antigens and present these donor-derived peptides on self (recipient) MHC to donor-reactive T-cells.²⁶⁸ A third, more recently described pathway is the *semi-direct* pathway, whereby recipient T-cells recognise donor MHC molecules transferred intact from donor cells to the surface of recipient DC.²⁶⁹ DC can acquire MHC molecules or other allo-peptides from other cells via a process of transfer of vesicles,²⁴⁷ or plasma membrane fragments.²⁷⁰

Following transplantation of an allograft, DC present allo-antigen derived from the donor in the context of MHC to recipient T-helper (CD4) cells. This constitutes “signal 1” of T-cell activation, and this is transduced through the T-cell receptor CD3 complex. “Signal 2” involves the DC giving the T-cell co-stimulation through the engagement of co-stimulatory molecules with their ligands on T-cells, particularly the interaction of CD80 and CD86 with CD28.^{44,271,272} The combination of these two signals initiates three intracellular pathways in T-cells: the calcium–calcineurin pathway, the RAS–mitogen-activated protein (MAP) kinase pathway, and the NF-κB pathway. These pathways activate transcription factors that trigger the expression of many new molecules, including interleukin-2 (IL-2), CD154 (also known as CD40 ligand, which interacts with CD40 on DC), and CD25, the IL-2 receptor. IL-2, acting via its receptor (through an autocrine mechanism) and other cytokines then initiate the “target of

rapamycin" (TOR) pathway to provide "signal 3," which leads to proliferation of a large number of effector T-cells.⁴⁴ Further downstream events include B cell activation and alloantibody production. Current immunosuppressive drugs target multiple parts of this pathway, but all have the drawback of being non-specific in their suppression.

The direct pathway has been classically thought of as the most important instigator of the immune response against the allograft, i.e. acute rejection. Migration of donor-derived DC out of the allograft to recipient lymphoid tissue allows presentation of highly immunogenic, donor-derived MHC antigens to naïve recipient T-cells. Kidney allografts that are purged of leukocytes have increased graft survival in the absence of immunosuppression.²⁷³ Interestingly, direct allo-recognition may have a role in the development of donor-specific tolerance as it is known that DC of donor origin may persist long-term in recipient tissue, a phenomenon known as micro-chimerism.²⁷⁴⁻²⁷⁶ However, the influence of the direct pathway decreases with time after transplantation. The indirect pathway, which involves the presentation of donor antigen within recipient MHC, is much less immunogenic than the direct pathway (fewer T-cells respond to *recipient* MHC than respond to *donor* MHC),²⁷⁷ but rejection can occur in the absence of direct allo-recognition,²⁷⁸ and a more recent study points to it having a much more significant role than previously thought.²⁷⁹ In addition, indirect allo-recognition predominates later after transplantation and is thought to be the main mechanism underlying chronic rejection,^{229,254} but along with the semi-direct pathway may also promote tolerance through the induction of regulatory T-cells.²⁸⁰

In the steady state, DC are present as immature APC in many tissues, including commonly transplanted organs (with the exception of immune-privileged sites such as the central area of the cornea). DC in this state internalise antigen efficiently and have low levels of T-cell stimulatory activity.^{72,73} In the presence of "danger signals" such as infection or, in the case of transplantation, inflammation triggered by surgery and ischaemia-reperfusion injury, DC resident in or infiltrating the graft mature in response to endogenous or exogenous mediators present within their local environment.^{240,254,281} Nuclear translocation of the transcription factor NF- κ B is important for this activation process in DC and is enhanced through interaction between molecules of the TNF receptor family on the DC surface with their ligands during T-cell–DC interaction and also ligation of TLR 2, 4 and 9 on the DC surface.^{118,119} Maturation of DC leads to reduced endocytosis of extracellular antigens, and translocation of long-lasting peptide-

loaded MHC to the cell surface. At the same time, DC upregulate surface co-stimulatory molecules including CD80, CD86, CD40, OX40 ligand, ICOS-L, and intercellular adhesion molecules (CD54 and CD58) required for interaction with T-cells and the establishment of the immunological synapse.²⁸² The expression of chemokine receptor (CCR)7 is increased, promoting DC migration to secondary lymphoid tissues in response to the CCR7 ligands, chemokine ligand (CCL)21 and CCL19.⁷³ As a result, mature DCs can powerfully stimulate naive and memory T-cells located in the T-cell areas of secondary lymphoid tissues.

A summary of the roles of DC in peripheral tolerance at steady state, and in the initiation of responses to allografts, is shown in Figure 1.5.1.

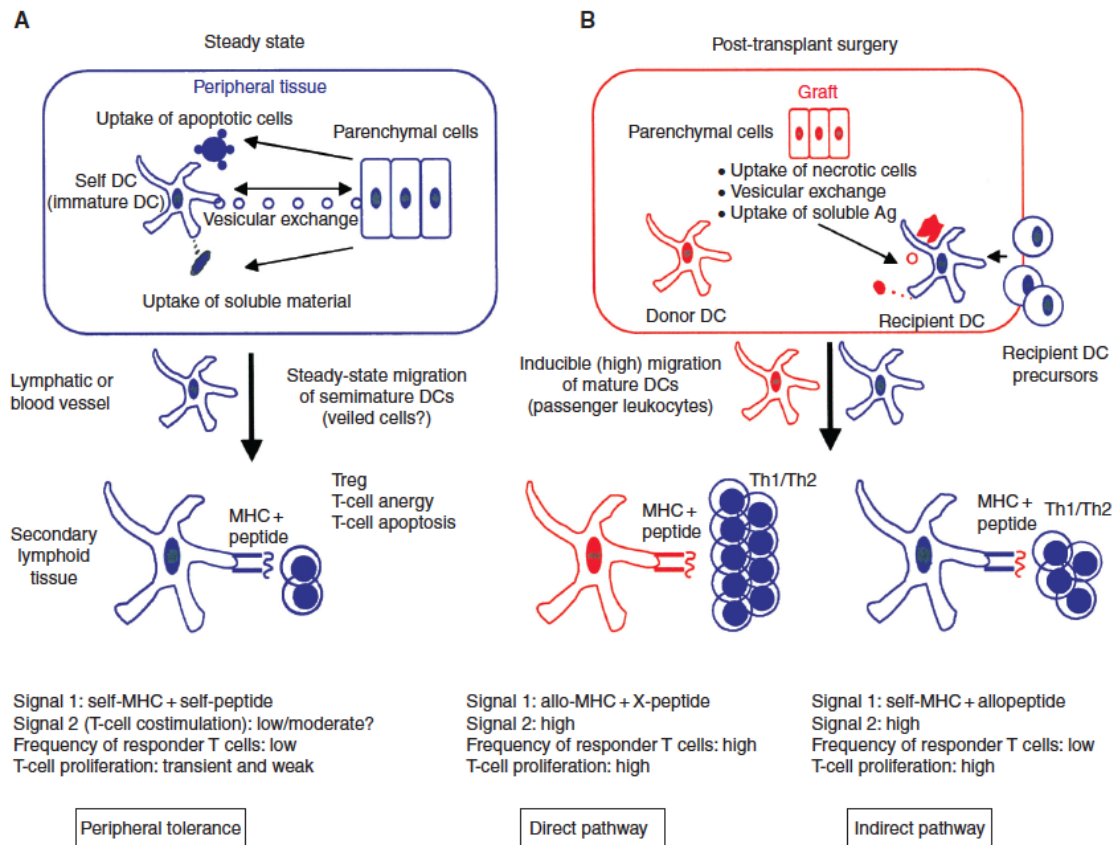


Figure 1.5.1. The role of dendritic cells (DC) in peripheral tolerance and graft rejection.

(A) During steady-state conditions (absence of proinflammatory or danger signals), peripheral tissue-resident DC capture self-antigens from neighboring parenchymal cells via uptake of apoptotic cells, vesicular exchange with living cells, or endocytosis of soluble molecules. DC mobilise [likely as semi-mature antigen-presenting cells (APC)] via lymphatic or blood vessels from the periphery to T-cell areas of secondary lymphoid organs. Once there, DC present self-antigens to autoreactive T cells that escaped thymic selection. Under physiological conditions, DC in T-cell areas of spleen or lymph nodes express low levels of T-cell co-stimulatory molecules and induce a transient and weak proliferation of autoreactive T cells followed by T-cell deletion, anergy, and, probably, generation of Treg cells.

(B) Following transplantation surgery, pro-inflammatory mediators released locally, ischaemia-reperfusion injury, and the presence of necrotic cells trigger full maturation of donor DC (donor tissues and cells are in red) and recipient DC (recipient cells are in blue) that infiltrate the graft as part of the inflammatory reaction. Both donor- and recipient-derived DC migrate out of the graft as passenger leukocytes. Once in the T-cell area of the secondary lymphoid organs, mature donor DC present allo-major histocompatibility complex (MHC) molecules to allo-reactive T cells (direct pathway) and mature recipient DCs present allo-peptides loaded into self-MHC molecules to recipient T cells recognising allo-peptides in the context of self-MHC molecules (indirect pathway).

Modified from a figure originally published in Morelli AE and Thomson AW. *Immunol Rev* 2003; 196: 125-146.

© 2003, John Wiley and Sons – used with permission.

1.5.2. Using DC to promote tolerance: Tolerogenic DC

Given the central role that DC play in initiating immunity and maintaining tolerance, they hold considerable attraction as a potential therapy for manipulating the immune response.

A large amount of work has been done to attempt to utilise DC to *enhance* the immune response: vaccines using autologous DC, cell-line derived DC or targeting DC with antigen *in vivo* have progressed into human clinical trials in HIV infection,^{283,284} and several types of cancer, including advanced melanoma,²⁸⁵⁻²⁸⁷ renal cell carcinoma,²⁸⁸ haematological malignancy,²⁸⁹ and advanced prostate cancer.²⁹⁰⁻²⁹² These studies have established the feasibility and safety of DC therapy in the clinical setting, even if they have not yet shown sufficient demonstrable efficacy to enable the widespread application of this therapy.

Numerous studies have established that *tolerogenic* DC can be generated *in vitro* and used to induce antigen-specific T-cell apoptosis or anergy,^{257,293-298} and promote the expansion of antigen-specific regulatory T-cell populations,^{263,299-302} which can suppress the immune response. Morelli and Thomson²²⁹ have proposed the desirable characteristics of tolerogenic DC generated *in vitro* for potential therapeutic use (modified here from a summary by Prasad)³⁰³:

1. Capable of antigen presenting function, with low levels of MHC surface expression, leading to weaker SIGNAL 1;
2. Maturation-resistant, immature, or alternatively-activated DC with low co-stimulatory molecule expression compared with inhibitory signal expression, leading to failure of SIGNAL 2;
3. Skewed away from Th1 promoting cytokines (especially IL12p70) towards IL-10 and indoleamine 2,3-dioxygenase (IDO) production;
4. Promote the generation and expansion of antigen-specific regulatory T-cells, and the apoptosis of antigen-specific effector T-cells; and
5. Capable of migration from the site of introduction to secondary lymphoid tissue, and remain resistant to maturation *in vivo*, as well as resistant to NK or T-cell induced death during this process.

The prevailing dogma in the literature has been that mature DC elicit an immunogenic response, and immature DC are tolerogenic.³⁰⁴ However, antigen presentation to T cells, and migratory properties *in vivo*, are both properties of mature DC that have been identified as important to tolerogenic DC (as discussed above). More recently, the phenotype of a tolerogenic DC has been proposed to include not only immature, but also maturation resistant, and alternatively-activated cells.²⁶⁴ It has also been recognised that immature DC generated *in vitro* may not necessarily be stable following injection *in vivo*, and could become immunogenic through maturation in response to pro-inflammatory cytokines and/or pathogen-derived molecules.

A variety of DC types have been explored for potential use in tolerogenic therapy, and tolerogenicity does not appear restricted to specific DC subsets, phenotypes or sources of origin. Unmodified tolerogenic DC have been used in a number of studies and have been found to lead to antigen-specific immunosuppression, with reduced mixed leukocyte reaction (MLR) responses *in vitro*, and the induction of Treg with Th2 (IL-10) cytokine responses.^{239,257} The seminal paper by Dhodapkar et al published in 2001 referred to above demonstrated *short term* antigen-specific inhibition of effector T-cell responses after subcutaneous administration of immature autologous DC pulsed with antigen to human volunteers,²⁵⁸ and studies in mice show unmodified immature myeloid DC can modestly prolong allograft survival.²⁹⁴ However, these DC did not induce the stable long-term inhibition of immune responses that would be needed in human transplantation.

A number of approaches have been used to try and enhance the tolerogenic capacity of DC for potential use in transplantation.^{229,254,305} Modification of *in vitro* culture conditions, genetic modification, and the use of immunosuppressive or anti-inflammatory drugs have all been exploited as techniques to promote DC tolerogenicity.

The function of DC generated *in vitro* can be influenced by manipulation of the cytokines in the culture environment. Generation of DC with low-dose GM-CSF (with or without IL-4) results in immature or maturation-resistant DC with T-cell inhibitory properties which are able to prolong allograft survival.^{297,306} DC treated with the regulatory cytokines IL-10³⁰⁷ or TGF- β ³⁰⁸ alone, or in combination³⁰⁹ remain immature, have reduced co-stimulatory molecules and reduced ability to stimulate T-cells, and can prolong allograft survival when given along with co-stimulatory blockade.^{308,309} In a

more recent study, DC expanded *ex vivo* with Flt3L were immature, expressed TGF- β , IL-10 and TNF- α , and homed to thymus, spleen and liver. These Flt3L DC showed evidence of inducing central tolerance via clonal deletion, and peripheral tolerance with donors-specific unresponsiveness, and led to long-term survival of donor skin grafts.³¹⁰

Genetic modification strategies can also enhance DC tolerogenicity.^{229,254} Interference with NF- κ B-dependent transcription of co-stimulatory molecule genes in bone-marrow derived DC by double-stranded oligodeoxyribonucleotides containing binding sites for NF- κ B, results in resistance to maturation by LPS, the induction of allogeneic T-cell hypo-responsiveness and prolongation of cardiac allograft survival.³¹¹ The addition of adenoviral transduction of the inhibitory co-stimulatory molecule CTLA4-Ig to this treatment resulted in superior induction of allogeneic T-cell hypo-responsiveness, the induction of activated T-cell apoptosis, indefinite cardiac allograft survival (in 40% of animals), and donor-specific tolerance.³¹² Other examples include the promotion of the deletion of antigen-specific T-cells through FasL (CD95L),³¹³ and the arrest of DC maturation with reduced expression of MHC class II, CD80 and CD86 following the silencing of RelB, which is the primary protein involved in NF- κ B associated DC maturation.³¹⁴ As yet genetically modified DC alone have not been successful in achieving transplant tolerance across MHC barriers.^{229,254,305}

A range of drugs and immunomodulatory agents have been used to promote DC tolerogenicity, based on influencing their generation, migration, maturation and immune function (reviewed by Morelli and Thomson, Hackstein and Thomson, and Leishman et al),^{229,254,315,316} including corticosteroids,³¹⁷ the calcineurin inhibitor cyclosporin,³¹⁸ rapamycin,³¹⁹ aspirin,³²⁰ mycophenolate mofetil,³²¹ activated Vitamin D ($1\alpha,25(\text{OH})_2\text{D}_3$),³²² and curcumin.³²³ All of these agents prevent DC maturation and/or activation or impair the ability of DC to produce IL-12p70. Some also prevent the nuclear translocation of NF- κ B family members, including RelB – which are required for DC differentiation.

Curcumin, an extract of *Curcuma longa* (turmeric), has a broad spectrum of anti-oxidant, anti-inflammatory, anti-microbial and anti-proliferative properties, via inhibition of the nuclear factor- κ B pathway,³²⁴ and has been shown recently to arrest maturation of DC and induce a tolerogenic phenotype that subsequently promotes

functional FoxP3⁺ T(regs) *in vitro* and *in vivo*.³²³ At present however, curcumin is not in clinical use as pharmacologic agent in transplantation.

Another agent of clinical relevance and particular interest is the immunosuppressive drug rapamycin. Rapamycin binds with an intracellular receptor, which is FK506-binding protein 12. This inhibits mammalian target of rapamycin (mTOR) protein signalling (“signal 3”), and impairs the maturation and T-cell allo-stimulatory function of DC.³¹⁹ DC that are conditioned in rapamycin poorly produce IL12-p70 and TNF α , are resistant to maturation by TLR ligands or CD40L. In a mouse model, they are able to render allogeneic T-cells unresponsive to further stimulation with donor antigen, can enrich for Foxp3⁺CD4⁺CD25⁺ regulatory T-cells and do not expand CD4⁺ effector cells.²⁹⁹ When rapamycin-conditioned DC of recipient origin are pulsed with donor antigen and administered pre-transplant in a cardiac allograft transplant model, along with a short course of rapamycin, heart-graft survival is indefinitely prolonged. This is associated with graft infiltration by Treg without evidence of graft vessel disease.²⁹⁹ In GVHD, rapamycin-conditioned DC promoted tolerance but still retained their migratory ability and chemokine expression.³²⁵ It is notable that unlike calcineurin inhibitors, rapamycin does not interfere with signal 1 (or 2) of T-cell interaction with DC, which are necessary for the induction of tolerance.³²⁶ In light of these findings and the unique immunomodulatory effects of mTOR inhibition,^{327,328} as well as their current established place in transplant immunosuppression, there is considerable potential in utilising these agents as adjuncts in translational studies of tolerogenic DC therapy in transplantation.

1 α ,25(OH)₂D₃, the active form of vitamin D₃, has been shown to inhibit the differentiation and maturation of DC *in vitro*.^{322,329} Vitamin D₃ treated DC have been shown in a number of studies to be resistant to maturation *in vitro*, and to prolong graft survival in mouse skin and cardiac transplant models.^{330,331} In addition, vitamin D₃ can be used along with corticosteroids and LPS to generate ‘alternatively-activated’ human MoDC that prime allogeneic naïve CD4 T-cells to retain a strong proliferative capacity with low IFN- γ and high IL-10 production; in contrast memory T-cells primed by these DC become hypo-responsive in terms of proliferation and cytokine production, and anergy is induced.³³² The findings of this last study are an important observation because effector memory T-cells have been considered resistant to co-stimulation blockade, high numbers of antigen-experienced memory T-cells are associated with an

increased risk of rejection, and are considered a major hurdle to the induction of tolerance in humans.²⁶⁴ Addressing these obstacles is an important component of developing tolerogenic DC therapy.

1.5.3. Tolerogenic DC therapy in transplantation

A large number of small animal studies of transplantation investigating the effects of recipient pre-conditioning with tolerogenic DC have been undertaken (see Table 1.5.1 and Table 1.5.2). These have used DC of various origins and phenotypes, with or without various adjuvant therapies. Both the targeting of the direct pathway using donor derived DC,^{293,294,297,306,308-310,312,331,333-341} and the indirect pathway using recipient DC,^{299,302,342-349} usually but not always with the addition of donor antigen, have been explored in these models. Taken together, these studies provide persuasive evidence that both donor and recipient derived DC infusion can suppress the allo-immune response.

To date, there has been very limited translation of these promising findings into pre-clinical (NHP) or clinical trials of tolerogenic DC therapy. The first study to report the administration of tolerogenic DC in a human clinical trial was the study discussed previously (see section 1.4.2) by Dhodapkar et al, although these findings were serendipitous as the study was designed to test DC therapy as a tool to enhance the immune response to a vaccine and not to promote tolerance.²⁵⁸ In rhesus monkeys, a study examined the infusion of DC rendered stably immature through culture with vitamin D3 and IL-10, with and without the administration of co-stimulation blockade using CTLA4-Ig.³⁵⁰ This study showed initial sensitisation followed by non-specific suppression (i.e. to both donor and third-party) of the allogeneic T-cell response in those animals that received DC infusion in addition to CTLA4-Ig.

In a very recent study, published following the studies outlined in this thesis, Ezzelerab et al have shown that these vitamin D3/IL-10 ‘regulatory’ donor DC can prolong median kidney allograft survival from 39.5 days to 113.5 days when administered along with short term CTLA4-Ig and rapamycin.³⁵¹ This paper represents a major advance for the field of DC therapy testing in NHP, however sustained improvements in allograft outcome remain to be established, and no trials of tolerogenic DC therapy have been performed in the setting of human transplantation.

Table 1.5.1. Efficacy of donor DC pre-treatment on allograft survival in small animal studies.

All DC were administered systemically. See Table 1.5.2 for definitions of abbreviations. Adapted from Morelli and Thomson,²²⁹ and Prasad,³⁰³ with additions and modifications.

Reference	Model	Donor DC type	DC Treatment	Recipient Treatment	MST (days)
Rastellini 1995 ³³³	Mouse islet	Liver DC	GM-CSF	STZ	30.3 (20 % > 60)
Fu 1996 ²⁹⁴	Mouse HHT	BM DC precursors ²⁵⁷	GM-CSF	-	22 ^a
Lu 1997 ³⁰⁸	Mouse HHT	BM iDC	GM-CSF TGF- β	Anti-CD40L	77 (40 % > 100)
Gao 1999 ³³⁴	Mouse HHT	Spleen DC	Long-term Allo-MLC	Anti-CD4	35 25 % > 120
Lutz 2000 ²⁹⁷	Mouse HHT	BM iDC	GM-CSF Low dose	-	> 100 ^b
Niimi 2001 ³³⁵	Mouse HHT	Spleen mDC	-	Anti-CD40L	> 100
O'Connell 2002 ³³⁶	Mouse HHT	Splenic CD8 α^+ mDC	GM-CSF overnight	-	35
Bonham 2002 ³¹²	Mouse HHT	BM iDC	NF- κ B ODN and Ad transfection CTLA4-Ig	-	>100 (40 %)
DePaz 2003 ³⁰⁶	Rat HHT	BM iDC	GM-CSF IL-4	ALS	>200 (50 %)
Sun 2003 ³³⁷	Mouse HHT	BM iDC	Ad transfection CTLA4-Ig	Anti-CD40L	>100 (50 %)
Coates 2004 ³⁵²	Mouse HHT	FLT3-L mobilised renal DC	Freshly sorted CD11c ⁺ DC	-	19 ^c
Abe 2005 ²⁹³	Mouse HHT	BM pre-pDC	FLT3-L	-	22 ^d
Bjorck 2005 ³³⁹	Mouse HHT	<i>In-vivo</i> FLT3-L mobilised Splenic PDC	Freshly sorted CD11c ⁺ PDC	Anti-CD40L	68 (50 % > 100)
Garrod 2006 ³⁴⁰	Mouse HHT	BM DC	Ad transfection IL-10 and CCR7	-	>100
Lan 2006 ³⁰⁹	Mouse HHT	BM "AA" DC	GM-CSF, IL-10, TGF- β , LPS	CTLA4-Ig CyA (d 0-9)	> 100
Wang 2006 ³⁵³	Mouse HHT	BM iDC	Ad transfection sTNFR1	-	>100 (50%)
Divito 2010 ³³¹	Mouse HHT	BM MR-DC	GM-CSF, IL-4, Vit D3	-	52
Yamano 2011 ³¹⁰	Mouse Skin	BM DC	Expanded <i>ex vivo</i> with Flt3L	-	51

^a The first study to test immature, co-stimulatory molecule deficient, myeloid *in-vitro* propagated donor DC on allograft survival. Donor BM DC alone, infused one week before transplant, produced only modest prolongation of MST compared with controls and 3rd party BM DC.

^b Only DC infused 7 days pre-transplant had this effect; DC infused at earlier and later time points were ineffective.

^c Renal DC from donor animals also prolonged allograft survival of third party grafts (MST 16 days).

^d MST was also prolonged by donor BM myeloid DC and third party BM pre-PDC.

Table 1.5.2. Efficacy of recipient DC pre-treatment on allograft survival in small animal studies.

DC were administered IV unless otherwise indicated. Adapted from Morelli and Thomson,²²⁹ and Prasad,³⁰³ with additions and modifications.

Reference	Model	Recipient DC type	DC Treatment	Recipient Treatment	MST (days)
Garrovillo 1999 ³⁴²	Rat HHT	BM iDC (intrathymic)	GM-CSF, IL-4 Donor MHC Class I peptide	ALS	>150 ^a
Garrovillo 2001 ³⁴³	Rat HHT	Thymic DC (iv)	Donor MHC Class I peptide	ALS	> 200 ^a
Mirenda 2004 ³⁴⁴	Rat Kidney	BM iDC ^b	dexamethasone	CTLA4-Ig (x1) CyA (d 0-10)	> 100
Taner 2005 ³⁴⁵	Mouse HHT	BM iDC (x3)	GM-CSF, IL-4 Rapamycin, Donor Splenic Lysate	-	>59 (40% > 100) ^c
Pecche 2005 ³⁴⁶	Rat HHT	BM iDC (adherent,x1)	Low dose GM-CSF, IL-4	-	22.5 ^d (20 % > 100)
Beriou 2005 ³⁴⁷	Rat HHT	BM iDC (> x1)	GM-CSF, IL-4	LF15-0195	>100 (92 % > 100)
Turnquist 2007 ³⁵⁰	Mouse HHT	BM iDC (x1)	GM-CSF, IL-4 Rapamycin, Donor Splenic Lysate	Rapamycin (d 0-9)	> 100
Horibe 2008 ³⁴⁸	Rat Skin	BM iDC (x2)	GM-CSF, IL-4 Rapamycin, Donor Splenic Lysate	ALS CyA (d 0-20)	> 113 (50 % > 180)
Kuo 2009 ³⁵⁴	Rat Hindlimb	BM iDC (x 1)	GM-CSF, Donor Splenic Lysate	ALS CyA (d 0-20)	> 200
Hill 2011 ³⁴⁹	Rat HHT	BM iDC (x1)	GM-CSF, IL-4	LF15-0195	>100 (80% >100)

^a Long-term survivors were challenged with a second allograft which was accepted while third party grafts were rejected without rejection of the primary heart graft.

^b Tolerogenic recipient DC expressed both recipient and donor MHC molecules to induce T-cell regulation via the indirect pathway.

^c Three doses of DC pulsed with allo-antigen and rapamycin; a single dose of such DC prolonged the MST to only 23.8 days, DC + tacrolimus prolonged the MST to 46.8 days.

^d Syngeneic and donor allogeneic DC both prolonged allograft survival; only 2 /10 animals in the syngeneic DC group had ST > 100 days

Abbreviations: iDC – immature DC; mDC – mature DC; PDC – plasmacytoid DC; STZ – streptozotocin; HHT-heterotopic heart transplant; BM – bone marrow; MST – median allograft survival time; GM-CSF – granulocyte-macrophage colony stimulating factor; TGF-transforming growth factor; CD40L- CD40 ligand (CD154) monoclonal antibody; allo-MLC – allogeneic mixed lymphocyte culture; IL-4 – interleukin-4; ALS – anti-lymphocyte serum; Ad transfection – DC genetically modified by adenoviral transfection to over-express various genes; CTLA4-Ig - CTLA4-immunoglobulin; FLT3-L- fms-like tyrosine kinase 3 Ligand; IL-10 – interleukin 10; CCR7 – chemokine receptor 7; AA – alternatively activated; CyA – cyclosporine A; Allo-Ag – DC pulsed with allo-antigen; d 0-9 – drug give on days 0-9 post-transplant then ceased; sTNFRI – soluble TNF receptor type I; LF15-0195 – analogue of deoxyspergualin.

In a recent phase I randomised clinical trial, ten patients with Type 1 diabetes received a course of four intradermal injections of 1×10^6 autologous DC, propagated *in vitro* from monocytes isolated via leukapheresis.³⁵⁵ Three of the patients received control DC generated in GM-CSF and IL-4, and seven patients received ‘immunosuppressive’ DC generated in GM-CSF, IL-4, and anti-sense oligonucleotides targeting CD40, CD80 and CD86 transcripts. Previous work had shown that tolerogenic DC generated with these oligonucleotides were able to prevent and cure diabetes in a non-obese diabetic mouse model.³⁵⁶ Although the treatment was well-tolerated in all patients, no specific effects of immunosuppressive DC therapy were observed, although there was an increase in the numbers of B220⁺ CD11c⁻ B-cells noted, of uncertain significance.³⁵⁵ Further studies of autologous DC therapy are planned, in rheumatoid arthritis,³⁵⁷ and as part of a European collaboration investigating the potential of various cell therapy products in organ transplantation.³⁵⁸

Treg are also being explored as a potential adoptive cellular therapy to induce tolerance.³⁵⁹⁻³⁶¹ In studies of mice, humans and macaques, DC have been used to generate and expand Treg *ex vivo* that have excellent antigen specific suppressor function when compared with naturally occurring Treg.³⁶²⁻³⁶⁸ Interestingly in several of these studies, including a human trial in 3 patients with myeloma,³⁶² it was injection of autologous mature DC that led to enhanced Foxp3⁺ Treg population *in vivo*, rather than immature DC as has been seen in other studies.²³⁹

A number of important questions remain unanswered regarding the optimal approaches to tolerogenic DC therapy.²²⁹ The type and source of DC (e.g. pDC versus MoDC or stem-cell/haematopoietic progenitor derived ‘myeloid’ DC), whether they are donor or recipient in origin, the route of administration (almost all animal studies have used the intravenous route; however human trials have used the subcutaneous or intradermal routes) and optimal dose schedules all remain to be determined. In addition, prevention of maturation *in vivo* post-administration, and associated sensitisation of the recipient, as well as the avoidance of donor DC destruction by recipient NK cells,³⁶⁹ and appropriate homing to secondary lymphoid tissues is important to ensure DC therapy is safe and efficacious. These issues will need to be resolved in NHP models before the translation of DC therapy into human clinical trials.

1.5.4. Targeting DC in situ to promote transplant tolerance

As an alternative to donor- or recipient-derived cellular DC therapy, which in the setting of deceased donor transplantation may pose logistical difficulties with obtaining timely donor precursors for DC generation *in vitro*, several approaches to targeting DC *in situ* have been proposed and are being explored. This approach utilises the intrinsic ability of DC in steady state in lymphoid tissue to maintain self-tolerance, and avoids the risk of activating the DC *ex vivo*.²²⁹

Using exosomes secreted from donor DC which are rich in MHC, donor antigens can be delivered to recipient DC and presented to T-cells via the indirect pathway, and in the presence of maturation arrest (using NF- κ B inhibition with de-oxyspergualin), can prolong rat heart graft survival.³⁷⁰ In addition, apoptotic donor cells, when captured by recipient DC in the steady state, inhibit NF- κ B pathways,³⁷⁰ can promote T cell anergy and death,³⁶⁶ and when given with co-stimulation blockade, can prolong cardiac allograft survival in a murine transplant model.³⁶⁶ Both of these approaches still require the propagation of donor DC *in vitro*, and thus have some of the same logistical difficulties as the aforementioned cellular therapies.

As discussed in section 1.3.4, DC express a range of pattern recognition receptors on their surface that are pivotal to their functions of antigen uptake and presentation.⁸² These include various TLRs, and the CLR. Many of these molecules are restricted in their expression to DC, with unique profiles for different DC subsets, as outlined in Table 1.3.2. Targeting recipient DC *in vivo*, using monoclonal antibodies to these markers, thus offers the potential to deliver donor antigen directly to specific DC populations, and the function of these molecules as key immune receptors implies that such targeting could be done to alter the outcomes of host immune responses. Several groups of investigators have used this approach to try and enhance activating immune responses, e.g. for vaccination purposes or in the tumour setting (reviewed in Palucka and Banchereau),³⁷¹ an approach requiring the maturation of the DC *in vivo*. In mice the delivery of donor antigen to quiescent (non matured) DC, via a monoclonal antibody to DEC-205, led to the development of antigen-specific tolerance.²⁹⁵ In several other studies, delivery of antigen to DC via antibodies targeting DEC-205, a marker of CD8⁺ DC,^{216,372,373} or 33D1, a marker of CD8⁻ DC,³⁷³ resulted in initial proliferation of antigen specific T-cells but subsequent deletion in the absence of any DC maturation

stimulus, i.e. antigen specific tolerance. In a more recent study, targeting self or foreign antigens to DC via the DC-asialoglycoprotein receptor (DC-ASGPR, another CLR) with a recombinant monoclonal antibody-antigen construct led to the generation of suppressive IL-10 producing CD4⁺ T-cells after vaccination in a humanised mouse model and in rhesus macaques.³⁷⁴

The limitation of such donor antigen-based approaches in the transplantation setting is the relatively restricted repertoire of donor antigen able to be delivered to DC using these mechanisms.²²⁹ In an alternative strategy, Jung et al have recently demonstrated that using an anti-human ICAM-1 antibody to target ICAM-1 on DC results in maturation arrest of human (Mo) or (humanised) mouse splenic DC in a semi-mature state, and can lead to tolerance (with suppression of IFN- γ and IL-2 responses) of porcine islet *xenografts* in humanised mice and non-human primates, where the latter receive low dose rapamycin and anti-CD154 (CD40L) to avoid NK and NK-mediated B-cell activation.³⁷⁵

Another potential approach is the use of DC-targeted therapies containing immunosuppressive or immunomodulatory drugs that could globally alter DC function (as discussed in section 1.5.2), and thus offer the opportunity to effectively manipulate DC immune responses to promote tolerance *in vivo*, while seeking to minimise the systemic toxicities associated with non-targeted immunosuppression. Such an approach that holds promise as means to effectively target and alter the function of DC *in situ* is the use of nanocarriers made with biomaterials, such as liposomes or nanoparticles, loaded with drugs that could influence DC function (see section 1.7 below).³⁷⁶

Jesudason, S., Collins, M.G., Rogers, N.M., Kireta, S. & Coates, P.T. (2012) Non-human primate dendritic cells.

Journal of Leukocyte Biology, v. 91(2), pp. 217-228

NOTE:

This publication is included on pages 50-73 in the print copy of the thesis held in the University of Adelaide Library.

It is also available online to authorised users at:

<http://dx.doi.org/10.1189/jlb.0711355>

1.7. Liposomes and nanoparticles

Biomaterial delivery vehicles composed of biocompatible lipids or polymers offer the potential to target drugs to particular cell-types and enable substantially increased efficiency in this delivery to target tissues in comparison with systemically administered free drugs. Biomaterials include a variety of nanocarriers including liposomes, polymer microparticles, nanoparticles, vesicles, and micelles, and these are increasingly being explored as a means of targeting therapeutics to various cell types including DC.^{376,451-453}

1.7.1. Liposomes

Liposomes, initially discovered in 1965,⁴⁵⁴ are spherical vesicles that consist of one or more phospholipid bilayers and contain one or more aqueous phases enclosed and between the bilayers, and a hydrophobic portion within the bilayer (see Figure 1.7.1). Phospholipids used in liposomes typically contain a hydrophilic head group and two hydrophobic chains enabling them to encapsulate both hydrophobic and hydrophilic drugs, protein or peptide antigens, or DNA.⁴⁵⁵

Liposomes range in size from small unilamellar vesicles <100nm to large multilamellar vesicles >1µm in diameter (see Table 1.7.1), and are biocompatible, water soluble and non-toxic. The size, charge and surface properties of liposomes can be manipulated during preparation, and can significantly affect their behaviour *in vivo*.^{456,457}

Table 1.7.1. Liposome vesicle types, size and lipid layers.

Modified from a table by Rogers.⁴⁵⁸

Vesicle type	Size (diameter)	Number of lipid bilayers
Micelle	<100nm	N/A
Unilamellar vesicle (UV)	Variable	1
Small unilamellar vesicle (SUV)	20-100nm	1
Medium unilamellar vesicle (MUV)	>100nm	1
Large unilamellar vesicle (LUV)	>100nm	1
Giant unilamellar vesicle (GUV)	>1000nm	1
Oligolamellar vesicle (OLV)	100-1000nm	5
Multilamellar vesicle (MLV)	>500nm	5-25

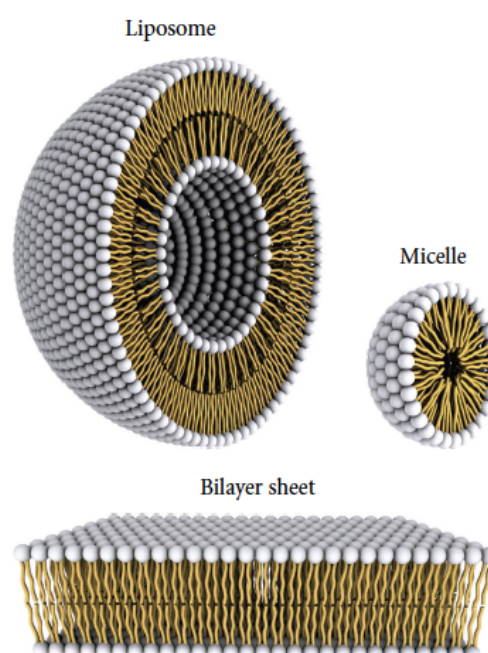


Figure 1.7.1. Aspects of liposomes and micelles.

This figure shows a representation of the steric organisation of a liposome (left) and a micelle (right). Liposomes have a lipidic bilayer (bottom) whereas micelles are constructed only of one lipid layer that has its apolar section turned inwards while its polar heads interact with the environment. As a result, the enclosed space in micelles is much more confined to that available in liposomes.

Reproduced from Bitounis D et al. *ISRN Pharmaceutics* 2012; 738432.

© 2012 Dimitrios Bitounis et al. Used under the terms of the Creative Commons Attribution Licence.

Following systemic administration, conventional liposomes – consisting of naturally occurring phospholipids and cholesterol, similar to the structure of cell membranes – are rapidly removed from the blood circulation (half life ~1-2 hours), through the process of opsonisation,^{459,460} and subsequent phagocytosis by macrophages and hepatic Kupffer cells of the reticuloendothelial system (RES).^{461,462} However, it has also been recognised that conventional nano-sized liposomes can accumulate in pathological areas (e.g. tumours or sites of inflammation or injury) through what is known as the enhanced permeability and retention effect.⁴⁶³ This is due to the development of ‘leaky’ vasculature that occurs in pathological areas, in contrast to normal tissues at steady state.

In order to improve the half-life of liposomes in the circulation, a small proportion (~5%) of functionalised sterically stabilising lipids can be incorporated into the structure of liposomes during their preparation.^{464,465} These liposome formulations are variously known as long-circulation-, sterically stabilised- or Stealth® liposomes. The most frequently utilised polymeric steric stabiliser is polyethylene glycol (PEG), which is water-soluble, has low toxicity, is non-immunogenic and exhibits resistance to opsonisation.⁴⁵⁵ The incorporation of PEG increases the half-life of liposomes in circulation to ~2 days via increased liposome stability, reduced non-specific interactions with blood components, and the avoidance of RES-mediated elimination.^{466,467}

The therapeutic efficacy of liposomes can be further improved through the use of targeting molecules on the liposomal surface, to facilitate delivery to specific cells or tissues *in vivo*, via the recognition and interaction with cellular surface antigens or receptors. Such targeting can be achieved with the use of antibodies or antibody fragments, vitamins, glycoproteins, peptides, oligonucleotides, or polysaccharides as well as other ligands recognised by cells.^{455,457} In particular, the use of antibodies grafted to the surface of liposomes – so called *immunoliposomes* – has emerged as an extremely promising means to target cells and tissues with high specificity. This was first described by Torchilin et al in 1979,⁴⁶⁸ and continues to be utilised as a means to target toxic chemotherapeutic agents to tumour cells, while minimising unwanted ‘off-target’ side effects, as well as in vaccines, and even in diagnostic imaging.^{452,455,457}

The basic structure of an immunoliposome incorporating targeting antibody grafted via surface PEG is shown in Figure 1.7.2. Important aspects of the evolution of liposomes in drug delivery have been reviewed by Torchilin,⁴⁵⁷ and are shown schematically in Figure 1.7.3.

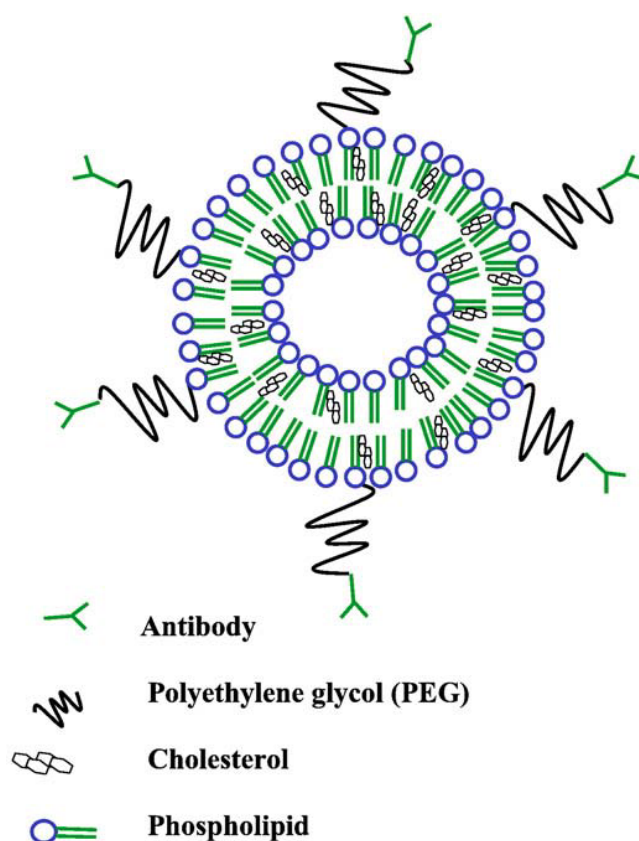


Figure 1.7.2. Sterically stabilised PEGylated immunoliposome. This schematic representation shows antibodies coupled to the distal end of the PEG-chains.

Reprinted from Kozłowska D, Foran P, MacMahon P, Shelly MJ, Eustace S, O'Kennedy R. Molecular and magnetic resonance imaging: The value of immunoliposomes. *Adv Drug Deliv Rev* 2009; 61: 1402-11.

© 2009, used with permission from Elsevier.

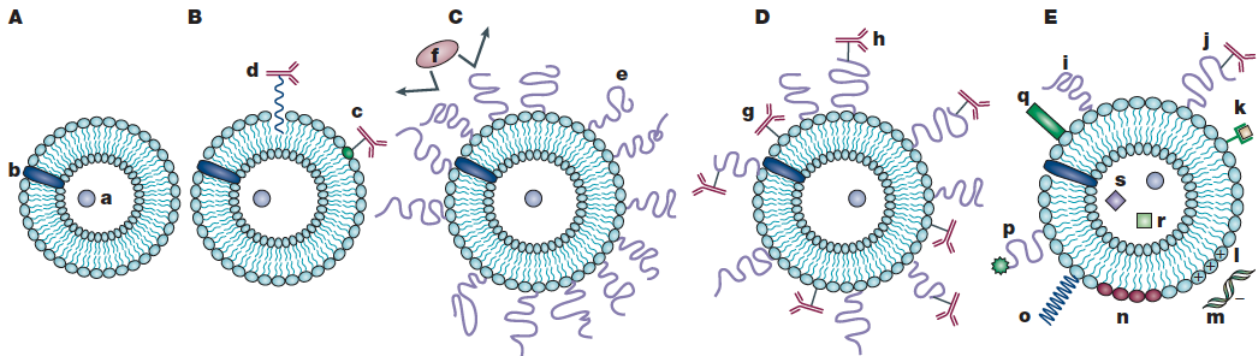


Figure 1.7.3. Evolution of liposomes.

(A) Early traditional phospholipids ‘plain’ liposomes with water soluble drug (a) entrapped into the aqueous liposome interior, and water-insoluble drug (b) incorporated into the liposomal membrane (these designations are not repeated on other figures).

(B) Antibody-targeted immunoliposome with antibody covalently coupled (c) to the reactive phospholipids in the membrane, or hydrophobically anchored (d) into the liposomal membrane after preliminary modification with a hydrophobic moiety.

(C) Long-circulating liposome grafted with a protective polymer (e) such as PEG, which shields the liposome surface from the interaction with opsonizing proteins (f).

(D) Long-circulating immunoliposome simultaneously bearing both protective polymer and antibody, which can be attached to the liposome surface (g) or, preferably, to the distal end of the grafted polymeric chain (h).

(E) New-generation liposome, the surface of which can be modified (separately or simultaneously) by different ways. Among these modifications are: the attachment of protective polymer (i) or protective polymer and targeting ligand, such as antibody (j); the attachment/incorporation of the diagnostic label (k); the incorporation of positively charged lipids (l) allowing for the complexation with DNA (m); the incorporation of stimuli-sensitive lipids (n); the attachment of stimuli-sensitive polymer (o); the attachment of cell-penetrating peptide (p); the incorporation of viral components (q). In addition to a drug, liposome can be loaded with magnetic particles (r) for magnetic targeting and/or with colloidal gold or silver particles (s) for electron microscopy.

Reprinted by permission from Macmillan Publishers Ltd: Torchilin VP. *Nat Rev Drug Discov* 2005; 4: 145-160. © 2005

1.7.1.1 Preparation of liposomes

There are several different methods that can be used to prepare liposomes.^{455,469} For the *thin lipid film hydration* method, a thin film of lipid is created by dissolving lipids in an organic solvent, and evaporation of the solvent with the use of a rotary evaporator. After removal of residual solvent, the solid thin film of lipid is rehydrated with an aqueous buffer at a temperature above the gel-liquid crystalline transition temperature of the lipid. This causes the lipids to swell and hydrate spontaneously, leading to the formation of multilamellar vesicle liposomes. These large vesicles are then either sonicated or extruded through polycarbonate filters of defined pore size to produce a suspension of small unilamellar liposomes of uniform size, e.g. 50-100nm in diameter.⁴⁵² The properties of the liposome formulation can be determined by the use of different phospholipid (with or without grafted PEG), cholesterol; drugs or other molecules of interest can also be encapsulated within the liposomes via passive entrapment or active loading techniques.⁴⁵² Other methods of liposome preparation include the *ultrasound* method, which produces small unilamellar vesicles via ultrasonication of aqueous dispersions of phospholipids; the *reverse phase evaporation* method, which produces large unilamellar and oligolamellar vesicles via the addition of lipids to a round bottom flask and the removal of solvent via distillation, followed by the re-dissolution in organic phase resulting in vesicle formation following which the solvent is evaporated to a semi-solid gel and non-encapsulated material is removed; the *freeze thaw extrusion* method, which enables the production of large unilamellar vesicles containing encapsulated proteins, and the *dehydration-rehydration* method, which produces oligolamellar vesicles.⁴⁵⁵

1.7.1.2 Conjugation methods for the preparation of immunoliposomes

To generate *immunoliposomes*, there are a number of different chemical approaches that have been utilised for the attachment of antibodies to liposomes; the details of these are beyond the scope of this thesis but have previously been reviewed in detail.⁴⁶⁹⁻⁴⁷¹

Coupling of antibody proteins directly to liposomes can be achieved by the generation of thioether bonds, in particular the reaction of thiols (sulfhydryl groups) and maleimide groups.^{455,470} This often requires the use of heterobifunctional cross-linking agents, due to the low frequency of sulfhydryl groups on many proteins.⁴⁷⁰ Alternatively, antibodies can be attached to sterically stabilised long-circulation liposomes at the distal end of the

PEG chain, an approach that is considered more efficient, and increases the availability of antibody for binding. One successfully and frequently used approach utilises 2-immunothiolane (Traut's reagent) to thiolate (i.e. add a sulfhydryl group to) antibody,^{472,473} and thus facilitate binding with PEG-derivatized lipid (i.e. PEG attached to phospholipid) via an attached maleimide group⁴⁷⁴; this is outlined schematically in Figure 1.7.4.⁴⁷⁰ This method has the advantages of a high coupling efficiency and the formation of stable covalent bonds.⁴⁷⁴

However, the use of whole antibodies with all of these methods can result in random orientation of antibodies on the surface of liposomes, and this may lead to faster clearance from circulation through interactions between Fc fragments and the RES.⁴⁷⁵ As a result, Fab fragments without the Fc portion, or alternatively recombinant single or double chain antibody (variable) fragments containing the variable regions of heavy and light chains (scFv, dsFv, respectively), have also been used; these can be conjugated to liposomes in specific orientation with the addition of C-terminal cysteine residues and the use of cross-linking molecules.⁴⁷⁶

Another approach that has been successfully used to produce targeted immunoliposomes that have therapeutic efficacy *in vivo* is known as the *post-insertion* method.⁴⁷⁷⁻⁴⁷⁹ This combinatorial approach involves the coupling of antibody (or other ligands) to the distal end of PEG-lipid derivatives in micellar phase, and subsequent transfer into the bilayers of pre-formed, drug loaded liposomes using a simple incubation step.^{478,480} These micelles consist of amphiphilic co-polymers (consisting of PEG and phospholipid, with hydrophobic and hydrophilic components that form via a process of self-assembly in aqueous solutions into a core-shell structure 10-100nm in size; the core is composed of hydrophobic lipids and the shell consists of a corona of polymeric PEG chains (see Figure 1.7.1).⁴⁸¹ The advantage of this approach is that a wide variety of ligands, including antibodies, can be inserted into liposomes containing a wide variety of drugs, as might be desired, e.g. in cancer chemotherapy on the basis of the drug sensitivity or receptor expression of the tumour (see Figure 1.7.5). In a comparison of immunoliposomes made using the conventional coupling techniques discussed above and the post-insertion method, there were no significant differences observed in efficacy both *in vitro* and *in vivo*.⁴⁷⁷

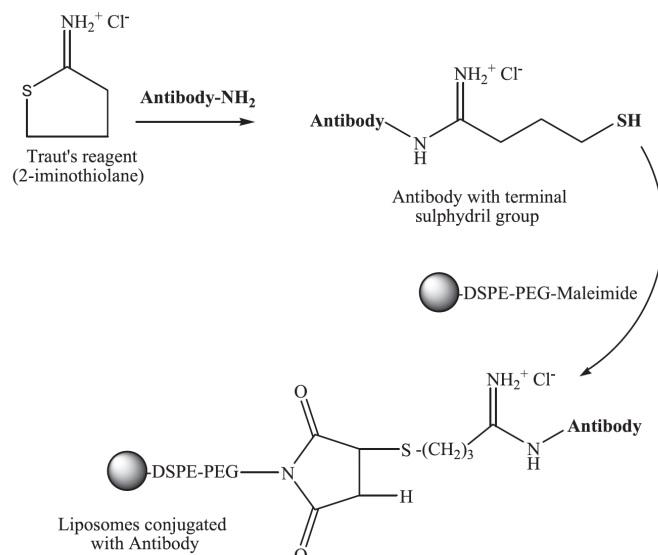


Figure 1.7.4. Thiolation of antibodies using Traut's reagent and conjugation of thiolated antibody to maleimide groups on the derivatized PEG.

Reprinted from Manjappa AS et al. Antibody derivatization and conjugation strategies: Application in preparation of stealth immunoliposome to target chemotherapeutics to tumour. *J Control Release* 2011; 150: 2-22.

© 2011 – used with permission from Elsevier.

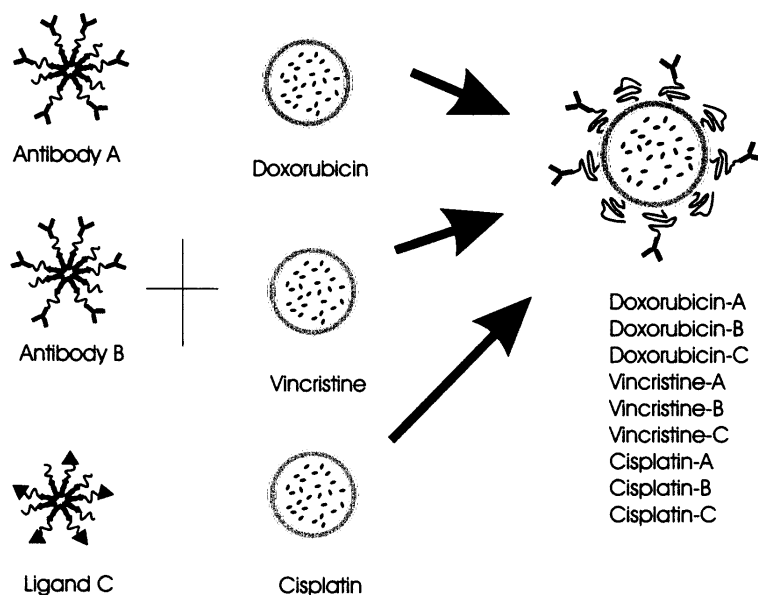


Figure 1.7.5. Cartoon depicting the combinatorial approach to the formation of ligand-targeted liposomal anticancer drugs.

Reprinted from Ishida T, Iden D, and Allen TA. A combinatorial approach to producing sterically stabilized (Stealth) immunoliposomal drugs. *FEBS Letters* 1999; 460: 129-133

© 1999 – Used with permission from Elsevier.

1.7.2. Polymeric nanoparticles

Nanoparticles are solid colloidal particles that can be used as carriers for drugs or other biologically active materials, and typically range in size from 10-400nm. Since the first demonstration of the controlled release of macromolecules using polymers by Langer and Folkman,⁴⁸² there have been a large number of studies utilising polymeric nanoparticles to develop specific drug delivery systems, particularly in the field of cancer therapy.⁴⁸³⁻⁴⁸⁵ Polylactic-co-glycolic acid (PLGA), polylactic acid (PLA), dextran and chitosan are among the biodegradable polymers that have been utilised in nanoparticle formulations, and Paclitaxel-loaded PLA-*block*-PEG micelles (Genexol-PM) have been tested as a therapeutic agent in clinical trials.⁴⁸⁶ However, PLGA has emerged as one of the most commonly used polymers, due to its excellent biocompatibility, biodegradability (it degrades to lactic and glycolic acid, which are both easily metabolised via the Krebs cycle, and eliminated as water and carbon dioxide; see Figure 1.7.6) and mechanical strength (it is a frequently used material in surgical sutures, e.g. VicrylTM),⁴⁸⁷ and the wide flexibility that is possible with the development of drug delivery systems utilising PLGA. Similar to liposomes, the surface of PLGA nanoparticles can be sterically stabilised with the use of PEG, which reduces uptake by the RES and prolongs the circulation half-life of the nanoparticles.⁴⁸⁸

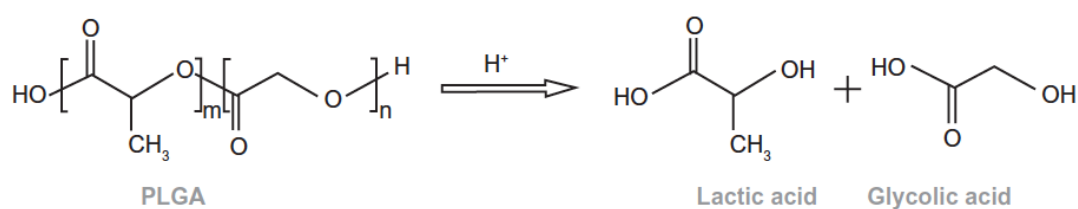


Figure 1.7.6. Chemical structure of polylactide-co-glycolide (PLGA), showing its degradation to lactic and glycolic acid.

Abbreviations: m=number of units of lactic acid; n=number of units of glycolic acid.

© 2011 Dinarvand et al. Republished with permission of Dove Medical Press Ltd, from *Int J Nanomedicine* 2011; 6: 877-895; permission conveyed through Copyright Clearance Center, Inc.

The design and functionality of PLGA nanoparticles can be tailored for multiple biomedical applications in terms of composition and colloidal features, the (co)polymers utilised in their formation, attachment of various ligands for targeting purposes, and the inclusions of various drugs (hydrophobic or hydrophilic) depending on the desired target cells, organs or pathology (e.g. cancers, inflammation).⁴⁸⁴ Some of these features are illustrated schematically in Figure 1.7.7.

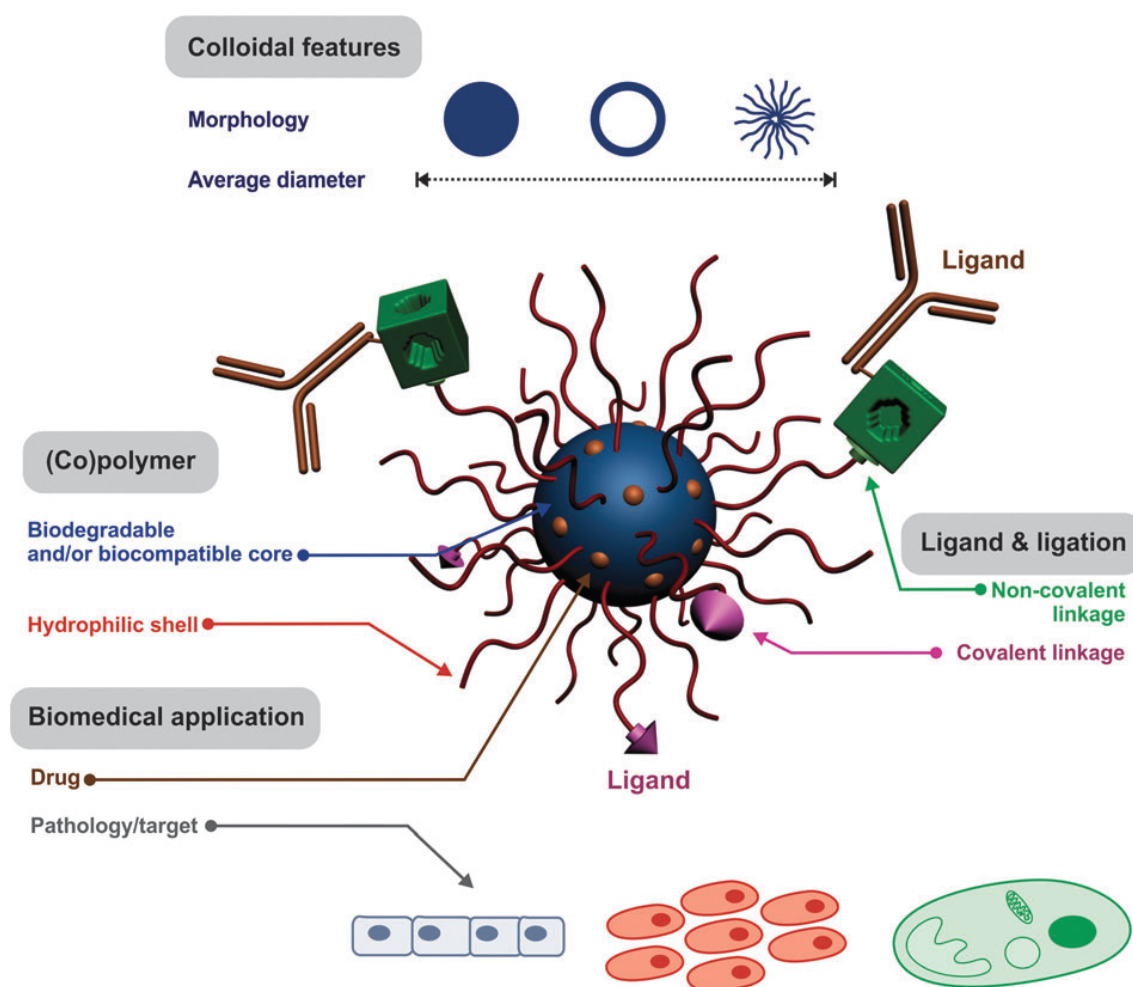


Figure 1.7.7. Schematic representation of aspects of the design of targeted nanoparticle systems.

Reproduced from Nicolas J et al. *Chem Soc Rev* 2013; 42: 1147-1235 – with permission of The Royal Society of Chemistry.

1.7.2.1 Preparation of PLGA nanoparticles

There are a number of methods of preparing polymeric PLGA nanoparticles that have been utilised^{483,484,489}; several of these methods involve a first step to prepare an emulsified system, and a second step that facilitates formation of the nanoparticles, which varies according to the method used.⁴⁸³

The *emulsification solvent evaporation* method^{483,490} involves the dissolution of polymer and drug in a water-immiscible volatile solvent (e.g. chloroform), following which this mixture is emulsified in an aqueous solution containing a surfactant stabiliser. This produces nano-sized droplets of organic solvent that serve as a template for nanoparticle formation. Emulsification is brought about with the use of a high-energy shearing source such as ultrasound or homogenisation; subsequently the organic solvent is removed under reduced pressure, which creates a fine dispersion of solid nanoparticles that can be collected with ultracentrifugation. Washes with distilled water are then used to remove surfactant residues, and any residual free drug.^{453,483,490} In order to entrap hydrophilic drugs (which are otherwise poorly incorporated), a double-emulsion technique is used that involves the addition of aqueous drug solution to organic polymer solution with stirring to produce a water-in-oil emulsion. This emulsion is then added into a second aqueous phase with the surfactant stabiliser (also with stirring) to form a water-in-oil-in-water emulsion; solvent removal by evaporation is performed as above.⁴⁹¹

Variations to the emulsification solvent evaporation method include *emulsification solvent diffusion*, which utilises an organic solvent that is partly soluble in water. The polymer solution is added to aqueous solution, with surfactant stabiliser along with stirring, generating an oil-in-water nano-droplet dispersion. This is then diluted in a large quantity of pure water, which enables the remaining organic solvent within the dispersed droplets to diffuse out, precipitating the polymeric nanoparticles. This approach has been used in a range of studies.^{483,492,493} Another variation is the *emulsification reverse salting-out* technique, which involves adding polymer and drug solution to a water miscible solvent (e.g. acetone), and then to an aqueous solution containing a salting-out agent (magnesium or calcium chloride), and a colloidal stabiliser, under stirring. If a sufficient quantity of water is added to this oil-in-water emulsion, nanoparticles are precipitated by the diffusion of acetone into the aqueous

phase induced by the sudden decrease in salt concentration. Remaining solvent and the salting-out agent are subsequently removed by cross-flow filtration.⁴⁹⁴

Dialysis can be used to form nanoparticles from pre-formed co-polymers where these can be dissolved in a water miscible organic solvent. By dialysing the polymer solution against water, nanoparticles precipitate into aqueous solution.⁴⁹⁵

Nanoprecipitation (also known as the solvent displacement method) is a technique used to prepare nanoparticles that involves two solvents that are miscible.⁴⁹⁶ It has the advantage of being a one-step procedure, does not require surfactants or salting-out solutions, and can be performed using a broad variety of benign solvents, such as dimethyl sulfoxide (DMSO) or acetone. It is a very effective method to incorporate lipophilic drugs into polymeric (PLGA) nanoparticles. Both the polymer and drug need to be soluble in the first (organic) solvent (e.g. acetone or acetonitrile), but insoluble in the second (aqueous) solvent. Nanoprecipitation occurs when polymer-drug containing solvent is added to the (non)-solvent, as shown in Figure 1.7.8. As soon as the polymer containing solvent diffuses into the dispersing medium (second solvent), the polymer precipitates to form a monodispersion of nanoparticles of 50-300nm in size, immediately entrapping the lipophilic drug.⁴⁹⁶ This rapid self-assembly process occurs through a complex series of interactions to minimise the system's free energy due to interfacial turbulence and has been thought to be governed by the so-called Marangoni effect.^{484,496} Nanoprecipitation has been successfully utilised to develop therapeutic nanoparticles with anti-cancer effects *in vitro* and *in vivo*.⁴⁹⁷⁻⁴⁹⁹

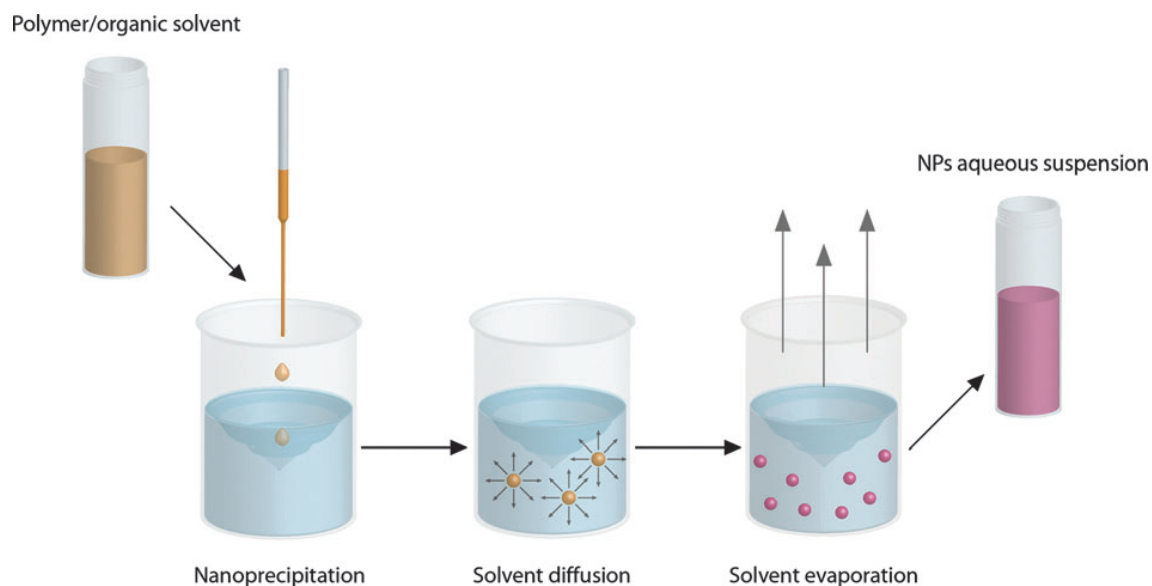


Figure 1.7.8. Preparation of polymeric nanocarriers by nanoprecipitation.

Reproduced from Nicolas J et al. *Chem Soc Rev* 2013; 42: 1147-1235 – with permission of The Royal Society of Chemistry.

1.7.2.2 Generation of targeted PLGA nanoparticles

The targeting of PLGA nanoparticles to specific cell types *in vivo* can be significantly enhanced with the use of targeting ligands including small molecules (e.g. vitamins, folic acid, curcumin – to target some cancers and β -amyloid plaques), carbohydrates (e.g. mannose to target lectin surface receptors), peptides (e.g. octreotide to target somatostatin receptors), aptamers (short single-stranded DNA or RNA oligonucleotides, e.g. to target prostate specific membrane antigen), and monoclonal antibodies which can be used to target specifically almost any molecule of interest.⁴⁸⁴ In the treatment of cancer, this offers the potential to target toxic chemotherapeutic drugs directly to tumour cells with the intention of minimising ‘off-target’ effects and the systemic toxicities associated with these agents.^{498,500} Targeting ligands can be added to (co)polymers prior to nanoparticle assembly, or to preformed nanoparticles; the latter is preferred however for the linkage of bulky ligands such as antibodies or proteins that might be denatured with the use of organic solvents.⁴⁸⁴

To facilitate the attachment of ligands to their surface, amphiphilic PLGA-*block*-PEG (PLGA-*b*-PEG) copolymers can be formulated and used to develop nanoparticles.⁵⁰¹ Because these block co-polymers consist of a hydrophobic PLGA portion and a hydrophilic PEG portion, this facilitates the generation of nanoparticles with a hydrophobic core and a hydrophilic shell via the methods described in section 1.7.2.1 (see Figure 1.7.9 and Figure 1.7.10 below). These amphiphilic copolymers can be synthesised via ring opening polymerization of lactide and glycolide in the presence of PEG moieties terminating in chemical initiators (e.g. PEG-COOH or PEG-maleimide), or alternatively via direct conjugation of PEG blocks to pre-formed PLGA.^{484,501}

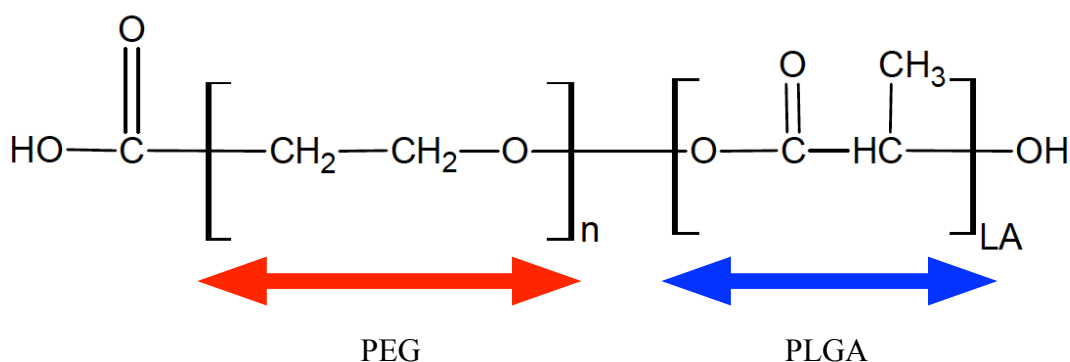


Figure 1.7.9. Chemical structure of PEG-*b*-PLGA copolymer with terminating carboxyl group.

In this amphiphilic PEG-*b*-PLGA copolymer, there is a hydrophilic PEG group (red), and a hydrophobic PLGA group (blue). In addition there is a carboxyl (–COOH) group attached as a chemical initiator to the PEG terminal (see text), which can be used for the conjugation of ligands via carbodiimide chemistry.

n=number of units of PEG; LA=number of units containing lactic acid (i.e. PLGA) – these can both be varied during preparation of these copolymers.

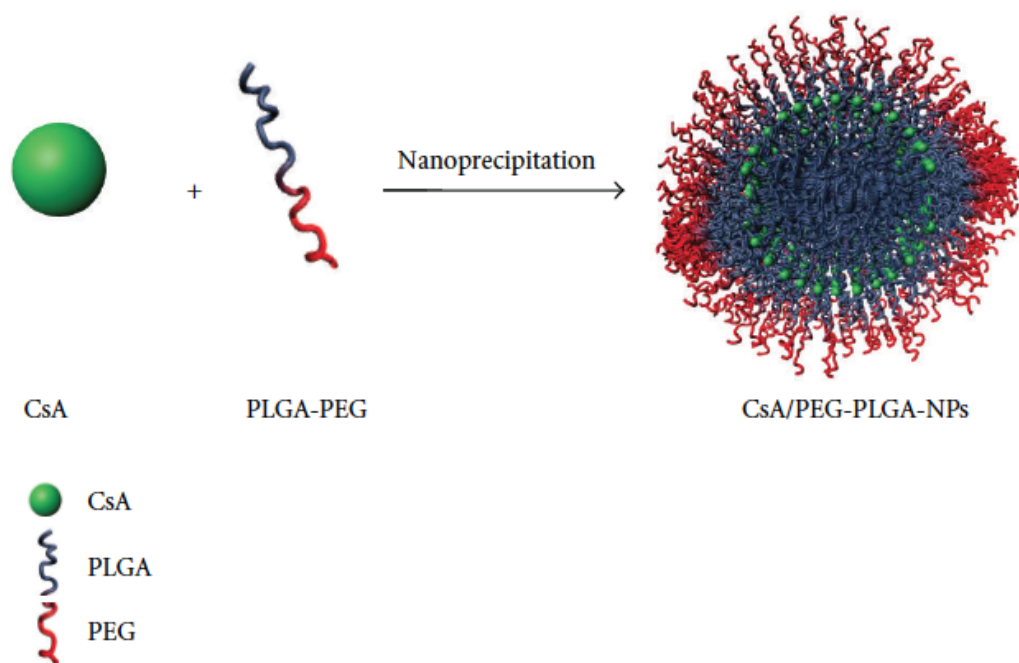


Figure 1.7.10. Schematic illustration of formation of drug containing PLGA nanoparticles using amphiphilic PLGA-*b*-PEG copolymers.

In this example, cyclosporine A (CsA) is shown as a model hydrophobic drug; the hydrophilic and hydrophobic portions of the PLGA-*b*-PEG copolymer are shown in red and blue, respectively. The hydrophobic core of this nanoparticle consists of CsA and PLGA; the hydrophilic shell consists of PEG moieties, which could be used to conjugate ligands such as targeting antibodies if a suitable initiator (e.g. COOH or maleimide, see text) was included at the distal end of the PEG.

Modified from an original figure from Tang L et al. *J Transplant* 2012; 2012: 896141.

© 2011 Li Tang et al. Used with permission under the terms of the Creative Commons Attribution Licence.

Carbodiimide chemistry is a frequently used and effective reaction method to conjugate ligands directly to PEG groups on the exterior of polymeric nanoparticles.^{484,498-500,502} Carboxyl ($-\text{COOH}$) groups at the terminal end of PEG chains in the hydrophilic shell of nanoparticles can be activated with the use of 1-ethyl-3-(3-dimethylaminopropyl) carbodiimide hydrochloride (EDC) and *N*-hydroxysuccinimide (NHS) and then reacted with primary amines on a targeting ligand (e.g. folic acid, peptides, sugars, or monoclonal antibodies) to form stable amide bonds (see Figure 1.7.11). The use of carbodiimide chemistry in the preparation of targeted drug-containing PLGA nanoparticles is illustrated schematically in Figure 1.7.12.

Other strategies that have been utilised include the use of *thiol-maleimide coupling* (similar to that discussed above for immunoliposomes),^{503,504} and *biotin-avidin ligation*.⁵⁰⁵ Further details of these and other methods of conjugation can be found in a detailed review by Nicolas et al.⁴⁸⁴

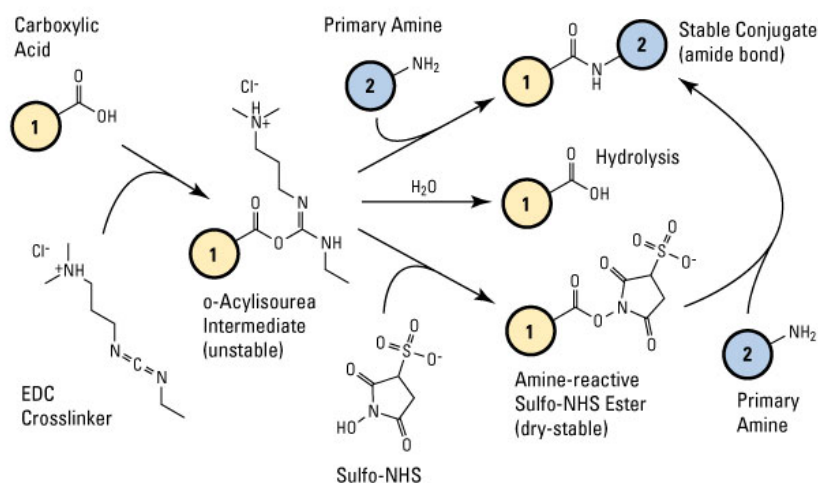


Figure 1.7.11. Sulfo-NHS plus EDC (carbodiimide) crosslinking reaction scheme.

Carboxyl-to-amine crosslinking with the popular carbodiimide, EDC, and sulfo-NHS (see text for definitions). Molecules (1) and (2) can be peptides, proteins or any chemicals that have respective carboxylate and primary amine groups. When they are peptides or proteins, these molecules are tens-to-thousands of times larger than the crosslinker and conjugation arms diagrammed in the reaction. Addition of NHS or Sulfo-NHS to EDC reactions (bottom-most pathway) increases efficiency and enables molecule (1) to be activated for storage and later use.

Source: <http://www.piercenet.com/browse.cfm?fldID=F3305493-0FBC-93DA-2720-4412D198A9C9>

© 2013 Thermo Fisher Scientific Inc – used with permission.

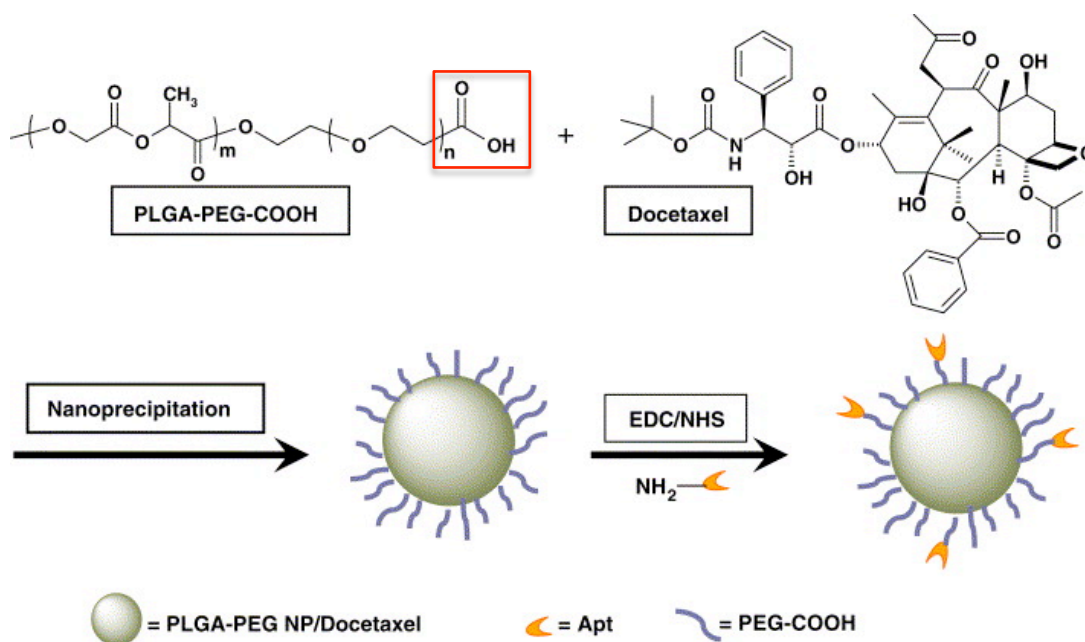


Figure 1.7.12. Schematic illustration of synthesis of targeted PLGA nanoparticles utilising carbodiimide chemistry.

In this example, PLGA-b-PEG-COOH and the hydrophobic anti-cancer drug docataxel were used to formulate PLGA-Docataxel nanoparticles using nanoprecipitation. The carboxyl groups (indicated by the red box) were activated with EDC-NHS to enable conjugation via carbodiimide chemistry to amine groups of a 5'-NH₂ modified A10 2'-fluoropyrimidine RNA aptamer targeting prostate smooth muscle antigen (PSMA).

Reprinted from Cheng J et al. Formulation of functionalized PLGA-PEG nanoparticles for in vivo targeted delivery. *Biomaterials* 2007; 28: 869-876.

© 2006 – used with permission from Elsevier.

1.8. Developing a non-human primate model of DC immunotherapy: the common marmoset monkey

In order to translate the potential of DC based immunotherapies, established in rodent studies, into suitability for evaluation in human clinical trials, it is necessary to test such a strategy in a robust NHP model of transplantation.^{38,39,506} The lesser degrees of complexity of the immune systems of lower order species, and their relative lack of environmental exposure to antigen and thus immunological memory, so-called heterologous immunity,^{42,43} have made it considerably easier to successfully induce tolerance in laboratory models such as the mouse and rat. It is thus necessary to confirm data on experimental therapies from small animal laboratory models in larger, more complex species (e.g. pigs, sheep or NHP) to establish suitability for human trials. The close similarity between NHP and humans mean that findings in NHP tolerance models are the most likely to be clinically applicable and relevant,³⁹ and thus most likely to closely reflect the situation in clinical human disease.

1.8.1. The common marmoset as a novel transplant model

The common marmoset (*Callithrix jacchus*) is a small New World primate that is being developed as a feasible pre-clinical model of transplantation at this laboratory. These animals are small in size (average weight 200-400g), not environmentally endangered and possess advantages in terms of ease of handling and animal husbandry, as well as considerably lower cost and housing requirements when compared with larger primates.⁵⁰⁷ In addition they are easy to breed, have a relatively short gestational period and usually produce multiple offspring (twins or triplets) from each pregnancy.⁵⁰⁷ Interestingly, co-twins or triplets exhibit placental sharing of foetal cells *in-utero* which leads to naturally occurring chimerism,⁵⁰⁸⁻⁵¹¹ including of immune cells and thus these animals appear to be an example of naturally occurring tolerance.⁵¹²⁻⁵¹⁴ This characteristic of marmosets is unique among primate species.

Although New World primates, including marmosets, have an evolutionary distance from humans of over 55 million years, they maintain close genetic similarity with humans. Between humans and marmosets, there is an average of 86% homology in immunity-related proteins,⁵¹⁵ (compared with 60% between mice and humans or marmosets), and over 90% homology for important co-stimulatory molecules⁵¹⁶ that are

involved in DC-T-cell interactions. In addition, many reagents such as cytokines and monoclonal antibodies to cell-surface proteins used in laboratory research are cross-reactive between humans and marmosets.⁵¹⁷⁻⁵²¹

Marmosets have an established role in biomedical research. They have been used as models of multiple sclerosis (experimental autoimmune encephalitis),⁵²²⁻⁵²⁵ to study Parkinsons disease,⁵²⁶ in pharmacology,⁵²⁷ drug-toxicity,⁵²⁸ hormonal release studies,⁵²⁹ and in the areas of bone disease,^{530,531} hypertension,⁵³² immunology and gene therapy,^{413,519,533,534} fertility research,^{535,536} as well as having had embryonic stem cell lines established.^{537,538}

Until recently, studies of the DC biology of marmosets have been limited³⁹⁹; work from this laboratory has extended this understanding considerably (see section 1.6).^{303,403} There is however a recent study of the therapeutic use of DC to repair spinal cord injury which made use of the naturally occurring tolerance due to chimerism in marmosets to generate DC from a ‘donor’ twin to transplant into injured spinal cord in a ‘recipient’ twin without incurring an immune response, and showed histological and clinical evidence of amelioration of injury.⁵³⁹ One drawback of both of these studies is that marmosets had to be killed to obtain bone marrow precursors for generation of DC^{399,539}; this approach would not be suitable for transplant studies, where a donor monkey needs to both act as a source of DC for pre-transplant infusion to a recipient and later act as the live donor of a kidney to the same recipient.

In order to develop the marmoset as a feasible transplant model, work from this laboratory has included developing rapid methods of sequence-based Class I and II MHC genotyping, to enable selection of maximally immunologically disparate animals for transplant studies.⁴⁰¹ This work has established that selecting marmosets on the basis of degree of mismatch at MHC Class II DRB predicts *in vitro* allo-reactivity as measured in MLR cultures. Work has also been done to establish marmoset blood grouping and cross-match (Coates et al, unpublished results). Surgical aspects of marmoset renal transplantation are also being developed, based on a rat model of renal transplantation.⁵⁴⁰ Several studies have reported the occurrence of spontaneous renal pathology in marmosets, but this has yet to be correlated to renal function or other serum or urine biochemical parameters.⁵⁴¹⁻⁵⁵¹ It is currently unknown whether this

phenomenon would have any impact on the use of marmosets as a kidney transplant model.

1.8.2. Marmosets as a potential NHP model for DC immunotherapy studies

Marmoset DC have been identified and characterised both *in vitro* and *in vivo* (as reviewed in detail in section 1.6). Marmoset DC have a number of characteristics that make them attractive to investigate the potential of tolerogenic DC in a transplant model.²²⁹ Firstly, both marmoset MoDC and haematopoietic progenitor derived DC (HPDC) (particularly the latter) obtained from G-CSF treated peripheral blood can be produced in sufficiently large numbers to enable adequate doses to be given to recipient animals in DC therapy studies. Lesser but potentially still adequate numbers of fresh myeloid DC are produced with FLT3-L mobilisation.³⁰³ Secondly, these DC can be isolated without killing the donor animal, leaving them available to act as live donor of tissue for transplant studies. Thirdly, the DC produced after G-CSF mobilisation have either a stably immature or semi-mature phenotype, with resistance to maturation stimuli. This characteristic implies greater tolerogenic potential if this is maintained *in vivo* following allogeneic DC infusion.

DC-SIGN, which is a specific DC marker present on myeloid DC and MoDC in humans,^{193,415} is present in lymphoid and other tissue DC in macaques,^{416,417} and African green monkeys (AGM),³⁹⁵ and highly expressed in AGM MoDC,³⁹⁵ but at low levels in macaque MoDC.⁴¹⁸ DC-SIGN has not previously been identified on marmoset DC isolated *in vitro*. Whether these differences between NHP and human DC reflect differences in antibody cross-reactivity, responses to growth factors (G-CSF or Flt3L) that vary between species, effects of culture media in different species, or true differences in DC biology and function is at present unclear.

1.8.3. DC immunotherapy studies in marmoset monkeys

Recently, a preliminary study of DC infusions between Class II MHC DRB-mismatched donors and recipients has been undertaken to establish the safety and feasibility of DC therapy in this species.³⁰³ Following a course of G-CSF mobilisation (10 mcg/kg daily for 5 days), immature MoDC were propagated *in vitro* from monocyte precursors isolated from peripheral blood of naive donor marmosets, using 2x 1mL blood samples taken over 2 days. Approximately 2×10^6 MoDC were generated from each donor, and

injected into 3 recipient animals intravenously. Donor specific allo-reactivity was monitored over a 3 month period using: 1) MLR of recipient peripheral blood mononuclear cells (PBMC) stimulated by irradiated PBMC from donor or third party animals; and 2) IFN- γ enzyme-linked immunospot (ELISPOT) assay to detect IFN- γ production by responder effector and memory T-cells, using a modified method optimised for marmoset cells.^{552,553}

Donor-derived DC therapy was well tolerated in all 3 recipients. Two of the three animals showed evidence of transient immune hypo-responsiveness which was non-specific as measured in MLR (i.e. to both donor and third party); the third animal showed evidence of donor-specific sensitisation, which was also transient but peaked later. IFN- γ secretion was lower in all 3 recipients for the first few weeks, with a nadir at week 4, after which it increased by about 2-3 months post infusion (see Figure 1.8.1).

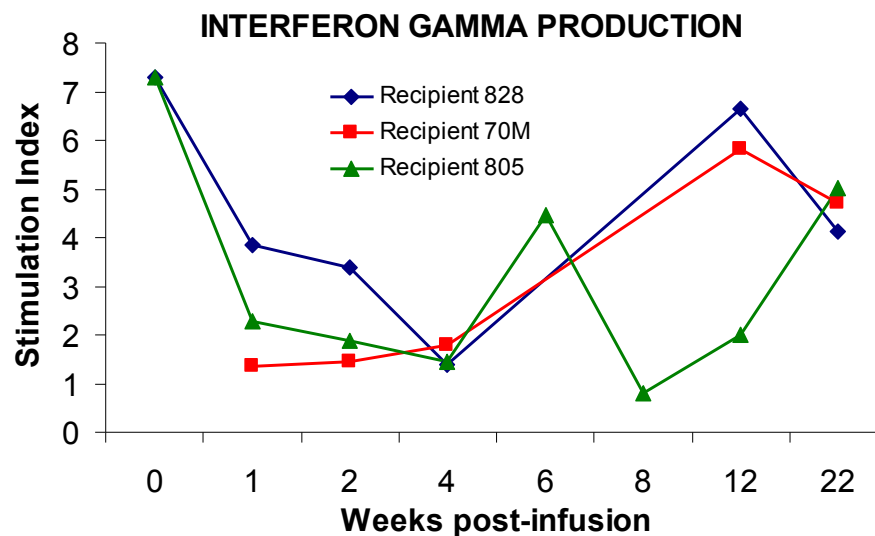


Figure 1.8.1. Marmoset recipient immune responses following the infusion of allogeneic donor-derived DC.

Marmoset MoDC propagated *in vitro* from G-CSF mobilised donors were infused into recipient marmosets that were mismatched at Class II MHC DRB. ELISPOT assays were performed at various time points to determine IFN- γ production by marmoset PBMC, using donor PBMC as stimulator cells, as a measure of donor reactivity.

Stimulation index = (IFN- γ production stimulated PBMC: Baseline PBMC). Time-point 0 represents pre-infusion data.

Image used courtesy of Dr Shilpanjali Jesudason (nee Prasad).³⁰³

Although the responses to allogeneic donor DC therapy reported were non-specific and transient, these findings provide preliminary data that suggest DC therapy can be administered safely in marmosets without adverse effects. Moreover, DC therapy is worthy of further investigation, and trials of alternative dosing schedules, routes of administration are needed to determine the optimal approach to DC administration in this model. It is also notable that unmodified, immature donor-derived MoDC therapy alone has not been sufficient to promote sustained donor-specific immune hypo-responsiveness in small animal studies,²⁹⁴ and it is likely that adjuvant therapy, perhaps with immunomodulatory drugs (e.g. rapamycin or curcumin), will be required to induce more sustainable tolerogenic effects.

Further studies are needed to elucidate the mechanisms of the immunologic effect of donor-derived DC therapy in marmosets, and whether it reliably suppresses the allo-immune response. An important aspect that should be explored in this NHP model is the trafficking behaviour of injected DC following administration via different routes *in vivo*, and to examine the interaction of administered DC with other immune cells in secondary lymphoid tissues. In addition, if appropriate DC-specific markers, e.g. DC-SIGN, can be identified in marmosets, it will be possible to explore targeting immunotherapies to recipient DC *in vivo*, with the use of monoclonal antibodies.

Ultimately, in order to determine the efficacy of DC immunotherapy in this NHP model, it will need to be administered in association with a transplant kidney allograft, and this will provide the most robust measure of whether desired tolerogenic effects have been achieved.

1.9. Literature Review: Conclusions

From this review of the literature, it is clear that DC immunotherapies offer considerable potential as a means to promote the induction of transplantation tolerance.

Although short to medium-term kidney transplant outcomes are excellent, current immunosuppressive regimens are associated with significant long-term toxicity. The induction of stable, true operational tolerance, or perhaps more feasibly the minimisation of immunosuppressive requirements, in kidney transplant recipients has the potential to offer considerable benefits in terms of mortality and morbidity. However, the current non-donor-specific approaches to tolerance induction being trialled in transplant recipients are high risk, not necessarily tolerogenic and may be associated with long-term immunodeficiency.

DC are critical to the normal homeostatic maintenance of tolerance, and play a pivotal role in the immune response following transplantation. There is a considerable body of evidence that cellular DC therapies of both donor and recipient origin are effective at inducing donor-specific tolerance in rodent models. A number of strategies to promote DC tolerogenicity have been shown to be effective *in vitro*, but to date there has been limited translation of these results into NHP transplant models. Proof of principle in terms of safety and feasibility of this type of therapy in humans has been established with DC vaccination studies, and one study of human volunteers receiving DC therapy that induced transient antigen-specific tolerance. In addition, targeting either donor antigen or immunosuppressive drugs to DC *in vivo*, perhaps with the use of nanocarriers such as liposomes or nanoparticles, which has established efficacy in the treatment of malignancy, has the potential to alter the immune response to a more tolerogenic phenotype. It is necessary to trial DC based immunotherapies in a robust pre-clinical NHP model, to establish efficacy and safety, before human clinical trials can be undertaken.

The common marmoset monkey has an established role in biomedical research, but has not previously been used in solid organ transplantation. This species has considerable advantages over other primates in terms of size, cost and ease of breeding, as well as being non-endangered in the wild. Work at this and other laboratories has extensively characterised the immune biology of this NHP, including developing techniques to

ensure the selection of maximally immunologically disparate animals for donor-recipient pairs to undergo DC infusion studies and transplantation. It remains to be determined whether previously observed spontaneous renal pathology in marmosets would have any impact on their use in kidney transplant studies. However, it is now possible to generate sufficiently large numbers of DC from the peripheral blood of marmosets mobilised with haematopoietic growth factors. These DC are stably immature, a desirable characteristic for tolerance induction (unlike other NHP dendritic cells characterised thus far), and are suitable for administration in transplant studies. Preliminary studies of donor-derived DC infusion therapy in marmoset monkeys have demonstrated safety and shown evidence of suppression of the immune response. To date, there have been no studies of specific DC targeting *in vivo* to promote a tolerogenic response in this or other NHP models.

1.10. Thesis aims and hypotheses

The major aim of the work presented in this thesis is to further develop the common marmoset monkey (*Callithrix jacchus*), as an NHP model with sufficient genetic disparity for pre-clinical transplantation studies in which to test dendritic cell based immunotherapy.

The hypotheses of this thesis are:

1. That the healthy adult marmoset monkey represents a suitable NHP model for pre-clinical transplantation studies, without significant spontaneous renal pathology that might compromise the feasibility of use as a kidney transplant model.
2. That donor derived marmoset DC can be propagated *in vitro* from precursors present in peripheral blood with sufficient numbers and viability for administration as a cellular therapy to allogeneic marmoset recipients, and that these administered DC exert their observed effects on the immune response following migration to secondary lymphoid organs.
3. That monoclonal antibodies targeting marmoset DC-SIGN can be developed that identify DC-SIGN expression on *in vitro* propagated DC or on tissue resident DC present *in vivo*, and that will be suitable for use in studies of DC immunotherapy in the marmoset transplant model.
4. That immunoliposomes or polymeric nanoparticles targeting DC-SIGN can be generated that are suitable for subsequent *in vivo* studies of targeted drug delivery to dendritic cells in the marmoset transplant model.

This work creates a platform whereby further studies of novel DC immunotherapy can be undertaken in the future, in this relevant preclinical NHP model, with the potential for translation to human clinical trials.

Chapter 2: MATERIALS AND METHODS

2.1. Introduction

This chapter describes general protocols and procedures related to laboratory techniques and animal-based procedures used for the studies described in this thesis. Manufacturer details can be found at the end of the chapter (section 2.8). Additional specific details of methodology may also be found in other relevant chapters.

2.2. Materials

2.2.1. Antibodies

All antibodies used in this thesis were anti-human monoclonal antibodies unless otherwise specified.

2.2.1.1 Isotype matched control monoclonal antibodies

1. Fluorescein isothiocyanate (FITC)-conjugated mouse IgG2b isotype control (clone 27-35) – BD Biosciences
2. Phycoerythrin (PE)-conjugated mouse IgG2a isotype control (clone G155-178) – BD Biosciences
3. PE-Cy5 (aka Cychrome, CyC)-conjugated mouse IgG2a isotype control (clone G155-178) – BD Biosciences
4. Allophycocyanin (APC)-conjugated mouse IgG1 K isotype (clone P3.6.2.8.1) – eBioscience
5. Unconjugated mouse IgG1k isotype control functional grade purified (clone P3.6.2.8.1) – eBioscience
6. Unconjugated mouse IgG1k isotype control (supernatant from X63 mouse myeloma cell line; stored and prepared in-house)

2.2.1.2 Primary monoclonal antibodies

All antibodies used in this thesis have been established as being cross-reactive with marmoset cells or tissues, unless otherwise specified.⁵¹⁷

1. FITC-conjugated CD3 (clone SP34) – BD Pharmingen
2. PE and APC-conjugated CD11c (clone S-HCL-3) – BD Pharmingen

3. FITC or PE-conjugated CD14 (clone M5E2) – BD Biosciences
4. FITC-conjugated CD20 (clone B-Ly-1) – DAKO Cytomation (DAKO)
5. FITC-conjugated CD56 (clone NCAM16.2) – BD Biosciences
6. FITC or PE or PE-Cy5-conjugated CD83 (clone HB15a) – Immunotech
7. FITC or PE-conjugated CD86 (clone FUN1) – BD Pharmingen
8. Unconjugated (purified), FITC or PE-conjugated CD209/DC-SIGN (clone DCN46; IgG2b) – BD Pharmingen
9. PE-Cy5 (aka CyC)-conjugated HLA-DR (clone G46-6) – BD Biosciences

2.2.1.3 Secondary polyclonal antibodies

1. FITC-conjugated sheep anti-mouse IgG F(ab')₂ fragment; catalogue number AQ326 – Chemicon (now Millipore)
2. PE-conjugated goat anti-mouse IgG1 (γ₁ chain specific); catalogue number 1070-09 – Southern Biotech
3. Anti-mouse IgG (Fc specific) – peroxidase antibody produced in goat; catalogue number A0168 – Sigma-Aldrich

2.2.2. Cytokines

- Recombinant human (rh) interleukin-4 (IL-4) – eBiosciences
- rh granulocyte macrophage-colony stimulating factor (GM-CSF) – Sandoz
- rh fetal liver tyrosine kinase 3 ligand (FLT3-L) – R&D Systems
- rh stem cell factor (SCF; Ancestim) – AMGEN Corporation
- rh thrombopoietin (TPO) – R&D Systems
- bacterial lipopolysaccharide (LPS) – Sigma Aldrich

2.2.3. Prepared buffers, media and solutions

- **Phosphate-buffered saline (PBS)** was prepared using sodium chloride (May & Baker), sodium phosphate (Amresco) and sodium dihydrogen orthophosphate (Ajax Finechem).
- **Roswell Park Memorial Institute (RPMI)-1640** media, also referred to as RPMI (Gibco BRL)

- **Fetal calf serum (FCS)** – added to PBS or media as described (JRH Biosciences)
- **Complete medium (CM)** - RPMI-1640 supplemented with 10%-20 % v/v fetal calf serum, 2mM L-glutamine (MultiCel), penicillin-streptomycin (MultiCel). Added cytokines and reagents included IL-4, GM-CSF, FLT3-L, SCF, TPO, and LPS.
- **Cell lysis buffer** – 0.15M ammonium chloride (Ajax Finechem), 0.01M sodium bicarbonate, 0.1mM EDTA, in MilliQ water
- **Staining buffer** for flow cytometry studies - PBS with 0.1% v/v FCS, 0.01% w/v sodium azide (Sigma Aldrich)
- **FACS lysing solution** – 10% concentrated FACS lysing solution (BD Biosciences) in distilled water
- **HEPES buffer** – 0.15M sodium chloride and 25mM HEPES (4-(2-hydroxyethyl)-1-piperazineethanesulfonic acid; Sigma-Aldrich) in MilliQ water
- **Human serum albumin (HSA)** – (Sigma-Aldrich)
- **Triton X-100** (Sigma-Aldrich) – used as a non-ionic detergent (Sigma-Aldrich)
- **Sodium dodecyl sulfate (SDS)** – used as a 2% (w/v) solution in buffer as an anionic detergent for solubilizing lipid preparations (Sigma-Aldrich)
- **Bicarbonate buffer** – sodium carbonate 1.59g and sodium bicarbonate 2.93g, in 1000ml of MilliQ water, adjusted to pH 9.6 (various manufacturers)
- **PBS-Tween wash buffer** – 0.5% w/v of Tween-20 added to PBS, adjusted to pH of 7.4
- **TMB substrate solution** – 3,3',5,5'-Tetramethylbenzidine solution (from Insulin ELISA kit; catalogue 10-1113-01, Mercordia)
- **Stop solution** – 0.5M sulfuric acid (H₂SO₄) solution (from Insulin ELISA kit; catalogue 10-1113-01, Mercordia)

2.2.4. Materials for immunoliposomes and polymeric PLGA nanoparticles

2.2.4.1 Immunoliposomes

- Chloroform; analytical grade (Chem-Supply)
- HEPES: 0.15M sodium chloride and 25mM 4(2-hydroxyethyl)piperazine-1-ethanesulfonic acid (Sigma Aldrich), in MilliQ water
- DPPC: 1,2-dipalmitoyl-*sn*-glycero-3-phosphocholine (Avanti Polar Lipids)

- mPEG-DSPE-2000: 1,2-distearoyl-phosphatidyl ethanolamine-methyl-polyethylene glycol conjugate (Lipoid)
- DSPE-PEG-mal: 1,2-distearoyl-*sn*-glycero-3-phosphoethanolamine-N-[maleimide (polyethylene glycol)-2000] (Laysan Bio Inc)
- Cholesterol; >95% pure (Sigma Aldrich)
- DiI: 1,1'-dioctadecyl-3, 3, 3', 3'-tetramethylindocarbocyanine perchlorate (Sigma Aldrich)
- Coumarin 6: 3-(2-benzothiazolyl)-N,N-diethylumbelliferylamine, 3-(2-benzothiazolyl)-7-(diethylamino) coumarin (Sigma Aldrich)
- Traut's reagent: 2-thiolaniline hydrochloride (Sigma Aldrich)
- DCN46: Unconjugated (purified) mouse anti-human CD209/DC-SIGN; clone DCN46 (BD Pharmingen)
- IgG isotype: Unconjugated mouse IgG1 κ isotype control functional grade purified; clone P3.6.2.8.1 (eBioscience)
- HSA: Human serum albumin (Sigma Aldrich)

2.2.4.2 Polymeric PLGA nanoparticles

- Acetonitrile; analytical grade (Sigma Aldrich, Australia)
- Acetone; analytical grade (Sigma Aldrich)
- PLGA-mPEG: methoxy poly(ethylene glycol)-*b*-Poly((D,L)lactic acid (Polysciotech)
- PLGA-PEG-COOH: Poly((D,L)lactide)-*b*-Poly(ethylene glycol)-carboxylic acid (Polysciotech)
- Coumarin 6: 3-(2-Benzothiazolyl)-N,N-diethylumbelliferylamine, 3-(2-Benzothiazolyl)-7-(diethylamino) coumarin (Sigma Aldrich)
- Curcumin (analytical grade; Sigma Aldrich)
- NHS: *N*-hydroxysuccinimide (Sigma Aldrich)
- EDC: *N*-(3-Dimethylaminopropyl)-*N'*-ethylcarbodiimide hydrochloride (Sigma Aldrich)
- DCN46: Unconjugated (purified) mouse anti-human CD209/DC-SIGN; clone DCN46 (BD Pharmingen)
- IgG isotype: Unconjugated mouse IgG1 κ isotype control functional grade purified; clone P3.6.2.8.1 (eBioscience)

2.3. Animals

2.3.1. *Animals*

Up to 32 healthy marmosets aged 2-14 years, weight 250-500g, were housed at the Queen Elizabeth Hospital at any one time. Most marmoset colonies in Australia, including our own, originate from animals imported in the 1980s from the United Kingdom, most from the Medical Research Council colony in Edinburgh, Scotland. Animals were initially bred from within the colony at Queen Elizabeth Hospital, and subsequently imported from the national marmoset-breeding colony within Australia.

2.3.2. *Marmoset colony maintenance*

The local Animal Ethics Committee (AEC) closely oversees the colony; currently this is the SA Pathology/Central Adelaide Health Network AEC. The AEC approved all procedures involving animals. The research described herein adheres to the American Society of Primatologists principles for the ethical treatment of non-human primates.

Maintenance of the colony is in accordance with guidelines set by the National Health and Medical Research Council (NHMRC) of Australia, as described in the *NHMRC Policy on the Care and Use of Non-human Primates for Scientific Purposes 2003*.⁵⁵⁴

The animals are monitored and observed daily, weighed regularly and any signs of illness or abnormal behaviour are identified. They have a diet of water ad libitum, fruit, vegetables, bread, mealworms, egg, marmoset pellets, supplemented with multivitamin and Vitamin D₃ and have access to daily outside runs. Standard operating procedures are in place for enclosure maintenance, diet, health checks, and environmental enrichment, as developed by Animal House staff with veterinary advice and input where necessary.

2.3.3. *Ethical clearance*

Procedures for marmoset colony maintenance and peripheral blood sampling were approved by the SA Pathology/Central Adelaide Health Network AEC. The current project approval is *68/11 - General Marmoset Colony Maintenance*; this expires on 31/8/2014.

All experimental procedures involving animals described in this thesis were approved by the SA Pathology/Central Adelaide Health Network AEC, and separately by the University of Adelaide AEC. The project approvals were: *The potential of donor derived dendritic cells to induce tolerance in common marmoset monkeys* (Project approvals 70/09 and M-2009-086 – both expiry dates 30 June 2012); and *Pre-clinical studies to investigate the use of liposomes to target dendritic cells in common marmoset monkeys* (Project approvals 68/11 – SA Pathology AEC, expiry 31/8/2013; and M-2011-167 – University of Adelaide AEC, expiry 31/1/2013).

2.3.4. Peripheral blood sampling

Between 0.2 and 2.0ml of peripheral blood was obtained via femoral venepuncture at any one time. Maximum blood loss was kept at a level less than 10ml/kg/month per animal. Animals bled frequently were given supplemental liquid iron to prevent anaemia.

The procedure for venepuncture was as follows:

- (1) Wear gown, gloves, hat and eye protection.
- (2) Catch marmoset and place in metal transport box; move to procedure room.
- (3) Remove monkey and place in harness with legs secured by Velcro straps.
- (4) Feed monkey yoghurt or banana during procedure.
- (5) Swab femoral region with 70% ethanol.
- (6) Using 27.5-gauge needle with syringe, draw 1ml of blood from femoral vein.
- (7) Remove needle and place pressure on site for 3-5 minutes.
- (8) If required, further blood could be collected from the contralateral femoral vein.
- (9) Check for any signs of bleeding once leg is removed from straps, and again before returning monkey to cage.

2.3.5. Urine collection and analysis

Urine was collected for dipstick analysis by catching the marmoset and holding over a clean metal tray. Urine samples (typically several drops only) were analysed by collecting with a syringe from the tray and transferring the sample onto a Multistix 10SG urinalysis testing strip (Bayer).

2.3.6. Euthanasia

Euthanasia was performed under isoflurane inhalational general anaesthesia via cardiac puncture and exsanguination. In these cases, full autopsy was performed and organs and tissues were collected and snap frozen or stored in formalin depending on planned usage. Blood and urine (where possible, via bladder puncture) were also collected and samples sent for SA Pathology laboratory analysis or processed for cell culture or other usage as required.

Appropriate tissue scavenging protocols were followed whenever euthanasia was performed, consistent with the NHMRC endorsed principles of replacement, reduction and refinement.

2.4. Cell culture protocols

2.4.1. Washes

All washes were performed in 10-50ml volumes by centrifuging at a relative centrifugal force (RCF) of 400-450g for 7 minutes at 4°C or room temperature, and decanting the supernatant unless otherwise specified.

2.4.2. Marmoset

2.4.2.1 Growth factor mobilisation of marmoset peripheral blood monocytes and haematopoietic progenitor cells

In order to maximise the yield of monocytes and/or haematopoietic progenitors from the peripheral blood of marmosets, recombinant human G-CSF (Lenograstim, AMGEN Corporation) was used to mobilise these cells into the circulation in DC propagation experiments. 10-15µg/kg/day was administered subcutaneously to marmosets for 5 days, as described in Prasad et al.⁴⁰³ No adverse effects were observed.

2.4.2.2 Peripheral blood mononuclear cell (PBMC) isolation

Whole blood (WB) was collected from non-mobilised or G-CSF mobilised animals via femoral venepuncture (as described under section 2.3.4) into 1ml lithium heparin paediatric blood collection tubes. WB samples of 300-1500µl volume were transferred into 10ml tubes; blood tubes were rinsed with PBS supplemented with 10% FCS (v/v) to ensure maximal WB retrieval. Blood was diluted up to 7ml volume with PBS, and underlaid with 2ml of Ficoll-PaqueTM Plus (Amersham Biosciences/GE Healthcare). Density gradient separation of marmoset PBMCs was performed by centrifuging the tubes at 800g for 25 minutes at 22°C, without braking. The PBMC layer was carefully collected and washed 2-3 times with PBS with 1% FCS. Contaminating red cells were removed by re-suspending the cell pellet in 2ml of warmed cell lysis buffer, incubating at 37°C for 5 minutes, and washing a further 3 times. Cells were resuspended in CM, RPMI-1640 or PBS/FCS, depending on planned usage. Viability and cell count were assessed with trypan blue (Sigma Aldrich) staining and a haemocytometer.

2.4.2.3 In vitro propagation of marmoset monocyte-derived dendritic cells (MoDC)

MoDC were propagated in vitro from G-CSF mobilised marmoset monocytes isolated from PBMC (as per section 2.4.2.2), as previously described.^{195,403}

Monocytes were isolated by plastic adherence as follows: marmoset PBMC (up to 2×10^6) were incubated in 6-well plates in 2ml of RPMI-1640 with 1% FCS for 90 minutes in a humidified incubator at 37°C, with 5% CO₂. Non-adherent cells were removed from plates or flasks by washing with PBS.

Immature MoDC were generated by culturing adherent cells for 6-7 days in CM supplemented with 40ng/ml (400U/ml) of IL-4 and 800U/ml of GM-CSF.

2.4.2.4 In vitro propagation of marmoset haematopoietic progenitor derived DC (HPDC)

Marmoset PBMC were isolated as per section 2.4.2.2. Non-enriched bulk PBMC were used as a source of CD34+ haematopoietic progenitor (HP) cells, as described by Prasad et al.⁴⁰³ PBMC ($0.5-1 \times 10^6$ /ml) were cultured in CM supplemented with Flt3L (100ng/ml), SCF (100ng/ml) and TPO (50ng/ml), adapted from human protocols,^{196,197} for up to 4 weeks. Media and cytokines were refreshed once or twice weekly by 50-100% replacement, and cells adjusted to $1-2 \times 10^6$ /ml. After 3-4 weeks in culture, HP cells were removed, washed several times and cultured further in CM supplemented with IL-4/GM-CSF (as for MoDC, per section 2.4.2.3) for 7 days.

2.4.2.5 Obtaining marmoset splenocytes for cell culture

Fresh marmoset spleens (whole or partial depending on planned experimental use) were collected at euthanasia and placed immediately in cold RPMI. Spleens were cut into small pieces on a petri dish and flushed through a 70µm cell strainer (BD) with RPMI into a 50ml tube using a sterile syringe plunger. The cell suspension was topped up with CM (10% FCS) and centrifuged at 450g for 7 minutes at 4°C, and washed a further 2 times with PBS/1% FCS. Contaminating red blood cells were removed by re-suspending the cell pellet in 2-5ml of warmed cell lysis buffer, incubating at 37°C for 5 minutes, and washing a further 3 times. Cells were counted before being resuspended at a density of 1×10^7 /ml in CM, or other media depending on planned usage.

2.4.2.6 Mixed leukocyte reaction (MLR)

2.4.2.6.1 One-way MLR

Allogeneic animals were chosen by *Caja*-DRB genotyping, which has been previously described and performed on all animals in the colony.^{401,402} PBMC were isolated from non-mobilised marmosets; stimulator PBMC from one animal were subjected to 30Gy irradiation. 1×10^5 cells from each animal were co-cultured in triplicate wells in a 96 well plate at 37°C in 5% CO₂ for 5 days. To obtain baseline data, 1×10^5 PBMC from each animal were also cultured alone. In the final 18-24 hours of incubation, each well was treated with 1µCi of tritiated thymidine ([³H] thymidine; Amersham Biosciences/GE Healthcare). Cells were harvested using a Tomtec Harvester 96 Mach III M (Tomtec). T-cell proliferation via [³H] thymidine incorporation was determined in a liquid scintillation counter (Wallac Oy Microbeta® Trilux1450, Perkin Elmer) and expressed as a mean (of replicate samples) counts per minute (cpm) ± SD. Allo-reactivity was confirmed if there was evidence of T-cell proliferation when cells from animals were cultured together, i.e. if the mean cpm (combined cells A and B) was significantly greater than the mean cpm (cells A) + mean cpm (cells B). The proliferative response was represented as the stimulation index (SI) = (mean cpm stimulation PBMC / mean CPM unstimulated PBMC). Statistical comparison between groups was performed using Student's t test, with p<0.05 deemed to be significant.

2.4.2.6.2 Dendritic cell MLR

DC were obtained as per sections 2.4.2.3 and 2.4.2.4 above. Allogeneic PBMC from animals chosen by *Caja*-DRB genotyping; or xenogeneic PBMC from random human buffy coats (section 2.4.3.1) were used as responder cells. Stimulator DC were subjected to 30Gy irradiation. DC were co-cultured with 1×10^5 allogeneic PBMC or Xenogeneic human PBMC in a 1:10 ratio in triplicate for 5 days. DC and PBMC were also cultured alone for baseline data. T-cell proliferation was determined as described in section 2.4.2.6.1. Statistical comparison between groups was performed using Student's t test, with p<0.05 deemed to be significant.

2.4.3. Human

2.4.3.1 Human peripheral blood mononuclear cell (PBMC) isolation

Buffy coats from healthy blood donors were obtained from the Australian Red Cross Blood Service (301 Pirie Street, Adelaide SA 5000). All samples were de-identified. 10-13ml of buffy coat WB was transferred into 50ml tubes, diluted up to 35ml with PBS and underlaid with 10-12ml of Ficoll-PaqueTM Plus. Density gradient separation of human PBMCs was performed by centrifuging the tubes at 600g for 20 minutes at 20-22°C without braking. The PBMC layer was carefully collected and washed 2-3 times with PBS. Contaminating red cells were removed by re-suspending the cell pellet in 1-2ml of warmed cell lysis buffer, incubating at 37°C for up to 5 minutes, and washing a further 3 times. Cells were resuspended in CM, RPMI-1640 or PBS/FCS, depending on planned usage. Viability and cell count were assessed with trypan blue staining and a haemocytometer.

2.4.3.2 In vitro propagation of human MoDC

MoDC were propagated in vitro from human monocytes isolated from PBMC (as per section 2.4.3.1), as previously described.^{195,403}

Monocytes were isolated by plastic adherence as follows: human PBMC (up to 5×10^7) were incubated in 75cm² flasks in 10ml of RPMI-1640 with 1% FCS in a humidified incubator at 37°C, with 5% CO₂ for 45-60 minutes. Non-adherent cells were removed from plates or flasks by washing with PBS.

Immature MoDC were generated by culturing adherent cells for 6-7 days in CM supplemented with 40ng/ml (400U/ml) of IL-4 and 800U/ml of GM-CSF. In some experiments, LPS (10ng/ml) was added as a maturation stimulus on day 5, and cells were cultured for a further 2 days to generate mature MoDC.

2.4.3.3 Generation of nylon wool T-cells (NWT)

Bulk human PBMC were used as a source of T-cells without the use of plastic adherence. After extensive washing with PBS, PBMC were adjusted to a density of 1×10^8 in 3ml of CM (10% FCS). Autoclaved nylon wool columns were pre-wetted with RPMI-1640, covered with parafilm, and placed in a 37°C incubator until equilibrated

(30 minutes or longer). PBMC (maximum 3ml/column) were added to the column to adsorb B cells, the ends were re-covered with parafilm and placed in the incubator for 30 minutes. T-cells were eluted from the column using 13ml of pre-warmed CM, counted, centrifuged, and resuspended at the desired concentration.

2.4.3.4 Mixed leukocyte reaction (MLR)

2.4.3.4.1 Dendritic cell MLR

DC were obtained as per section 2.4.3.2 above, collected from flask supernatant, washed 3 times with PBS and resuspended at 2×10^5 /ml in CM. Stimulator DC were subjected to 30Gy irradiation. DC were co-cultured with 1×10^5 allogeneic NWT at a 1:10-1:1000 ratio in quintuplicate in a 96-well plate (total volume 200 μ l) for 5 days. DC and NWT were also cultured alone to establish baseline proliferation. In the final 18-24 hours of incubation, each well was treated with 1 μ Ci of tritiated thymidine ($[^3\text{H}]$ thymidine). T-cell proliferation was determined as described in section 2.4.2.6.1 above. Statistical comparison between groups was performed using Student's t test, with $p < 0.05$ deemed to be significant.

2.4.3.4.2 Two-way MLR

PBMC were isolated from buffy coats as per section 2.4.3.1 above. 1×10^5 cells from each of 2 allogeneic donors were co-cultured in quintuplicate in a 96 well plate (total volume 200 μ l) for 5 days. Cells were not irradiated. To obtain baseline data, 1×10^5 PBMC from each donor were also cultured alone. In the final 18-24 hours of incubation, each well was treated with 1 μ Ci of tritiated thymidine ($[^3\text{H}]$ thymidine). T-cell proliferation and statistical analyses were performed as described in sections 2.4.2.6.1 and 2.4.3.4.1 above.

2.4.4. Cryopreservation of cells

Where necessary, fresh or cultured cells were cryopreserved at a density of up to 1×10^7 cells per vial for cell lines, and up to 5×10^7 cells per vial for primary cells. RPMI-1640 was supplemented with 20% FCS (v/v); a portion of this solution was supplemented with 20% v/v DMSO (Chem-Supply). Cells were suspended in 900 μ l of RPMI with 20% v/v FCS per vial, and an equal volume of RPMI-FCS-DMSO was added slowly drop-wise to the cells while shaking the tube. 1.8ml of the cell suspension was added to

each cryopreservation vial, and vials were frozen in an isopropanol controlled freezing container placed overnight in a freezer at -80°C . For long-term storage, vials were transferred to liquid nitrogen or kept at -80°C .

When cryopreserved cells were required for experimental use, they were removed from storage and the vial was placed immediately in a 37°C water bath. When the cell suspension was just visibly thawed, the vial was removed from the water bath and cells were placed in a sterile tube. DMSO was diluted out of solution slowly by adding 10ml of cold RPMI-1640 slowly over a period not less than 5 minutes, while shaking the tube. Cells were washed with RPMI-1640 for 7 minutes at 450g, counted and resuspended into PBS or media depending on planned usage.

2.5. Immunofluorescence and microscopy

Tissues were snap frozen and embedded in OCT (Tissue-Tek®, Sakura), and stored at -80 degrees. When required, tissues were sectioned at 3-4µm using a cryostat, placed onto slides and fixed in cold acetone for 5 minutes. In other experiments, cytopsin samples of cultured cells were prepared from an aliquot of cells resuspended in RPMI supplemented with 10% v/v FCS at a density of 2.5×10^5 cells/ml. Cells (200µl) were immobilised onto glass microscope slides using a Shandon Cytospin (Thermo Scientific) and centrifuged at 300rpm for 5 minutes, before being air dried and fixed with cold acetone for 5 minutes.

Slides were air-dried and washed with PBS. If required, slides were incubated with the appropriate cross-reactive directly conjugated mouse anti-human antibody for 30 minutes, before being washed twice with PBS. Nuclei were counterstained with 60nM 4',6-diamidino-2-phenylindole dihydrochloride (DAPI, Molecular Probes) for up to 5 minutes. Slides were washed again in PBS, mounted with fluorescent mounting medium (DAKO), imaged using structured illumination microscopy on a Zeiss Apotome microscope (Carl Zeiss Pty Ltd), and photographed.

During cell culture experiments, cells were regularly observed in culture using light microscopy. Cells were also prepared on glass slides by cytopsin centrifugation as in above and stained with May-Graunwald Giemsa stain, kindly prepared and processed by the Haematology Laboratory, SA Pathology (Queen Elizabeth Hospital). Cytopsin slides were then viewed and photographed.

2.6. Flow cytometry

Cell samples were resuspended in staining buffer (usually 10^5 - 10^6 cells/100 μ l), blocked with 10% v/v heat inactivated rabbit serum (ICN Pharmaceuticals), and incubated for 20 minutes at 4°C. Samples were aliquotted into polypropylene FACS tubes and incubated with appropriate amounts of monoclonal antibodies for 20 minutes in the dark at 4°C. Cells were fixed at room temperature with 10% FACS lysing solution (BD Pharmingen), 2ml/tube, and washed twice in staining buffer, and resuspended in filtered saline (0.15 M NaCl). All flow cytometry was performed using a FACS Canto II flow cytometer (BD Biosciences) and analysed using and FCS Express software version 3 (De Novo Software). In most cases, 10,000 to 20,000 events were recorded. Data are reported in comparison to isotype-matched controls; compensation samples were not required.

In addition, where multiple colour staining was used, overlap of fluorescence between detection channels was compensated for at the start of each experiment, using monoclonal antibodies with the highest fluorescence for each channel and a small portion of the sample to be tested. Data are reported in comparison to isotype-matched controls; in some experiments, fluorescence minus one (FMO) controls were also used.

2.7. Molecular biology techniques: cloning of marmoset and human DC-SIGN

2.7.1. Cloning of marmoset and human DC-SIGN

2.7.1.1 Polymerase chain reaction (PCR)

Oligonucleotides used for cloning were synthesised by Sigma Aldrich. PCR was performed in a 50µL reaction mix, using AmpliTaq Gold® PCR Master Mix (Applied Biosystems), forward and reverse primers (0.5mM at final concentration, Geneworks), relevant cDNA (1µL), and sterile water. The reaction master mix was prepared in a DNA-free room, and cDNA added last. Two drops of sterile mineral oil (Sigma Aldrich) were added to prevent evaporation. All reactions were performed in a Perkin Elmer Cetus DNA thermocycler (Perkin Elmer), and amplification began with 10 minutes pre-heating at 95°C, denaturation for 30 seconds at 95°C, annealing for 30 seconds at 65-68°C (dependent on the calculated T_M of the relevant primers), and extension for 1 minute at 72°C, for 40 cycles. The presence of PCR product was confirmed with 2% agarose gel electrophoresis (see section 2.7.1.2). PCR product was purified using DNA Clean and Concentrator-5 kit (Zymo Research). The amount of DNA was quantitated using a NanoDrop 1000 spectrophotometer (Thermo Scientific).

2.7.1.2 Agarose gel electrophoresis

To confirm the presence of appropriate products after PCR (or digestion of plasmids, see below), 2.5µL of 6x loading buffer was mixed with 12.5µL of the PCR product and electrophoresed through 2% w/v agarose (Amresco) gels using a Bio-Rad Minigel apparatus (Bio-Rad). However, products for gel extraction were run on 1% w/v agarose gels. SPP1/EcoRI (Geneworks) was used as a DNA molecular weight marker; 2µL was mixed with 2.5µL of 6x loading buffer and 10µL of water. All samples were loaded onto the gel and electrophoresed at 85V for approximately 90 minutes. Gels were stained with GelRed™ (Biotium) solution for 10 minutes and photographed under UV illumination using the InGenius gel documentation system (Syngene).

2.7.1.3 Ligation of DNA fragments into cloning vectors

As the quantity of PCR products was insufficient for immediate sequencing, products were ligated into the cloning vector pGEM®-T easy (Promega). Ligation reactions were set up as per Table 2.7.1 and incubated for 2 hours at room temperature. Approximately 30ng of PCR product DNA (marmoset or human DC-SIGN) was used in each reaction.

Table 2.7.1. Ligation reaction for pGEM®-T easy vector

Ligation reaction	
PCR product	X μ L (up to 5 μ L)
2x rapid ligation buffer	5 μ L
pGEM®-T easy vector	1 μ L (50ng)
T4 DNA ligase	1 μ L
Sterile water	to 10 μ L

2.7.1.4 Transformation of competent *E. coli* cells

DH5 α competent *Escherichia coli* (*E. coli*) cells (Invitrogen) were thawed on ice; 5 μ L of ligation mix (section 2.7.1.3) was added immediately and incubated for 30 minutes. Following incubation, cells were heat-shocked for 20 seconds at 42°C, placed on ice for 2 minutes, supplemented with 950 μ L of pre-warmed SOC medium (Sigma Aldrich) and incubated at 37°C with continuous shaking at 225rpm for 1 hour. Two hundred millilitres (200 μ L) of transformed cells were plated onto pre-warmed LB-agar (Oxoid Ltd) plates containing ampicillin 50 μ g/ml (Boehringer Ingelheim Ltd), Xgal (5-bromo-4-chloro-3-indolyl-beta-D-galactopyranoside) 40 μ g/ml (Amresco), and IPTG (isopropyl β -D-1-thiogalactopyranoside) 0.2mM (Amresco), and incubated overnight at 37°C. Uncut plasmid with no insert and/or pUC19 DNA was used as a positive control to demonstrate transformation efficiency, whilst untransformed *E. coli* cells served as a negative control.

White recombinant colonies containing inserts were selected, resuspended in 2mL LB with ampicillin (50-100 μ g/ml) and incubated overnight at 37°C, 225rpm. Plasmid DNA

was prepared using the Zyppy Plasmid Miniprep kit (Zymo Research) and digested with the restriction enzyme *NotI* (New England Biolabs) at 37°C for 1 hour in a 10 µL reaction along with associated buffer (Buffer 3), 10x BSA and sterile water, to release the DNA inserts. Digested plasmid was loaded onto a 2% agarose gel and run at low voltage; DNA was visualised by Gel Red (Biotium) staining.

Sequencing was performed on four plasmid clones (2 each of marmoset DC-SIGN and human DC-SIGN from independent PCR reactions) to confirm that the correct sequences were obtained (Sequencing facility, Department of Haematology, Flinders Medical Centre, Adelaide, Australia). Standard primers (T7 and SP6) for pGEM®-T easy were used. Sequences were aligned with published sequences for marmoset and human DC-SIGN (GenBank accession numbers EU_041929.1 and NM_021155, respectively) using Vector NTI software (Invitrogen).

2.7.2. Transfection of CHO cell line with marmoset or human DC-SIGN

Due to the low level of DC-SIGN expression on propagated marmoset DC, and the difficulty in obtaining sufficient numbers of these cells, a CHO cell line was transfected with marmoset (and human) DC-SIGN to facilitate screening of a panel of monoclonal antibodies for binding to marmoset DC-SIGN.

2.7.2.1 Cell lines

Chinese Hamster Ovary (CHO) cells (American Type Culture Collection) were grown in CM until >90% confluence was achieved. At this time, cells were detached using trypsin/EDTA solution 0.25%/0.125% (Sigma Aldrich) and washed in PBS containing 5% v/v FCS. Cells were counted and used to seed an appropriate number of flasks, depending on experimental requirements. All cells were incubated at 37°C in 5% CO₂.

2.7.2.2 Generation of pCI mammalian expression vector containing DC-SIGN

The mammalian expression vector pCI (Promega) was prepared by *NotI* (New England Biolabs) restriction enzyme digestion (incubated for 1 hour at 37°C) with associated buffer (Buffer 3), 10x BSA and sterile water, followed by dephosphorylation with calf intestinal alkaline phosphatase (ALP, Promega). The correct sequence of marmoset or human DC-SIGN was ligated into the cloning vector pGEM®-T easy (Promega), used

to transform *E. Coli* DH5 α competent cells and plated onto LB-agar plates (containing ampicillin, Xgal and IPTG), followed by plasmid preparation (as described in sections 2.7.1.3 and 2.7.1.4). Plasmid DNA was prepared by *NotI* (New England Biolabs) restriction enzyme digestion and the product run on a 1% agarose gel at low voltage. The product was purified from the gel using DNA Gel Recovery Kit[®] (Zymo Research); the amount of DNA obtained was quantified with the NanoDrop 1000 spectrophotometer.

Purified cloned marmoset or human DC-SIGN was sub-cloned into the pCI expression vector at a 1:1 ratio, and used to transform *E. coli* DH5 α competent cells and plated onto LB-agar plates containing ampicillin 50 μ g/ml. After overnight culture, white colonies were selected, each was placed into 2mL LB culture (with ampicillin 100 μ g/ml) and incubated again overnight at 37°C at 225rpm. Plasmid DNA was obtained (Zyppy Plasmid Miniprep Kit[®]), from a sample of the culture. Correct size and orientation of the DNA insert in the pCI expression vector were confirmed by digestion with *NotI*, and with *XmaI/ApaI* (New England Biolabs), followed by agarose gel electrophoresis. LB broth culture samples (1mL) of *E.coli* containing the correct pCI-DC-SIGN plasmids (and pCI without an insert as control) were used in larger volume LB broth overnight cultures (with ampicillin 100 μ g/ml) in order to generate sufficient quantities of Plasmid DNA. A Zyppy Maxiprep kit (Zymo Research) was used to prepare the plasmid DNA following culture, and the amount of DNA was quantitated using the NanoDrop 1000 spectrophotometer.

2.7.2.3 Cell line transfection

Plasmid DNA of the pCI mammalian expression vector containing marmoset or human DC-SIGN were used to transfect an established Chinese Hamster Ovary (CHO) cell line using Lipofectamine[™] 2000 (Invitrogen) according to the manufacturer's instructions. Expression vector without inserted DNA was also used for generating control CHO cell transfectants. Cells were incubated for 24-48 hours in CM following transfection, and collected using trypsin/EDTA 0.25%/0.125% (Sigma Aldrich). Trypsin activity was neutralised with neat FCS and cells were washed twice in CM prior to use.

2.8. Manufacturers

Agilent Technologies – Santa Clara, CA, USA
Ajax Finechem – Seven Hills, NSW, Australia
American Reagent – Sharley, NY, USA
American Type Culture Collection – Manassas, VA, USA
Amersham Biosciences (now GE Healthcare) – Brown Deer, WI, USA
AMGEN Corporation – Thousand Oaks, CA, USA
Amresco – Solon, OH, USA
Applied Biosystems – Scoresby, VIC, Australia
Avanti Lipids – Alabaster, AL, USA
Bayer – Leverkusen, Germany
BD Medical – North Ryde, NSW, Australia
BD, BD Biosciences, and BD Pharmingen – Franklin Lakes, NJ, USA; San Jose, CA, USA
Beckman Coulter – Hialeah, FL, USA
Bio-Rad laboratories – Hercules, CA, USA
Biotium – Hayward, CA, USA
Boehringer Ingelheim Ltd – Ingelheim am Rhein, Germany
Buchi Labortechnik – Flawil, Switzerland
Capitol Scientific – Austin, TX, USA
Carl Zeiss Pty Ltd – Oberkochen, Germany
Chem-Supply – Gillman, SA, Australia
Chemicon (now Millipore) – Bedford, MA, USA
DAKO – Glostrup, Denmark
DeNovo Software – Thornhill, Ontario, Canada
eBioscience – San Diego, CA, USA
Electron Microscopy Sciences – Fort Washington, PA, USA
Geneworks – Thebarton, SA, Australia
Gibco BRL – Geithersburg, MD, USA
GraphPad Software Inc. – La Jolla, CA, USA
Greiner Bio-One – Monroe, NC, USA
Hitachi – Tokyo, Japan
ICN Pharmaceuticals – Costa Mesa, CA, USA
Immunotech – Prague, Czech Republic; Marseilles, Cedex, France
Invitrogen – Melbourne, VIC, Australia
JRH Biosciences – Lenexa, Kansas, USA

Laysan Bio Inc – Alabama, USA
Lipoid – Ludwigshafen, Germany
Malvern Instruments – Worcestershire, United Kingdom
May & Baker – West Footscray, VIC, Australia
Mercordia – Uppsala, Sweden
Micro Star Technologies – Huntsville, TX, USA
Microsoft Corporation – Redmond, WA, USA
Microtek – Carson, CA, USA
Molecular Probes – Eugene, OR, USA
MutiCel Trace Scientific – Clayton, VIC, Australia
Neubody (now Biosensis) – Thebarton, SA, Australia
New England Biolabs – Ipswich, MA, USA
Nunc Nalge International – Naperville, IL, USA
Olympus – South-end-on-Sea, Essex, United Kingdom
Oxoid Ltd – Hampshire, United Kingdom
PerkinElmer – Waltham, MA, USA
Pfizer Australia – West Ryde, NSW, Australia
Pierce Biotechnology (now ThermoFisher)– Rockford, IL, USA
PolysciTech – West Lafayette, IN, USA
Promega – Madison, WI, USA
R&D Systems – Minneapolis, MN, USA
Sakura – Flemington, The Netherlands
Sandoz – Pyrmont, NSW, Australia
Sigma-Aldrich – St Louis, MO, USA;
Sorvall – Newtown, CT, USA
Southern Biotech – USA
Statacorp – College Station, TX, USA
Syngene – Cambridge, United Kingdom
Thermo Fisher Scientific – Middletown, VA, USA
Thermo Scientific – Rockford, IL, USA
Tomtec – Hamden, CT, USA
Zymed (now Invitrogen) – Camarillo, CA, USA
Zymo Research – Orange, CA, USA

**Chapter 3: ESTABLISHING THE
BASIS FOR A MARMOSET RENAL
TRANSPLANT MODEL:
CHARACTERISATION OF MARMOSET
RENAL HISTOLOGY AND
CORRELATION WITH SERUM AND
URINARY FINDINGS**

Acknowledgment

In the studies presented in Chapter 3, several others contributed to the work described. Dr Natasha Rogers contributed to the assessment of biopsies, initial data analysis, and preparing an initial draft manuscript. John Brealey (SA Pathology) processed and photographed the electron microscopy samples, and obtained the measurements of GBM thickness. A manuscript presenting data from the studies in Chapter 3 is currently in preparation:

- Collins MG, Rogers NM, Jesudason S, Kireta S, Brealey J, and Coates PT. Spontaneous glomerular mesangial lesions in common marmoset monkeys (*Callithrix jacchus*): a benign non-progressive glomerulopathy [Manuscript in preparation].

In all other respects the work presented is the original work of the author.

3.1. Introduction

In the field of transplantation, many promising approaches to tolerance have been developed in small animal models, but relatively few have translated to the human clinical setting. The lesser degrees of complexity of the immune systems of lower order species, and their relative lack of environmental exposure to antigen and thus immunological memory, i.e. so-called heterologous immunity,^{42,43} make it considerably easier to successfully induce tolerance in small animal laboratory models such as the mouse and rat. It is thus necessary to confirm data on experimental therapies from these small animal models in larger, more complex species such as pigs, sheep or NHP, to establish suitability for human trials. The close similarity between NHP and humans mean that findings in NHP tolerance models are the most likely to be clinically applicable and relevant,³⁹ and thus most likely to closely reflect the situation in clinical human disease.

The common marmoset, *Callithrix jacchus*, is a New World monkey that has been used in laboratory research studies in the areas of fertility,⁵³⁵ autoimmune disease,^{522,525} hypertension,⁵³² toxicology,^{555,556} and drug screening.^{527,528} Marmosets retain important similarities to humans in terms of genetic homology, anatomy, disease profile and other biological features, while possessing many of the cost and maintenance advantages of small animal models.⁵⁰⁷ Their small size promotes ease of animal husbandry, they are not endangered, and they have a relatively rapid generational turnover.⁵⁵⁵ In a significant recent advance, transgenic marmosets have been successfully produced, and thus it is likely that the marmoset will become of increasing interest as a biomedical research model.⁵⁵⁷

A focus of the work of this laboratory, and this thesis, is the development of a marmoset model of transplantation that might be utilised to test the tolerogenic potential of dendritic cell based immunotherapies. As a pre-requisite for this work, a broad range of techniques have been developed including the rapid genotyping of marmoset MHC class II genes,^{401,402} the propagation of DC from precursors in bone marrow or peripheral blood,^{399,403} the establishment of the cross-reactivity of human or NHP specific reagents with marmoset samples,^{517,520} and normal ranges for key

haematological parameters. Another essential component of this model will be the establishment of a kidney (or other organ) transplant model.

Spontaneous renal lesions have been reported in a range of Old World⁵⁵⁸⁻⁵⁶⁰ and New World primates,⁵⁶⁰⁻⁵⁶⁴ including the common marmoset monkey.^{541-548,550,551,565} The nature of these have not been fully characterised but in some cases they have been attributed as a significant cause or contributor to the death of these primates. In the case of marmosets, the wasting marmoset syndrome,⁵⁶⁶ characterised by a chronic lymphocytic enteritis associated with a glomerulopathy and clinically presenting with failure to thrive, weight loss, generalised weakness and diarrhoea has been thought to have parallels to the human diseases IgA nephropathy and coeliac disease.⁵⁵⁰ It has not been established whether these histologically observed findings are specifically associated with renal failure or urinary abnormalities, however, and some investigators have proposed that the renal lesions may be a feature of normal marmoset ageing.⁵⁶⁵

In order to establish the feasibility of the marmoset as a potential kidney transplant model, it is therefore necessary to characterise further the nature of this reported spontaneous renal pathology.

The aims of this chapter are:

1. To characterise the nature of spontaneous renal pathology that occurs in marmoset monkeys using histology, immunofluorescence, electron microscopy, and serum and urine biochemistry, in both healthy animals euthanized in the course of experimental studies, and those euthanized for weight loss.
2. To determine whether the observed findings would be likely to have any impact on the suitability of using marmoset monkeys in a model of kidney transplantation.

3.2. Methods

3.2.1. Animals

Details of the animal procedures used in this chapter, marmoset colony maintenance, and ethical clearance are described in Chapter 2 (section 2.3), and also below.

Marmoset tissue, blood and urine samples for this study were collected during the period 2003 to 2012.

3.2.1.1 Peripheral blood sampling

Between 0.2 and 2.0ml of peripheral blood was obtained via femoral venepuncture at any one time. Maximum blood loss was kept at a level less than 10ml/kg/month per animal. Animals bled frequently were given supplemental liquid iron to prevent anaemia.

3.2.1.2 Urine collection and analysis

Urine was collected for dipstick analysis by catching the marmoset and holding over a clean metal tray. Urine samples (typically several drops only) were analysed by collecting with a syringe from the tray and transferring the sample onto a Multistix 10SG urinalysis testing strip (Bayer). Urine analysis was performed using on clean catch samples on a periodic basis every 2-3 years among animals remaining in the colony.

3.2.1.3 Euthanasia

Euthanasia was performed under isoflurane inhalational general anaesthesia via cardiac puncture and exsanguination. In these cases, full autopsy was performed and organs and tissues were collected and snap frozen or stored in formalin depending on planned usage (in addition to this study). Blood and urine (where possible, via bladder puncture) were also collected and samples sent for SA Pathology laboratory analysis or processed for cell culture or other usage as required.

3.2.2. Evaluation of marmoset renal tissues

3.2.2.1 Histological analysis

Kidney tissue from euthanized animals was immersion-fixed in 10% formalin, embedded in paraffin, sectioned and stained with haematoxylin and eosin (HE) or Periodic Acid Schiff's (PAS) stain. Sections were assessed by two investigators (the candidate and Dr Natasha Rogers) as follows: (1) glomerular number and the presence of glomerular obsolescence were counted from 5 randomly selected cortical areas at 100x magnification; (2) the degree of mesangial expansion was assessed at 200x magnification in >20 glomeruli (where possible) from each section using a semi-quantitative scoring system (1 – normal; 2 – focal or mild changes; 3 – diffuse or moderate/severe changes)⁵⁴⁸; and (3) glomerular diameter was measured in 15 glomeruli from each section (where possible) at 20x magnification: two perpendicular measurements were performed and the mean was used. Glomeruli were included in the measurement analysis if the hilar vessels were visible and the two concurrent measurements differed by <30µm.

To validate that mesangial scoring was consistent between investigators, a subset of the sections were independently and blindly assessed by both investigators and scores were compared; in these cases composite results are reported.

3.2.2.2 Immunofluorescence

Kidney tissue was frozen in OCT and sectioned at 3-4µm in the cryostat, placed onto slides and fixed in cold acetone for 5 minutes. Air-dried slides were washed in phosphate buffered saline (PBS) and the appropriate cross-reactive rabbit polyclonal anti-human FITC conjugated antibody (IgG, IgM, IgA, C3, or appropriate negative control, 1:10 dilution in PBS, all DAKO) was added for 30 minutes. Slides were washed twice with PBS, dried and mounted with a coverslip using 18.5µl sodium barbitone-buffered glycerol pH 8.6. Sections were examined using an Olympus BX40 microscope within 24 hours. Positive staining was graded using a standard semi-quantitative grading system (negative to 3+).

3.2.2.3 Electron microscopy

Marmoset kidney cortex was dissected into cubes of approximately 0.5mm in each dimension. Tissue cubes were fixed for at least one hour in EM fixative (4% formaldehyde and 1.5% glutaraldehyde in sodium cacodylate buffer, pH 7.2). Fixed tissue was post-fixed in 2% osmium tetroxide in sodium cacodylate buffer, *en bloc* stained with 2% uranyl acetate and dehydrated through 70%, 90% and 100% ethanol. Then, tissue was processed through 1,2-epoxypropane, a 50/50 mixture of 1,2-epoxypropane and Procure 812 resin (Electron Microscopy Sciences) and two changes of 100% resin. Tissue and resin were transferred to Beem capsules and placed in an oven overnight at 90°C.

Survey sections of tissue blocks were stained with Toluidine Blue. Areas of interest were thin-sectioned at approximately 100nm thickness on a Porter-Blum ultramicrotome (Sorvall) using a diamond knife (Micro Star Technologies). Sections were stained with Reynolds' lead citrate and examined in a Hitachi H-600 transmission electron microscope. All sections in the microscope were standardized using z-axis height adjustment. Magnifications were calibrated against a carbon-grating replica. Glomeruli were photographed at 2,000X magnification and negatives were developed using traditional photographic techniques. Negatives were coupled with a transparency grid (lines intersecting at 8mm intervals) and digitized at 400dpi using a ScanMaker 8700 (Microtek). Glomerular basement membrane (GBM) thickness was measured perpendicularly across the membrane. Tangentially sectioned GBM were not measured. Membranes were considered to be sectioned tangentially if either endothelial cell fenestrations or podocyte pedicles were visible *en face*. Additionally membrane material adjacent to mesangial cell cytoplasm was not measured. One hundred and fifty (150) measurements were taken per specimen and the data were imported to a GraphPad Prism statistical package (GraphPad Software) for analysis.

3.2.3. Assessment of blood and urine parameters

Renal function was assessed by measurement of serum creatinine using the Jaffe picric acid reaction (OSR 6178, Beckman Coulter); creatinine and other biochemistry were analysed on an Olympus AU640 autoanalyser (Beckman Coulter), by SA Pathology at The Queen Elizabeth Hospital (Adelaide, Australia). Measurements were compared to both human (as reported by the laboratory) and International Species Information

System (ISIS) Physiological reference ranges (www.isis.org).⁵⁶⁷ Animals showing evidence of glomerular staining for immunoglobulins had blood testing for anti-nuclear antibodies using the HEp-2 cell line method (SA Pathology, The Queen Elizabeth Hospital).

In addition to urine dipstick analysis for protein (section 3.2.1.2) urine protein was formally assessed using the benzethonium chloride method (Thermofisher Scientific) for some samples.

3.2.4. *Statistical analysis*

Results are presented as mean (standard deviation, SD), or median (interquartile range, IQR). Specific statistical tests performed are referred to in the relevant sections of the text. In all cases, an alpha level of 5% ($p \leq 0.05$) was used as the limit for statistical significance. All statistical tests were two-tailed.

Data were analysed and statistical analyses were performed using Microsoft Excel for Mac 2011 (Microsoft Corporation), GraphPad Prism version 6 for Mac OS X (GraphPad Software), or Stata version 11.2 (Statacorp).

3.3. Results

3.3.1. *Animals*

Renal tissue was obtained from 25 marmosets, 19 euthanized for research purposes (experimental group) and 6 for progressive weight loss (weight loss group). Mean age was 6.5 ± 3.2 years, and the weight loss group were a mean of 3.3 years older at the time of death ($p=0.040$; unpaired t test). Detailed histology, immunofluorescence, and electron microscopy data for each animal is shown in Table 3.3.1. Table 3.3.2 displays a summary of all the quantitative data.

3.3.2. *Histology*

There was negligible glomerular obsolescence ($<5\%$ of all visualised glomeruli) seen in all kidneys examined. The overall mean of the individual animal mean mesangial scores using the semi-quantitative grading system was 2.45 (standard deviation (SD) of the mean 0.18); the majority of glomeruli were scored as 2+ or greater (Table 3.3.1), representing moderate mesangial expansion. There was a small difference observed between the weight loss and experimental group scores (mean score difference 0.16; $p=0.05$), but this did not represent a pathologically relevant difference (Table 3.3.2). There was a 13% difference in the mean scores ($p<0.0001$) between investigators for the subset of validation biopsies analysed independently ($n=8$); however none of the mean scores differed by more than 20%.

Glomerular diameter measurements (Figure 3.3.2) varied within and between animals (Table 3.3.1 and Figure 3.3.3) with a range of 87-241 μm with an overall mean of individual animal means of 162 μm (SD 16 μm), and were approximately normally distributed (Figure 3.3.4). There was a difference in the mean diameter observed between the weight loss and the experimental groups (mean 149 μm versus 165 μm ; $p=0.0003$).

No other glomerular pathology was observed; specifically no segmental sclerosis, necrosis or crescents were seen. There was no significant interstitial fibrosis, lymphocytic infiltrations, tubular degeneration, haemosiderosis or extramedullary haematopoiesis seen.

3.3.3. Immunofluorescence

Immunofluorescence staining of glomeruli from a subset of marmoset monkeys (n=11) demonstrated IgM deposits in all kidneys (Table 3.3.1 and Figure 3.3.5). This was associated with positive staining for IgA and IgG and C3 deposition in some but not all cases. Not all monkeys had tissue sent for immunofluorescence during the 9-year time period of this study, for unknown reasons, and samples were only analysed where tissue was available.

Peripheral blood from 10 of these animals screened negative for antinuclear antibodies, using the HEp-2 cell line based method (SA Pathology).

3.3.4. Electron microscopy

Electron microscopic examination of glomeruli in 20 marmoset monkeys demonstrated electron dense mesangial deposits in 14 (70%) of animals, with a further 2 animals showing sparse deposits, i.e. evidence of deposits in 80% of monkeys (Table 3.3.1 and Figure 3.3.6). In some animals ischaemic changes were noted in some glomeruli but no other specific glomerular pathology was observed.

Assessment of glomerular basement membrane thickness in 23 marmoset monkeys (Figure 3.3.7, Table 3.3.1) showed normally distributed measurements ($p=0.52$; Shapiro-Wilk normality test), with an overall mean of 449nm (SD 69nm). No difference was observed between the experimental and weight loss groups ($p=0.71$; Table 3.3.2).

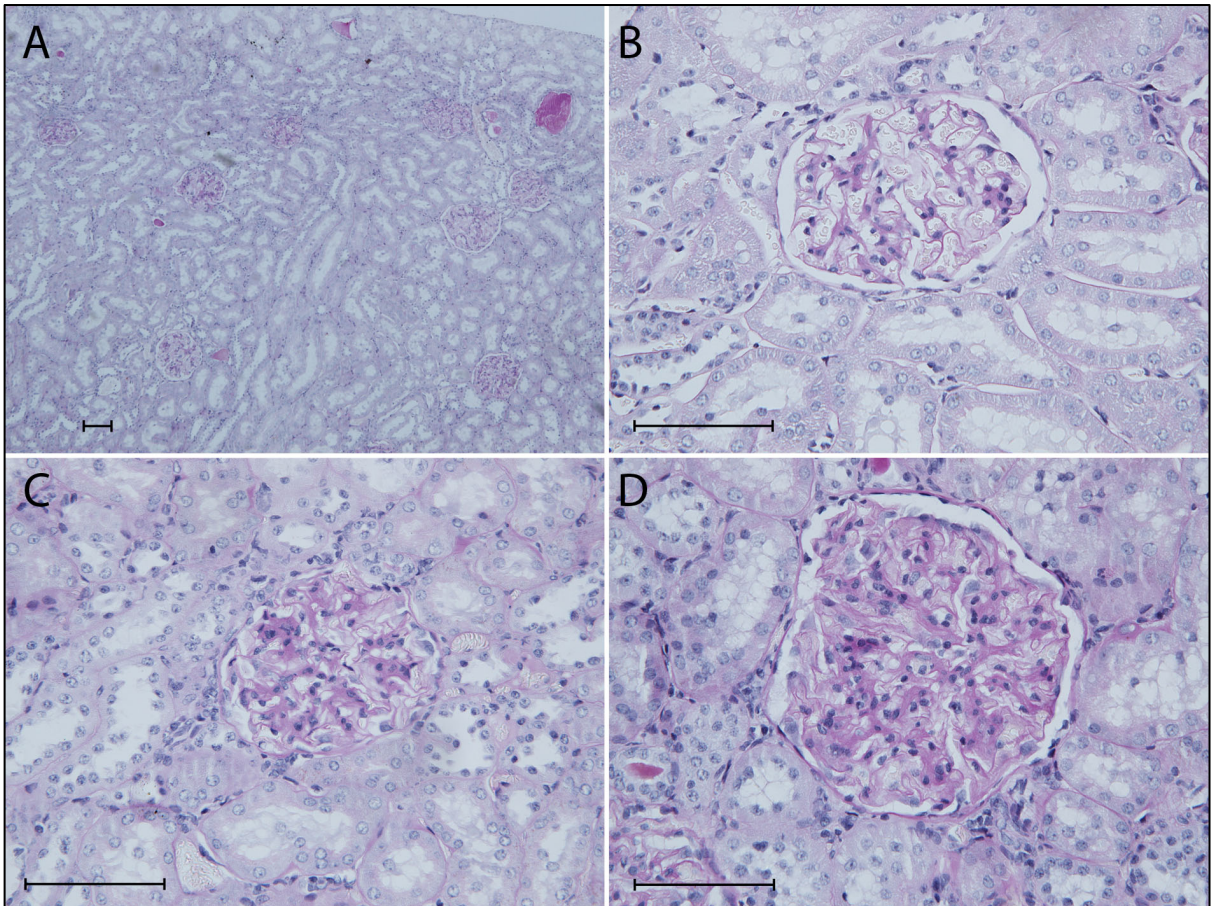


Figure 3.3.1. Representative marmoset kidney light microscopy images showing mesangial expansion and hypercellularity.

(A) Low power view of renal cortex; (periodic acid-Schiff; PAS) stain. Glomeruli show evidence of variable degrees of mesangial expansion and hypercellularity, without glomerular obsolescence. No significant interstitial fibrosis, lymphocytic infiltration, tubular degeneration, haemosiderosis or extramedullary haematopoiesis is seen. (B), (C) and (D) High power views of glomeruli showing examples of semi-quantitative grading of mesangial changes; PAS stain. (B) – Grade 1; no significant abnormality; (C) – Grade 2; mild-moderate and/or focal mesangial expansion/hypercellularity; (D) – Grade 3; moderate-severe diffuse/global mesangial expansion/hypercellularity; in this case glomerulomegaly is also evident.

Scale lines indicate 100 μ m.

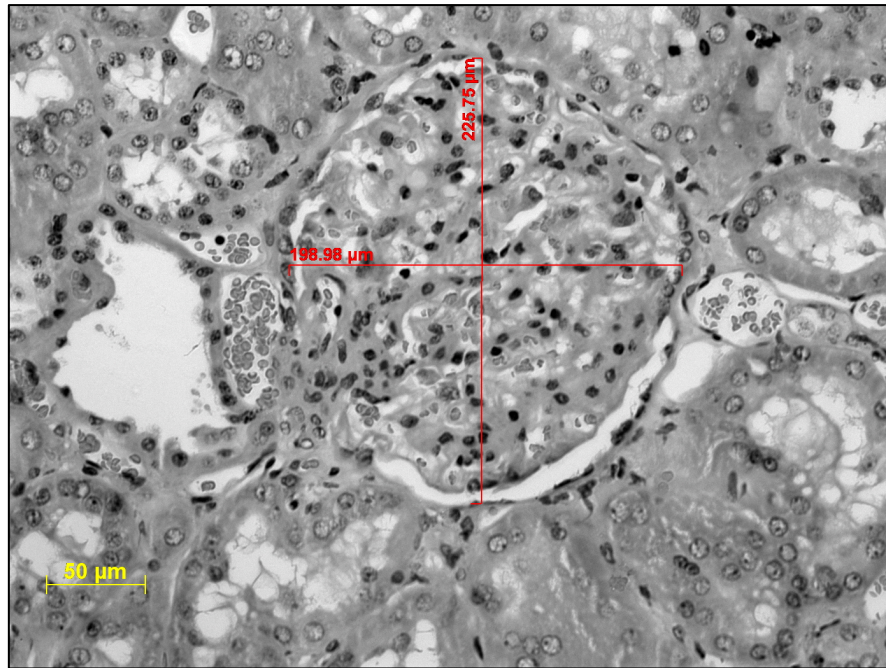


Figure 3.3.2. Representative image of the measurement method used to assess marmoset glomerular diameter in this study.

Up to 15 non-sclerotic glomeruli were photographed from each marmoset kidney at 200x magnification using a Zeiss Apotome microscope; glomerular diameter was determined by taking the mean of two perpendicular measurements across the glomerulus. Glomeruli were included in this analysis where they were sectioned such that the hilar vessels were visible, with a difference between perpendicular measurements of $\leq 30\mu\text{m}$, as shown in this figure (see section 3.4 for further discussion).

Haematoxylin and Eosin staining; scale lines show measurements as indicated.

Table 3.3.1. Renal histology, immunofluorescence and ultrastructural analysis in 25 adult marmoset monkeys.

Animal number	Age / gender	Indication for euthanasia	Mesangial score mean (SD)	Glomerular diameter (µm) mean (SD)	Immunofluorescence deposits				EM deposit	GBM thickness (nm) mean (SD)
					IgM	IgA	IgG	C3		
68*	- / F	Experiment	2.33 (0.70)	205 (19)	++	+++	trace	negative	Present	511 (118)
69	7.6 / F	Experiment	2.25 (0.67)	177 (15)	+++	trace	++	+	Sparse	413 (83)
70	10.0 / F	<i>Weight loss</i>	2.51 (0.63)	145 (13)			ND		Present	480 (95)
71	5.1 / F	Experiment	2.40 (0.61)	149 (7)	+++	+++	trace	+++	Present	524 (117)
72	5.5 / F	Experiment	2.43 (0.65)	149 (19)			ND		Present	538 (97)
77	4.0 / F	Experiment	2.37 (0.49)	164 (18)			ND		Present	527 (87)
81	2.1 / F	Experiment	2.29 (0.61)	163 (12)			ND		ND	266 (50)
85	12.7 / M	Experiment	2.54 (0.61)	183 (21)	+++	+++	+++	++	ND	ND
86	3.1 / M	Experiment	2.21 (0.41)	146 (14)			ND		Absent	353 (70)
108	3.1 / F	Experiment	2.23 (0.43)	144 (13)			ND		Present	386 (71)

* In the case of animals 68, 814, and 861, exact date of birth or date of death information was not available, therefore age could not be calculated. All animals were older than 2 years, however, so had reached maturity.

SD = standard deviation; EM = electron microscopy; GBM = glomerular basement membrane

Animal number	Age / gender	Indication for euthanasia	Mesangial score mean (SD)	Glomerular diameter (µm) mean (SD)	Immunofluorescence deposits				EM deposit	GBM thickness (nm) mean (SD)
					IgM	IgA	IgG	C3		
657	9.9 / F	Experiment	2.39 (0.68)	187 (26)	+++	trace	+++	trace	Present	560 (136)
732	7.9 / F	Experiment	2.16 (0.59)	128 (14)	+	++	+	+++	Present	496 (102)
800	11.5 / F	<i>Weight loss</i>	2.41 (0.50)	154 (13)			ND		ND	ND
801	4.8 / F	Experiment	2.46 (0.59)	168 (24)	++	negative	negative	ND	Sparse	421 (76)
804	11.4 / F	<i>Weight loss</i>	2.70 (0.46)	167 (17)			ND		ND	ND
814*	- / F	Experiment	2.63 (0.49)	160 (22)	+++	++	++	ND	Present	454 (96)
815	4.6 / F	Experiment	2.20 (0.67)	196 (15)	++	negative	negative	++	Absent	451 (120)
816	4.9 / F	<i>Weight loss</i>	2.64 (0.56)	132 (18)	+	negative	negative	trace	Absent	375 (73)
824	11.3 / F	Experiment	2.81 (0.40)	170 (18)			ND		ND	ND
860	3.8 / F	Experiment	2.40 (0.60)	143 (9)	++	++	trace	+	Present	428 (91)
861*	- / F	<i>Weight loss</i>	2.53 (0.51)	180 (11)			ND		Sparse	445 (76)
865	4.4 / F	Experiment	2.47 (0.51)	158 (13)			ND		Present	485 (96)
873	7.7 / F	<i>Weight loss</i>	2.65 (0.49)	129 (15)			ND		Present	448 (82)
874	3.8 / F	Experiment	2.67 (0.48)	151 (13)			ND		Present	427 (88)
875	4.5 / F	Experiment	2.62 (0.49)	157 (19)			ND		Present	434 (95)

Table 3.3.2. Summary of renal histology and ultrastructural quantitative data.

Indication for euthanasia	Number	Age (years) mean (SD)	Gender (M:F)	Mesangial score mean (SD)	Glomerular size (µm) mean (SD)	GBM thickness (nm) mean (SD)
Experiment	19	5.8 (3.0)	2:17	2.41 (0.18)	164 (26)	451 (18)
Weight loss	6	9.1 (2.8)	0:6	2.57 (0.11)	149 (25)	437 (22)
		<i>p=0.040</i>		<i>p=0.05</i>	<i>p=0.0003</i>	p=0.71
Overall	25	6.5 (3.2)	4:25	2.45 (0.55)	162 (16)	449 (69)

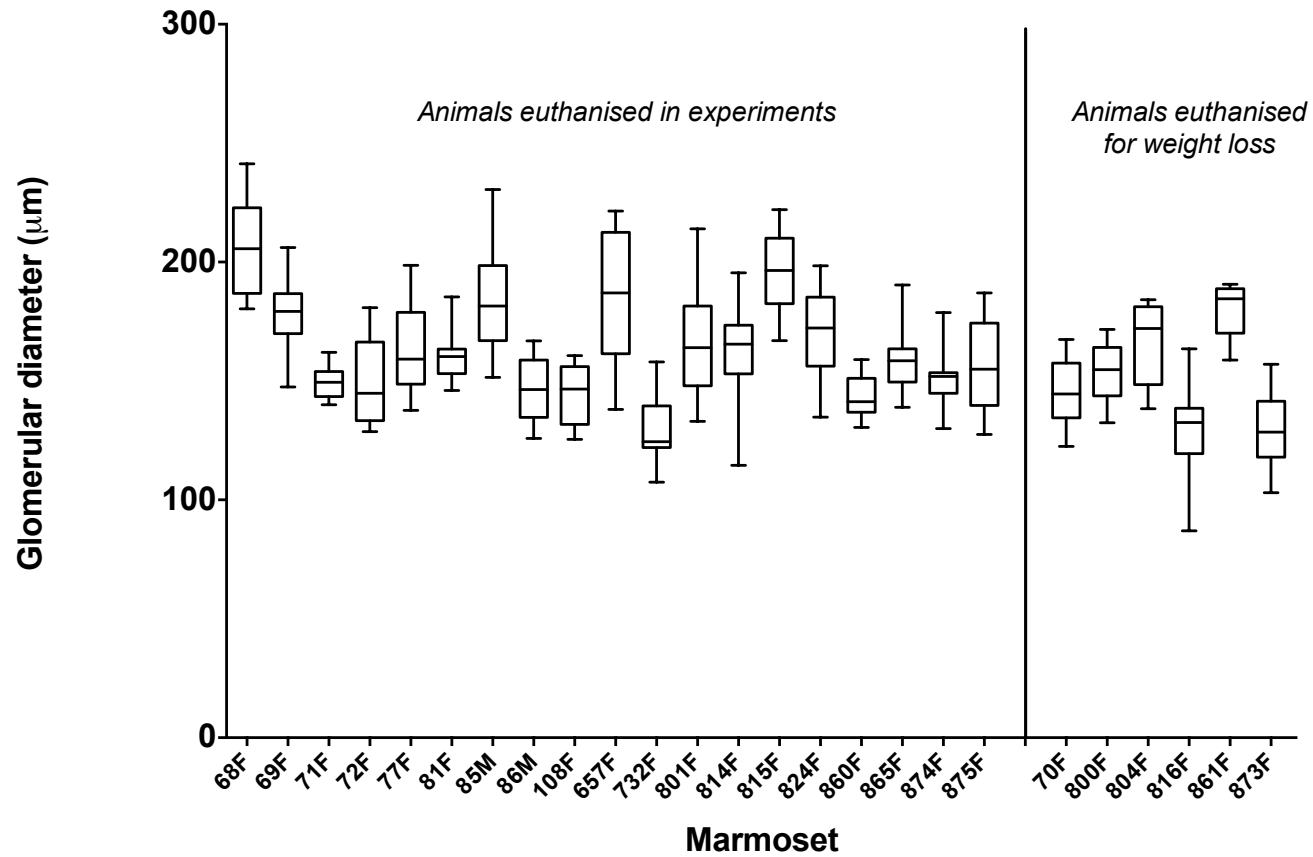


Figure 3.3.3. Glomerular diameter in 25 adult marmoset monkeys.

Up to 15 glomeruli were measured in each marmoset; the mean of two perpendicular measurements was used to determine the glomerular diameter, as described in the text. The graph shows box and whisker plots with the 25th, 50th and 75th percentiles shown by the lines of the box, and the range by the ends of whiskers. The glomeruli of animals euthanised for weight loss were slightly smaller (mean 149µm versus 165µm; $p=0.0003$).

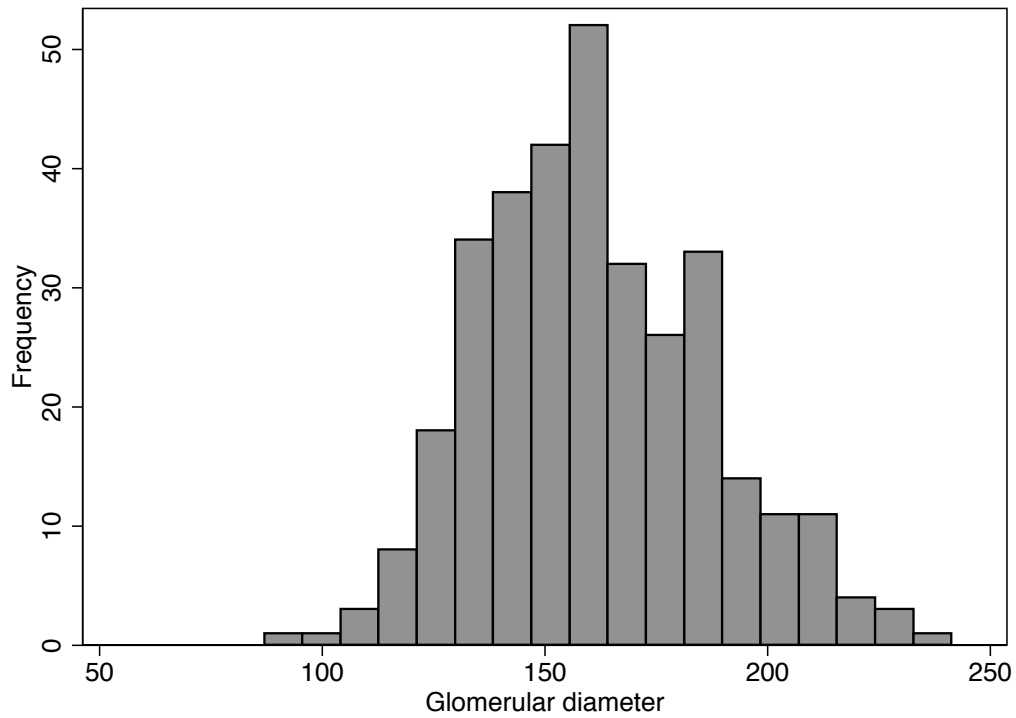


Figure 3.3.4. Frequency distribution of the diameters of 333 non-sclerotic glomeruli in 25 adult marmoset monkeys aged up 14 years.

Glomerular diameter (μm) was measured by taking the mean of two perpendicular measurements for each glomerulus, as described in the text. Glomerular diameter was approximately normally distributed with a slight tail to the right (median of 159, mean of 161, skewness of 0.32 and kurtosis 2.88).

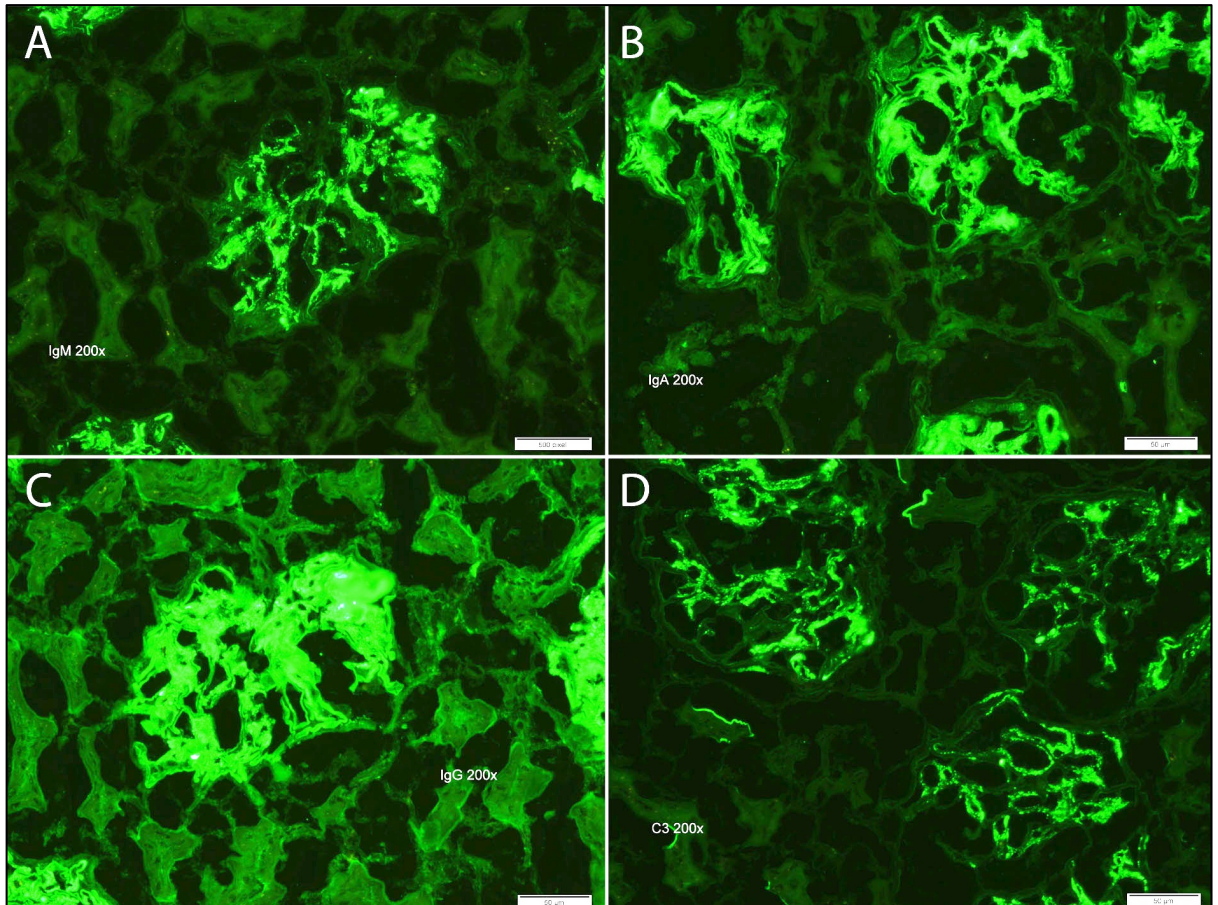


Figure 3.3.5. Representative immunofluorescence microscopy images of marmoset kidneys showing mesangial immunoglobulin deposits.

High power views of marmoset glomeruli (original magnification 200x). Glomerular deposits, particularly in a mesangial pattern are seen of (A) Immunoglobulin M (IgM) – 3+, (B) IgA – 3+, (C) IgG – 3+, and (D) Complement component C3 – 2+. All marmoset kidneys examined demonstrated IgM positivity; not all kidneys demonstrated other deposits (see Table 3.3.1).

Scale bars indicate 50µm.

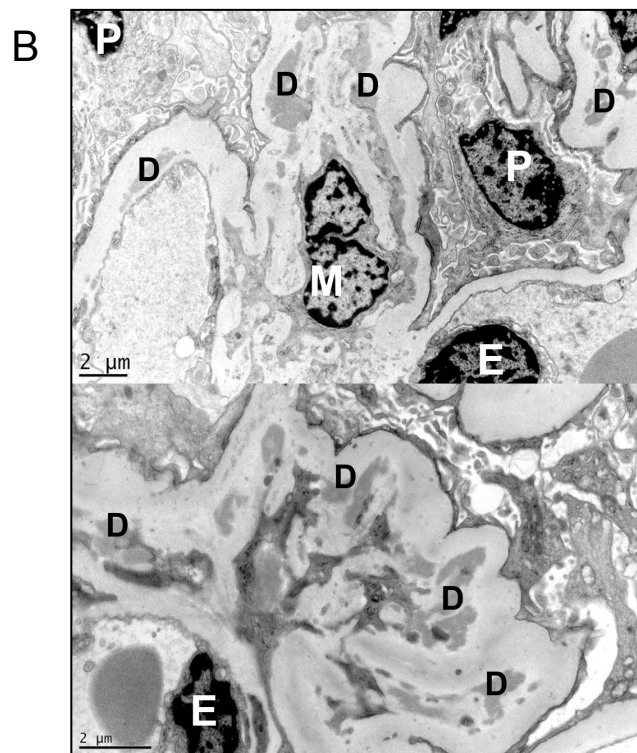
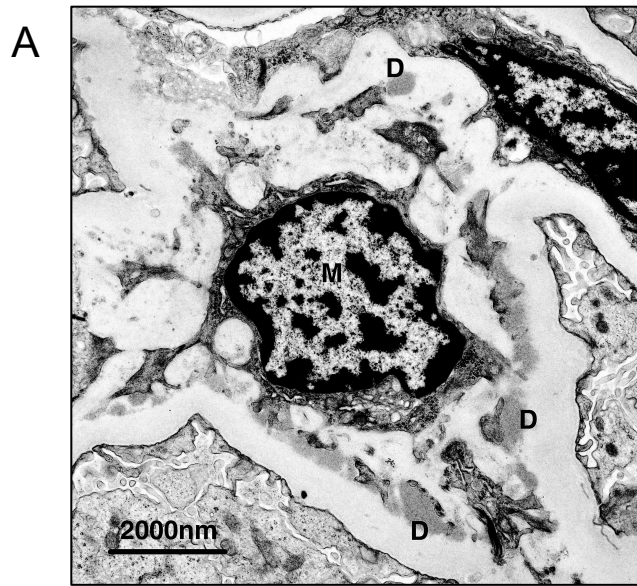


Figure 3.3.6. Representative electron microscopic images of marmoset kidney showing the presence of mesangial deposits.

The majority of marmoset glomeruli that were examined ultrastructurally showed mesangial deposits. *Panel A:* Images from an animal humanely killed in the course of fertility experiments. Typical deposits (labelled D) are seen in close proximity to a mesangial cell (M). *Panel B:* Images from an animal euthanized for ongoing weight loss. The upper panel demonstrates deposits (D) seen in relation to a mesangial cell (M), podocyte (P), and an endothelial cell (E). The lower panel shows similar findings, at higher power.

Scale lines show measurements as indicated.

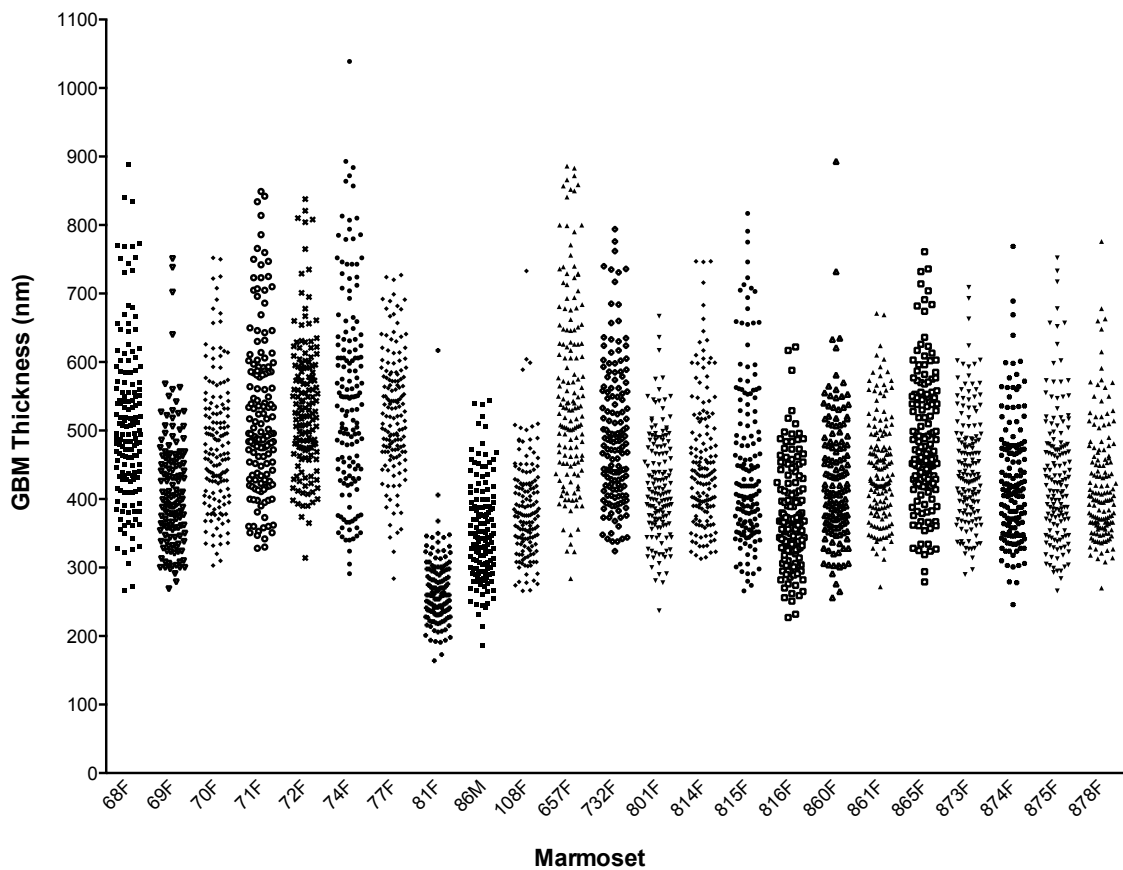


Figure 3.3.7. Ultrastructural analysis of glomerular basement membrane (GBM) thickness in 23 marmoset monkeys.

Electron microscopy was performed of renal cortex obtained from 23 marmoset monkeys. Measurements of GBM thickness (nm) were performed as described in the text; 150 measurements were taken for each animal, and are shown by individual points on the graph. One animal (81F) demonstrated evidence of thin basement membranes. Summary statistics for these measurements are shown in Table 3.3.1 and Table 3.3.2.

3.3.5. *Biochemistry parameters and urinary protein*

Renal function from 34 animals (n=7 still alive and 27 deceased, including 22 of the 25 animals in the histology analysis, and 5 others who had not had renal tissues analysed) performed both during life and at the time of euthanasia was assessed; results are shown in Figure 3.3.8 and Table 3.3.3. Serum creatinine appeared to have a bimodal distribution, with peaks at approximately 20 and 40 $\mu\text{mol/L}$. There was considerably variability both within and between animals, and there was no association with age, cause of death (experimental group versus weight loss), or time of collection (random versus at euthanasia). Both the median (interquartile range), and mean (SD) values were in keeping with the ISIS reference range, as shown in Table 3.3.3.

Assessment of other biochemical parameters in marmoset peripheral blood (see Table 3.3.3) showed hypernatraemia (mean sodium 146; SD 12) and hypoalbuminaemia (mean 28.1; SD 9.5) in the majority of animals tested. The remaining biochemical parameters measured were within internationally recognised limits.

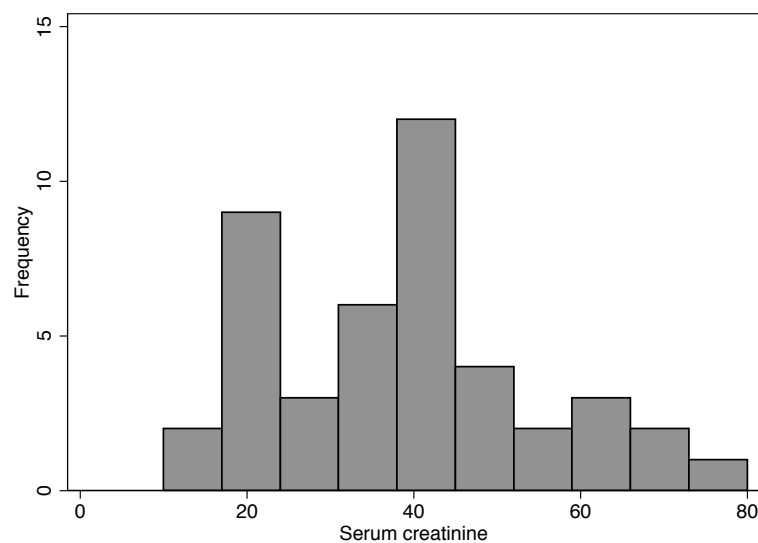


Figure 3.3.8. Frequency distribution of serum creatinine ($\mu\text{mol/L}$) results from 45 peripheral blood samples taken from 34 marmoset monkeys aged up to 14 years.

Serum creatinine was measured periodically in live animals within the colony, and at euthanasia, over the period 2003 to 2012. Marmoset serum creatinine values follow a bimodal distribution, with peaks at approximately 20 $\mu\text{mol/L}$ and 40 $\mu\text{mol/L}$, respectively.

Table 3.3.3. Serum biochemistry in adult marmoset monkeys.

Parameter	Units	Sample size	Marmoset		Human reference range*	ISIS reference values**
			Mean (SD)	Median (IQR)		Mean (SD)
Creatinine	µmol/L	45	38 (16)	39 (23.5-50)	50-120	44 (18)
Urea	mmol/L	20	6.9 (2.5)	6.8 (4.7-7.8)	2.7-8.0	8.211 (0.7140)
Sodium	mmol/L	35	156 (12)	153 (147-167)	135-145	149 (6)
Potassium	mmol/L	35	4.6 (1.4)	4.1 (3.9-4.9)	3.5-4.5	4.1 (2.0)
Chloride	mmol/L	21	106 (3.8)	106 (104-108)	100-109	106 (8)
Bicarbonate	mmol/L	21	29 (6.2)	31 (22-34)	18-26	22.5 (3.3)
Phosphate	mmol/L	24	1.42 (0.33)	1.30 (1.14-1.71)	0.65-1.45	1.81 (0.94)
Calcium	mmol/L	17	2.37 (0.47)	2.58 (2.18-2.68)	2.1-2.55	2.48 (0.08)
Glucose	mmol/L	12	5.8 (2.1)	5.2 (4.7-7.0)	3.2-5.5	10.60 (3.663)
Albumin	g/L	32	28.1 (9.5)	28.5 (24.3-36)	34-48	41 (7)

* Human reference ranges are as reported by the laboratory (SA Pathology, Queen Elizabeth Hospital). ** ISIS – International Species Information System Reference Physiological Values (International Units) – as published in Mahoney (2005).⁵⁶⁷ SD = standard deviation; IQR = interquartile range.

Urine dipstick analysis for protein of samples from 34 animals showed trace or 1+ protein in the majority (69%) of samples, with a significant minority of samples revealing more significant proteinuria (2+ or 3+; found in 25%); see Figure 3.3.9. Urinary dipstick protein measurements from 84 urine samples taken from 34 marmoset monkeys aged up to 14 years. Proteinuria fluctuated over time, but there did not appear to be any relationship between urine protein, age or cause of death, even in the animals found to have with higher degrees of proteinuria. Very few samples (n=6; from 4 animals) did not show proteinuria, and all these animals were dipstick positive 1+ or greater at other times. Other measurements of urine protein such as protein-creatinine index or albumin-creatinine ratio were performed in some animals (Table 3.3.4) but were difficult to interpret due to the very low excretion of creatinine detected in many marmoset urine samples. There was a wide range of urine protein and albumin measurements in comparison to the dipstick measures, suggesting a degree of laboratory error, perhaps due to this or to the low sample volumes (typically <1ml from a marmoset clean catch urine, or 1-2 ml via bladder puncture at autopsy). Regardless, the vast majority of urine protein measurements showed significant proteinuria, above the human reference range.

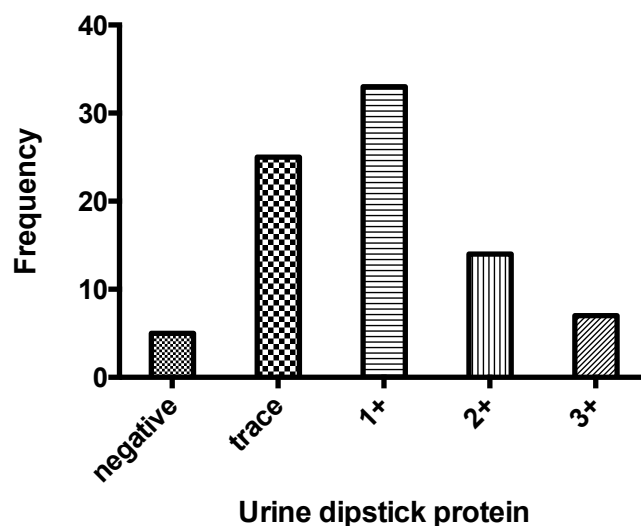


Figure 3.3.9. Urinary dipstick protein measurements from 84 urine samples taken from 34 marmoset monkeys aged up to 14 years.

Urinary dipstick protein was measured periodically in live animals within the colony, and at euthanasia, over the period 2003 to 2012. The majority of samples (n=58, 69%) taken demonstrated a value of trace or 1+ protein; very few samples (n=5) were negative.

Table 3.3.4. Urine biochemistry and dipstick parameters in adult marmoset monkeys.

Parameter	Units	Sample size	Marmoset		Human reference range	ISIS reference values
			Mean (SD)	Range*		
Urine protein	g/L	15	0.62 (1.3)	0-1.79	<0.16	-
Urine protein-creatinine index		15	12.3 (24.3)	0-94.6	<2.1	-
Urine albumin	mg/L	13	219 (426)	4.3-1140	<35 (random)	-
Urine albumin-creatinine ratio	mg/mmol	13	100 (190)	3.3-670	<3.5	-
Urine protein (dipstick)		84	1.13 (0.79)		-	-
Urine blood (dipstick)		39	0.42 (0.73)		-	-

* For the formal urine protein measurements, only the range is given; there were few values with a wide range of results. SD = standard deviation; IQR = interquartile range.

3.4. Discussion

The studies outlined in this chapter represent a comprehensive survey of renal pathology and biochemical parameters in a colony of outbred common marmoset monkeys, and confirm the universal and benign nature of the glomerular lesions that are frequently observed in this Callithricid primate species. There were no significant differences in glomerular findings observed between animals suspected clinically of developing wasting (weight loss) and those euthanized for experimental reasons. This study reports for the first time on the nature of these glomerular lesions in relation to serum and urine biochemical findings.

By light microscopy, the majority of marmoset glomeruli showed evidence of mesangial expansion, as has been reported previously.^{541,542,545-548,551} The semi-quantitative scoring method indicated that this was of at least mild to moderate degree in all animals. However, there was minimal glomerular obsolescence, and no evidence of renal tubular changes or interstitial fibrosis. Although some marmoset glomeruli (particularly those with mesangial scores of 3) were significantly enlarged, the overall distribution of glomerular size (mean $161 \pm 16 \mu\text{m}$) was similar to reported normal values for human glomeruli; in various studies these have been reported as a mean of $168 \pm 12 \mu\text{m}$,⁵⁶⁸ and $147 \pm 19 \mu\text{m}$.⁵⁶⁹ There was also no indication of renally-based extramedullary haematopoiesis,⁵⁵¹ nor mononuclear or lymphocytic infiltration suggestive of a chronic tubulointerstitial nephritis that has been previously reported,^{544,548} even in marmosets euthanized due to clinical suspicion of wasting marmoset syndrome. Similar appearances were observed regardless of animal age, although mesangial scores were slightly lower in the animals with underlying illness at the time of euthanasia.

Mesangial expansion is a consequence of increased mesangial matrix deposition, and results from increased type IV (and to a lesser extent type I) collagen production and/or decreased proteolysis, although in this study we did not confirm collagen type by immunohistochemistry. Type IV collagen is also a component of basement membrane structure, and in this study marmoset glomerular basement membrane thickness (mean $449 \pm 69 \text{nm}$), reported for the first time in this species, was greater than measurements typically seen in the human population⁵⁷⁰; more recently a study reported a typical

GBM thickness of 329 ± 45 nm in a series of live kidney donors.⁵⁷¹ These findings may reflect a localised abnormality in collagen production or processing. Immune complex deposition promotes thromboxane synthesis and subsequent mesangial contraction, which are smooth muscle cell-derived. Increased mesangial cell pressure in marmosets has been proposed to underlie protrusions of mesangial cytoplasm through endothelial gaps.⁵⁴⁶

In parallel with the presence of mesangial expansion by light microscopy, there was a predominance of mesangial IgM deposits by immunofluorescence, often in conjunction with IgA, IgG and C3. Concurrently, electron dense mesangial deposits were observed in the majority of marmoset kidneys by electron microscopy. Similar deposits in human kidneys are characteristically seen in immune complex nephropathies such as systemic lupus erythematosus,⁵⁷² obesity related focal segmental glomerulosclerosis,⁵⁶⁸ and IgA nephropathy,⁵⁷³ although the presence of IgM deposits does not seem to confer any prognostic significance in these diseases. As previously noted, none of the animals in this study had evidence of glomerular sclerosis or other glomerular pathology. Moreover, animals with immunoglobulin deposits did not show any evidence of anti-nuclear antibodies using a HEp2 cell line based assay. Immunoglobulin deposition may occur in otherwise normal human kidneys, for unknown reasons.^{574,575} The event precipitating immunoglobulin deposition in marmosets is unknown; the animals used in this study have all been bred in captivity with no evidence of infection. The genetics of MHC class II has previously been characterised in the marmosets at the Queen Elizabeth Hospital colony and a range of class II genotypes have been identified, confirming the genetic diversity of these animals.⁴⁰¹

Measurement of glomerular size was performed using a similar approach to the modified maximal planar area method,⁵⁷⁶ as described by Kambham et al.⁵⁶⁸ This method estimates glomerular diameter using the mean of two perpendicular measurements across the glomerulus, at the points of maximal glomerular diameter. In this study, measurements were taken from Bowman's capsule rather than the glomerular capillary tuft itself, in order used to facilitate reproducibility between two investigators, and because of the presence of ischaemic shrinkage in some glomeruli. It is thus acknowledged this may introduce a systemic bias towards an increased estimate of size, at least when comparing with Kambham et al. However, most glomeruli in fact had

minimal Bowman's space evident; other methods of size estimation do include the total volume of Bowman's capsule in the measurement, and most approaches are subject to at least some degree of bias compared with the gold-standard but laborious Cavalieri method.⁵⁷⁷ In this study, a small but statistically significant *reduction* in glomerular size was noted in animals with weight loss; the significance of this finding is unclear. However, this observation and the lack of any other observed glomerular pathology do not support the existence of any association between renal disease and cause of illness in these animals.

Evaluation of marmoset serum and urine biochemistry showed that while serum creatinine remains within previously published internationally established ranges,⁵⁶⁷ mild to moderate proteinuria, when assessed semi-quantitatively by urine dipstick, is almost universal in marmosets. It should be noted that no established reference range for urine protein excretion currently exists in marmosets, and these data are based on human reference ranges. This apparent proteinuria did not progress with age or over time. Laboratory measurements of urine protein-creatinine indices varied over a wide range, at least in part due to low urinary creatinine measurements, but overall were difficult to interpret. There was little detectable microscopic haematuria. Others have proposed that marmosets might represent a good model of spontaneously occurring IgA nephropathy, but the lack of microscopic haematuria or progressive renal dysfunction observed in this study does not support this conclusion.⁵⁵⁰

Taken together, these findings support the conclusion that marmosets spontaneously develop glomerular lesions characterised by mesangial expansion, IgM deposition, and glomerular basement membrane thickening, and that these are associated with a mild degree of proteinuria. The cause of these lesions are unclear, but may relate to circulating IgM immune complexes that could occur as a result of environmental, dietary or infectious exposures.⁵⁴³ However, these lesions do not progress to renal dysfunction either histologically or biochemically, and do not appear to contribute directly to illness in marmosets, at least in this colony. Rather than contributing to the cause of wasting marmoset syndrome, as has been thought,⁵⁴¹ it may be the case that spontaneous marmoset glomerular pathology represents a unrelated epiphenomenon that has been documented at the same time as the identification of the symptoms of wasting disease in these animals. Indeed, in this study there was no evidence of the tubulo-

interstitial lesions found in the wasting syndrome that have been reported by others,^{544,548} implying that these are different processes. In contrast to reports from colonies elsewhere,^{548,550} the marmosets in this colony are not utilised in pharmacological or toxicology studies. Drug exposure could conceivably be an important factor in the development of tubulo-interstitial lesions, i.e. via the induction of a drug induced interstitial nephritis in some cases.

In conclusion, the studies in this chapter demonstrate the feasibility of utilising the common marmoset monkey as a NHP model of kidney transplantation. The mild and benign nature of the observed glomerular pathology in marmosets should have no impact on the histological assessment of rejection or other transplant related pathology, provided these common findings are taken into account (e.g. when assessing for the presence or absence of glomerulitis).⁵⁷⁸ This study confirms that renal function remains normal in marmosets with glomerular lesions and is within standard reference ranges; however urinary protein may be a less useful marker due to the universal detection of mild to moderate proteinuria in these animals.

**Chapter 4: DONOR-DERIVED
DENDRITIC CELL THERAPY:
TRAFFICKING OF ALLOGENEIC AND
AUTOLOGOUS MARMOSSET DENDRITIC
CELLS *IN VIVO***

4.1. Introduction

Donor derived DC therapy has shown considerable potential as a tolerogenic therapy to prevent rejection and prolong allograft survival in rodent models of transplantation, as discussed in Chapter 1 and in recent reviews.^{229,264} However, translation of these findings in rodents to humans has proven difficult due to heterologous immunity, the increased complexity of the human response to an allograft, and even in part due to observed species differences between mice and human DC.⁸⁶ In addition, DC are typically sourced from bone marrow in rodents, but from peripheral blood monocytes in humans.³⁰⁵ However, there are now established methods to propagate DC *in vitro* from peripheral blood precursors in non-human primates, and these animals offer a means to translate the rodent findings towards human clinical trials.^{350,380,390,395,396,403} To date, several studies have shown that intravenously administered NHP donor immature or ‘regulatory’ phenotype (Mo)DC can modify the allo-immune response.^{303,350,351}

Marmoset MoDC and haematopoietic progenitor derived DC (HPDC) generated *in vitro* have previously been shown to have an immature or semi-mature phenotype, respectively, with reduced allo-stimulatory potential compared to human MoDC.⁴⁰³ This makes them attractive to use as a NHP model of tolerogenic DC therapy that might be investigated in a transplant model. In a previous study, *intravenous* infusion of 2×10^6 MoDC into allogeneic marmoset recipients led to a non-specific reduction in IFN- γ secretion as measured in a modified ELISPOT assay, with evidence of a non-specific reduction in immune responsiveness in 2 of 3 recipients in mixed leucocyte reaction.³⁰³ This study provides proof of principle that marmoset ‘tolerogenic’ DC therapy can be used to manipulate the immune response.

The mechanisms by which tolerogenic DC therapies effect their actions on the immune response include the induction of T-cell anergy, clonal deletion or the generation and expansion of T-regulatory cells.^{229,305} However, the fate of administered cells *in vivo* is not well characterised. In particular it is unknown whether normal trafficking of allogeneic DC to the spleen, liver and secondary lymphoid tissues occurs following intravenous administration, or whether migration to the draining lymph node occurs following subcutaneous administration. Both of these interactions are thought to be important for the initiation of appropriate tolerogenic immune responses, and as yet the

optimal route of administration of tolerogenic DC immunotherapy is unknown.^{264,579}

Understanding the trafficking behaviour of allogeneic DC in a relevant primate model of DC immunotherapy is an important component of translating this therapy further towards transplant studies in NHP, and ultimately human clinical trials.

The aims of this chapter are:

1. To propagate marmoset DC *in vitro* from G-CSF mobilised marmoset peripheral blood monocytes and haematopoietic cells as precursors, label these cells with fluorescent markers, and confirm that these cells are suitable as a potential source of immature DC to use as a cellular therapy in the marmoset transplant model.
2. To administer *in vitro* propagated and fluorescently labelled marmoset DC (generated as per Aim (1) above), derived from a MHC-mismatched (allogeneic) donor, or alternatively autologous DC, to marmoset recipients via both subcutaneous and intravenous injection, and determine whether these administered cells show evidence of trafficking *in vivo*.

4.2. Methods

4.2.1. *Animals*

Healthy adult marmoset monkeys (aged up to 14 years) from within the colony at The Queen Elizabeth Hospital were used for the studies described in this chapter. Where possible, older aged animals were used as recipients, to minimise inappropriate euthanasia of animals that might be suitable for use in other studies. The SA Pathology/Central Adelaide Health Network and University of Adelaide animal ethics committees approved and had oversight of all procedures involving the animals.

Recombinant human (rh) G-CSF (10-15µg/kg/day) was given for 5 days to marmosets selected to be donors of monocytes and/or haematopoietic progenitors for DC propagation⁴⁰³; no adverse effects of this treatment were observed. The procedures for administering G-CSF, peripheral blood sampling, and euthanasia are as described in Chapter 2 (section 2.3).

4.2.2. *Cell culture*

Marmoset MoDC and HPDC were propagated from precursors in marmoset peripheral blood following 5 days of mobilisation with G-CSF. Detailed protocols for isolation of marmoset PBMC, marmoset MoDC and HPDC culture, reagents and media used, and mixed leucocyte reactions (MLR) are described in Chapter 2 (section 2.4.2).

Human PBMC were sourced from buffy coats obtained by the South Australian Red Cross blood service from de-identified healthy blood donors, and isolated as described in section 2.4.3.1.

4.2.2.1 *In vitro propagation of marmoset MoDC and HPDC*

Monocytes were isolated from marmoset PBMC by plastic adherence; non-adherent cells were removed from plates or flasks by washing. Immature MoDC were generated by culturing monocytes for 6-7 days in CM supplemented with 40ng/ml (400U/ml) recombinant human (rh)-IL-4 and 800U/ml rh-GM-CSF.

Non-enriched bulk PBMC were used as a source of CD34⁺ haematopoietic progenitor (HP) cells, and cultured in CM supplemented with rh-Flt3L (100ng/ml), SCF (100ng/ml) and TPO (50ng/ml), for up to 4 weeks. Media and cytokines were refreshed once or twice weekly. After 3-4 weeks in culture, HP cells were removed, washed and cultured in CM supplemented with IL-4/GM-CSF for 7 days to generate HPDC.

4.2.3. Fluorescent labelling of *in vitro* propagated marmoset DC

Marmoset MoDC and HPDC propagated *in vitro* were fluorescently labelled prior to planned infusion studies to enable identification in marmoset tissues post infusion. Two different fluorescent labels were used, to enable differentiation of different cell types *in vivo*.

4.2.3.1 CFSE labelling

Marmoset HPDC (or MoDC in some studies) were labelled with carboxyfluorescein diacetate succinimidyl ester (CFSE, Molecular Probes) using a protocol based on Quah et al.⁵⁸⁰ As DC generated *in vitro* are terminally differentiated and are not expected to proliferate, CFSE was not used to monitor proliferation, but rather for its stable long-term fluorescence and ease of identification in flow cytometry analysis.

Cells were resuspended in 1ml of PBS with 5-10% v/v FCS at a minimum concentration of 0.5×10^6 /ml in a fresh tube. The tube was laid horizontally to prevent pre-mature mixing. 110µl of PBS was added to the non-wetted portion of the tube, and 1.1µl of 5mM stock solution (in DMSO) of CFSE was resuspended in this. The tube was capped, inverted several times, vortexed to ensure adequate mixing and covered (to protect from light). Cells and CFSE were incubated for 5 minutes at room temperature. Cells were washed by topping up with PBS/5% FCS and centrifuged at 300g RCF for 5 minutes; this wash was repeated several times. Cells were resuspended in PBS or media depending on planned usage. Fluorescence was determined with flow cytometry.

4.2.3.2 DiI labelling

Marmoset MoDC were labelled with 1,1'-dioctadecyl-3,3',3'-tetramethylindodicarbocyanine perchlorate (DiI, Molecular Probes). Cells for labelling were resuspended at 1×10^6 /ml in PBS, 2µg/ml of DiI was added and cells were

incubated at 37°C for 30 minutes. Labelled cells were washed with PBS/5% FCS extensively in a similar manner to CFSE labelling above (section 4.2.3.1).

4.2.4. Confirmation of suitability of propagated labelled marmoset DC for DC infusion

In order to confirm the suitability of labelled marmoset DC to use for the *in vivo* studies of DC trafficking, DiI or CFSE labelled DC were analysed for stimulation potential in a xenogeneic MLR with human cells, and viability (after CFSE staining only).

4.2.4.1 Xenogeneic mixed leucocyte reaction (MLR)

Marmoset MoDC labelled with either DiI, CFSE, or untreated, were analysed for their ability to stimulate T-cell proliferation in a xenogeneic DC MLR, as per Chapter 2 (section 2.4.2.6.2). Marmoset DC were irradiated with 30Gy and used as stimulator cells, and co-cultured with 1×10^5 xenogeneic human PBMC in a 1:10 ratio in triplicate for 5 days. Marmoset MoDC and human PBMC were also cultured alone for baseline data. T-cell proliferation was determined as described in section 2.4.2.6.1.

4.2.4.2 Viability after CFSE staining

Because of the potential for cellular toxicity of CFSE in some settings,⁵⁸¹ viability of CFSE stained HPDC was assessed. Untreated and CFSE labelled HPDC (1×10^6 /ml) (either on the day of labelling or after 48 hours of culture in CM supplemented with GM-CSF/IL-4) were resuspended in 100µl of PBS, and 200µl (5µg/ml) of 7-amino-actinomycin D (7AAD; eBioscience) was added. 200µl of normal saline was used as a control. Cells were incubated for 10 minutes at room temperature, and then analysed immediately with a FACS Canto II flow cytometer (BD Biosciences) and data was analysed using FCS Express version 3 software (DeNovo). Compensation tubes consisted of cells stained with CFSE or 7AAD alone.

4.2.5. Selection of donor and recipient animals for DC administration studies

Marmoset donor and recipient pairings for the allogeneic studies in this chapter were selected to maximise allo-reactivity on the basis of the degree of *Caja*-DRB (marmoset MHC Class II) genotype mismatching between the animals.⁴⁰¹ For each recipient

animal, 2 allogeneic donors, one donor for MoDC and HPDC, respectively, were utilised.

For the study involving the administration of autologous DC, the same animal was used as both the donor and recipient. In this case, two courses of G-CSF were required to ensure adequate numbers of precursors would be present in peripheral blood for the purposes of propagating HPDC and MoDC, respectively.

4.2.5.1 Confirmation of allo-reactivity between donor and recipient animals

To confirm the degree of allo-reactivity predicted on the basis of *Caja*-DRB mismatching, one-way MLR (as described in Chapter 2, section 2.4.2.6.1) was undertaken using PBMC from each marmoset donor and recipient pair. To minimise excessive blood sampling of donor animals, stimulator PBMC for MLR were obtained from blood collected following G-CSF mobilisation and primarily intended for use as the source of monocytes of haematopoietic progenitors for DC culture. Stimulator PBMC were irradiated with 30Gy prior to culture. Responder cells were PBMC obtained from designated recipient animals; these animals had not received any G-CSF prior to blood sampling. Stimulator and responder PBMC (1×10^5 cells) were co-cultured in triplicate for 5 days; to obtain baseline data, 1×10^5 PBMC from each animal were also cultured alone. T-cell proliferation was determined, and for the purposes of comparison between different donor-recipient pairings was converted to a stimulation index, as per section 2.4.2.6.1.

4.2.6. Administration of labelled DC via subcutaneous and intravenous infusion

Following labelling of marmoset MoDC and HPDC with DiI and CFSE respectively, cells were washed extensively with PBS and resuspended in sterile 0.9% sodium chloride (NaCl) containing 0.1% v/v heparin (1000u/ml; Pfizer Australia). Cell viability and counts were confirmed prior to the final suspension with the use of trypan blue staining. Approximately $1-2 \times 10^6$ MoDC and $1-2 \times 10^7$ HPDC were resuspended in 200 μ l and 500 μ l of 0.9% NaCl/heparin, respectively, and protected from light until the time of administration to the animals. The dose of MoDC chosen was based on achieving a comparable dose (on a weight basis) to those used in previous studies of DC trafficking

in primates.³⁷⁹ A higher dose was chosen for the HPDC to maximise the likelihood of observing trafficked fluorescent cells in tissues after infusion.

Labelled donor DC were administered to recipient marmosets using 0.5ml or 1ml insulin syringes (fitted with 29g needles; BD Medical). CFSE-labelled HPDC were injected intravenously into the left femoral vein; intravenous placement of the needle was confirmed by the aspiration of venous blood prior to administration of DC. Immediately after the IV injection, DiI-labelled MoDC were injected subcutaneously into the right upper thigh of the animal; the site was marked by the placement of 5.0 silk suture.

Following DC administration, recipients were monitored for 20 minutes for any adverse effects, before being returned to their enclosure for routine monitoring.

4.2.7. Collection and analysis of marmoset tissues following DC administration

Forty-eight hours after the administration of labelled marmoset DC, recipient animals were euthanized under inhalational anaesthesia to collect tissues, as described in section 2.3.6. This time point was chosen on the basis of previous studies in mice⁵⁸²⁻⁵⁸⁷ and NHP^{379,390} indicating that subcutaneously injected DC would be likely to be present within the draining lymph node, and intravenously injected DC within the spleen and liver, at this time point. While under anaesthesia and prior to cardiac puncture, methylene blue (1%; American Reagent) was injected slightly proximal to the site of the suture marking the subcutaneous injection site, to enable the identification of the draining inguinal lymph node. Tissue samples were snap frozen using liquid nitrogen and embedded into OCT and transferred to -80°C for storage. Tissues collected for this study included the skin and subcutaneous tissue at the marked injection site, draining inguinal lymph node, kidneys, lungs, liver, spleen and mesenteric/para-aortic lymph nodes. Other scavenged tissues, peripheral blood, urine and bone marrow were also collected. In some studies, a sample of fresh lymph node (draining and contralateral), or spleen was collected for flow cytometry analysis. Fresh tissues were prepared for flow cytometry as per isolation of (spleen) cells for culture purposes (section 2.4.2.5).

Marmoset tissues were analysed by immunofluorescence microscopy as described in Chapter 2 (section 2.5) for the presence of DiI-MoDC or CFSE-HPDC. Additionally,

flow cytometry analysis (without monoclonal antibodies) of fresh lymph nodes and spleen was performed to detect the presence of DiI or CFSE positive cells, as per section 2.6.

It was not possible to include non-injected animals as a control group (e.g. to exclude auto-fluorescence) due to the need for euthanasia of an otherwise healthy marmoset to obtain such tissues. Thus, each animal served as their own control by including immunofluorescence staining of tissues likely to be uninvolved e.g. lymph nodes contralateral to the subcutaneous injection site.

4.3. Results

4.3.1. *Suitability of in vitro propagated and fluorescently labelled marmoset DC for DC infusion studies*

Marmoset MoDC were propagated *in vitro* and labelled with DiI or CFSE as a fluorescent label to enable identification of infused cells in marmoset tissues. Labelling did not alter the stimulation potential of these cells in a xenogeneic MLR (Figure 4.3.1), confirming that functionally these cells would be suitable to use for DC infusion studies.

In addition, viability of marmoset DC after prolonged HP culture and HPDC differentiation was excellent, with 7AAD staining only a small population of cells (approximately 1.5%). No difference was observed between unlabelled or CFSE labelled cells (Figure 4.3.2).

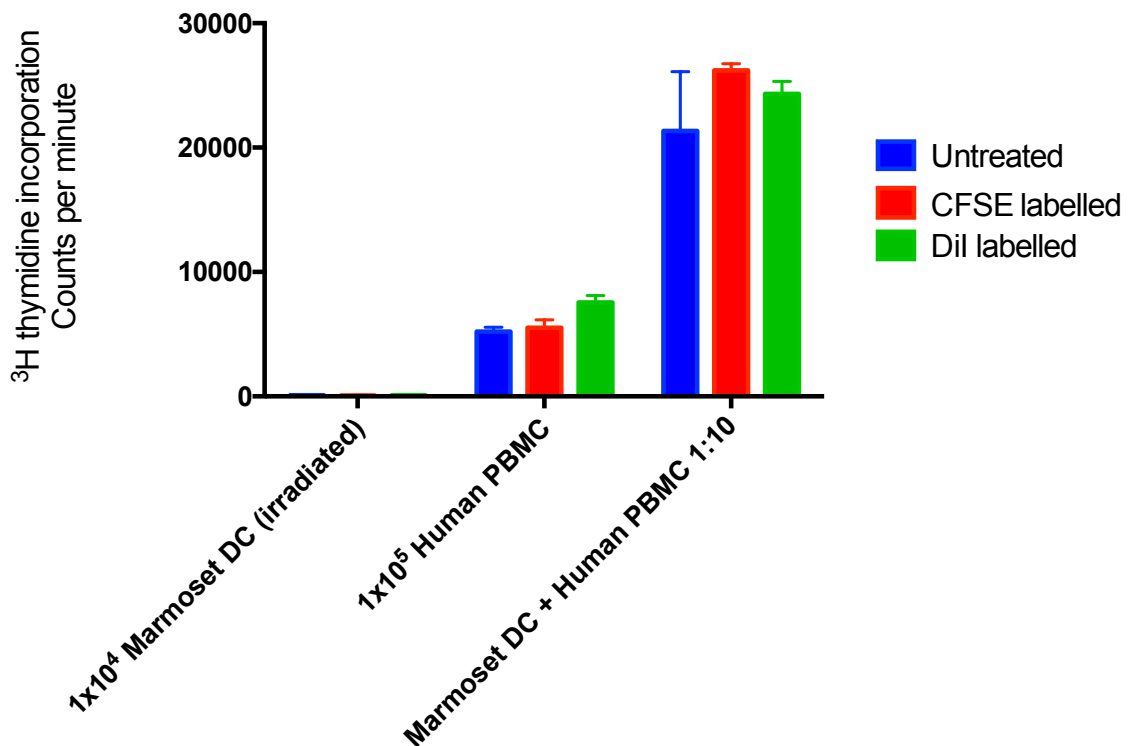


Figure 4.3.1. Fluorescent labelling of *in vitro* propagated marmoset MoDC with CFSE or DiI does not alter stimulation potential in a xenogeneic mixed leucocyte reaction.

Marmoset MoDC (day 6 in culture with GM-CSF/IL-4) were labelled with CFSE or DiI as described in the text, were assessed for stimulatory capacity in xenogeneic MLR. All stimulator MoDC were irradiated with 30Gy prior to co-culture with human PBMC at a 1:10 ratio. T-cell proliferation was assessed by ³H-thymidine incorporation. No significant difference in T-cell proliferation was observed between DiI or CFSE labelled cells and untreated cells (p=0.36, one way ANOVA).

Results shown are mean ± standard deviation and are representative of two experiments.

DC = marmoset MoDC; PBMC = peripheral blood mononuclear cells.

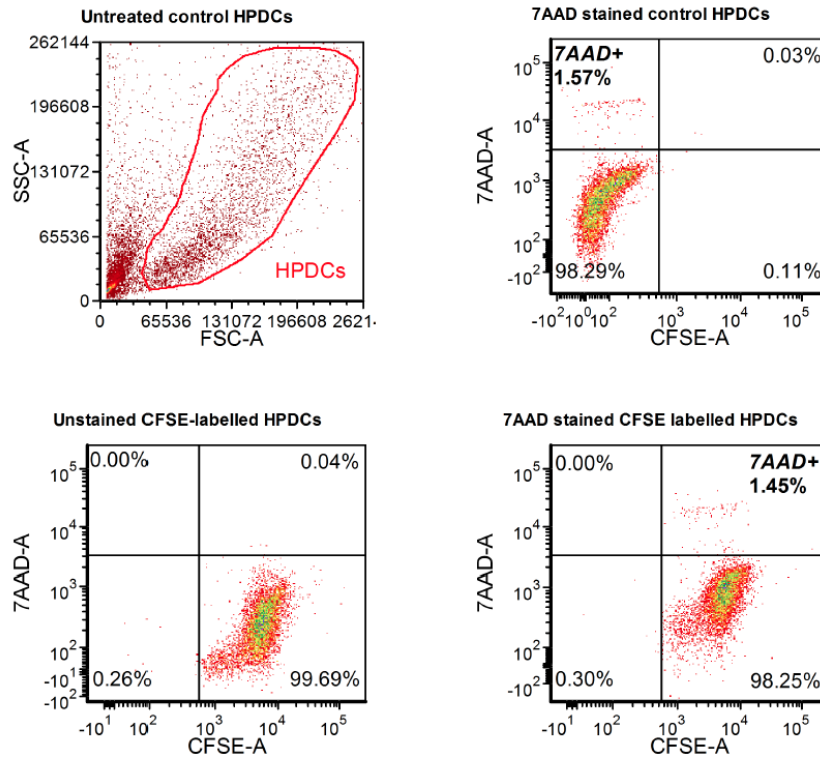


Figure 4.3.2. Marmoset HPDC propagated *in vitro* have excellent viability, which is not altered by labelling with CFSE.

After HP culture and differentiation into DC by culture in GM-CSF/IL-4, marmoset HPDC were labelled with CFSE, and cultured for a further 48 hours. Unlabelled HPDC were also cultured as controls. Labelled and control cells were washed and stained at room temperature with 7AAD as a cell viability indicator, with unstained HPDC as a further control, and analysed immediately by flow cytometry. Cells were gated according to forward and side scatter characteristics (top left panel), and CFSE staining was confirmed in 99% of cells (bottom left panel). 7AAD stained a small population of HPDC, which was similar for both unlabelled (1.57%; top right panel) and CFSE labelled (1.45%; bottom left panel).

Data are representative of 2 separate experiments.

HPDC = haematopoietic progenitor derived dendritic cells.

4.3.2. Selection of donor-recipient pairs

Marmoset donor-recipient pairings were selected on the basis of *Caja*-DRB (MHC Class II) genotype, to ensure at least one DRB mismatch between donors and recipients.⁴⁰¹ All animals in the colony had been genotyped for *Caja*-DRB genes prior to this study. The median age of donors was 11.2 years (range 10.3-13.7) and the median age of recipients was 12.7 years (11.3-14). Details of selected donors and recipients are shown in Table 4.3.1.

Table 4.3.1. *Caja*-DRB (Class II MHC) genotyping of the marmoset donors and recipients used in studies of DC trafficking.

Study	Recipient	DRB typing [†]	Donor	DRB typing	Mismatches
1	824F	1605, 1623, 0302, 0303	70M	1605, 1624 , 0302, 0302	1
			811F	1605, 1623, 0303, 0304	1
2	734F (auto)	1623, 1623, 0303, 0304	-	-	N/A
3 [‡]	85M	1605, 1624, 0302, 0302	79M	1605, 1608 , 0302, 0304	2
			82M [§]	1605, 1610 , 1608 , 0303 , 0303	3
4	85M	1605, 1624, 0302, 0302	75F	1605, 1608 , 0302, 0304	2
			863F	1604 , 1604 , 0302, 0303	2

[†] Marmoset MHC class II genes identified in the colony include *Caja*-DRB1*03 (individual alleles are shown as 03--), *Caja*-DRB*W16 (individual alleles shown as 16--), and *Caja*-DRB*W12. All animals in the colony are known to be positive for the *Caja*-DRB*W1201 allele.

[‡] DC infusions from 79M and 82M into recipient 85M (study 3) were not proceeded with due to inadequate numbers of DC propagated in culture (see discussion in text).

[§] Several animals in the colony have been genotyped and found to have 3 *Caja*-DRB*W16 alleles, including animal 82M. This is presumably related to haematopoietic chimerism from circulatory exchange known to occur between marmoset twins *in utero*.

4.3.3. Yield of marmoset MoDC and HPDC following culture

The yield of marmoset MoDC and HPDC after *in vitro* propagation and culture are shown in Figure 4.3.3 and Figure 4.3.4.

Due to an inadequate yield of propagated DC (both HPDC and MoDC) from cultures for the second allogeneic DC trafficking study (study #3 in Table 4.3.1, donor marmosets 82 and 79), it was necessary to abandon this study prior to DC administration. Thus, 2 further donor animals were G-CSF mobilised in order to propagate MoDC and HPDC (study #4, donor marmosets 863 and 75).

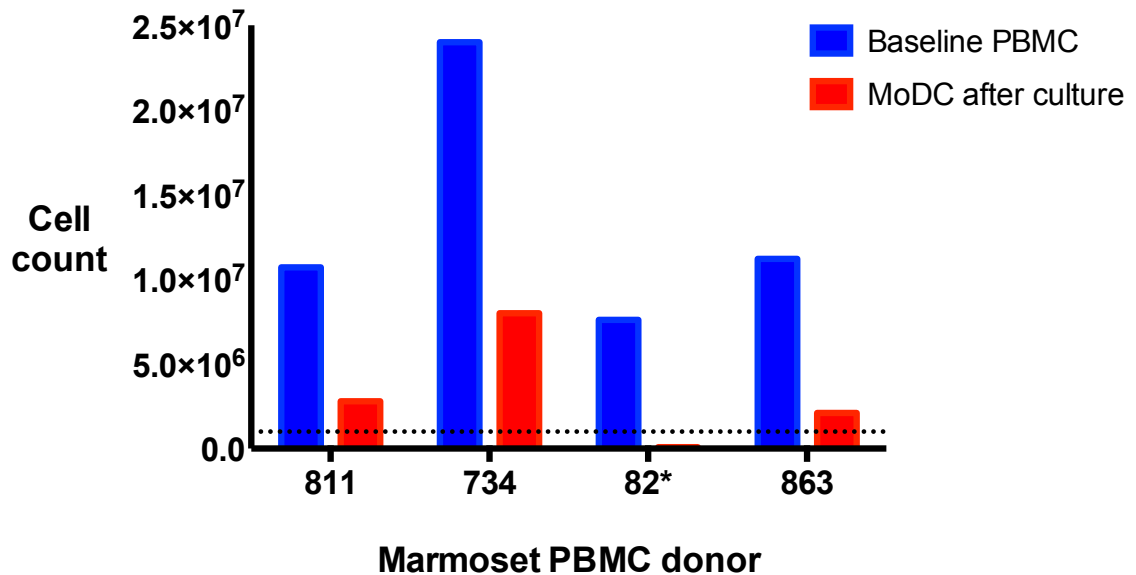


Figure 4.3.3. Yield of marmoset peripheral blood mononuclear cells (PBMCs) and immature monocyte-derived dendritic cells (MoDC) following G-CSF mobilisation and subsequent MoDC culture.

Marmoset donors were mobilised with 5 days of subcutaneously administered recombinant human (rh-) G-CSF 10-15µg/kg/day, and bled up to 3-4mls of peripheral venous blood over 2 days. Following Ficoll density gradient separation and lysis of red blood cells, PBMCs were isolated. Baseline PBMC counts were between 7.6×10^6 and 2.4×10^7 cells. After isolation of monocytes by plastic adherence and culture in complete medium (CM) supplemented with GM-CSF/IL-4 for up to 7 days, the yield of marmoset immature MoDC was 2.1×10^6 to 8×10^6 cells.

*MoDC culture from one animal (marmoset 82) failed to produce an adequate cell count for infusion (arbitrarily set at 1×10^6 cells, dotted line), this was due to a fungal infection encountered during cell culture.

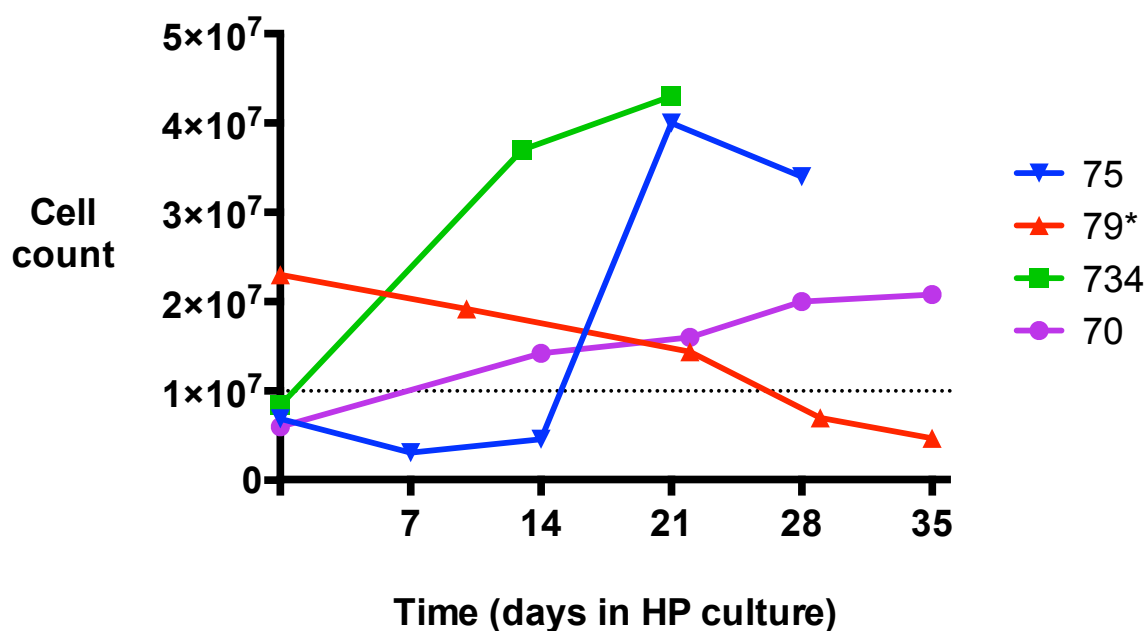


Figure 4.3.4. Yield of haematopoietic progenitor (HP) culture of G-CSF mobilised marmoset PBMCs, and subsequent differentiation of haematopoietic progenitor derived dendritic cells (HPDC).

Marmoset donors were mobilised with 5 days of subcutaneously rh-G-CSF 10-15µg/kg/day, and bled up to 3-4mls of peripheral venous blood over 2 days. One donor (marmoset 70) underwent planned euthanasia due to extremes of age following G-CSF mobilisation, and blood collected was via cardiac puncture. Following Ficoll density gradient separation and lysis of red blood cells, PBMCs were isolated. Bulk PBMCs were cultured in complete medium (CM) supplemented with FLT-3L, SCF and TPO to enrich for (CD34⁺) haematopoietic progenitors, for up to 4 weeks (HP culture). After HP culture, cells were washed and cultured for a further 7 days in CM supplemented with GM-CSF/IL-4 to propagate HPDC.

The duration of HP culture prior to HPDC propagation varied; see text for description. In all cases, the last point on the graph represents the final HPDC cell count, i.e. the yield. This ranged from 2.08x10⁷ to 4.3x10⁷ cells (excluding marmoset 79). The arbitrary threshold count for HPDC to be used for infusion was set at 1x10⁷ cells (dotted line).

*Cell counts progressively fell throughout HP culture for marmoset 79, and evidence of fungal infection was observed in some wells, so these cells were not used for infusion studies.

4.3.4. Confirmation of allo-reactivity between donors and recipients in allogeneic mixed leucocyte reaction

Mixed leucocyte reactions (MLRs) were performed between using PBMCs from each allogeneic donor-recipient pair from study #1 and #4, and confirmed significant allo-reactivity between 3 of the 4 donor-recipient pairs (see Figure 4.3.5). This is shown by the difference of the stimulation indices from baseline (i.e. a reference point of 1). One pair (75F versus 85M, HPDC donor for study #4) did not reach statistical significance due to high baseline proliferation in several single cells wells of the MLR.

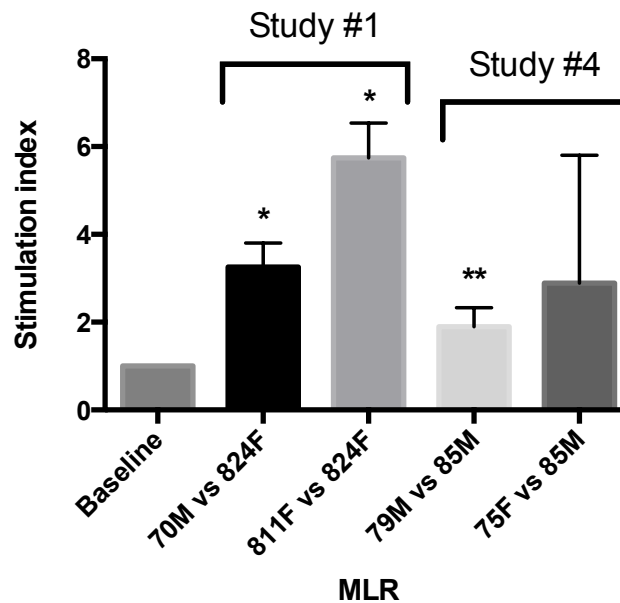


Figure 4.3.5. Confirmation of allo-reactivity between allogeneic marmoset donors and recipients in allogeneic mixed leucocyte reactions (MLR).

Marmoset PBMC from marmoset donor-recipient pairs (study #1 and study #4 as per Table 4.3.1) were assessed for stimulatory capacity in allogeneic MLR. Stimulator (donor) PBMCs were irradiated with 30Gy prior to co-culture with recipient PBMC at a 1:1 ratio. T-cell proliferation was assessed by ^3H -thymidine incorporation, and converted to a stimulation index to enable comparison between pairings. A reference stimulation index (baseline) of 1 was used as a comparison. 3 of the 4 pairs showed significant allo-reactivity; one pair was not statistically significant; analysis of the data suggested this was due to an unexpectedly high baseline proliferation of recipient marmoset PBMCs in some wells of the MLR.

Results shown are mean \pm standard deviation and are a composite of 4 separate experiments.

PBMC = peripheral blood mononuclear cells.

* = $p < 0.001$; ** = $p < 0.01$ (Students unpaired t test; versus baseline)

4.3.5. Administration of allogeneic and autologous DC to marmoset recipients and collection of tissues

Three marmoset recipients simultaneously received approximately $6-7 \times 10^6$ /kg DiI-labelled MoDC ($\sim 2 \times 10^6$ total cells for an average animal of 300g) and approximately $6-7 \times 10^7$ /kg CFSE-labelled HPDC ($\sim 2 \times 10^7$ in total), via subcutaneous and intravenous routes respectively. Two recipients (824 and 85, study #1 and #4) received allogeneic DC from two MHC-mismatched donors; the other recipient (734, study #2) received autologous DC. No adverse effects were observed in any of the animals.

4.3.6. Trafficking of subcutaneously administered marmoset MoDC in vivo

Figure 4.3.6 shows that after 48 hours, DiI labelled MoDC were found at the site of subcutaneous injection for both allogeneic and autologous recipients, although fewer were seen in the autologous setting. However, no evidence of trafficking of subcutaneously injected MoDC to the draining lymph node was seen in either allogeneic recipient using immunofluorescence microscopy. Flow cytometry of one recipient's draining lymph node (marmoset 85, study #4) confirmed the lack of any DiI positive cells (Figure 4.3.7).

Unfortunately, no lymph node tissue was recovered from the autologous recipient (marmoset 734, study #2), despite the use of methylene blue as a localising agent.

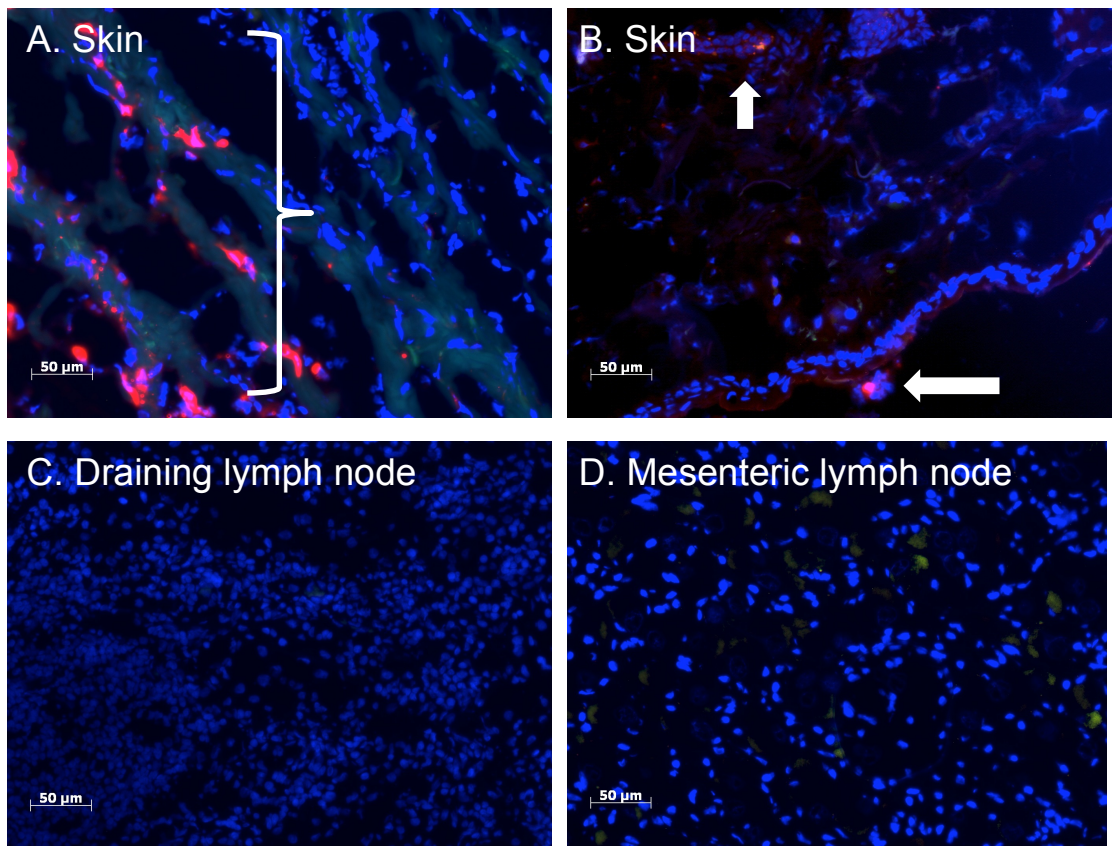


Figure 4.3.6. Marmoset MoDC labelled with DiI and injected subcutaneously are present at the site of injection after 48 hours but do not migrate to the draining lymph node.

Immunofluorescence microscopy of representative sections of marmoset tissue obtained at euthanasia 48 hours after subcutaneous injection of DiI-labelled marmoset MoDC. DiI labelled injected cells are shown in red and are detected in the rhodamine channel on the Zeiss microscope; cell nuclei are stained blue with DAPI counterstain. (A) Marmoset 824 skin (allogeneic recipient; study #1) showing multiple areas of DiI positive cells (bracket) in the dermis; (B) Marmoset 734 skin (autologous recipient; study #2) showing two nodules of DiI positivity (arrows) that appear to be in the epidermis/upper dermis and at the base of the dermis; (C) Marmoset 824 draining (R) inguinal lymph node identified via methylene blue, with no evidence of DiI positivity (D) Marmoset 824 mesenteric lymph node (as a control).

Immunofluorescence microscopy of the draining lymph node of Marmoset 85M (study #4) showed similar appearances, with no evidence of DiI positive cells. Unfortunately, the draining lymph node was not recovered at euthanasia of marmoset 734 (autologous recipient; study #2), despite the use of methylene blue for identification purposes.

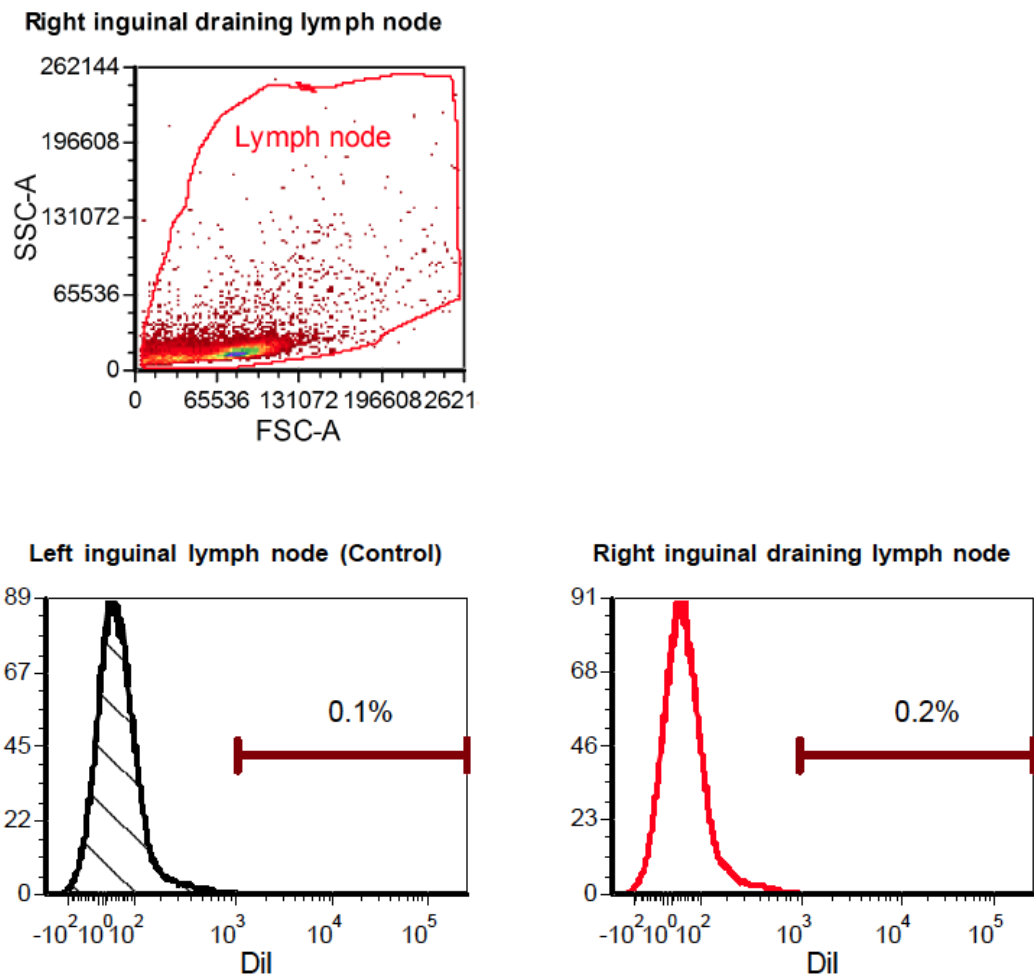


Figure 4.3.7. DiI positive marmoset MoDC are not found in the draining lymph node at 48 hours following subcutaneous injection.

48 hours after subcutaneous injection of DiI labelled allogeneic marmoset MoDC, lymph nodes were obtained at euthanasia and analysed by flow cytometry for the presence of DiI positive cells, using the PE channel of the FACS Canto II. Cells were included in the analysis gate on the basis of forward and side scatter characteristics (upper panel). There were no DiI positive cells seen in either a control lymph node (lower left panel) or the draining lymph node (right lower panel).

4.3.7. Trafficking of intravenously administered marmoset HPDC in vivo

Although a large dose of CFSE-labelled HPDC was administered intravenously to the two allogeneic marmoset recipients, there was no evidence of any CFSE-positive cells observed in any examined tissues (lungs, liver, kidney, lymph nodes or spleen) after euthanasia at 48 hours (Figure 4.3.8). Flow cytometry of fresh spleen in one recipient (85, study #4) also did not identify any distinct population of CFSE positive cells (Figure 4.3.9).

In the marmoset that received autologous HPDC (734, study #2), there were several areas of CFSE positivity noted in the spleen at 48 hours, and also a few CFSE staining cells seen in the liver (Figure 4.3.10). However, no CFSE positivity was observed in lungs, kidney or lymph nodes. In this case, flow cytometry was not performed.

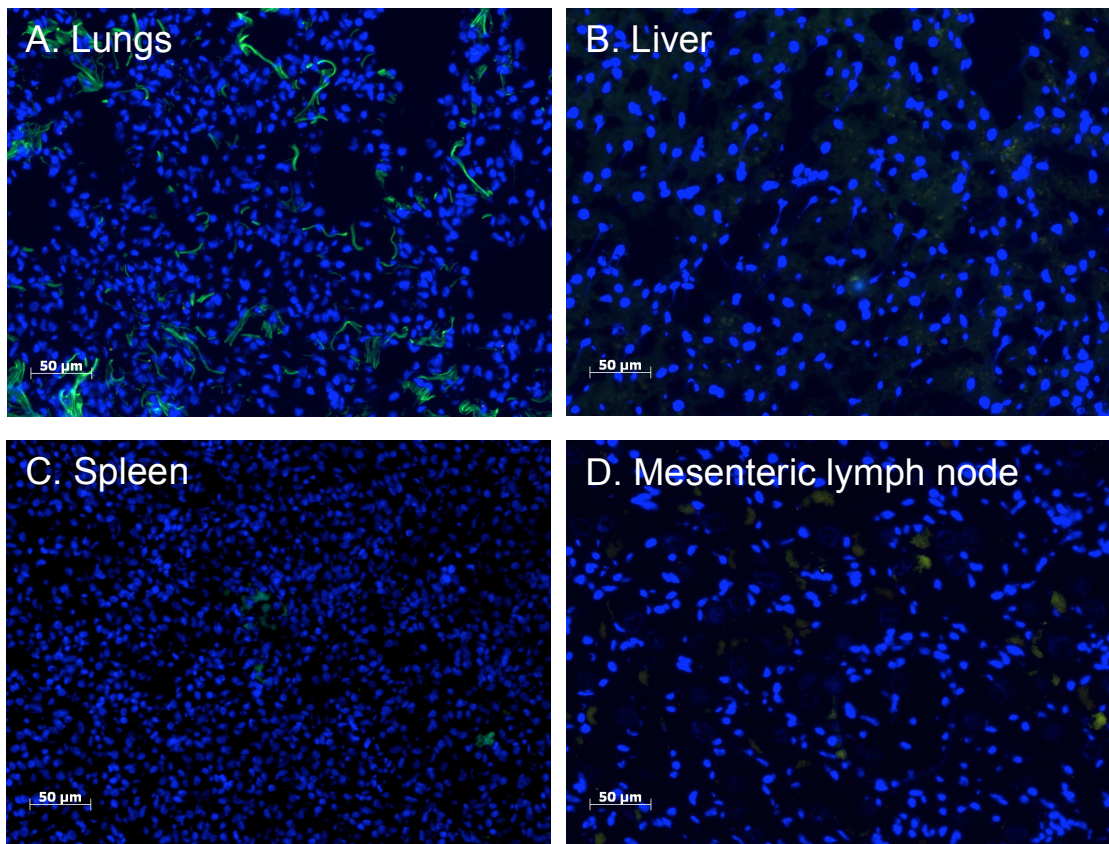


Figure 4.3.8. Allogeneic marmoset HPDC labelled with CFSE and injected intravenously are not detectable in tissues after 48 hours.

Immunofluorescence microscopy of representative sections of marmoset tissue obtained at euthanasia 48 hours after intravenous injection of *allogeneic* CFSE-labelled marmoset HPDC. CFSE injected cells (if present) should be stained green as they are detected in the GFP (green fluorescent protein) channel on the Zeiss microscope; cell nuclei are stained blue with DAPI counterstain. Tissues shown are from marmoset 824 (study #1): (A) lungs showing background auto-fluorescence of bronchial cartilage; (B) liver; (C) spleen; (D) mesenteric lymph node. No evidence of CFSE staining was identified in any of the tissues examined.

Immunofluorescence microscopy was performed on tissues taken from both marmoset 824 and 85M (study #1 and #4, respectively) and similar appearances were found, with no evidence of CFSE positive cells.

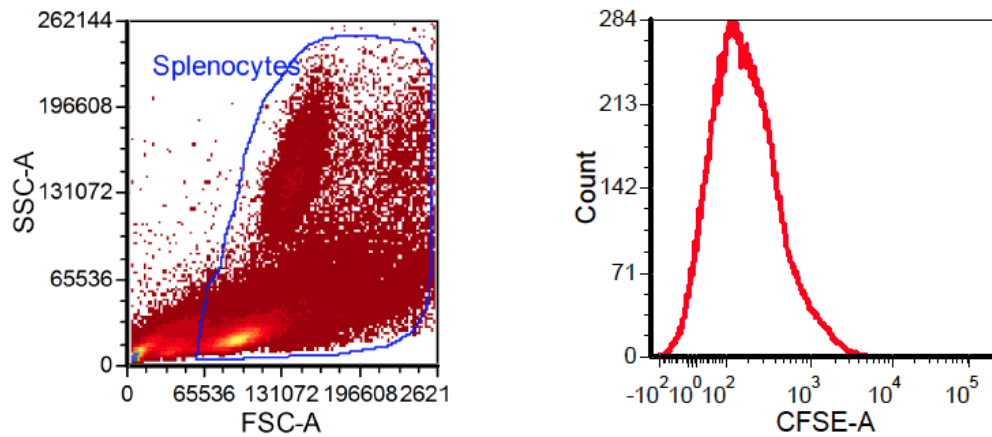


Figure 4.3.9. CFSE positive allogeneic marmoset HPDC are not found in the spleen at 48 hours following intravenous injection.

48 hours after intravenous injection of CFSE labelled allogeneic marmoset HPDC, a sample of fresh spleen was obtained at euthanasia and analysed by flow cytometry for the presence of CFSE positive cells. Cells were included in the analysis gate on the basis of forward and side scatter characteristics (left panel). No distinct population of CFSE positive cells was seen, i.e. there was only a single peak observed (right panel), although the lack of any control fresh spleen tissue from another animal (not given CFSE labelled DC) should be noted.

The spleen cells used in the analysis were taken from study #4, i.e. allogeneic recipient 85M.

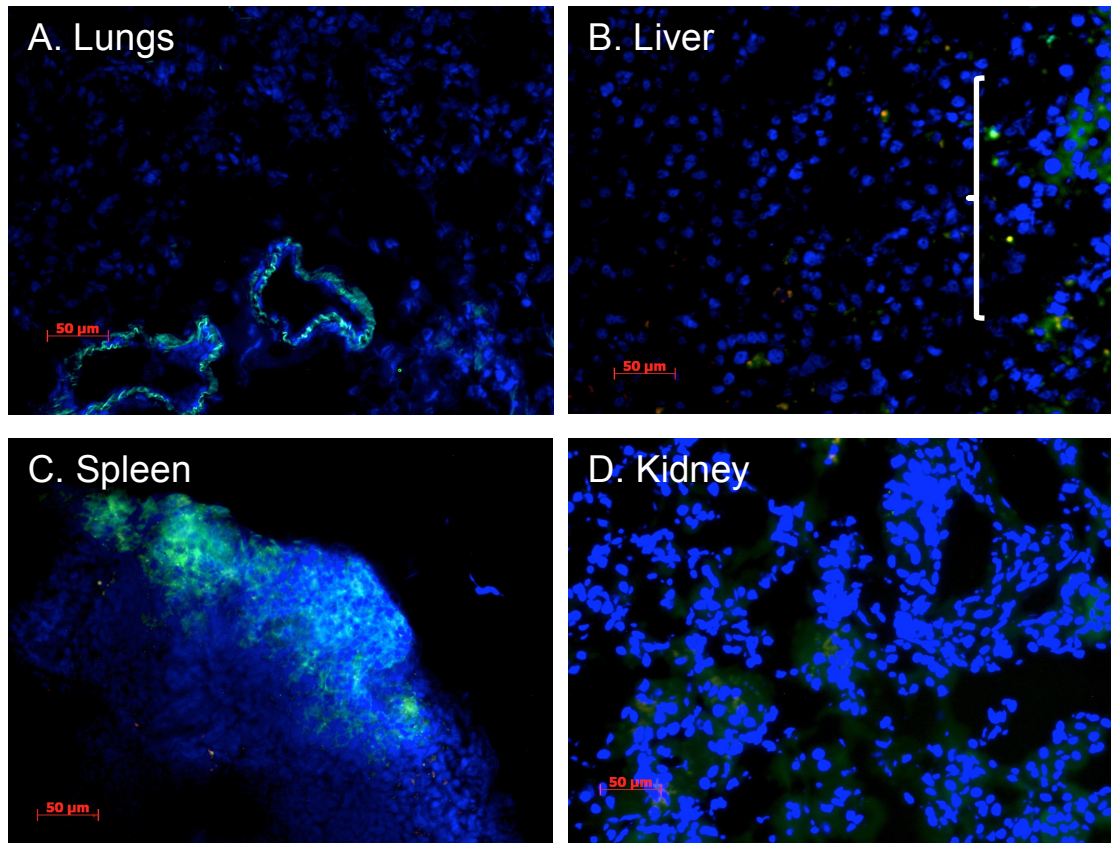


Figure 4.3.10. Autologous marmoset HPDC labelled with CFSE and injected intravenously are detectable in spleen and possibly liver after 48 hours.

Immunofluorescence microscopy of representative sections of marmoset tissue obtained at euthanasia 48 hours after intravenous injection of *autologous* CFSE-labelled marmoset HPDC. CFSE injected cells stain green as they are detected in the GFP (green fluorescent protein) channel on the Zeiss microscope; cell nuclei are stained blue with DAPI counterstain. Tissues shown are from marmoset 734 (study #2): (A) lungs showing background auto-fluorescence of bronchial cartilage; (B) liver showing scattered CFSE positive cells; (C) spleen showing some peripheral nodules of CFSE positive cells; (D) kidney, no CFSE staining.

4.4. Discussion

In this chapter, a series of studies were undertaken in order to investigate the trafficking of *in vitro* propagated DC following subcutaneous or intravenous injection in the marmoset non-human primate model. Two allogeneic studies were undertaken, with an autologous study as a control. The purpose of this study was both to determine whether *in vitro* propagated marmoset DC possess migratory capacity *in vivo*; and secondly to investigate the behaviour of injected allogeneic DC compared with autologous DC in a robust non-human primate model. This is the first reported study of allogeneic DC trafficking in a primate model.

Marmoset MoDC and HPDC were propagated *in vitro* from G-CSF mobilised peripheral blood using methods previously established in our laboratory,^{303,403} and based on human protocols.¹⁹⁵⁻¹⁹⁷ These DC have previously been shown to have an immature and semi-mature phenotype respectively when propagated using these methods in this laboratory.⁴⁰³ In this study, sufficient numbers of DC were propagated from peripheral blood samples of 1-2 ml taken from live donor monkeys for the studies of DC infusion (Figure 4.3.3 and Figure 4.3.4), although one planned experiment (study #3) had to be abandoned due to inadequate growth of cells in culture. This confirms the feasibility of this method of DC propagation for kidney transplant studies, where a donor animal would need to remain alive and healthy to provide a kidney some time after donating DC. This is in contrast to other approaches to sourcing DC from marmosets, which involve killing the donor animal.^{399,539} Additionally, labelling with CFSE had no effect on viability (Figure 4.3.2), and DiI and CFSE did not alter the allo-stimulation potential of marmoset DC in mixed leucocyte reaction (Figure 4.3.1), confirming the suitability of the fluorescently labelled cells for these studies.

Following subcutaneous injection of DiI labelled MoDC, DiI positive cells were visible at the site of injection at 48 hours but not in the draining lymph node in allogeneic recipients (Figure 4.3.6). Fewer DiI positive cells were seen in skin of the autologous recipient but regrettably no lymph node tissue was recovered from this animal, so that migration to the draining lymph node could not be assessed. No DiI positive cells were seen in any other examined tissues. The lack of detectable *allogeneic* DC present in the

draining lymph node was a surprising finding, and indeed for the final recipient (study #4), flow cytometry of the draining and contralateral nodes was undertaken to try and increase the sensitivity to detect DC; but no DiI fluorescence was detected (Figure 4.3.7). In a study of subcutaneous injection of *autologous* fluorescently labelled MoDC in chimpanzees using similar methods to those reported here,⁵⁸⁸ DC were noted to be present in the skin at 24 hours, but not at later time points; DC were seen in the draining lymph node between 24 and 48 hours and were still present in lower numbers at 120 hours. A later study using intradermal injection of immature and mature DC in rhesus macaques³⁹⁰ showed that both cell types were present in the draining lymph node at 36 hours but that mature DC elicited an inflammatory response in the skin and were still present there; immature DC were not found in the skin at this time-point.

The reasons for the apparent lack of migration ability of subcutaneously injected DC in this study are unclear. Whether marmoset *in vitro* propagated MoDC and HPDC express chemokine receptors involved in migration to draining lymph nodes such as CCR8 and CCR7 is currently unknown, however the identification of anti-human chemokine receptor antibodies that are cross-reactive with marmoset cells⁵²⁰ makes such studies both feasible and necessary to advance this model. Additionally, studies of cell migration behaviour *in vitro* could be undertaken to investigate this further, using techniques such as Transwell® migration^{589,590} or a chemotaxis chamber.³⁹⁰

Studies in mice,^{584,586,587,591} primates,^{588,592} and humans^{593,594} have shown that following subcutaneous injection of mature or immature DC, only a small proportion (<1%) ever reach the draining lymph node. Moreover, several of these studies^{593,594} have demonstrated that a greater proportion of DC can be found in the lymph node following intradermal rather than subcutaneous route of administration. Regardless, only a small proportion of injected monocyte-derived DC need to reach the lymph node in order to elicit strong antigen-specific immune responses, and many cells will remain at the injection site, lose viability and be cleared by infiltrating macrophages by 48 hours.⁵⁹⁵ In this study, although DiI positive cells were visible at the site of injection, it is not known whether these cells remained viable; additionally comparatively few cells were present in the skin compared with the high numbers injected ($\sim 2 \times 10^6$ for an average animal weighing 300g). This observation implies that a significant proportion of the cells had been lost, and raises the possibility that clearance of injected cells by

inflammatory macrophages^{390,595} or NK cells³⁶⁹ may have occurred, particularly in the case of the allogeneic DC.

Following intravenous infusion of a total dose of approximately 2×10^7 CFSE labelled HPDC, CFSE positive cells were visible in the spleen and liver of the recipient of autologous DC, confirming the migratory capacity of these cells, but not in the recipients of allogeneic DC (Figure 4.3.8). To date, there are few reported studies of tracking of intravenously injected DC in NHP,⁵⁹² and none investigating migration to internal organs such as spleen, lungs or liver. Studies in mice (using bone-marrow or splenic DC)⁵⁸²⁻⁵⁸⁷ and humans (using monocyte-derived DC)^{593,596,597} of DC trafficking *in vivo* using scintigraphy, positron emission tomography, or magnetic resonance imaging, or *in vitro* using scintigraphy or bioluminescence, have shown that intravenously injected *autologous* DC home to large vascular organs, typically to the lungs in the first 24 hours and thereafter to the spleen and liver. In a study involving higher resolution analysis of tissue distribution to smaller and deeper tissues in mice,⁵⁹⁸ intravenous bone marrow derived DC were shown to eventually also home to specific lymph nodes in the pancreatic area and draining the lungs. In the present study, no CFSE positivity was observed in the lungs in any of the marmosets at the 48-hour time point, which is consistent with previous observations. However, although CFSE positive cells were found in the spleen and liver of the recipient of autologous DC, no CFSE positivity was seen in the recipients of allogeneic DC. In mice at least, intravenously injected allogeneic DC appear to home to tissues normally,⁵⁸⁶ so it seems unlikely that this observation is due to impaired migratory capacity of intravenously injected allogeneic DC in comparison to autologous DC. Alternatively these cells may have been cleared or destroyed by recipient NK cells, as has been observed with donor DC in a classic skin transplant study.³⁶⁹

A potential criticism of this study is that each recipient animal received both MoDC and HPDC simultaneously. However, it is important to note that the primary purpose of this study was to determine the trafficking behaviour of injected DC in marmoset recipients, rather than to investigate the immune responses of recipients to DC therapy. In addition, at the time of commencing this study and obtaining ethics committee approval, it was intended that further studies would be undertaken of donor-derived DC therapy in marmosets followed by kidney transplantation using animals in the colony at Queen

Elizabeth Hospital. As such, the study was designed to comply with ethical imperatives and the NHMRC endorsed principle of minimising the numbers of primates used in research.⁵⁵⁴

A limitation of this study is that in order to determine the behaviour of injected DC *in vivo*, it was necessary to kill recipient marmosets to obtain tissues for analysis. This limited the numbers of studies that could be performed, even with the use of simultaneous MoDC and HPDC injections as outlined above. Although the analysis of whole organs with immunofluorescence microscopy techniques and flow cytometry enables a high degree of resolution and the potential to identify individual fluorescently labelled cells, other non-invasive methods can be used successfully to track the behaviour of cells *in vivo*.⁵⁸³ Radiolabelling and scintigraphy,^{593,594,599} magnetic resonance imaging,⁶⁰⁰ and positron emission tomography⁵⁸⁷ have all been used to track DC *in vivo* with an acceptable degree of spatial resolution. More recently the technique of bioluminescence imaging has been developed and used in studies of DC migration in mice, e.g. using DC transduced with viral vectors containing firefly luciferase.⁶⁰¹ This technique could conceivably be applied in marmosets, given their relatively small size (adult weight typically 300-400g), and underlines the suitability of this non-human primate model for studies of this type.

Morelli and colleagues have recently demonstrated in an elegant series of cardiac transplant studies in mice that intravenously injected *allogeneic* (donor) tolerogenic DC are unable to directly regulate donor-specific T-cells *in vivo*.³³¹ It was shown that these donor DC die quickly after injection, and that donor antigen is reprocessed and presented to T-cells by endogenous (recipient) DC via the indirect pathway. A subsequent study demonstrated that the immunosuppressive and graft prolonging effects of donor DC therapy is mediated by and dependent on endogenous conventional DC.⁶⁰² *Autologous* DC used as vaccines and loaded with tumour antigens have similarly been shown to mediate their effect on CD8 T-cells via antigen transfer to endogenous APC (typically DC).⁶⁰³ In an earlier study done in our laboratory, infusion of *in vitro* propagated immature (Mo)DC into allogeneic marmoset recipients resulted in reduced anti-donor and anti-third party responses in 2 out of 3 animals (described in Chapter 1, section 1.8.3).³⁰³ A study in rhesus macaques had similar findings.³⁵⁰ The results of these NHP studies of DC immunotherapy, and the lack of allogeneic cells in spleen or

liver observed in the present study, taken together with the observations of Morelli and colleagues,^{331,602} suggest that while allogeneic DC have effects on the immune response, these do not necessarily occur via the direct interaction of infused donor cells with recipient T-cells. Rather, similar to the effects on immune responses observed with donor-specific transfusion,^{604,605} donor derived tolerogenic DC therapy may act merely as a source of donor antigen for recipient DC, perhaps via the apoptosis of donor cells.⁶⁰⁶ Additionally, there is evidence that in some settings donor DC therapy results in sensitisation of the recipient towards donor antigens.⁶⁰⁷

This study does not directly address the question of which route of administration would be most efficacious to promote a tolerogenic response to donor-derived DC therapy. However, the results provide some insight into the outcome *in vivo* after injection of allogeneic DC via different sites. Following intravenous injection, DC appear to be rapidly cleared and were not visible as intact cells in any of the tissues examined at 48 hours. As discussed above, apoptotic DC can be tolerogenic,⁶⁰⁶ and systemic administration may facilitate the greatest exposure of recipient DC to injected donor antigen in the absence of local inflammatory stimuli, even if the injected DC do not directly interact with T-cells.³³¹ Following subcutaneous injection however, DC were still present at the site of injection after 48 hours, and no evidence of migration of these cells to the draining lymph node was seen. Many studies of subcutaneous or intradermal injection of DC have been in the context of tumour vaccination studies,^{608,609} and designed to promote an immune activating rather than a tolerogenic response, although autologous immature DC administered subcutaneously can inhibit the immune response.²⁵⁸ It is possible that rather than migrating to the draining lymph node and initiating a tolerogenic response, as hoped for with this approach, allogeneic DC might initiate a localised inflammatory response in the presence of donor antigen (whether or not the DC were viable or remained immature in phenotype) resulting in immune activation⁷² through the involvement of recipient Langerhans cells, and other local infiltrating immune cells such as monocytes or macrophages. Although this study did not specifically investigate for evidence of an inflammatory reaction present at the site of injection, other primate studies have made this observation.³⁹⁰ To date, no direct comparisons between subcutaneous or intradermal and intravenous administration of tolerogenic DC therapies have been reported, although tumour vaccination studies have

indicated that subcutaneous rather than intravenous administration of DC is more effective at promoting a vaccine-induced immune activating response,⁵⁸⁴ and many investigators propose that the intravenous route is more appropriate for tolerance induction.^{264,579}

In conclusion, while donor-derived DC therapy has demonstrated potential in rodent models and primate studies to promote a tolerogenic immune response, this study suggests that the mechanisms by which this occurs is not via normal DC trafficking and interaction with recipient T-cells, at least in this primate model. This appears to be regardless of whether the route of administration of DC is intravenous or subcutaneous. Data from recent studies suggests that the beneficial effects of donor derived DC therapy may in fact occur largely through acquisition and reprocessing of donor antigen by recipient DC, for presentation to T-cells via the indirect pathway.

In light of these findings and recent published data, the logistical difficulties inherent in cellular therapy, and the ethical implications of undertaking further studies of donor-derived DC therapy followed by kidney transplantation surgery in marmosets, it was decided to pursue an alternative strategy of DC immunotherapy via targeting marmoset DC *in situ* for the subsequent studies reported in this thesis.

**Chapter 5: DEVELOPMENT OF
MONOCLONAL ANTIBODIES TO
TARGET DC-SIGN ON MARMOSET
DENDRITIC CELLS TO FACILITATE
TARGETED THERAPY**

5.1. Introduction

Monoclonal antibodies have a well established place in biomedical science, with applications ranging from cell or antigen identification in basic research,⁶¹⁰ diagnostic tests,⁶¹¹ through to therapeutic agents for the treatment of human disease.⁶¹² All monoclonal antibodies share the unique characteristic that they bind their unique target molecule with extremely high specificity and sensitivity, enabling precise selection of almost any target of interest. Since the discovery of hybridoma technology in 1975,⁶¹³ it has become feasible to generate large numbers of mouse monoclonal antibodies against almost any target molecule that is capable of being used as an immunogen; screening of these can be done to select antibody clones of high affinity, and stable cell lines can be produced to ensure their indefinite availability for future use.^{614,615} Further developments in this technology have improved the suitability of antibodies for use in therapeutics, in particular the ability to generate chimeric and fully humanised antibodies,⁶¹⁶ thus avoiding the problems associated with species immune differences.⁶¹⁷

The use of monoclonal antibodies to target specific cell types by binding to specific cell-surface proteins in conjunction with drugs or drug-carriers offers the potential to develop cell-specific therapies. DC play a pivotal role in the generation of immune responses, in particular to a transplanted organ or tissue, and thus these cells represent a highly desirable target for such therapies. DC express numerous surface receptors that could be utilised as targets in this manner. The C-type lectin DC-SIGN is one such receptor that is particularly attractive for such an approach, as it is highly specific for DC (with some low level expression on macrophages), and has important roles in antigen uptake and cross-presentation to T-cells.^{193,218,220,415,618}

In this thesis, a series of studies have been undertaken with the overall aim to develop DC based immunotherapy in a NHP transplant model, the common marmoset monkey. It is necessary to investigate such therapies in a suitable pre-clinical model prior to proceeding to human clinical trials,³⁹ and the marmoset monkey is becoming established as an important and useful model for DC therapies in a transplant context.^{303,399,402,403,539} In contrast to the studies undertaken in the previous chapter of using *donor* derived DC as a cellular therapy to facilitate tolerogenic responses to an

organ transplant, this and the following chapter will consider an alternative approach based on targeting *recipient* DC *in situ* via DC-SIGN using monoclonal antibodies as the means to specifically target these cells.

To date, it has yet to be established whether currently available anti-human antibodies that bind human DC-SIGN are cross-reactive with marmoset DC-SIGN. Studies of *in vitro* propagated marmoset DC have not identified DC-SIGN expression,⁴⁰³ and although the marmoset DC-SIGN peptide has been sequenced and found to have approximately 80% homology with human DC-SIGN,^{458,619} it is unknown whether the marmoset DC-SIGN has similar structure or functionality *in vivo*. In addition, there are currently no published studies of the surface markers or phenotype of marmoset tissue DC, so it is uncertain whether DC-SIGN would be a suitable target to use for DC targeted immunotherapy in this species.

The aims of this chapter are:

1. To develop monoclonal antibodies targeting marmoset DC-SIGN that could be used in subsequent studies of DC immunotherapy in the marmoset pre-clinical model of transplantation.
2. To clone marmoset DC-SIGN, and express it on the surface of a Chinese Hamster Ovary (CHO) cell line, to ensure that a suitable marmoset DC-SIGN⁺ cell would be available to use for screening of generated monoclonal antibodies.
3. To determine if DC-SIGN expression can be detected on the surface of marmoset DC – i.e. (1) marmoset *in vitro* propagated DC, or (2) marmoset *in vivo* tissue DC isolated from lymphoid tissue – using generated monoclonal antibodies or a commercially available anti-human DC-SIGN.

5.2. Methods

5.2.1. Cell culture

Protocols for cell culture are outlined in detail in Chapter 2 (section 2.4); additional details where necessary are described in the sections below.

5.2.2. Cloning of marmoset and human DC-SIGN

Marmoset and human DC-SIGN were cloned from stored marmoset and human cDNA, extracted from frozen marmoset spleen, thymus and liver, and human MoDC, respectively.⁴⁵⁸ Protocols for PCR, agarose gel electrophoresis, ligation into cloning vectors, transformation of competent *E. Coli*, and transfection of CHO cell lines are outlined in Chapter 2 (section 2.7).

5.2.2.1 Primers

PCR primers were chosen based on confirmed sequences of human and marmoset DC-SIGN, and are listed in Table 5.2.1.

Table 5.2.1. Sense and anti-sense primers used for cloning of human and marmoset DC-SIGN

Gene	GenBank* Accession number	Sense primer 5'-3'	Anti-sense primer 5'-3'	Product size (bp)	T _M (°C)
Human DC-SIGN	NM_021155	ggggTgACATgAg TgACTCCAA	CTACgCAggAgggggg gTTTg	1215	60
Marmoset DC-SIGN	EU041929.1	ATgAgTgACTCC CAggAACC	CAggAgAgAAgCCT TTCTTCATC	1113	68

* Sequence available at <http://www.ncbi.nlm.nih.gov/genbank/>. Accessed November 2010.

bp = base pairs

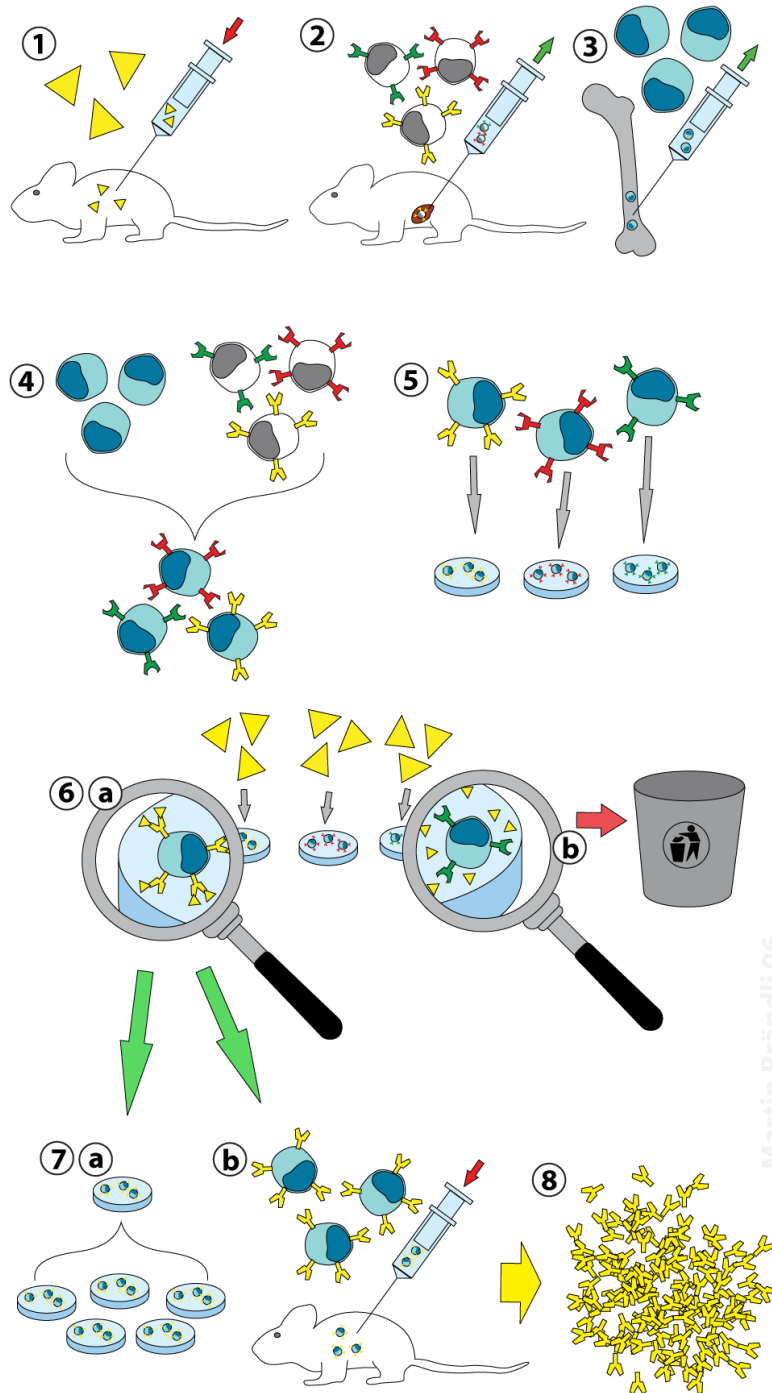
T_M = predicted primer annealing temperature

5.2.3. Development of monoclonal antibodies targeting marmoset DC-SIGN

Monoclonal antibodies against marmoset DC-SIGN were generated under a commercial arrangement with Neobody Pty Ltd (now Biosensis; Thebarton, SA). The process is outlined schematically in Figure 5.2.1. Briefly, five Balb/c mice were immunised using 3mg of a mixture of three antigenic peptides derived from the amino acid sequence of marmoset DC-SIGN, and conjugated to keyhole limpet haemocyanin (KLH) as an adjuvant. The sequences were chosen by Neobody on the basis of their likely antigenicity and cross-reactivity with both human and marmoset DC-SIGN, and were taken from different locations within the whole peptide sequence. The sequences of the three peptides that were used were:

Antigenic peptide #1	QQEIQELLQLKAAVGE
Antigenic peptide #2	NSVTACQEVGAQLVII
Antigenic peptide #3	FTLLAGVLVAILVQVS

Antibody titres were evaluated using ELISA and hybridoma fusion was carried out between splenocytes and myeloma cells. After screening for binding against peptides #1, #2, and #3 using ELISA (performed by Neobody), 15 positive clones (supernatants) from hybridomas were confirmed as having reactivity against peptides #1 and #2, but not against peptide #3. These 15 hybridoma supernatants were submitted to this laboratory for further testing as per section 5.2.4 below.



Martin Brändli 06

Figure 5.2.1. Summary of the steps in the process of generating monoclonal antibodies with the use of hybridoma technology.

(1) Immunisation of a mouse; (2) Isolation of B cells from the spleen; (3) Cultivation of myeloma cells; (4) Fusion of myeloma and B cells; (5) Separation of cell lines; (6) Screening of suitable cell lines; (7) in vitro (a) or in vivo (b) multiplication; and (8) Harvesting.

Reprinted from a figure by Martin Brändli; © 2010. Used with permission, under the terms of the Creative Commons Attribution-Share Alike 2.5 Generic licence.

5.2.4. Screening of monoclonal antibodies for binding to marmoset and human DC-SIGN

Marmoset and human monocyte derived DC were generated as described in Chapter 2 (sections 2.4.2 and 2.4.3, respectively), and used on day 5-7 of culture with GM-CSF/IL-4, without the addition of maturation stimuli. CHO cells transfected with marmoset or human DC-SIGN were generated as per section 2.7.2, and were used 24-48 hours post transfection.

Cells ($2-5 \times 10^6$ /ml in staining buffer) were Fc-receptor blocked with 10% v/v heat inactivated rabbit serum, and incubated for 20 minutes at 4°C. Cells were then incubated with 50µL of each of the hybridoma supernatants, 100-500ng of purified (unconjugated) DC-SIGN antibody (BD clone DCN46), or 50µL supernatant from a mouse myeloma cell-line producing IgG1κ clone (X63; stored in-house), for 20 minutes at 4°C. Cells were washed in FACS wash, and further incubated with a secondary sheep anti-mouse IgG FITC for 25 minutes, fixed in FACS lysing solution (BD Biosciences) and washed twice in FACS wash buffer. Cells were also incubated with DC-SIGN FITC or isotype control FITC, and fixed and washed as above. Binding of hybridoma supernatants and DC-SIGN FITC (BD clone DCN46) to cells was established by flow cytometry (FACS Canto II, BD Biosciences) and data was analysed using FCS Express software version 3 (DeNovo).

Antibodies showing evidence of binding to marmoset DC-SIGN were further tested for binding to DC-SIGN in human spleen and marmoset lymphoid (spleen and thymus) tissues, using immunofluorescence microscopy as outlined in Chapter 2 (section 2.5).

5.2.5. Generation of purified monoclonal antibodies against marmoset DC-SIGN

Following the selection of two hybridoma supernatants for purification (clones 9E6A8 and 9E6E12), Neobody Pty Ltd produced purified antibodies from these hybridomas. Briefly, selected hybridoma clones were sub-cloned by limiting dilution, and cell lines were created. Hybridomas were brought up conditioned media purified using protein G purification. Antibodies were dialysed against 1x PBS at a pH of 7.4. The presence of purified antibody was confirmed with the use of sodium dodecyl sulfate polyacrylamide gel electrophoresis (SDS-PAGE); and isotyping was performed using a Mouse MonoAB ID kit (HRP) (Zymed; now Invitrogen, Camarillo, CA, USA). Antibody was

resuspended in PBS with 0.03% (w/v) sodium azide, and the concentration was determined using spectrophotometry.

5.2.6. Identification of DC-SIGN positive cells in marmoset spleen and confirmation of monoclonal antibody binding

Marmoset splenocytes were obtained following euthanasia as described in section 2.4.2.5. Fresh splenocytes were analysed by flow cytometry, as described in Chapter 2 (section 2.6), with modifications as outlined here. Cells were collected into FACS tubes, washed extensively, and resuspended in staining buffer. After blocking with rabbit serum, splenocytes underwent multi-colour staining with Lineage markers (CD3, CD20 and CD56, all FITC), Class II PE-Cy5, CD11c APC, and DC-SIGN PE (clone DCN46). Isotype matched antibodies conjugated to FITC, PE-Cy5, APC and PE respectively were used as negative controls. In some experiments, 1 µg of the selected purified (unconjugated) monoclonal antibody clones (as per section 5.2.5), or an isotype unconjugated mouse IgG (clone P3.6.2.8.1) were substituted for DC-SIGN PE; these cells were incubated with these antibodies alone, followed by an additional incubation step with 20 µl of a secondary PE-conjugated goat anti-mouse IgG1 antibody for 25 minutes, prior to staining with conjugated antibodies. Compensation controls included the following:

1. Unstained cells (isotype matched controls)
2. FL-1 compensation: CD3 and CD20 FITC
3. FL-2 compensation: CD11c PE
4. FL-3 compensation: Class II PE-Cy5
5. FL-5 compensation: CD11c APC

Following staining as above, multi-colour flow cytometry was performed using a FACS Canto II flow cytometer (BD Biosciences). Approximately 200,000 events were recorded for experimental samples (5000 were recorded for compensation controls and 100,000 for isotype controls). Doublet discrimination was not performed. Cells were selected for inclusion in the analysis gate according to forward and side scatter characteristics (Figure 5.2.2.)

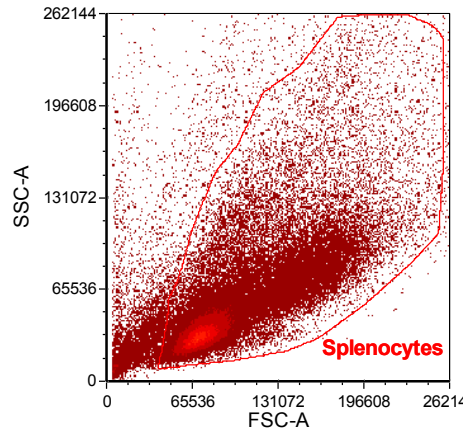


Figure 5.2.2. Forward and side scatter plot showing representative gate used to select marmoset splenocytes in the flow cytometry studies to identify DC-SIGN positive cells.

5.2.7. Confirmation of binding of purified monoclonal antibodies to marmoset and human DC-SIGN

Following purification, antibodies generated under section 5.2.5, in addition to purified BD clone DCN46, were tested to confirm binding with marmoset and human DC-SIGN using transfected CHO cells. In these experiments, a range of antibody concentrations (100ng-1µg) were utilised. X63 supernatant or isotype purified mouse IgG (clone P3.6.2.8.1) were used as controls; other aspects of the protocol were as described in section 5.2.4 above.

5.3. Results

5.3.1. Cloning of human and marmoset DC-SIGN

5.3.1.1 Cloning of DC-SIGN, ligation into pGEM®-T easy vector and sequencing

Marmoset and human DC-SIGN were cloned from stored cDNA (as per section 2.7.1) using specific primers and a Taq Polymerase (AmpliTaq Gold®, Applied Biosystems) to generate PCR products with 3' adenine overhangs to facilitate ligation into the pGEM®-T easy cloning vector (Figure 5.3.1). Agarose gel electrophoresis confirmed the generation of single PCR products of appropriate size (1215bp and 1113bp respectively). Ligation into pGEM®-T easy was followed by transformation of DH5 α *E. Coli* competent cells. Bacterial growth on LB-Agar plates (containing ampicillin, Xgal and IPTG) enabled the selection of white colonies containing the plasmid with the insert present. Successful transformation with plasmid confers ampicillin resistance (enabling growth), and interruption of the β -galactosidase enzyme gene by the presence of a PCR insert prevents a blue colour change, generating white colonies. A plasmid miniprep was used to isolate plasmid DNA, and *NotI* digestion and agarose gel electrophoresis confirmed the presence of DC-SIGN inserts of the correct size.

Following further culture of colonies containing the correct inserts, and maxiprep to isolate sufficient volumes of plasmid DNA, plasmid containing the insert DC-SIGN was sequenced. Sequence analysis confirmed the successful cloning of marmoset and human DC-SIGN (Figure 5.3.2 and Figure 5.3.3, respectively).

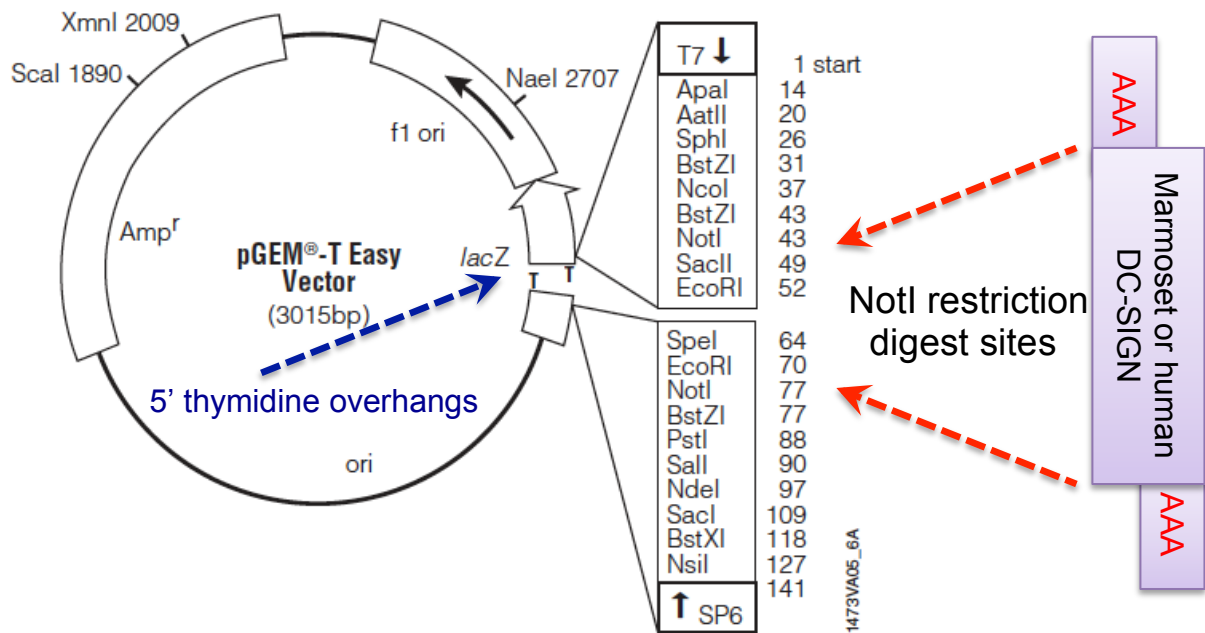


Figure 5.3.1. Schematic representation of cloning of marmoset and human DC-SIGN into the pGEM®-T-easy vector.

Marmoset and human DC-SIGN were cloned as described in the text, and were propagated using specific primers (section 5.2.2.1). PCR products, containing 3' adenine overhangs (represented by AAA on the ends of the PCR product; red text) were cloned into pGEM®-T easy plasmid vector containing 5' thymidine overhangs (represented by T on the vector; blue arrow). The NotI restriction enzyme digest site is indicated (red arrows).

LacZ = β -galactosidase gene (generates blue colonies, interrupted by presence of insert); Amp^r = ampicillin resistance gene

Modified from a figure by Natasha Rogers (2011).⁴⁵⁸

pGEM®-T easy vector map © 2010 Promega Corporation.

		1	50				
	marm2	(1)	-----		marm2	(540)	AGTGGGTGAATTGCCAGAGAAATCCAAGCAGCAGATCTACCAGAAACTGA
	marmA	(1)	-----		marmA	(540)	AGTGGGTGACTTGCCAGAGAAATCCAAGCAGCAGATCTACCAGAAACTGA
DC SIGN	Marmoset EU041929	(1)	-----		DC SIGN Marmoset EU041929	(540)	AGTGGGTGACTTGCCAGAGAAATCCAAGCAGCAGATCTACCAGAAACTGA
	pGEM-Teasy-marmDC-SIGN	(1)	GGGCGAATTGGGCCGACGTCGCATGCTCCCGGCCCATGGCGGCCGG		pGEM-Teasy-marmDC-SIGN	(601)	AGTGGGTGACTTGCCAGAGAAATCCAAGCAGCAGATCTACCAGAAACTGA
		51	100			651	700
	marm2	(1)	-----ATGAGTGA		marm2	(590)	CCGAGTTGAAGGCTGCAGTGGGTAAGCTCCCAGAGAAATCCAAGCAACA
	marmA	(1)	-----ATGAGTGA		marmA	(590)	CCGAGTTGAAGGCTGCAGTGGGTAAGCTCCCAGAGAAATCCAAGCAACA
DC SIGN	Marmoset EU041929	(1)	-----ATGAGTGA		DC SIGN Marmoset EU041929	(590)	CCGAGTTGAAGGCTGCAGTGGGTAAGCTCCCAGAGAAATCCAAGCAACA
	pGEM-Teasy-marmDC-SIGN	(51)	GGAATTCGATTATGAGTGA		pGEM-Teasy-marmDC-SIGN	(651)	CCGAGTTGAAGGCTGCAGTGGGTAAGCTCCCAGAGAAATCCAAGCAACA
		101	150			701	750
	marm2	(40)	TTCTGGAGGAGGAAGAACTTGGATCCAACAGACTCGAGGCTACAAGAG		marm2	(640)	GAGATCTACCAGGAAGTACCAGCTGAAGGCTGCAGTGGAAACCGCTGTG
	marmA	(40)	TTCTGGAGGAGGAAGAACTTGGATCCAACAGACTCGAGGCTACAAGAG		marmA	(640)	GAGATCTACCAGGAAGTACCAGCTGAAGGCTGCAGTGGAAACCGCTGTG
DC SIGN	Marmoset EU041929	(40)	TTCTGGAGGAGGAAGAACTTGGATCCAACAGACTCGAGGCTACAAGAG		DC SIGN Marmoset EU041929	(640)	GAGATCTACCAGGAAGTACCAGCTGAAGGCTGCAGTGGAAACCGCTGTG
	pGEM-Teasy-marmDC-SIGN	(101)	TTCTGGAGGAGGAAGAACTTGGATCCAACAGACTCGAGGCTACAAGAG		pGEM-Teasy-marmDC-SIGN	(701)	GAGATCTACCAGGAAGTACCAGCTGAAGGCTGCAGTGGAAACCGCTGTG
		151	200			751	800
	marm2	(90)	CTTAGCAGGGTGTCTTGGTCAGGCCCCCTGGTGTGCAACTCCCTCCT		marm2	(690)	CCGCCCTGTCCCTGGGAATGGACATCTTCCAAGGAAACTGTTACTTCA
	marmA	(90)	CTTAGCAGGGTGTCTTGGTCAGGCCCCCTGGTGTGCAACTCCCTCCT		marmA	(690)	CCGCCCTGTCCCTGGGAATGGACATCTTCCAAGGAAACTGTTACTTCA
DC SIGN	Marmoset EU041929	(90)	CTTAGCAGGGTGTCTTGGTCAGGCCCCCTGGTGTGCAACTCCCTCCT		DC SIGN Marmoset EU041929	(690)	CCGCCCTGTCCCTGGGAATGGACATCTTCCAAGGAAACTGTTACTTCA
	pGEM-Teasy-marmDC-SIGN	(151)	CTTAGCAGGGTGTCTTGGTCAGGCCCCCTGGTGTGCAACTCCCTCCT		pGEM-Teasy-marmDC-SIGN	(751)	CCGCCCTGTCCCTGGGAATGGACATCTTCCAAGGAAACTGTTACTTCA
		201	250			801	850
	marm2	(140)	TCACACTCTGGCTGGGGTCTGGTGGCCATCCTTGTTCAGAGTGTCCAG		marm2	(740)	TTTCTAACTCCAGCGCAACTGGCCCAACTCTGTCCAGCGCTGCCAGGAA
	marmA	(140)	TCACACTCTGGCTGGGGTCTGGTGGCCATCCTTGTTCAGAGTGTCCAG		marmA	(740)	TTTCTAACTCCAGCGCAACTGGCCCAACTCTGTCCAGCGCTGCCAGGAA
DC SIGN	Marmoset EU041929	(140)	TCACACTCTGGCTGGGGTCTGGTGGCCATCCTTGTTCAGAGTGTCCAG		DC SIGN Marmoset EU041929	(740)	TTTCTAACTCCAGCGCAACTGGCCCAACTCTGTCCAGCGCTGCCAGGAA
	pGEM-Teasy-marmDC-SIGN	(201)	TCACACTCTGGCTGGGGTCTGGTGGCCATCCTTGTTCAGAGTGTCCAG		pGEM-Teasy-marmDC-SIGN	(801)	TTTCTAACTCCAGCGCAACTGGCCCAACTCTGTCCAGCGCTGCCAGGAA
		251	300			851	900
	marm2	(190)	GTCCCCAGCTCCATAAGTCAGGGCAATCCAAGCAAGAGGAGATCTACCA		marm2	(790)	GTGGGGGCCAGCTTGTGCATAATCAAAGTGTAGGAGCAGAACTTCCT
	marmA	(190)	GTCCCCAGCTCCATAAGTCAGGGCAATCCAAGCAAGAGGAGATCTACCA		marmA	(790)	GTGGGGGCCAGCTTGTGCATAATCAAAGTGTAGGAGCAGAACTTCCT
DC SIGN	Marmoset EU041929	(190)	GTCCCCAGCTCCATAAGTCAGGGCAATCCAAGCAAGAGGAGATCTACCA		DC SIGN Marmoset EU041929	(790)	GTGGGGGCCAGCTTGTGCATAATCAAAGTGTAGGAGCAGAACTTCCT
	pGEM-Teasy-marmDC-SIGN	(251)	GTCCCCAGCTCCATAAGTCAGGGCAATCCAAGCAAGAGGAGATCTACCA		pGEM-Teasy-marmDC-SIGN	(851)	GTGGGGGCCAGCTTGTGCATAATCAAAGTGTAGGAGCAGAACTTCCT
		301	350			901	950
	marm2	(240)	GGAAGTGA		marm2	(840)	ACAGCTGCAGTCTTCCAGAAGCAACCGCTTGGCCTGGATGGGACTTTCAG
	marmA	(240)	GGAAGTGA		marmA	(840)	ACAGCTGCAGTCTTCCAGAAGCAACCGCTTGGCCTGGATGGGACTTTCAG
DC SIGN	Marmoset EU041929	(240)	GGAAGTGA		DC SIGN Marmoset EU041929	(840)	ACAGCTGCAGTCTTCCAGAAGCAACCGCTTGGCCTGGATGGGACTTTCAG
	pGEM-Teasy-marmDC-SIGN	(301)	GGAAGTGA		pGEM-Teasy-marmDC-SIGN	(901)	ACAGCTGCAGTCTTCCAGAAGCAACCGCTTGGCCTGGATGGGACTTTCAG
		351	400			951	1000
	marm2	(290)	AGCAAGAGGAGATCTACCAGGAGCTGACCCAGCTGAAGCCCGCAGTGGGT		marm2	(890)	ACCTAAAGCAGGAAGGCACATGGCAGTGGTGGATGGCTCACTCTGTCA
	marmA	(290)	AGCAAGAGGAGATCTACCAGGAGCTGACCCAGCTGAAGCCCGCAGTGGGT		marmA	(890)	ACCTAAAGCAGGAAGGCACATGGCAGTGGTGGATGGCTCACTCTGTCA
DC SIGN	Marmoset EU041929	(290)	AGCAAGAGGAGATCTACCAGGAGCTGACCCAGCTGAAGCCCGCAGTGGGT		DC SIGN Marmoset EU041929	(890)	ACCTAAAGCAGGAAGGCACATGGCAGTGGTGGATGGCTCACTCTGTCA
	pGEM-Teasy-marmDC-SIGN	(351)	AGCAAGAGGAGATCTACCAGGAGCTGACCCAGCTGAAGCCCGCAGTGGGT		pGEM-Teasy-marmDC-SIGN	(951)	ACCTAAAGCAGGAAGGCACATGGCAGTGGTGGATGGCTCACTCTGTCA
		401	450			1001	1050
	marm2	(340)	GAGCTCCCAGAGAAATCCAAGCAACAGGAGTCTACCAGGAGCTGACACG		marm2	(940)	CCAGCCTCAGGCGGTATTGGAACCAAGGAGAGCCCAACAATATCGGGGA
	marmA	(340)	GAGCTCCCAGAGAAATCCAAGCAACAGGAGTCTACCAGGAGCTGACACG		marmA	(940)	CCAGCCTCAGGCGGTATTGGAACCAAGGAGAGCCCAACAATATCGGGGA
DC SIGN	Marmoset EU041929	(340)	GAGCTCCCAGAGAAATCCAAGCAACAGGAGTCTACCAGGAGCTGACACG		DC SIGN Marmoset EU041929	(940)	CCAGCCTCAGGCGGTATTGGAACCAAGGAGAGCCCAACAATATCGGGGA
	pGEM-Teasy-marmDC-SIGN	(401)	GAGCTCCCAGAGAAATCCAAGCAACAGGAGTCTACCAGGAGCTGACACG		pGEM-Teasy-marmDC-SIGN	(1001)	CCAGCCTCAGGCGGTATTGGAACCAAGGAGAGCCCAACAATATCGGGGA
		451	500			1051	1100
	marm2	(390)	GCTGAAGGCCGAGTGGGTGAGCTCCCAGAGAAATCCAAGCAGCAGGAAA		marm2	(990)	GGAAAGACTGCGCGGAATTTAACGGCAATGGCTGGAACGACGACAGATGTA
	marmA	(390)	GCTGAAGGCCGAGTGGGTGAGCTCCCAGAGAAATCCAAGCAGCAGGAAA		marmA	(990)	GGAAAGACTGCGCGGAATTTAACGGCAATGGCTGGAACGACGACAGATGTA
DC SIGN	Marmoset EU041929	(390)	GCTGAAGGCCGAGTGGGTGAGCTCCCAGAGAAATCCAAGCAGCAGGAAA		DC SIGN Marmoset EU041929	(990)	GGAAAGACTGCGCGGAATTTAACGGCAATGGCTGGAACGACGACAGATGTA
	pGEM-Teasy-marmDC-SIGN	(451)	GCTGAAGGCCGAGTGGGTGAGCTCCCAGAGAAATCCAAGCAGCAGGAAA		pGEM-Teasy-marmDC-SIGN	(1051)	GGAAAGACTGCGCGGAATTTAACGGCAATGGCTGGAACGACGACAGATGTA
		501	550			1101	1150
	marm2	(440)	TCTACCAGGAGCTGACACGGCTGAAGGCTGCAGTAAAGTGGTGGCAGAC		marm2	(1040)	CGCCGCCAAATTTCTGGATCTGCAAAAAGTCCGAGCCTCTCTCCAGG
	marmA	(440)	TCTACCAGGAGCTGACACGGCTGAAGGCTGCAGTAAAGTGGTGGCAGAC		marmA	(1040)	CGCCGCCAAATTTCTGGATCTGCAAAAAGTCCGAGCCTCTCTCCAGG
DC SIGN	Marmoset EU041929	(440)	TCTACCAGGAGCTGACACGGCTGAAGGCTGCAGTAAAGTGGTGGCAGAC		DC SIGN Marmoset EU041929	(1040)	CGCCGCCAAATTTCTGGATCTGCAAAAAGTCCGAGCCTCTCTCCAGG
	pGEM-Teasy-marmDC-SIGN	(501)	TCTACCAGGAGCTGACACGGCTGAAGGCTGCAGTAAAGTGGTGGCAGAC		pGEM-Teasy-marmDC-SIGN	(1101)	CGCCGCCAAATTTCTGGATCTGCAAAAAGTCCGAGCCTCTCTCCAGG
		551	600			1151	1200
	marm2	(490)	AGGTCCAAGCAACAGGAGATCTACCAGGAAGTGTGCAGCTGAAGGCTGC		marm2	(1090)	GATGAAGAAAGGCTTCTCTCTG-----
	marmA	(490)	AGGTCCAAGCAACAGGAGATCTACCAGGAAGTGTGCAGCTGAAGGCTGC		marmA	(1090)	GATGAAGAAAGGCTTCTCTCTG-----
DC SIGN	Marmoset EU041929	(490)	AGGTCCAAGCAACAGGAGATCTACCAGGAAGTGTGCAGCTGAAGGCTGC		DC SIGN Marmoset EU041929	(1090)	GATGAAGAAAGGCTTCTCTCTG-----
	pGEM-Teasy-marmDC-SIGN	(551)	AGGTCCAAGCAACAGGAGATCTACCAGGAAGTGTGCAGCTGAAGGCTGC		pGEM-Teasy-marmDC-SIGN	(1151)	GATGAAGAAAGGCTTCTCTCTG-----
		601	650			1201	1250

Figure 5.3.2. Nucleotide sequence alignment of marmoset DC-SIGN.

Marmoset DC-SIGN was sequenced in the pGEM®-T easy vector, using T7 and SP6 primers (Sequencing done at Flinders Sequencing Facility; section 2.7.1.3). Sequencing results were aligned using Vector NTI software. Several single nucleotide polymorphisms are highlighted.

Legend: *marm2* and *marmA* = results from 2 different PCRs; *DC SIGN Marmoset EU041929* = published marmoset DC-SIGN sequence from Genbank; *pGEM-Teasy-marmDC-SIGN* = previously cloned marmoset DC-SIGN from this laboratory.⁴⁵⁸

1 50

human clone2 (1) -----

DC SIGN NM_021155 Human (1) -----

Human DC SIGN cloned A' rc (1) -----

pGEM-Teasy-humanDC-SIGN (1) GGGCGAATGGGCCCGACGTCGCATGCTCCCGCCGCCATGGCGCCGGC 100

51 100

human clone2 (1) -----**GGGCTGAC**ATGAGTGACTCCAAGGAACCAAGACTGCAGC

DC SIGN NM_021155 Human (1) -----ATGAGTGACTCCAAGGAACCAAGACTGCAGC

Human DC SIGN cloned A' rc (1) -----**GGGCTGAC**ATGAGTGACTCCAAGGAACCAAGACTGCAGC

pGEM-Teasy-humanDC-SIGN (51) GGAATTTCGATT**GGGCTGAC**ATGAGTGACTCCAAGGAACCAAGACTGCAGC 150

101 150

human clone2 (40) **AGCTGGGCCTCCTGGAGGAGGAACAGCTGAGAGGCCTGGATTCCGACAG**

DC SIGN NM_021155 Human (32) **AGCTGGGCCTCCTGGAGGAGGAACAGCTGAGAGGCCTGGATTCCGACAG**

Human DC SIGN cloned A' rc (40) **AGCTGGGCCTCCTGGAGGAGGAACAGCTGAGAGGCCTGGATTCCGACAG**

pGEM-Teasy-humanDC-SIGN (101) **AGCTGGGCCTCCTGGAGGAGGAACAGCTGAGAGGCCTGGATTCCGACAG** 200

151 200

human clone2 (90) **ACTCGAGGATACAAGACTTAGCAGGGTGTCTTGGCCATGGTCCCTCGGT**

DC SIGN NM_021155 Human (82) **ACTCGAGGATACAAGACTTAGCAGGGTGTCTTGGCCATGGTCCCTCGGT**

Human DC SIGN cloned A' rc (90) **ACTCGAGGATACAAGACTTAGCAGGGTGTCTTGGCCATGGTCCCTCGGT**

pGEM-Teasy-humanDC-SIGN (151) **ACTCGAGGATACAAGACTTAGCAGGGTGTCTTGGCCATGGTCCCTCGGT** 250

201 250

human clone2 (140) **GCTGCAACTCCTCTCCTTCACGCTCTTGGCTGGGCTCCTTGTCCAAGTGT**

DC SIGN NM_021155 Human (132) **GCTGCAACTCCTCTCCTTCACGCTCTTGGCTGGGCTCCTTGTCCAAGTGT**

Human DC SIGN cloned A' rc (140) **GCTGCAACTCCTCTCCTTCACGCTCTTGGCTGGGCTCCTTGTCCAAGTGT**

pGEM-Teasy-humanDC-SIGN (201) **GCTGCAACTCCTCTCCTTCACGCTCTTGGCTGGGCTCCTTGTCCAAGTGT** 300

251 300

human clone2 (190) **CCAAGTCCCCAGCTCCATAAGTCAGGAACAATCCAGCAAGACCGCATC**

DC SIGN NM_021155 Human (182) **CCAAGTCCCCAGCTCCATAAGTCAGGAACAATCCAGCAAGACCGCATC**

Human DC SIGN cloned A' rc (190) **CCAAGTCCCCAGCTCCATAAGTCAGGAACAATCCAGCAAGACCGCATC**

pGEM-Teasy-humanDC-SIGN (251) **CCAAGTCCCCAGCTCCATAAGTCAGGAACAATCCAGCAAGACCGCATC** 350

301 350

human clone2 (240) **TACCAGAACCTGACCCAGCTTAAAGCTGCAGTGGGTGAGCTCTCAGAGAA**

DC SIGN NM_021155 Human (232) **TACCAGAACCTGACCCAGCTTAAAGCTGCAGTGGGTGAGCTCTCAGAGAA**

Human DC SIGN cloned A' rc (240) **TACCAGAACCTGACCCAGCTTAAAGCTGCAGTGGGTGAGCTCTCAGAGAA**

pGEM-Teasy-humanDC-SIGN (301) **TACCAGAACCTGACCCAGCTTAAAGCTGCAGTGGGTGAGCTCTCAGAGAA** 400

351 400

human clone2 (290) **ATCCAAGCTGCAGGAGATCTACCAGGAGCTGACCCAGCTGAAGGCTGCAG**

DC SIGN NM_021155 Human (282) **ATCCAAGCTGCAGGAGATCTACCAGGAGCTGACCCAGCTGAAGGCTGCAG**

Human DC SIGN cloned A' rc (290) **ATCCAAGCTGCAGGAGATCTACCAGGAGCTGACCCAGCTGAAGGCTGCAG**

pGEM-Teasy-humanDC-SIGN (351) **ATCCAAGCTGCAGGAGATCTACCAGGAGCTGACCCAGCTGAAGGCTGCAG** 450

401 450

human clone2 (340) **TGGGTGAGCTTCCAGAGAAATCTAAGCTGCAGGAGATCTACCAGGAGCTG**

DC SIGN NM_021155 Human (332) **TGGGTGAGCTTCCAGAGAAATCTAAGCTGCAGGAGATCTACCAGGAGCTG**

Human DC SIGN cloned A' rc (340) **TGGGTGAGCTTCCAGAGAAATCTAAGCTGCAGGAGATCTACCAGGAGCTG**

pGEM-Teasy-humanDC-SIGN (401) **TGGGTGAGCTTCCAGAGAAATCTAAGCTGCAGGAGATCTACCAGGAGCTG** 500

451 500

human clone2 (390) **ACCCGGCTGAAGGCTGCAGTGGGTGAGCTTCCAGAGAAATCTAAGCTGCA**

DC SIGN NM_021155 Human (382) **ACCCGGCTGAAGGCTGCAGTGGGTGAGCTTCCAGAGAAATCTAAGCTGCA**

Human DC SIGN cloned A' rc (390) **ACCCGGCTGAAGGCTGCAGTGGGTGAGCTTCCAGAGAAATCTAAGCTGCA**

pGEM-Teasy-humanDC-SIGN (451) **ACCCGGCTGAAGGCTGCAGTGGGTGAGCTTCCAGAGAAATCTAAGCTGCA** 550

501 550

human clone2 (440) **GGAGATCTACCAGGAGCTGACCTGGCTGGAAGCTGCAGTGGGTGAGCTTC**

DC SIGN NM_021155 Human (432) **GGAGATCTACCAGGAGCTGACCTGGCTGGAAGCTGCAGTGGGTGAGCTTC**

Human DC SIGN cloned A' rc (440) **GGAGATCTACCAGGAGCTGACCTGGCTGGAAGCTGCAGTGGGTGAGCTTC**

pGEM-Teasy-humanDC-SIGN (501) **GGAGATCTACCAGGAGCTGACCTGGCTGGAAGCTGCAGTGGGTGAGCTTC** 600

551 600

human clone2 (490) **CAGAGAAATCTAAGATGCAGGAGATCTACCAGGAGCTGACTCGGCTGAAG**

DC SIGN NM_021155 Human (482) **CAGAGAAATCTAAGATGCAGGAGATCTACCAGGAGCTGACTCGGCTGAAG**

Human DC SIGN cloned A' rc (490) **CAGAGAAATCTAAGATGCAGGAGATCTACCAGGAGCTGACTCGGCTGAAG**

pGEM-Teasy-humanDC-SIGN (551) **CAGAGAAATCTAAGATGCAGGAGATCTACCAGGAGCTGACTCGGCTGAAG** 650

601 650

human clone2 (540) **GCTGCAGTGGGTGAGCTTCCAGAGAAATCTAAGCAGCAGGAGATCTACCA**

DC SIGN NM_021155 Human (532) **GCTGCAGTGGGTGAGCTTCCAGAGAAATCTAAGCAGCAGGAGATCTACCA**

Human DC SIGN cloned A' rc (540) **GCTGCAGTGGGTGAGCTTCCAGAGAAATCTAAGCAGCAGGAGATCTACCA**

pGEM-Teasy-humanDC-SIGN (601) **GCTGCAGTGGGTGAGCTTCCAGAGAAATCTAAGCAGCAGGAGATCTACCA**

651 700

human clone2 (590) **GGAGCTGACCCGGCTGAAGGCTGCAGTGGGTGAGCTTCCAGAGAAATCTA**

DC SIGN NM_021155 Human (582) **GGAGCTGACCCGGCTGAAGGCTGCAGTGGGTGAGCTTCCAGAGAAATCTA**

Human DC SIGN cloned A' rc (590) **GGAGCTGACCCGGCTGAAGGCTGCAGTGGGTGAGCTTCCAGAGAAATCTA**

pGEM-Teasy-humanDC-SIGN (651) **GGAGCTGACCCGGCTGAAGGCTGCAGTGGGTGAGCTTCCAGAGAAATCTA** 700

701 750

human clone2 (640) **AGCAGCAGGAGATCTACCAGGAGCTGACCCGGCTGAAGGCTGCAGTGGGT**

DC SIGN NM_021155 Human (632) **AGCAGCAGGAGATCTACCAGGAGCTGACCCGGCTGAAGGCTGCAGTGGGT**

Human DC SIGN cloned A' rc (640) **AGCAGCAGGAGATCTACCAGGAGCTGACCCGGCTGAAGGCTGCAGTGGGT**

pGEM-Teasy-humanDC-SIGN (701) **AGCAGCAGGAGATCTACCAGGAGCTGACCCGGCTGAAGGCTGCAGTGGGT** 800

751 800

human clone2 (690) **GAGCTTCCAGAGAAATCTAAGCAGCAGGAGATCTACCAGGAGCTGACCCA**

DC SIGN NM_021155 Human (682) **GAGCTTCCAGAGAAATCTAAGCAGCAGGAGATCTACCAGGAGCTGACCCA**

Human DC SIGN cloned A' rc (690) **GAGCTTCCAGAGAAATCTAAGCAGCAGGAGATCTACCAGGAGCTGACCCA**

pGEM-Teasy-humanDC-SIGN (751) **GAGCTTCCAGAGAAATCTAAGCAGCAGGAGATCTACCAGGAGCTGACCCA** 850

801 850

human clone2 (740) **GCTGAAGGCTGCAGTGGAAACGCTGTGCCACCCCTGTCCC****TGGGAATGGA**

DC SIGN NM_021155 Human (732) **GCTGAAGGCTGCAGTGGAAACGCTGTGCCACCCCTGTCCC****TGGGAATGGA**

Human DC SIGN cloned A' rc (740) **GCTGAAGGCTGCAGTGGAAACGCTGTGCCACCCCTGTCCC****TGGGAATGGA**

pGEM-Teasy-humanDC-SIGN (801) **GCTGAAGGCTGCAGTGGAAACGCTGTGCCACCCCTGTCCC****TGGGAATGGA** 900

851 900

human clone2 (790) **CATTCTTCCAAGGAAACTGTTACTTCATGCTTAATCCAGCGGAATCGG**

DC SIGN NM_021155 Human (782) **CATTCTTCCAAGGAAACTGTTACTTCATGCTTAATCCAGCGGAATCGG**

Human DC SIGN cloned A' rc (790) **CATTCTTCCAAGGAAACTGTTACTTCATGCTTAATCCAGCGGAATCGG**

pGEM-Teasy-humanDC-SIGN (851) **CATTCTTCCAAGGAAACTGTTACTTCATGCTTAATCCAGCGGAATCGG** 950

901 950

human clone2 (840) **CACGACTCCATCACCGCTGCAAAGAAGTGGGGGCCAGCTCGTCTGTAAT**

DC SIGN NM_021155 Human (832) **CACGACTCCATCACCGCTGCAAAGAAGTGGGGGCCAGCTCGTCTGTAAT**

Human DC SIGN cloned A' rc (840) **CACGACTCCATCACCGCTGCAAAGAAGTGGGGGCCAGCTCGTCTGTAAT**

pGEM-Teasy-humanDC-SIGN (901) **CACGACTCCATCACCGCTGCAAAGAAGTGGGGGCCAGCTCGTCTGTAAT** 1000

951 1000

human clone2 (890) **CAAAAGTGTGAGGAGCAGAACTTCCTACAGCTGCAGTCTTCCAGAAGTA**

DC SIGN NM_021155 Human (882) **CAAAAGTGTGAGGAGCAGAACTTCCTACAGCTGCAGTCTTCCAGAAGTA**

Human DC SIGN cloned A' rc (890) **CAAAAGTGTGAGGAGCAGAACTTCCTACAGCTGCAGTCTTCCAGAAGTA**

pGEM-Teasy-humanDC-SIGN (951) **CAAAAGTGTGAGGAGCAGAACTTCCTACAGCTGCAGTCTTCCAGAAGTA** 1050

1001 1050

human clone2 (940) **ACCGCTTCACTGGATGGGACTTTCAGATCTAAATCAGGAAGGCACGTGG**

DC SIGN NM_021155 Human (932) **ACCGCTTCACTGGATGGGACTTTCAGATCTAAATCAGGAAGGCACGTGG**

Human DC SIGN cloned A' rc (940) **ACCGCTTCACTGGATGGGACTTTCAGATCTAAATCAGGAAGGCACGTGG**

pGEM-Teasy-humanDC-SIGN (1001) **ACCGCTTCACTGGATGGGACTTTCAGATCTAAATCAGGAAGGCACGTGG** 1100

1051 1100

human clone2 (990) **CAATGGGTGGACGGCTCACCTCTGTTGCCAGCTTCAAGCAGTATTGGAA**

DC SIGN NM_021155 Human (982) **CAATGGGTGGACGGCTCACCTCTGTTGCCAGCTTCAAGCAGTATTGGAA**

Human DC SIGN cloned A' rc (990) **CAATGGGTGGACGGCTCACCTCTGTTGCCAGCTTCAAGCAGTATTGGAA**

pGEM-Teasy-humanDC-SIGN (1051) **CAATGGGTGGACGGCTCACCTCTGTTGCCAGCTTCAAGCAGTATTGGAA** 1150

1101 1150

human clone2 (1040) **CAGAGGAGAGCCCAACAACTGGGGGAGGAAGACTGCGCGGAATTTAGTG**

DC SIGN NM_021155 Human (1032) **CAGAGGAGAGCCCAACAACTGGGGGAGGAAGACTGCGCGGAATTTAGTG**

Human DC SIGN cloned A' rc (1040) **CAGAGGAGAGCCCAACAACTGGGGGAGGAAGACTGCGCGGAATTTAGTG**

pGEM-Teasy-humanDC-SIGN (1101) **CAGAGGAGAGCCCAACAACTGGGGGAGGAAGACTGCGCGGAATTTAGTG** 1200

1151 1200

human clone2 (1090) **GCAATGGCTGGAACGACGCAAAATGTAATCTTGCCAAATTTGGATCTCG**

DC SIGN NM_021155 Human (1082) **GCAATGGCTGGAACGACGCAAAATGTAATCTTGCCAAATTTGGATCTCG**

Human DC SIGN cloned A' rc (1090) **GCAATGGCTGGAACGACGCAAAATGTAATCTTGCCAAATTTGGATCTCG**

pGEM-Teasy-humanDC-SIGN (1151) **GCAATGGCTGGAACGACGCAAAATGTAATCTTGCCAAATTTGGATCTCG** 1250

1201 1250

human clone2 (1140) **AAAAAGTCCGACGCTCCTGCTCCAGGATGAAGAACAGTTCTTTCTCC**

DC SIGN NM_021155 Human (1132) **AAAAAGTCCGACGCTCCTGCTCCAGGATGAAGAACAGTTCTTTCTCC**

Human DC SIGN cloned A' rc (1140) **AAAAAGTCCGACGCTCCTGCTCCAGGATGAAGAACAGTTCTTTCTCC**

pGEM-Teasy-humanDC-SIGN (1201) **AAAAAGTCCGACGCTCCTGCTCCAGGATGAAGAACAGTTCTTTCTCC** 1300

1251 1300

human clone2 (1190) **AGCCCTGCCACCCCAACCCCTCTCGCTAGATCACTAGTGAATTC**

DC SIGN NM_021155 Human (1182) **AGCCCTGCCACCCCAACCCCTCTCGCTAGATCACTAGTGAATTC**

Human DC SIGN cloned A' rc (1190) **AGCCCTGCCACCCCAACCCCTCTCGCTAGATCACTAGTGAATTC**

pGEM-Teasy-humanDC-SIGN (1251) **AGCCCTGCCACCCCAACCCCTCTCGCTAGATCACTAGTGAATTC**

Figure 5.3.3. Nucleotide sequence alignment of human DC-SIGN.

Human DC-SIGN was sequenced in the pGEM®-T easy vector, using T7 and SP6 primers (Sequencing done at Flinders Sequencing Facility; section 2.7.1.3). Sequencing results were aligned using Vector NTI software. Several single nucleotide polymorphisms are highlighted.

Legend: *human clone2* and *Human DC SIGN cloned A' rc* = results from 2 different PCRs; *DC_SIGN NM_021155 Human* = published human DC-SIGN sequence from Genbank; *pGEM-Teasy-humanDC-SIGN* = previously cloned human DC-SIGN from this laboratory.⁴⁵⁸

5.3.1.2 Ligation into pCI mammalian expression vector

To enable transfection of a mammalian cell line (CHO cells) with marmoset or human DC-SIGN, *NotI* digested DC-SIGN from the maxiprep (section 5.3.1.1) was gel purified and ligated into the pCI mammalian expression vector (Figure 5.3.4). DH5 α *E. Coli* competent cells were again transformed, and grown on LB-agar plates containing ampicillin. White colonies (containing plasmids conferring ampicillin resistance) were screened for marmoset or human DC-SIGN inserts of the correct size and orientation using *NotI* and *XmaI/ApaI* restriction digests, respectively, and agarose gel electrophoresis (Figure 5.3.5). Analysis with Vector NTI® software indicated that *XmaI/ApaI* restriction digest would elaborate inserts of ~800-900bp or ~300-350bp depending on whether DC-SIGN was correctly or incorrectly oriented, respectively. Colonies determined to contain plasmids with DC-SIGN of the correct size and orientation were used in a maxiprep to isolate plasmid DNA.

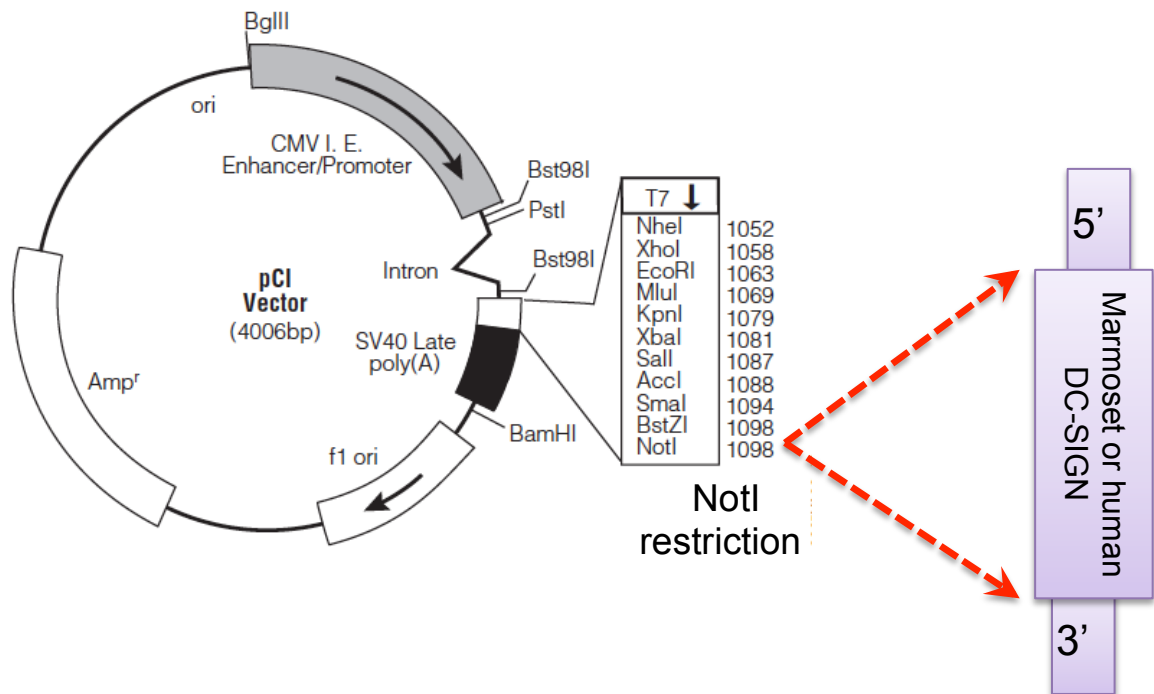


Figure 5.3.4. Schematic representation of sub-cloning of marmoset and human DC-SIGN into the pCI mammalian expression vector.

Marmoset and human DC-SIGN were excised from pGEM®-T easy vector with *NotI* restriction enzyme, subjected to agarose gel electrophoresis, recovered using a DNA Gel Recovery Kit® (Zymo Research), and sub-cloned into *NotI* digested pCI mammalian expression vector. The diagram indicates the correct 5'-3' orientation of marmoset/human DC-SIGN within the plasmid vector to ensure successful transcription via the CMV enhancer/promoter region. Amp^r = ampicillin resistance gene

Modified from a figure by Natasha Rogers (2011).⁴⁵⁸

pCI mammalian expression vector map © 1994-2006 Promega Corporation.

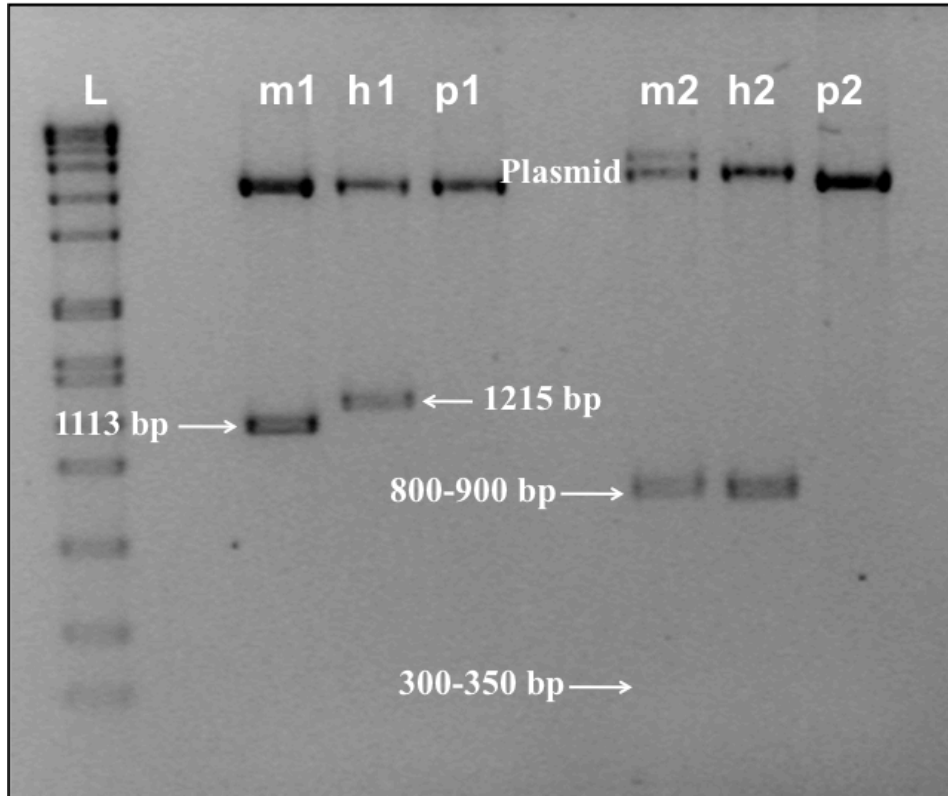


Figure 5.3.5. Cloned marmoset and human DC-SIGN were successfully ligated into pCI mammalian expression vector in the correct orientation.

Agarose gel electrophoresis was performed following restriction digest of pCI mammalian expression vector containing human or marmoset DC-SIGN. This result confirms marmoset or human DC-SIGN is present within pCI in correct orientation:

- *NotI* digest elaborates plasmid and a DC-SIGN fragment of 1215 bp (human) or 1113 bp (marmoset)
- *XmaI/ApaI* digest should elaborate a fragment of approximately 800-900bp if in correct orientation (300-350bp if incorrect orientation)

L = SPP1 molecular weight marker; m = marmoset DC-SIGN in pCI; h = human DC-SIGN in pCI; p = pCI alone; 1 = *NotI* restriction digest (to confirm product size); 2 = *XmaI/ApaI* restriction digest (to confirm correct orientation); Plasmid = plasmid fragment.

5.3.1.3 Amino acid sequence of marmoset and human DC-SIGN and selection of antigenic peptide sequences

Following DNA sequencing, the amino acid sequence alignment of human and cloned marmoset DC-SIGN were compared. The three antigenic peptides #1, #2 and #3 used for mouse immunisations to generate monoclonal antibodies were selected from within the marmoset DC-SIGN sequence, based on their likely immunogenicity. Sequence alignments are shown in Figure 5.3.6. There was approximately 80% homology observed between marmoset and human DC-SIGN, with the most significant difference noted being a deletion of 26 amino acids within the marmoset peptide, as reported previously.⁴⁵⁸

		1		50
	Antigen 1, 2, 3 DC SIGN		-----	F
DC_SIGN NM_021155	Human protein sequence	(1)	MSDSK ¹ EPRLQ ² QL ³ GL ⁴ LEEE ⁵ QLRGL ⁶ GF ⁷ RO ⁸ TRGYKSLAGCLGHG ⁹ PLVLQ ¹⁰ LLS ¹¹ F	
	Marm2seq Protein	(1)	MSDSQ ¹ EPRLQ ² Q ³ MF ⁴ LEEE ⁵ ---E ⁶ LGF ⁷ Q ⁸ TRGYKSLAGCLGHG ⁹ PLVLQ ¹⁰ LLS ¹¹ F	
		51		100
	Antigen 1, 2, 3 DC SIGN		TLLAG ¹ VLVA ² ILVQ ³ VS-----	
DC_SIGN NM_021155	Human protein sequence	(51)	TLLAG ¹ ----L ² LVQ ³ VS ⁴ KVPSSIS ⁵ Q ⁶ ES ⁷ RQDAIYQNL ⁸ TQLKAAV ⁹ GELSEK ¹⁰ SK	
	Marm2seq Protein	(48)	TLLAG ¹ VLVA ² ILVQ ³ VS ⁴ KVPSSIS ⁵ Q ⁶ GS-----K	
		101		150
	Antigen 1, 2, 3 DC SIGN		-----	
DC_SIGN NM_021155	Human protein sequence	(97)	LQ ¹ E ² IYQELT ³ QLKAAV ⁴ GELPEKSK ⁵ LQ ⁶ E ⁷ IYQELT ⁸ RLKAAV ⁹ GELPEKSK ¹⁰ LQ ¹¹ E ¹² I	
	Marm2seq Protein	(75)	QE ¹ E ² IYQELT ³ WLKAAV ⁴ GELPEKSK ⁵ QE ⁶ E ⁷ IYQELT ⁸ QLKAAV ⁹ GELPEKSK ¹⁰ QE ¹¹ V	
		151		200
	Antigen 1, 2, 3 DC SIGN		-----	Q ¹ E ² IYQEL
DC_SIGN NM_021155	Human protein sequence	(147)	YQELT ¹ WLKAAV ² GELPEKSK ³ MQ ⁴ EIYQEL ⁵ TRLKAAV ⁶ GELPEKSK ⁷ Q ⁸ EIYQEL	
	Marm2seq Protein	(125)	YQELT ¹ RLKAAV ² GELPEKSK ³ Q ⁴ EIYQEL ⁵ TRLKAAV ⁶ SEL ⁷ DRSK ⁸ Q ⁹ EIYQEL	
		201		250
	Antigen 1, 2, 3 DC SIGN		LQ ¹ LKAAVGE-----	
DC_SIGN NM_021155	Human protein sequence	(197)	TR ¹ LKAAVGE ² LPEKSKQ ³ Q ⁴ EIYQEL ⁵ TRLKAAV ⁶ GE ⁷ LPEKSKQ ⁸ Q ⁹ EIYQEL ¹⁰ TQ ¹¹ LK	
	Marm2seq Protein	(175)	LQ ¹ LKAAVGE ² LPEKSKQ ³ Q ⁴ -IYQ ⁵ KLTE ⁶ LKAAV ⁷ GLPEKSKQ ⁸ Q ⁹ EIYQEL ¹⁰ TQ ¹¹ LK	
		251		300
	Antigen 1, 2, 3 DC SIGN		-----	NSV ¹ TAC ² Q ³ EVGAQLV ⁴ IT ⁵ ---
DC_SIGN NM_021155	Human protein sequence	(247)	AAVERL ¹ CH ² PCPWE ³ WTF ⁴ FQGN ⁵ CYF ⁶ NS ⁷ NSQRN ⁸ W ⁹ HDSI ¹⁰ TAC ¹¹ KEVGAQLV ¹² V ¹³ IKS	
	Marm2seq Protein	(224)	AAVERL ¹ CR ² PCPWE ³ WTF ⁴ FQGN ⁵ CYF ⁶ NS ⁷ NSQRN ⁸ W ⁹ PNSV ¹⁰ TAC ¹¹ Q ¹² EVGAQLV ¹³ IT ¹⁴ IKS	
		301		350
	Antigen 1, 2, 3 DC SIGN		-----	
DC_SIGN NM_021155	Human protein sequence	(297)	AE ¹ EQN ² F ³ LQ ⁴ LQ ⁵ SSRS ⁶ NR ⁷ FT ⁸ WMGLSDI ⁹ NQ ¹⁰ EGTWQ ¹¹ VDGSP ¹² LL ¹³ PS ¹⁴ FK ¹⁵ Q ¹⁶ Y ¹⁷ W ¹⁸ NR ¹⁹ G	
	Marm2seq Protein	(274)	DE ¹ EQN ² F ³ LQ ⁴ LQ ⁵ SSRS ⁶ NR ⁷ LA ⁸ WMGLSDI ⁹ KQ ¹⁰ EGTWQ ¹¹ VDGSP ¹² LS ¹³ PS ¹⁴ LR ¹⁵ Y ¹⁶ W ¹⁷ NR ¹⁸ Q ¹⁹ G	
		351		400
	Antigen 1, 2, 3 DC SIGN		-----	
DC_SIGN NM_021155	Human protein sequence	(347)	EP ¹ NN ² V ³ GEEDCAEF ⁴ SN ⁵ GW ⁶ ND ⁷ DC ⁸ NLAK ⁹ FWICKKSA ¹⁰ ASC ¹¹ SRDEE ¹² Q ¹³ FL ¹⁴ SPAP	
	Marm2seq Protein	(324)	EP ¹ NN ² V ³ GEEDCAEF ⁴ SN ⁵ GW ⁶ ND ⁷ DC ⁸ SA ⁹ AK ¹⁰ FWICKKSA ¹¹ ASC ¹² SRDEE ¹³ RL ¹⁴ LS---	
		401		
	Antigen 1, 2, 3 DC SIGN		-----	
DC_SIGN NM_021155	Human protein sequence	(397)	ATP ¹ NPPPPA	
	Marm2seq Protein	(371)	-----	

Figure 5.3.6. Comparison of the amino acid sequences of marmoset and human DC-SIGN, showing the alignment of antigens #1, #2 and #3 within the marmoset peptide.

Sequence alignment was performed with Vector NTI® software; differences between the amino acid sequences are highlighted. There is approximately 80% homology observed between marmoset and human DC-SIGN; the antigenic peptides chosen have complete homology with marmoset DC-SIGN.

Marm2seq protein = cloned marmoset DC-SIGN amino acid sequence; *DC_SIGN NM_021155 Human protein sequence* = published human amino-acid sequence, as per GenBank.

Amino acid positions of the antigenic peptides in relation to the human sequence are as follows: #1 – 193; #2 – 283; #3 – 50

5.3.2. Screening of hybridoma supernatants for binding to marmoset and human MoDC

Marmoset and human MoDC were incubated with 15 hybridoma supernatants (numbered #7 to #21 inclusive in these studies) generated as described in section 5.2.3, a secondary anti-mouse FITC, and analysed by flow cytometry. Initial screening revealed a small population of *in vitro* propagated marmoset MoDC that were stained with several of the hybridoma supernatants, particularly #20 and #21 (Figure 5.3.7). Similar screening experiments using human MoDC did not show any evidence of cell staining by the supernatants, despite strong staining by the anti-human DC-SIGN antibody DCN46 (data not shown).

5.3.3. Screening of hybridoma supernatants for binding to marmoset and human DC-SIGN transfected CHO cells

Due to a lack of strong binding of either DCN46 or the marmoset DC-SIGN hybridoma supernatants to the surface of *in vitro* propagated marmoset MoDC, a CHO cell line was transfected with cloned marmoset or human DC-SIGN using Lipofectamine™ 2000. DC-SIGN transfected CHO cells were stained with hybridoma supernatants and a secondary antibody as above, and analysed by flow cytometry.

Significant binding to both marmoset and human DC-SIGN was seen with five of the supernatants (#14, #15, #17, #20 and #21), as shown in Figure 5.3.8 and Figure 5.3.9, respectively. The strongest staining was observed with supernatants #20 and #21.

5.3.4. Immunofluorescence microscopy: binding of hybridoma supernatants to DC-SIGN in marmoset and human lymphoid tissues

Immunofluorescence microscopy of marmoset spleen and thymus, and human spleen stained with five of the hybridoma supernatants that demonstrated the strongest binding to marmoset/human DC-SIGN transfected CHO cells, as well as the anti-human DC-SIGN antibody DCN46, was undertaken. In marmoset thymus and spleen (Figure 5.3.10 and Figure 5.3.11), supernatant #20 and #21 showed evidence of strong binding, as did DCN46. In human spleen tissue, DCN46 binding was observed (as expected; this was the positive control), and there was weak binding seen of supernatant #20, but not #21 (Figure 5.3.12).

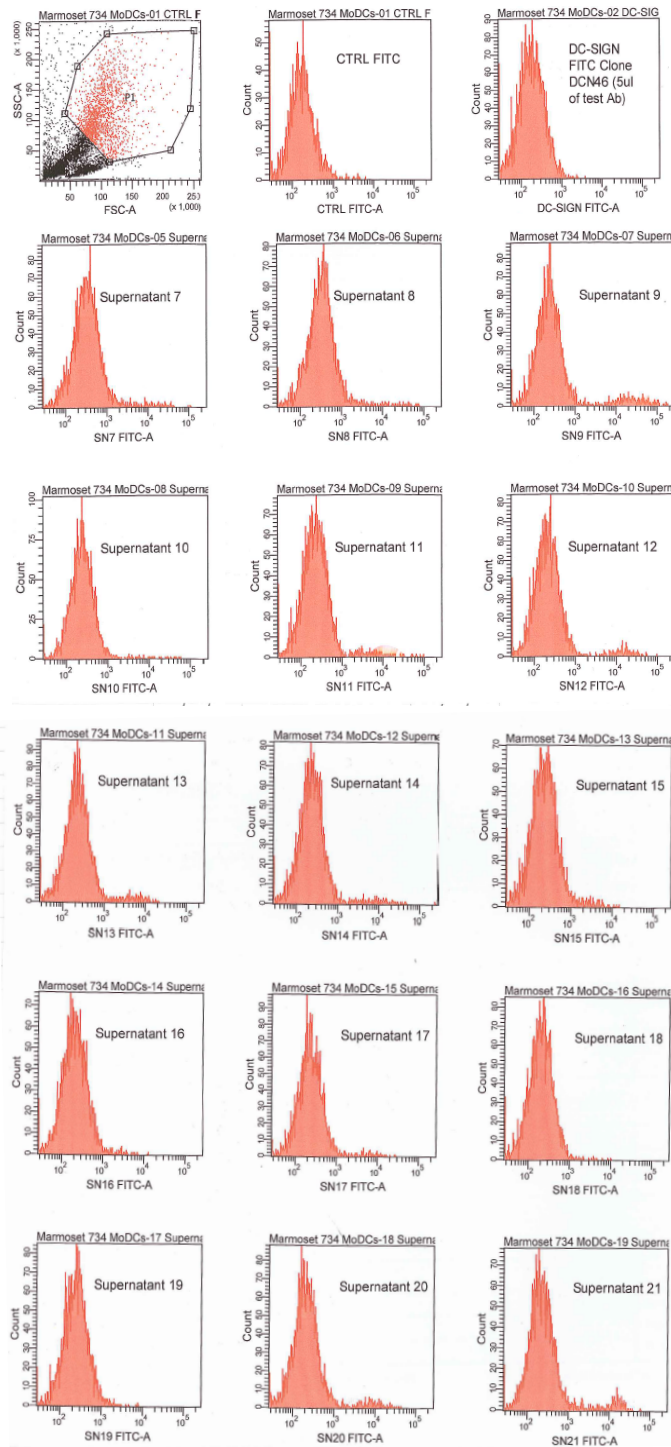


Figure 5.3.7. Flow cytometry screening of binding of hybridoma supernatants to marmoset MoDC.

Marmoset MoDC were stained with 15 hybridoma supernatants (numbered #7-#21 inclusive) targeting marmoset DC-SIGN and a secondary sheep anti-mouse FITC. X63 supernatant was used as a negative control (not shown here). In addition, FITC conjugated isotype control and DC-SIGN (clone DCN46) were also used as additional controls (shown here). There were a small population of cells observed to show binding with several of the supernatants, particularly supernatants #20 and #21. No binding of DCN46 to marmoset MoDC was seen. In similar experiments with human MoDC, no binding was seen.

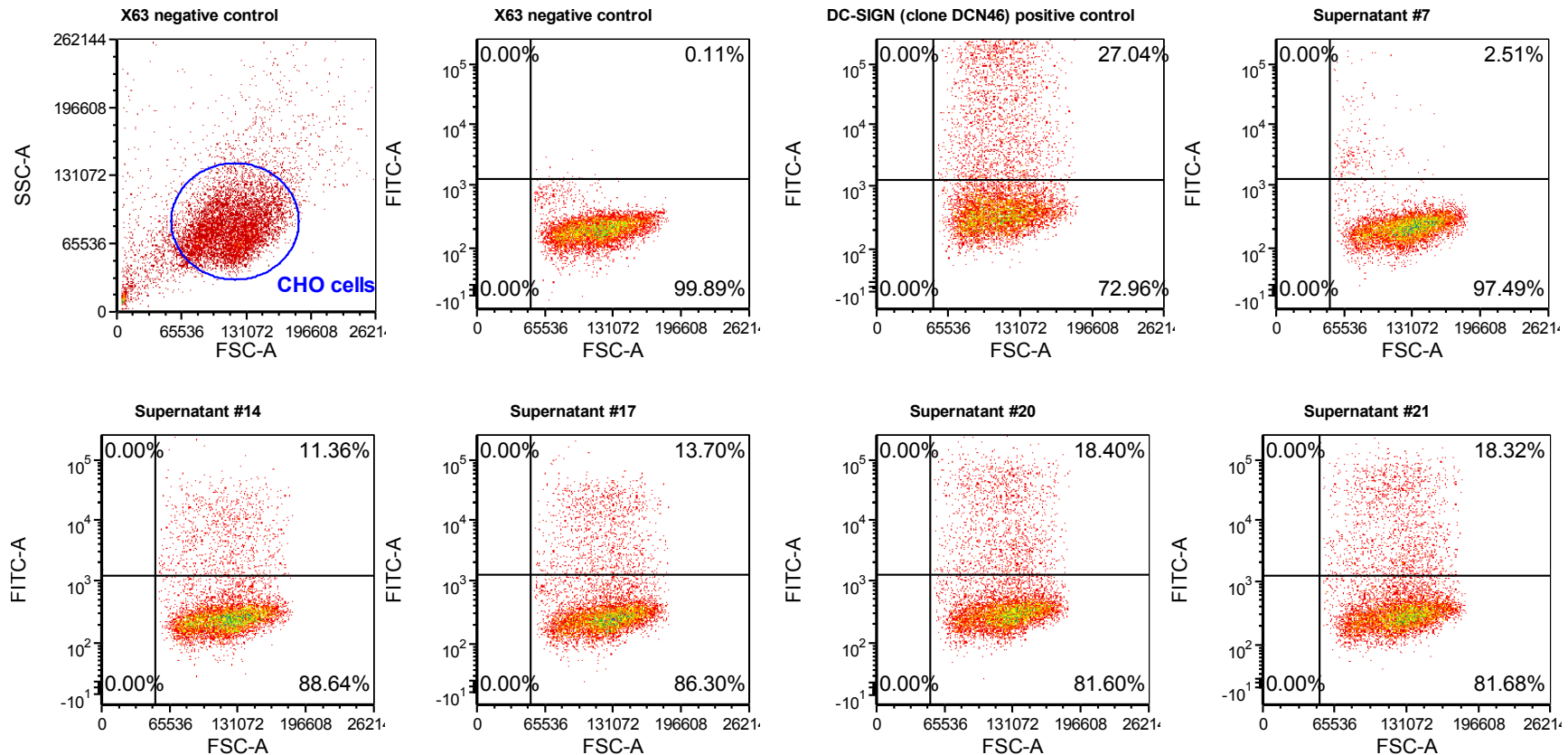


Figure 5.3.8. Hybridoma supernatants bind to marmoset DC-SIGN expressed on the surface of CHO cells.

Flow cytometry of CHO cells transfected with marmoset DC-SIGN within the mammalian expression vector pCI using Lipofectamine™ 2000, screened for positive staining using generated hybridoma supernatant clones. X63 and DCN46 (unconjugated) were used as negative and (human DC-SIGN) positive controls, respectively. Secondary staining with sheep anti-mouse FITC conjugated antibody (clone AQ326). The strongest staining was observed with supernatant clones #14, #15 (not shown), #17, #20 and #21. Other clones screened were negative (not shown).

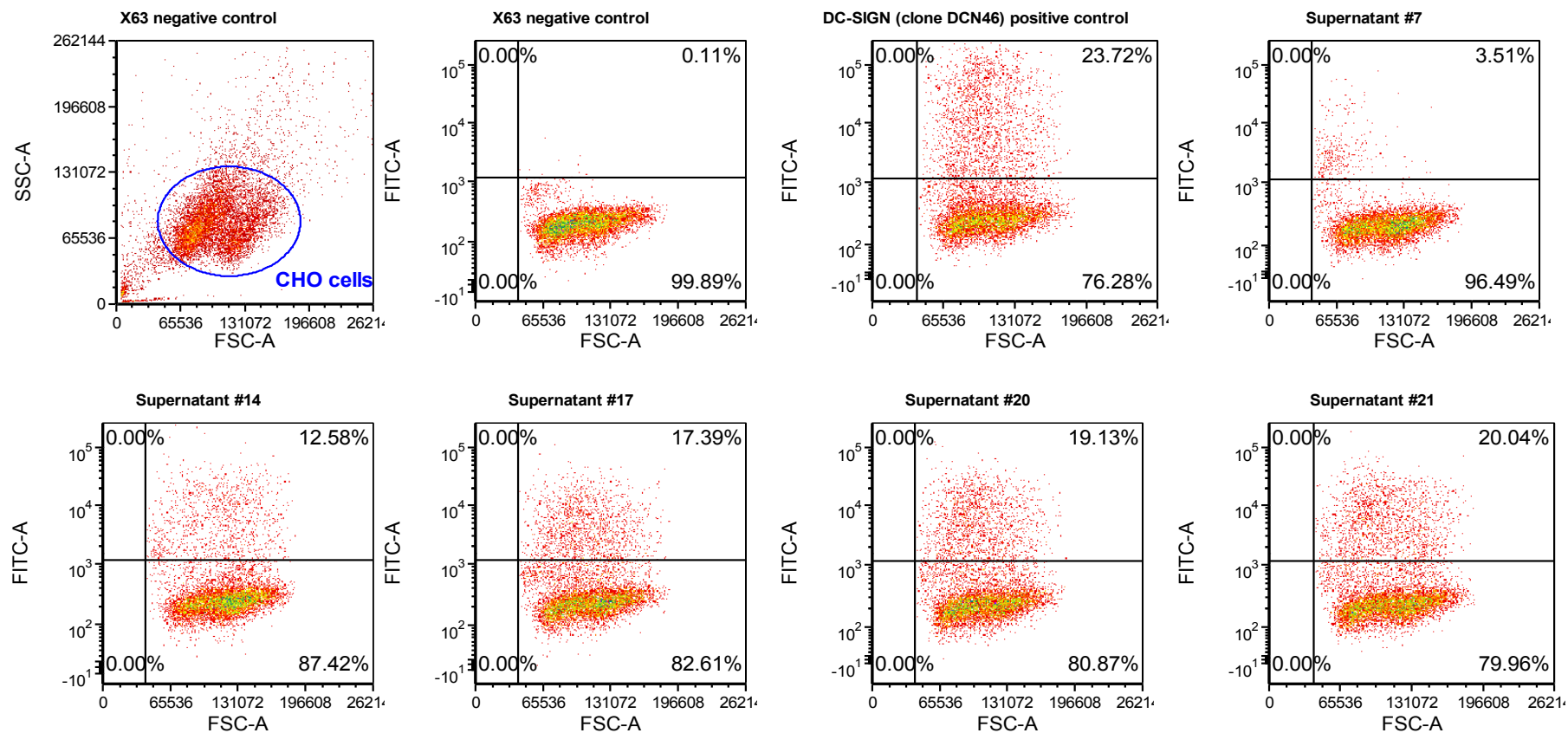


Figure 5.3.9. Hybridoma supernatants bind to human DC-SIGN expressed on the surface of CHO cells.

Flow cytometry of CHO cells transfected with human DC-SIGN within the mammalian expression vector pCI using Lipofectamine™ 2000, screened for positive staining using generated hybridoma supernatant clones. X63 and DCN46 (unconjugated) were used as negative and positive controls, respectively. Secondary staining with sheep anti-mouse FITC conjugated antibody (clone AQ326). The strongest staining was observed with supernatant clones #14, #15 (not shown), #17, #20 and #21. Other clones screened were negative (not shown).

MARMOSET THYMUS

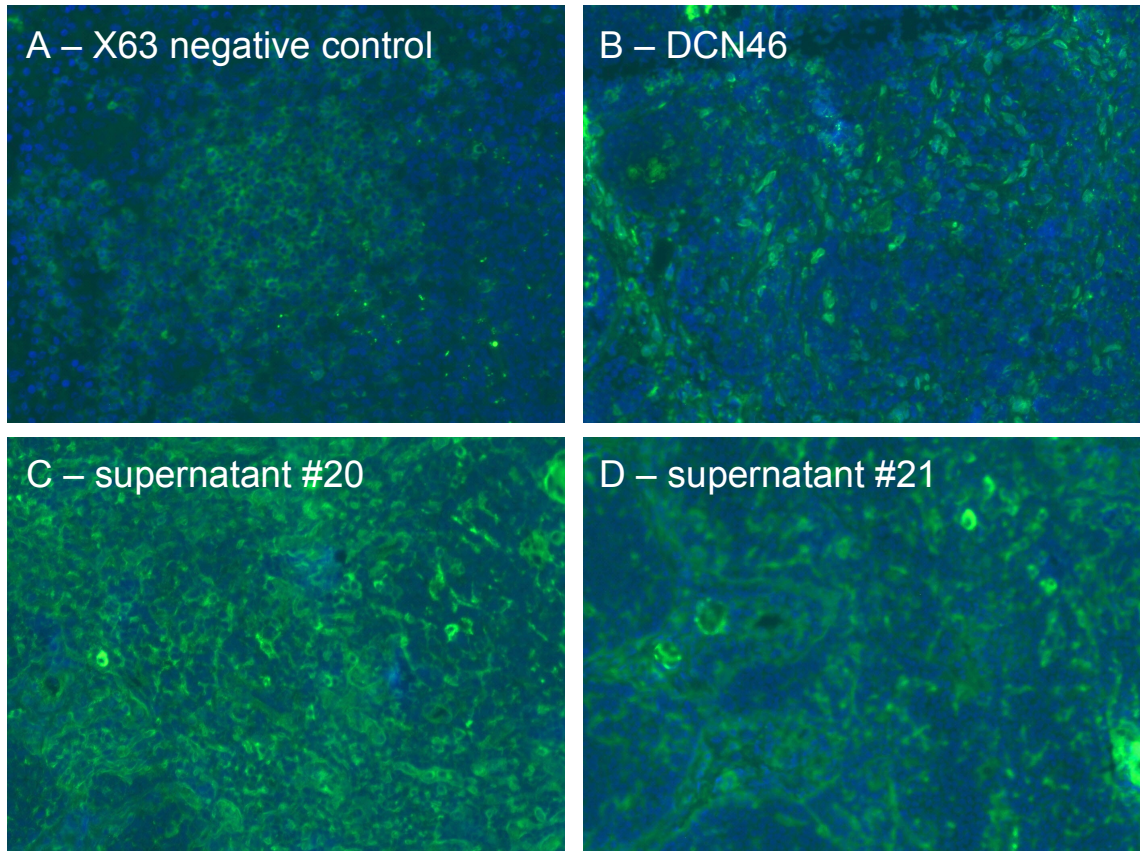


Figure 5.3.10. Hybridoma supernatants targeting marmoset DC-SIGN and anti-human DC-SIGN (DCN46) bind to cells in marmoset thymus.

Immunofluorescence microscopy of sections of marmoset thymus tissue stained with hybridoma supernatants or control antibodies and then a secondary sheep anti-mouse FITC. Binding is shown by green staining; cell nuclei are stained blue with DAPI counterstain. (A) Marmoset thymus stained with X63 negative control; (B) marmoset thymus stained with unconjugated anti-human DC-SIGN (DCN46); (C) and (D) marmoset thymus stained with supernatants #20 and #21, respectively. **There was evidence of staining of marmoset thymus cells with DCN46, and both hybridoma supernatants #20 and #21.** There was minimal staining of marmoset thymus cells observed with the other supernatants tested (# 14, #15 and #17 – data not shown).

Original magnification = x200.

MARMOSET SPLEEN

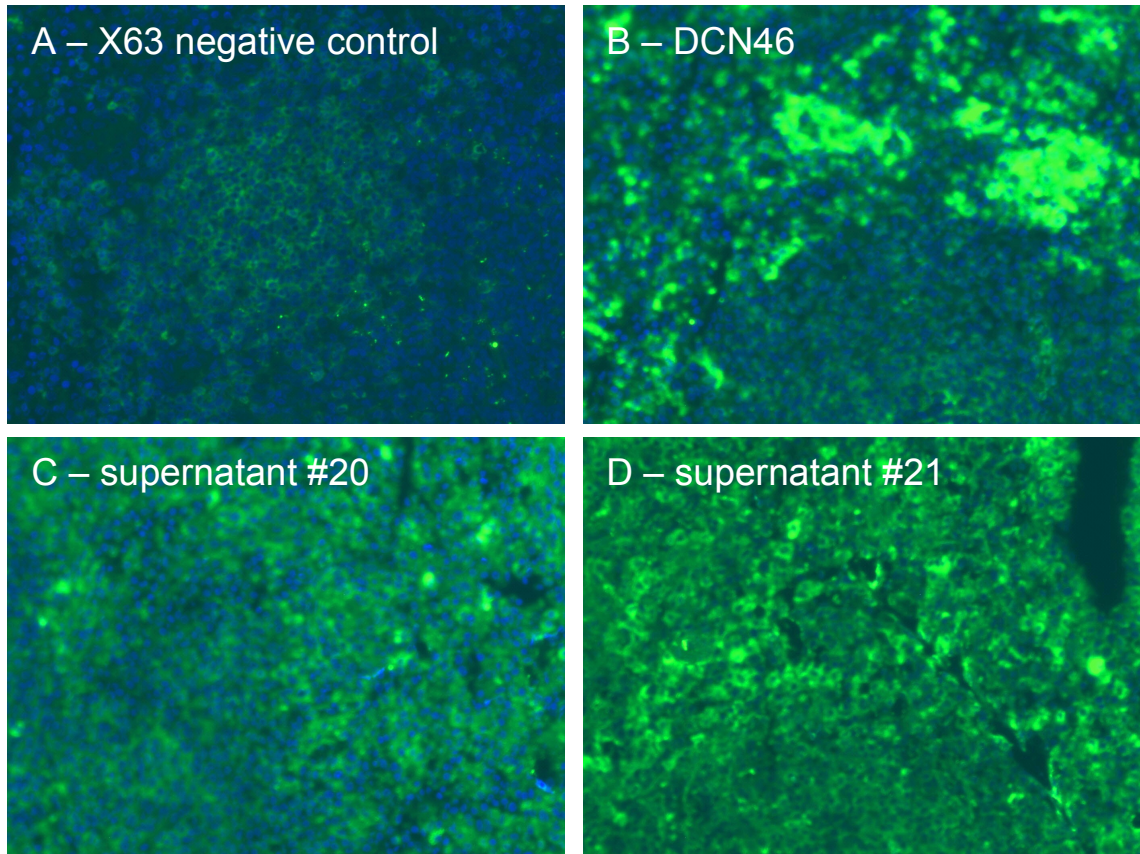


Figure 5.3.11. Hybridoma supernatants targeting marmoset DC-SIGN and anti-human DC-SIGN (DCN46) bind to cells in marmoset spleen.

Immunofluorescence microscopy of sections of marmoset spleen tissue stained with hybridoma supernatants or control antibodies and then a secondary sheep anti-mouse FITC. Binding is shown by green staining; cell nuclei are stained blue with DAPI counterstain. (A) Marmoset spleen stained with X63 negative control; (B) marmoset spleen stained with unconjugated anti-human DC-SIGN (DCN46); (C) and (D) marmoset spleen stained with supernatants #20 and #21, respectively. **There was evidence of staining of marmoset spleen cells with DCN46, and both hybridoma supernatants #20 and #21.** There was minimal staining of marmoset spleen cells observed with the other supernatants tested (# 14, #15 and #17 – data not shown).

Original magnification = x200.

HUMAN SPLEEN

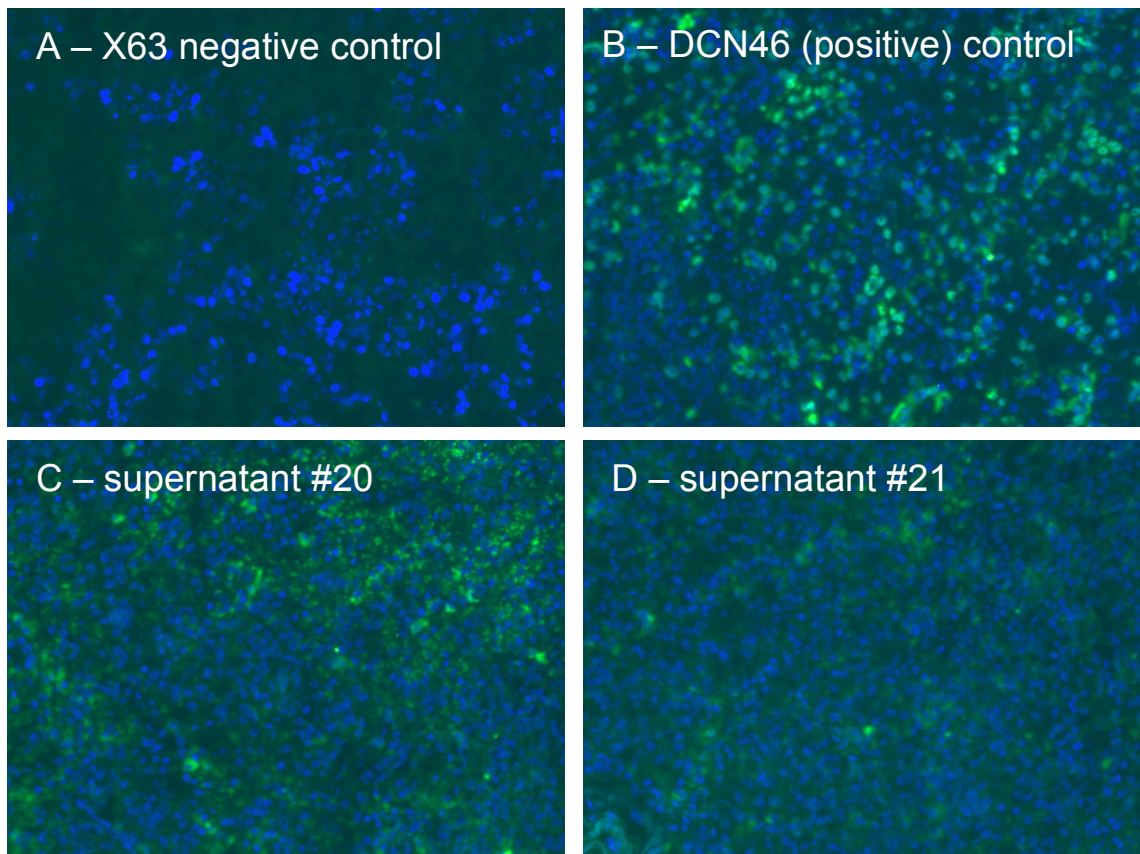


Figure 5.3.12. Hybridoma supernatants targeting marmoset DC-SIGN bind to cells in human spleen.

Immunofluorescence microscopy of sections of human spleen tissue stained with hybridoma supernatants or control antibodies and then a secondary sheep anti-mouse FITC. Binding is shown by green staining; cell nuclei are stained blue with DAPI counterstain. (A) Human spleen stained with X63 negative control; (B) human spleen stained with unconjugated anti-human DC-SIGN (DCN46) as a positive control; (C) and (D) human spleen stained with supernatants #20 and #21, respectively. **There was evidence of weak staining of human spleen cells with hybridoma supernatant #20 but not #21.** There was minimal staining of human spleen cells observed with the other supernatants tested (# 14, #15 and #17 – data not shown).

Original magnification = x200.

5.3.5. Generation of purified monoclonal antibodies targeting marmoset DC-SIGN from hybridoma supernatants

Following the results of the studies outlined in sections 5.3.3 and 5.3.4 above, two of the hybridoma clones were selected for purification of monoclonal antibody, #20 and #21 (clones 9E6E12 and 9E6A8 respectively). Antibody purification and QC testing were performed commercially by Neobody Pty Ltd (data not shown here).

5.3.6. Identification of DC-SIGN positive cells in marmoset spleen; lack of staining with generated monoclonal antibodies.

Marmoset spleen cells were stained and underwent multi-colour flow cytometry analysis to identify the presence of DC-SIGN positive cells (Figure 5.3.13). A gating strategy was used to identify cells that are negative for lineage markers (CD3, CD20 and CD56, i.e. T cells, B cells and NK cells, but not excluding cells of monocyte/macrophage lineage, i.e. CD14⁺), and expressing Class II and the myeloid marker CD11c. Within this cell population, approximately 20% of cells (<1% of the overall splenocyte gated population) express DC-SIGN as shown by staining with the anti-human DC-SIGN antibody DCN46. When the same strategy was used and cells were stained with the generated monoclonal antibodies (9E6A8 and 9E6E12; purified from hybridoma clones #21 and #20 respectively), no staining was seen.

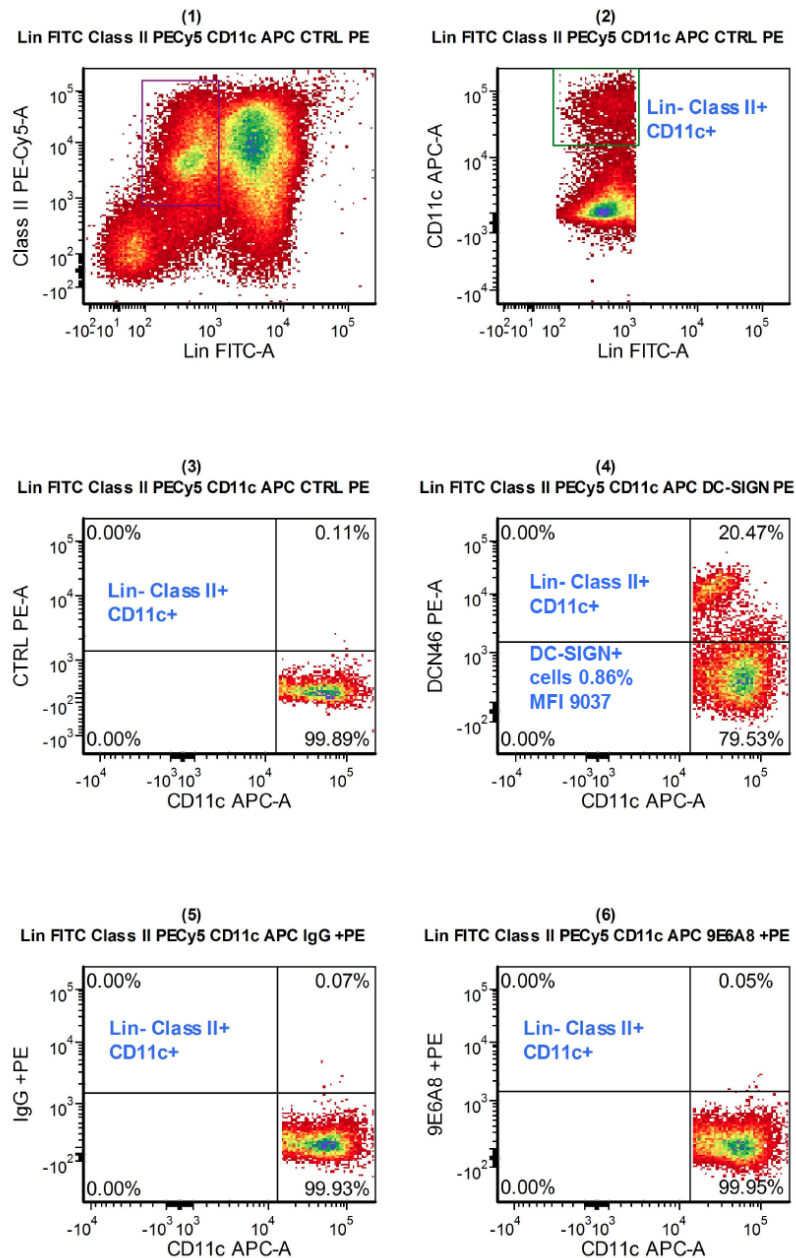


Figure 5.3.13. Anti-human DC-SIGN (DCN46) stains a population of Lineage⁻ Class II⁺ Cd11c⁺ marmoset spleen cells, but no staining is observed with generated monoclonal antibodies.

Marmoset spleen cells were stained with FITC-conjugated Lineage (Lin) markers (see text), Class II-PECy5 and CD11c-APC. Anti-human DC-SIGN (DCN46) stained a population of cells in the Lin⁻ Class II⁺ Cd11c⁺ fraction, representing 0.86% of the overall splenocyte gated population. Generated monoclonal antibody (9E6A8, purified from hybridoma supernatant #21) did not demonstrate any staining using the same strategy; similar results were observed with monoclonal antibody 9E6E12 (from supernatant #20).

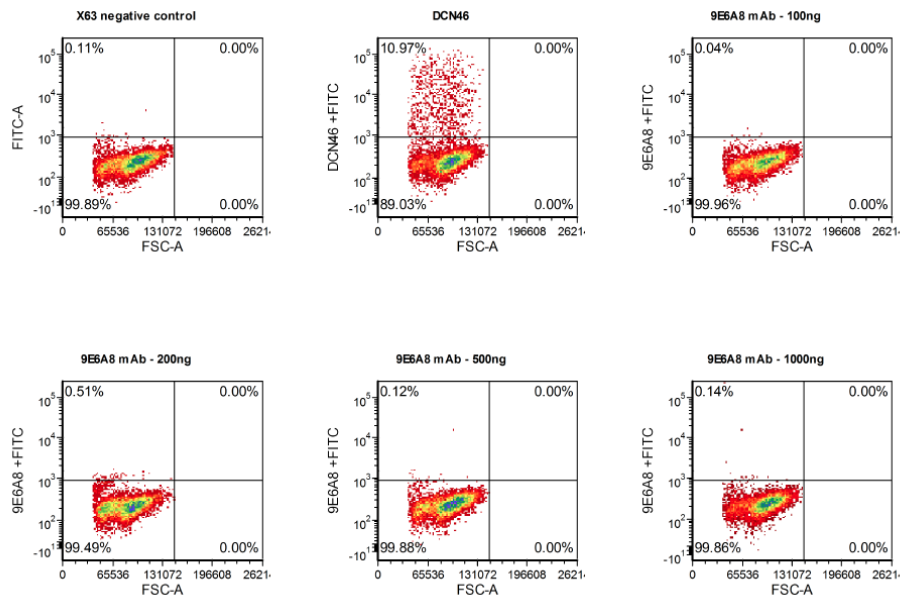
Panels (1) and (2) show the gating strategy for Lin⁻ Class II⁺ CD11c⁺ cells; (3) and (4) show isotype control PE and DCN46 PE stained gated cells respectively; (5) and (6) show un conjugated mouse IgG + secondary anti-mouse PE, and 9E6A8 + secondary anti-mouse PE staining, respectively. >200,000 events were collected per sample; data are representative of 3 experiments

5.3.7. Studies of binding of purified monoclonal antibodies to marmoset and human DC-SIGN

CHO cells transfected with marmoset or human DC-SIGN were incubated with a range of quantities of purified monoclonal antibody clone 9E6A8, unconjugated anti-human DC-SIGN (DCN46), or X63 as a negative control. Anti-mouse FITC was used to confirm antibody binding, and cells were analysed using single colour flow cytometry. Although both marmoset and human DC-SIGN transfected CHO cells showed binding by DCN46, there was no evidence of binding by 9E6A8 at any of the concentrations tested (see Figure 5.3.14). These studies were repeated several times with different preparations of 9E6A8 supplied by Neobody (including supernatant used for the purified antibody; data not shown) with similar results; in addition further studies of supernatant from purified 9E6E12 also showed no evidence of binding (data not shown).

Subsequent correspondence with Neobody indicated that there had been problems with contamination of the hybridoma cultures encountered during production, and it was thought that this might have affected the functionality of the final produced antibody.

(A) Marmoset DC-SIGN transfected CHO cells



(B) Human DC-SIGN transfected CHO cells

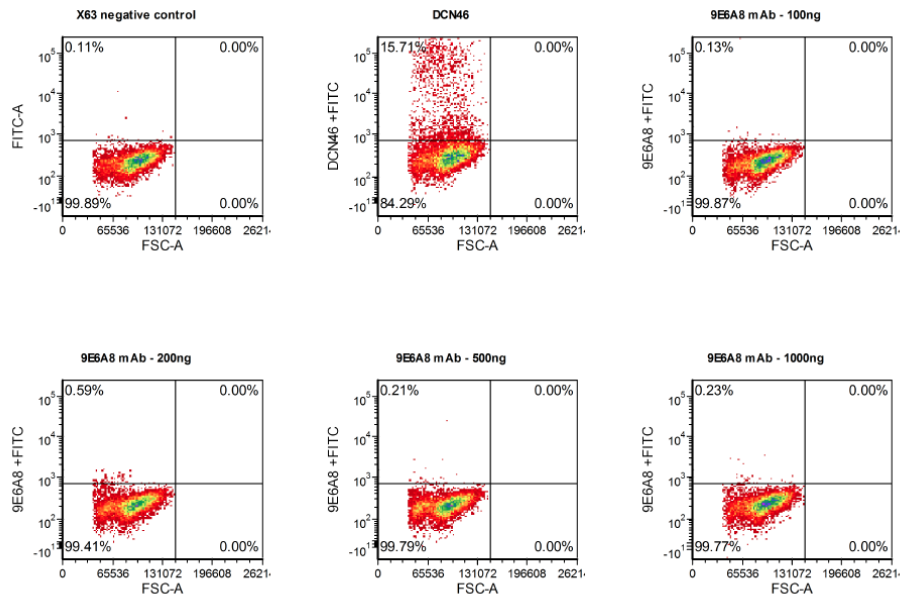


Figure 5.3.14. Anti-human DC-SIGN (DCN46) – but not generated monoclonal antibody 9E6A8 – binds to CHO cells transfected with marmoset and human DC-SIGN

Despite a range of quantities of monoclonal antibody being used, there was no evidence of 9E6A8 binding to CHO cells transfected with either marmoset or human DC-SIGN. Similar results were observed with supernatants of both 9E6A8 and clone 9E6E12 (data not shown; see text). Strong binding by DCN46 to both marmoset and human DC-SIGN was observed, consistent with previous results.

5.4. Discussion

This chapter presents the results of a strategy to develop a monoclonal antibody targeting marmoset DC-SIGN that would ideally also be cross-reactive with human DC-SIGN. Such an antibody could potentially be investigated in the marmoset transplant model as a means to target therapeutics to DC *in situ* via DC-SIGN. Although two of the initially produced hybridoma supernatants showed promising binding to marmoset DC-SIGN transfected CHO cells, and to putative tissue dendritic cells in marmoset spleen and thymus, the final purified antibody clones (9E6A8 and 9E6E12) did not demonstrate confirmed binding. After investigation by the commercial company involved in the generation of the hybridomas, it was determined that contamination of the cultures had occurred, and this may have caused the lack of functionality observed for the purified antibodies. The exact nature of the contamination has not been disclosed to this laboratory. Alternatively, other factors present within the hybridoma cultures⁶²⁰ (e.g. the tissue culture media used) for the initially screened supernatants but excluded by the purification process may have affected the epitope specificity of the monoclonal antibodies. Regrettably, it has not been possible to address these issues within the timeframe for the studies outlined in this thesis. Nevertheless, these studies have demonstrated that the anti-human DC-SIGN antibody DCN46 (BD Biosciences) does have cross reactivity with marmoset DC-SIGN, and appears suitable to use in further studies of targeting marmoset DC-SIGN⁺ cells.

The studies reported here demonstrate for the first time that anti-human DC-SIGN antibodies (DCN46) not only bind to marmoset DC-SIGN expressed in a cell-line, but also to putative tissue-resident DC present in marmoset spleen and thymus. This is an important finding, as this provides a rational basis to target marmoset tissue resident DC *in situ* with antibodies targeted to marmoset DC-SIGN, and thus underlines the feasibility of evaluating DC-targeted cell-specific therapy in this NHP transplant model. Multi-colour flow cytometry of freshly isolated marmoset spleen confirms that these cells are positive for Class II and CD11c, can be found in the lineage (CD3, CD20 and CD56) negative fraction, and represent <1% of the total splenocyte gated population. In this study, monocyte/macrophage markers (e.g. CD14, CD11b, CD16) were not included in the lineage cocktail due to other studies indicating that these markers may present on NHP myeloid DC; it was thus desirable to avoid excluding these

cells.^{85,387,388} However, the inclusion of CD56 in the lineage cocktail may not necessarily be appropriate as others have reported that CD56 is not a marker of NK cells in NHP, and may be present on some NHP DC.^{388,434} Further studies are ongoing to fully delineate the expression of DC surface markers in marmosets and the phenotype of these cells (unpublished results; Jesudason S, Kireta S, Collins MG et al).

Prior to these studies, DC-SIGN had not been detected on the surface of *in vitro* propagated marmoset MoDC using anti-human DC-SIGN antibodies,^{403,621} despite this marker being highly expressed on human MoDC.²¹⁸ It has been uncertain whether this observation was due to lack of cross-reactivity of the antibody with marmoset DC-SIGN, or the absence of DC-SIGN expression on *in vitro* propagated marmoset MoDC. Alternatively, the use of recombinant human IL-4 – which may not be completely cross-reactive in marmosets, and is critical to the expression of DC-SIGN in MoDC⁶²² – during *in vitro* propagation of marmoset DC might lead to inadequate induction of marmoset DC-SIGN. However, previous studies having confirmed intact signalling via STAT-6 following culture of monocytes with rh-IL-4 in this species,⁴⁰³ making this less likely. Interestingly, the initial screening studies of binding of the hybridoma supernatants (Figure 5.3.7) to marmoset MoDC did show staining of a small population of MoDC, suggesting the possibility of some level of DC-SIGN expression. Regrettably, it has not been possible to further investigate this finding due to the limited availability of the initially screened supernatants, and the lack of a functional purified antibody at the conclusion of the production process. Nevertheless, the demonstration of binding by anti-human DC-SIGN to marmoset tissue resident cells in spleen and thymus supports the conclusion that DC-SIGN is not highly expressed on *in vitro* propagated marmoset DC.

To generate monoclonal antibodies targeting marmoset DC-SIGN, a standard hybridoma technology approach was utilised.⁶¹³ Mouse immunisations were performed using a mixture of three different immunogenic peptides (linked with the adjuvant KLH) from throughout the marmoset DC-SIGN peptide that were thought to be likely to be cross-reactive with the human peptide due to only small amino acid differences. This approach may have led to significant numbers of the hybridomas produced not being optimal to target DC-SIGN due to differences between the structure of the isolated peptides and the quaternary structure of DC-SIGN expressed on the surface of cells.⁶²³ Others have used whole cells expressing DC-SIGN (i.e. human immature MoDC) as an

immunogen, but this was not possible here due to the lack of any easily obtainable cells known to strongly express marmoset DC-SIGN.^{218,622} An alternative approach might have been to use the extracellular domain of marmoset DC-SIGN expressed within a plasmid or vaccinia virus, which has also been used successfully to generate antibodies to DC-SIGN.⁶²⁴

Human DC-SIGN consists of a carbohydrate recognition domain, a neck region, and a cytoplasmic domain, and is known to undergo tetramerization at the cell surface,⁶²³ through the interaction of hydrophobic repeat residues in the neck region (see Figure 1.3.5). It is unknown whether the marmoset DC-SIGN protein exhibits the same quaternary structure at the cell surface, but the high level of homology (80%) and the presence of a similar arrangement of tandem repeats suggests that it would. In these studies, the two hybridoma clones observed to have the highest reactivity against marmoset DC-SIGN (#20 and #21) were both known to be reactive against antigen #1 in ELISA, consisting of a 17-amino acid sequence beginning at position 193, which is analogous to being within the neck region of human DC-SIGN (see Figure 1.3.5 and Figure 5.3.6). DCN46 is also known to target the neck region of DC-SIGN⁶²⁵⁻⁶²⁷; antibodies targeting the neck region of DC-SIGN have advantages over other regions of the protein in terms of delivery of antigen to DC and cross-presentation.⁶²⁸

Because of the lack of a readily available method to propagate DC-SIGN⁺ marmoset DC *in vitro*, marmoset DC-SIGN was cloned, and transfected into a CHO cell line using a mammalian expression vector and Lipofectamine 2000.⁶²⁹ Human DC-SIGN transfected CHO cells were also generated, to provide a positive control for antibody binding, using DCN46. This method results in transient expression of DC-SIGN with a relatively low transfection efficiency (10-25% observed in these studies) that reduces with time, has to be optimised, and results in a much lower DC-SIGN staining intensity than that observed with human immature MoDC.²¹⁸ This reduces the ability of these studies to obtain a high degree of resolution between different antibody binding affinities (i.e. between the hybridoma clones). An alternative approach for future studies might be the generation of a stable DC-SIGN expressing cell line, which has been achieved by others, albeit with more labour intensive requirements.^{622,630}

In conclusion, ultimately the studies reported in this chapter were not successful in generating a monoclonal antibody specifically targeting marmoset DC-SIGN. However,

there is now sufficient evidence of cross-reactivity of the anti-human antibody DCN46 to marmoset DC-SIGN to proceed to use this antibody in studies of targeted therapy to marmoset DC. DCN46 has been confirmed to bind both marmoset DC-SIGN transiently expressed in a CHO cell line, and also to Lineage⁻ CD11c⁺ Class II⁺ putative DC in marmoset spleen and thymus. These findings support the feasibility of using this antibody to deliver cell-specific therapy to resident DC in marmoset lymphoid tissues.

**Chapter 6: DEVELOPMENT OF
IMMUNOLIPOSOMES AND
NANOPARTICLES TARGETING HUMAN
AND MARMOSET DC-SIGN TO
MODIFY DENDRITIC CELL FUNCTION**

Acknowledgment

In the studies presented in Chapter 6, others contributed to the work described. The preparation and physicochemical characterisation of the immunoliposomes and PLGA nanoparticles was done in collaboration with Dr Benjamin Thierry and Lisa Kitto of the University of South Australia. In addition Lisa Kitto assisted under my supervision with the performance of some of the immunoliposome cell culture studies, BCA analysis and the DC-SIGN ELISA, and reported some of the data in her Honours thesis:

- Kitto LJ. Immunotargeted liposomes for therapeutic delivery to dendritic cells [Bachelor of Pharmacy (Honours) thesis]. Adelaide: University of South Australia; 2012.

In all other respects, including the design and implementation of these studies, and the written account in this thesis, the work presented is the original work of the author.

6.1. Introduction

DC are specialised antigen presenting cells that are pivotal in the initiation and maintenance of immune responses.^{71,72} Following antigen exposure, and depending on the context, DC can elicit either an immune activation response or promote tolerance or anergy. In addition to endogenous factors, a number of different immunosuppressive agents have been shown to affect DC function *in vitro* and *in vivo* and may promote a tolerogenic phenotype.^{315,323,631} In the field of transplantation, there has been considerable work done to try and harness the tolerogenic potential of DC and reduce or eliminate the need for systemic immunosuppression,^{229,632} although these are yet to reach clinical application.

It has been demonstrated that immunoliposomes^{455,479,633,634} and PLGA nanoparticles^{498,500,635} can be used successfully to target chemotherapeutic and other agents to neoplastic cells. In a major advance, a recent phase 1 human clinical trial has reported efficacy and safety data for doxorubicin loaded immunoliposomes targeting epidermal growth factor receptor (EGFR)-expressing tumour cells in 26 patients with advanced solid tumours administered the drug between 2007 and 2010.⁶³⁶ Targeting strategies are focused towards cell-specific chemotherapeutic drug delivery to avoid ‘off-target’ unwanted side effects such as myelosuppression and gastrointestinal or cardiac toxicity that are frequently dose-limiting and contribute to reduced therapeutic efficacy. Alternatively, targeted nanocarriers may be used to effectively deliver antigens to dendritic cells as a vaccination strategy, e.g. to promote anti-tumour immune responses.⁶³⁷ Targeting may be facilitated via passive uptake of particulate nanocarriers,^{638,639} or by active targeting via the use of monoclonal antibodies grafted to the surface of nanocarriers.⁶⁴⁰⁻⁶⁴²

Specific targeting of dendritic cells via their surface receptors using drug-containing nanocarriers, such as liposomes or nanoparticles, has considerable potential as a therapy to alter the immune response to a transplant. The delivery of immunosuppressive or immunomodulatory drugs directly to DC has the potential to reduce the significant toxicity associated with current standard ‘non-targeted’ immunosuppression.⁴⁴ This strategy would seek to manipulate the indirect pathway of allorecognition,²⁶⁸ by altering the function of DC *in situ*. Such an approach may have considerable advantages in the

setting of acute transplantation over cellular therapy based approaches in terms of logistics, timeliness and cost.²²⁹ To date there have been not been studies specifically evaluating such an approach.

DC express numerous surface receptors, including the C-type lectins, which are involved in antigen uptake, migration and adhesion. DC-SIGN is a C-type lectin that is abundantly expressed on immature tissue and monocyte derived DC, and is downregulated on mature DC; it has a vital role in DC function and is a highly specific marker for DC.^{193,218,220,415,618} DC-SIGN is also expressed on NHP DC,⁶²¹ but does not have a direct functional orthologue in mouse DC populations.⁶⁴³

The aims of this chapter are:

1. To develop immunoliposomes and polymeric nanoparticles targeting DC-SIGN that could be used in further *in vivo* studies of targeted drug delivery to dendritic cells in the common marmoset (*Callithrix jacchus*) NHP model; and
2. To determine whether treatment of dendritic cells with an immunomodulatory drug (Curcumin) contained within DC-SIGN targeted immunoliposomes or nanoparticles has specific effects on DC function *in vitro*.

6.2. Methods

6.2.1. Materials

Materials used for the preparation of immunoliposomes and PLGA nanoparticles are listed with details of manufacturers in Chapter 2 (section 2.2.4 and section 2.8).

6.2.2. Preparation and characterisation of immunoliposomes

PEG liposomes were prepared as described by Tuscano et al,⁴⁷⁹ and Wicki et al,⁶⁴⁴ and then incubated with micelles conjugated to monoclonal antibodies to generate immunoliposomes using a post-insertion method (see Chapter 1, section 1.7.1.2).⁴⁷⁹ DCN46 (anti-human DC-SIGN; IgG2b – BD Pharmingen) was used to target to DC-SIGN on the surface of dendritic cells; an IgG isotype antibody (clone P3.6.2.8.1; IgG1 κ – eBiosciences) was used as a negative control. Human serum albumin (HSA, Sigma Aldrich) was used in place of antibodies in some studies. The lipophilic fluorescent marker dye DiI (peak excitation 549nm; peak emission 565nm) was incorporated into the lipid bilayer of blank PEG-liposomes, as it is known to stably incorporate into cell membranes.

6.2.2.1 Preparation of PEG liposomes and incorporation of DiI

Liposomes (5mM) were prepared by thin lipid film hydration (see Chapter 1, section 1.7.1.1). DPPC and cholesterol at a 3:2 molar ratio were combined with 5mol% mPEG-DSPE-2000 (polyethylene glycol (M_r 2000) covalently linked via a carbamate bond to DSPE (distearoyl-phosphatidyl-ethanolamine)) and 0.3mol% DiI in chloroform. In some preparations, 0.3mol% coumarin 6 was used as an alternative to DiI to minimise interference with the protein quantitation assay. Solvent was evaporated for 3 hours in the dark to produce a thin lipid film using a rotary evaporator (Büchi Rotavapor® R-210, Büchi Labortechnik). Liposomes were rehydrated with HEPES buffer (25mM) in a 55°C water bath for 90 minutes in the dark. Following rehydration, liposomes were extruded for 10 cycles through 400nm and 200nm Nucleopore™ polycarbonate membranes (Capitol Scientific). Liposome vials were sealed, stored in the dark at 4°C, and used within 7 days.

6.2.2.2 Preparation of PEG-maleimide-micelles

Micelles were prepared by thin lipid film hydration. DSPE-PEG-mal (maleimide-derivatized mPEG-DSPE) and mPEG-DSPE-2000 were combined at a 4:1 molar ratio in chloroform. Solvent was evaporated under nitrogen gas (N₂) to produce a thin lipid film. The lipid film was rehydrated with deoxygenated HEPES buffer (25mM) in a 55°C water bath for approximately 30 minutes. Once rehydration was complete, micelles were immediately incubated with purified, thiolated DCN46 (alternatively IgG or HSA) as described below.

6.2.2.3 Conjugation of monoclonal antibodies to micelles

DCN46 (60µg), or alternatively isotype IgG, was thiolated by incubating with Traut's reagent at a 1:10 molar ratio for 1 hour at room temperature. For some preparations where subsequent protein quantitation experiments were planned (section 6.2.5 below), either 60µg or 300µg of HSA was used as an alternative to antibody. Thiolated DCN46 was then purified using a Zebra™Spin desalting column (Thermo Scientific). Briefly, the desalting column was equilibrated with HEPES (25mM) by adding buffer to the column and centrifuging for 1 minute at 1500g (RCF) 3 times. Once equilibrated, thiolated DCN46 was added to the column and centrifuged for 2 minutes at 1500g. The DCN46 flow through was collected and immediately incubated with micelles at a 1:5 molar ratio, under N₂ conditions with continuous stirring overnight.

6.2.2.4 Synthesis and purification of immunoliposomes via post-insertion of micelles into liposomes

DiI-PEG liposomes (1ml) were incubated with 100µl of the DCN46-micelle preparation at a 1:0.05 molar ratio in a 55°C water bath for 1 hour. DCN46 immunoliposomes were purified from the mixture using a Sepharose®CL-4B separation column (Sigma Aldrich). Briefly, the column was equilibrated with HEPES (25mM). Following equilibration, the DCN46 immunoliposome preparation was added to the top of the column and the flow through was collected in separate aliquots according to time and appearance. The collection with the highest lipid concentration (determined by colour intensity) was utilised.

6.2.2.5 Characterisation of immunoliposome preparations

Blank liposome and immunoliposome preparations were diluted 1:100 with sodium chloride (10mM) prior to analysis. Size, polydispersity and zeta potential estimations were analysed using a Zetasizer Nano (Malvern Instruments). Polydispersity is a measure of the heterogeneity of particle sizes in a mixture. Zeta potential is defined as the potential difference across phase boundaries between solids and liquids; in the case of colloid interfaces (as in liposomes or polymeric nanoparticles) it refers to the charge difference between the surface of the dispersion particle and the medium in which it is dispersed. Samples were tested in triplicate.

The concentration of DPPC phospholipid was determined indirectly by measuring the DiI concentration in liposome and immunoliposome preparations. Lipids in the samples were dissolved in ethanol (1:10 dilution) prior to analysis. A Cary Eclipse fluorescence spectrophotometer (Agilent Technologies) with excitation and emission wavelengths set to 525nm and 575nm respectively was used to measure the DiI absorbance of each sample. Results were compared with a standard curve of DiI fluorescence at known concentrations. Samples and standards were tested in triplicate.

6.2.3. Preparation and characterisation of PLGA nanoparticles targeting DC-SIGN

PLGA nanoparticles containing either the fluorescent hydrophobic molecule Coumarin 6 (peak excitation 450nm; peak emission 540nm) or the (also hydrophobic) NF- κ B inhibitor Curcumin were prepared by nanoprecipitation,⁴⁹⁶ as described in Chapter 1 (section 1.7.2.1) and outlined below. In order to target nanoparticles to DC-SIGN on the surface of dendritic cells, drug-containing PLGA nanoparticles were conjugated to DCN46 (anti-human DC-SIGN, BD Pharmingen) or an irrelevant IgG isotype as a control using carbodiimide chemistry (see section 1.7.2.2). In some experiments, HSA was used in place of these antibodies. Following preparation, the nanoparticles were stored in the dark at 4°C, and were ultrasonicated for a minimum of 5 minutes prior to use.

6.2.3.1 Preparation of PLGA nanoparticles containing Coumarin 6 or Curcumin

PLGA-mPEG and PLGA-PEG-COOH (10mg/ml in acetonitrile) were combined at a ratio of 1mg: 0.575mg in a round bottom flask. Coumarin 6 (2mg/ml in acetone) was added to at a 0.3% mass (w/w) ratio to PLGA. Alternatively, Curcumin (1mg/ml in acetone) was added to at a 5% w/w ratio to PLGA. Ultrapure (milliQ H₂O) at a two-fold volume was added dropwise slowly to the solution over 10 minutes while shaking the flask. Residual organic solvent was removed by rotary evaporation in the dark over 45-60 minutes at reduced pressure. The resulting PLGA nanoparticles containing either Coumarin 6 or Curcumin were centrifuged at 10,000g for 15 minutes at 4°C, and supernatant was carefully removed. The nanoparticles were resuspended in ultrapure water, and stored in the dark at 4°C until use.

6.2.3.2 Conjugation of monoclonal antibodies to PLGA nanoparticles

In order to bind monoclonal antibodies to the surface of drug containing PLGA nanoparticles, unbound available amine groups on immunoglobulin molecules were conjugated to free carboxyl terminals of the polymer using carbodiimide chemistry (see Chapter 1, section 1.7.2.2).⁴⁹⁸ Free carboxyl groups on the PEG-PLGA-COOH component of the PLGA nanoparticles were activated using a solution of EDC (15mg) and NHS (20mg) that had been combined in ultrapure water. The PLGA nanoparticles were reacted with the NHS/EDC preparation at a 2:1 volume ratio, at room temperature, and mixed gently. The resulting activated PLGA nanoparticle preparation was

centrifuged at 10,000g at 4°C for 15 minutes, supernatant was removed and the nanoparticles were resuspended in filtered HEPES buffer.

Monoclonal antibodies (DCN46 or IgG isotype) were added to the activated nanoparticles at a 1:5 mass ratio of IgG to activated PLGA nanoparticles (PEG-PLGA-COOH equivalent) and incubated at room temperature for a minimum of 6 hours, or overnight. In some preparations utilised in characterisation experiments, HSA at the same mass ratio was used as an alternative to antibodies. The antibody conjugated PLGA-nanoparticles were then purified by centrifuging at least twice at 4°C for 15 minutes at 15,000g with removal of supernatant. The final preparation was resuspended in HEPES buffer, and stored in the dark at 4°C until use.

6.2.3.3 Characterisation of PLGA nanoparticles

Size, polydispersity and zeta potential (see description in section 6.2.3.3 above) of the conjugated PLGA nanoparticles were assessed using dynamic light scatter on a Zetasizer Nano (Malvern Instruments). PLGA preparations were subjected to ultrasonication prior to taking measurements or use in subsequent cell culture experiments.

6.2.4. DC-SIGN binding assay – enzyme-linked immunosorbent assay (ELISA)

Immunoliposomes and PLGA nanoparticles conjugated to DCN46 were tested for the ability to bind DC-SIGN in a modified ELISA assay. Unconjugated and IgG-conjugated preparations were used as negative controls.

A 96-well ELISA plate (Maxisorp, Nunc Nalge International) was coated with 100µl/well of recombinant human DC-SIGN/CD209 Fc chimera fusion protein (R&D systems) at a concentration of 4µg/ml in bicarbonate buffer (pH 9.6). The plate was incubated at 37°C for 2 hours followed by overnight incubation at 4°C. Unbound fusion protein was removed and the plate was washed several times with PBS-Tween wash buffer. 200µl/well of PBS/10% FCS was added as a blocking agent and the plate was incubated for 2 hours at room temperature, and washed with PBS-Tween. Samples of DCN46 or IgG immunoliposomes, or blank liposomes, or alternatively DCN46-PLGA, IgG-PLGA or unconjugated PLGA nanoparticles were added at various dilutions in PBS, 100µl/well. Serially diluted samples of unconjugated anti-human DC-SIGN antibody (clone DCN46) were used as standards; alternatively DC-SIGN antibody was used as a positive control and PBS was used as a negative control. The plate with samples and standards/controls (in duplicate) was then incubated for 2 hours at room temperature, washed with PBS-Tween, and goat anti-mouse IgG (Fc specific) peroxidase antibody (Sigma-Aldrich) was added (50µl/well, diluted 1:9000 in PBS), before a further incubation for 1 hour at 37°C. After further washes, TMB substrate solution was added (100µl/well), the plate was incubated for 15-20 minutes at 37°C, and the reaction was stopped by adding 100µl/well of stop solution (0.5M H₂SO₄). The absorbance was measured within 30 minutes using a BioRad microplate reader at 450nm.

Raw data was imported using Microplate Manager 5.2.1 software (BioRad) and the degree of DC-SIGN binding activity was estimated by comparison with a standard curve generated using the anti-DC-SIGN standards, or assessed qualitatively versus the positive and negative controls. Microsoft Excel software (Microsoft Corporation) and GraphPad Prism version 5.0d or 6.0b for Mac OS (GraphPad software) were used for analysis.

6.2.5. Protein quantification assay

To estimate the yield of antibody (either DCN46, IgG, or alternatively HSA) in immunoliposome preparations, a bicinchoninic acid (BCA) protein quantitation assay was used (Pierce® BCA Protein Assay Kit, or Micro BCA Protein Assay Kit – Pierce Biotechnology/ThermoFisher). In some experiments, Coumarin 6 (peak excitation 450nm; peak emission 540nm) was used in place of DiI in the liposome preparations, to minimise interference with the absorbance measurement of the BCA assay (562nm).

Protein content was measured in immunoliposomes (conjugated to DCN46 or HSA), with unconjugated liposomes assayed as controls. To reduce the likelihood of phospholipid interference in the BCA assay, liposomes were lysed in HEPES buffer containing either 5% (w/v) Triton X-100 (Sigma-Aldrich), or alternatively 2% (w/v) SDS (Sigma-Aldrich). In the latter case, lipids were maintained in 2% SDS for up to 20 hours to maximise lipid dissolution.⁶⁴⁵

BCA assays were performed according to the manufacturers instructions in the 96-well plate format with some modifications. Standards were prepared using bovine serum albumin (BSA) supplied with the kit. Samples containing lipids and protein were assayed after SDS lysis undiluted, and at 1:10 and 1:100 dilutions in HEPES. Standards (in triplicate) and samples (in duplicate) were assayed in 50µl of buffer per well of a 96-well flat-bottomed polystyrene plate (Greiner Bio-One). BCA kit Reagent A was mixed with Reagent B at a 50:1 ratio and added to samples and standards at a working ratio of 4:1 (200µl per well). The plate was covered and incubated at 37°C for 30-60 minutes, cooled to room temperature and the absorbance was measured using a BioRad microplate reader at 562nm. Alternatively, samples and standards in 150µl of buffer were assayed using a Micro BCA kit. Micro BCA reagents A, B and C were mixed in a 25:24:1 ratio and 150µl of this working reagent was added to each well. The plate was covered and incubated at 37°C for up to 2 hours, cooled to room temperature and the absorbance read as above.

Raw data was imported using Microplate Manager 5.2.1 software (BioRad) and protein concentration was estimated by comparison with a standard curve generated using the BSA standards. Microsoft Excel software (Microsoft Corporation) was used for analysis.

6.2.6. Cell culture

Human PBMC were sourced from buffy coats obtained by the South Australian Red Cross blood service from de-identified healthy blood donors. Protocols for human monocyte-derived DC (MoDC) generation, obtaining marmoset splenocytes, reagents and media, DC and two-way mixed lymphocyte reactions are described in Chapter 2.

6.2.7. Immunoliposome and PLGA nanoparticle uptake by human MoDC

6.2.7.1 MoDC culture with immunoliposomes or PLGA nanoparticles

Human immature MoDC were generated as described in section 2.4.3.2. On day 6 or 7 of culture with GM-CSF/IL-4, immature MoDC (which express high levels of DC-SIGN) were collected from flasks and counted. MoDC (either fresh or thawed following cryopreservation where this was required (section 2.4.4)) were resuspended at a density of $0.5\text{-}1.0 \times 10^6/\text{ml}$ in CM, and cultured in a volume of 0.5ml/well in 24-well plates. Heat inactivated rabbit serum (10% v/v) was added as an Fc receptor blocking agent and incubated with the cells for 30 minutes.

DiI immunoliposomes incorporating either DCN46, or IgG, or alternatively unconjugated DiI liposomes were added to the MoDC culture (0.1mM DPPC lipid equivalent per 0.5ml well). As an additional negative control, cells were incubated in media alone, with an equivalent amount of PBS added to each well. Cells and liposomes were incubated overnight (16 hours) in a humidified incubator at 37°C with 5% CO₂.

Fluorescent PLGA nanoparticles containing coumarin-6 and conjugated to the monoclonal antibodies DCN46, IgG, or unconjugated, were added to MoDC culture at an approximate concentration of 7µg of PLGA-PEG-COOH equivalent in 10µl of HEPES buffer per 0.5ml well (14µg/ml). As a negative control, MoDC were also cultured with media alone. Cells and nanoparticles were co-cultured for 60 minutes at either 37°C or 4°C. To confirm the specificity of nanoparticle targeting to DC-SIGN, MoDC were incubated with unconjugated anti-human DC-SIGN antibody (DCN46) for 30 minutes at 4°C prior to adding PLGA nanoparticles as a competitive binding assay in some experiments.

6.2.7.2 Flow cytometry of MoDC for immunoliposome or PLGA nanoparticle uptake

Following culture as above, MoDC were analysed by flow cytometry, as described in Chapter 2 (section 2.6), with modifications as outlined here. Cells were collected into FACS tubes, washed extensively to remove unbound liposomes or nanoparticles, and resuspended in staining buffer. As a positive control, a portion of MoDC that had been cultured in media alone were incubated with DC-SIGN PE (in the case of immunoliposomes) or DC-SIGN FITC (PLGA nanoparticles) or isotype FITC antibodies for 20 minutes at 4°C. After equilibration to room temperature, all cells were fixed with FACS lysing solution and single colour flow cytometry was performed as described in section 2.6.

Uptake of immunoliposomes was measured by determining the degree of DiI fluorescence (with DC-SIGN PE as a positive control) in the PE channel of a FACS Canto II flow cytometer (BD Biosciences). Uptake of PLGA nanoparticles was measured by determining the degree of Coumarin 6 fluorescence (with DC-SIGN FITC as the positive control) in the FITC channel of the cytometer. For each sample, 20,000 events were collected. Cells were selected for inclusion in the analysis gate according to forward and side scatter characteristics (Figure 6.2.1).

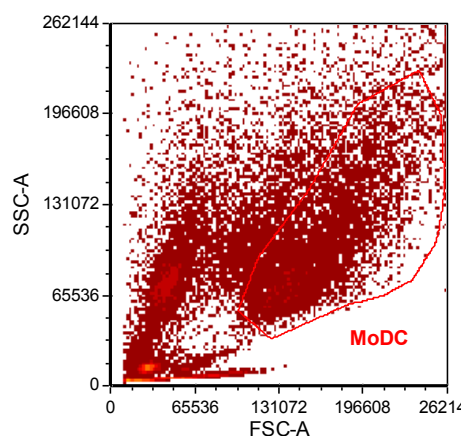


Figure 6.2.1. Forward and side scatter plot showing representative gate used to select DC-SIGN positive MoDC in the flow cytometry studies of immunoliposome and PLGA nanoparticle uptake.

6.2.7.3 Immunofluorescence microscopy

A sample of MoDC cultured as in section 6.2.7.1 were prepared as a cytospin sample and immunofluorescence microscopy was performed as described in Chapter 2 (section 2.5) to determine the cellular uptake of DiI or Coumarin 6.

6.2.8. PLGA nanoparticle uptake by marmoset splenocytes

6.2.8.1 Marmoset splenocyte culture with nanoparticles

Marmoset splenocytes were obtained following euthanasia as described in section 2.4.2.5. Spleen cells were resuspended at a density of 1×10^7 /ml in CM. Cells were incubated overnight at 37°C in the dark, in 6-well plates (2ml/well). Fluorescent PLGA nanoparticles containing coumarin-6 and conjugated to the monoclonal antibodies DCN46, IgG, or unconjugated at a concentration of $\sim 28 \mu\text{g}$ of PLGA-PEG-COOH equivalent in 40 μl of HEPES buffer per 2ml well (i.e. $\sim 14 \mu\text{g}/\text{ml}$) prior to incubation. As a negative control, splenocytes were also cultured with media alone.

6.2.8.2 Flow cytometry of marmoset splenocytes for PLGA nanoparticle uptake

Following culture as above, splenocytes were analysed by flow cytometry, as described in Chapter 2 (section 2.6), with modifications as outlined here. Cells were collected into FACS tubes, washed extensively, and resuspended in staining buffer. After blocking with rabbit serum, splenocytes underwent multi-colour staining with Class II PE-Cy5 and CD11c APC to identify the population likely to contain DC-SIGN positive cells (as described in Chapter 5, section 5.3.6 above) that might be targeted by PLGA nanoparticles. Both isotype and FMO controls were used. Coumarin-6 fluorescence was read in the FITC channel (FL1), due to their similar excitation and emission spectra. Compensation controls included the following:

1. Unstained cells
2. FL-1 compensation: CD3 FITC
3. FL-3 compensation: Class II PE-Cy5
4. FL-5 compensation: CD11c APC

Uptake of PLGA nanoparticles was measured by determining the degree of Coumarin 6 fluorescence in the FITC channel of a FACS Canto II flow cytometer (BD Biosciences). Between 100,000 and 200,000 events were recorded. Doublet discrimination was not performed. Cells were selected for inclusion in the analysis gate according to forward and side scatter characteristics (Figure 6.2.2)

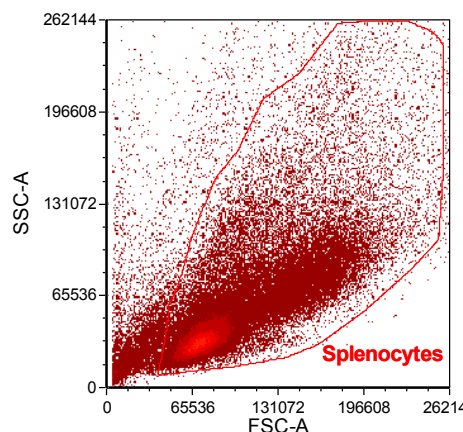


Figure 6.2.2. Forward and side scatter plot showing gate used to select marmoset splenocytes in the flow cytometry studies of PLGA nanoparticle uptake.

6.2.9. Curcumin-containing PLGA nanoparticles – effects on human MoDC

6.2.9.1 MoDC culture and treatment with Curcumin PLGA nanoparticles

Human MoDC were generated as described in section 2.4.3.2. On day 5 of culture with GM-CSF/IL-4, curcumin-containing PLGA nanoparticles conjugated to DCN46, or irrelevant IgG, were added to selected wells in the 6-well plate at an approximate concentration of 7 μ g of PLGA-PEG-COOH equivalent in 10 μ l of HEPES buffer per 0.5ml well (14 μ g/ml), similar to the approach used in section 6.2.7.1 above. MoDC treated with the PLGA nanoparticles were matured 24 hours later by the addition of LPS (10ng/ml) to cells on day 6 of culture. Untreated cells, both immature and mature MoDC, were also cultured as controls.

The experimental treatment groups after 7 days culture were thus as follows:

1. Immature MoDC – 7 days of GM-CSF/IL-4 culture
2. Mature MoDC – as per (1) but treated with LPS on day 6
3. Mature MoDC – as per (2) but pre-treated for 24 hours with DCN46 conjugated Curcumin-PLGA nanoparticles on day 5 prior to LPS maturation
4. Mature MoDC – as per (2) but pre-treated for 24 hours with IgG conjugated Curcumin-PLGA nanoparticles on day 5 prior to LPS maturation

6.2.9.2 Flow cytometry for DC maturation markers

Following culture as above, MoDC were analysed by flow cytometry as described in Chapter 2 (section 2.6). Cells were collected into FACS tubes, washed extensively to remove unbound nanoparticles, and resuspended in staining buffer. Samples of MoDC ($\sim 10^5$ cells/tube) were stained with the following monoclonal antibodies: Class II PE-Cy5, CD80 FITC, CD86 FITC, CD83 FITC, and DC-SIGN FITC. Isotype matched FITC and PE-Cy5 antibodies were used as controls. After equilibration to room temperature, all cells were fixed with FACS lysing solution, washed, and single colour flow cytometry was performed as described in section 2.6.

6.2.9.3 Mixed leucocyte reaction

MoDC treated with nanoparticles and controls (as per section 6.2.9.1 above) were analysed for their capacity to stimulate T-cell proliferation in a dendritic cell MLR, using the methods described in Chapter 2 (section 2.4.3.4.1). All stimulator MoDC were irradiated prior to being added to the MLR. Nylon wool T-cells were used as responder cells.

In addition, curcumin-containing PLGA nanoparticles conjugated to either DCN46 or IgG were added directly to a two-way MLR (Chapter 2, section 2.4.3.4.2) at varying doses to determine the effects of PLGA nanoparticle-encapsulated curcumin on alloproliferation.

6.3. Results

6.3.1. Immunoliposomes

6.3.1.1 Characterisation of immunoliposomes

The size, polydispersity and zeta potential of the DiI containing liposome preparations were determined in triplicate using dynamic light scattering. Results are shown in Table 6.3.1.

Table 6.3.1 Physicochemical characteristics of liposome preparations

Sample	Size* (nm)	Polydispersity index	Zeta potential* (mV)
Unconjugated liposomes	162 ± 0.92	0.06 ± 0.02	-27 ± 2.7
DCN46 immunoliposomes	173 ± 2.9	0.191 ± 0.02	-21 ± 2.6
IgG immunoliposomes	166 ± 1.2	0.118 ± 0.02	-23 ± 1.0

* Mean ± standard deviation

Conjugation of DCN46 and IgG to immunoliposomes via micellar incorporation led to a small increase in size (~4-11nm; p=0.0011, one-way ANOVA) and a small increase (i.e. reduction of negative charge) of zeta potential (~+4-6mV; p=0.043; one-way ANOVA) compared with unconjugated liposomes. All liposome preparations were monodispersed, as shown by polydispersity indices less than 0.3, although the DCN46 and IgG conjugated immunoliposomes were less monodispersed than the unconjugated liposomes (p=0.0006; one-way ANOVA).

Repeated measurements of these physicochemical characteristics in DCN46 immunoliposomes and the unconjugated liposome preparations at 1, 20 and 97 days after storage in buffer at 4°C showed no significant differences in any of the measured properties over time.

The concentration of DPPC phospholipid in liposome preparations was determined indirectly by measuring the DiI concentration in liposome and immunoliposome preparations. Results were compared with a standard curve of DiI fluorescence at known concentrations. Unconjugated liposomes (~1mM DPPC equivalent) were diluted approximately 5-fold following the process of antibody conjugation and purification (DCN46 and IgG immunoliposome preparations were approximately 0.2-0.24mM of DPPC equivalent), and in all subsequent studies appropriate adjustments were made to ensure an equivalent amount of phospholipid/DiI was utilised in each experimental group.

6.3.1.2 Immunoliposomes conjugated with DCN46 bind to DC-SIGN in an ELISA

Using a modified ELISA assay, the functionality of DCN46-conjugated immunoliposomes was confirmed. However, the amount of functional DCN46 detected in the immunoliposome preparations was low (compared with the concentrations initially added to the micelles, 60µg/ml) in this semi-quantitative assay (Figure 6.3.1).

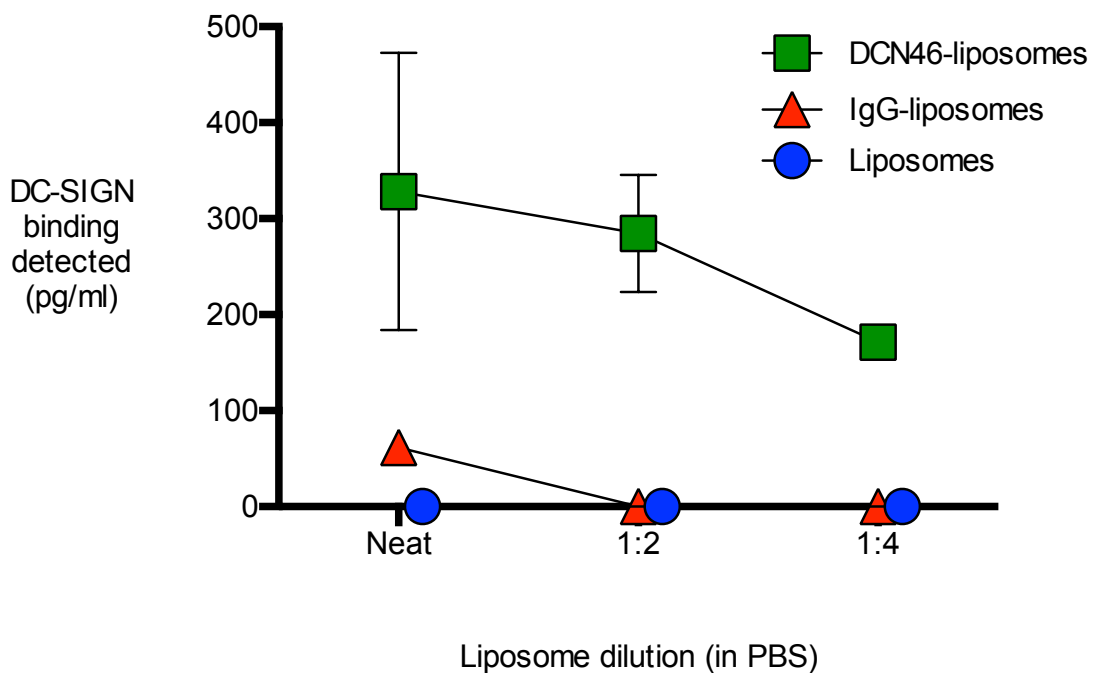


Figure 6.3.1. Immunoliposomes conjugated to DCN46 show evidence of binding to DC-SIGN in a semi-quantitative ELISA assay.

Serially diluted samples of unconjugated liposomes, or immunoliposomes conjugated to DCN46 (DC-SIGN antibody) or an irrelevant IgG were assayed for binding in an ELISA plate coated with recombinant human DC-SIGN-Fc chimera. Serially diluted samples of purified DC-SIGN antibody were used as standards. At all dilutions tested (neat, 1:2 and 1:4), there was evidence of DCN46 binding to DC-SIGN. Semi-quantitative analysis indicated a low level of functional DCN46 (range ~200 to ~500 pg/ml) compared with the amount of DCN46 added to the micelles (60µg/ml), in the neat preparations. Results for DCN46 immunoliposomes versus unconjugated liposomes are representative of two separate experiments; IgG-immunoliposomes were included in one of the experiments. Results shown are mean ± standard deviation. At all dilutions tested, the difference between DCN46 immunoliposomes and IgG or unconjugated liposomes was significant ($p < 0.001$; unpaired t test).

6.3.1.3 DCN46 immunoliposomes do not show significant uptake by human MoDC after overnight culture

Immunoliposome preparations containing the fluorescent dye DiI and conjugated to DCN46, irrelevant IgG, or unconjugated, were cultured with human MoDC overnight at 37°C. Flow cytometry for DiI fluorescence in the PE channel did not show evidence of DiI immunoliposome uptake by human MoDC, whether conjugated to DCN46 or not (Figure 6.3.2).

Immunofluorescence microscopy of cells after overnight culture with the liposome preparations showed similar results (Figure 6.3.3).

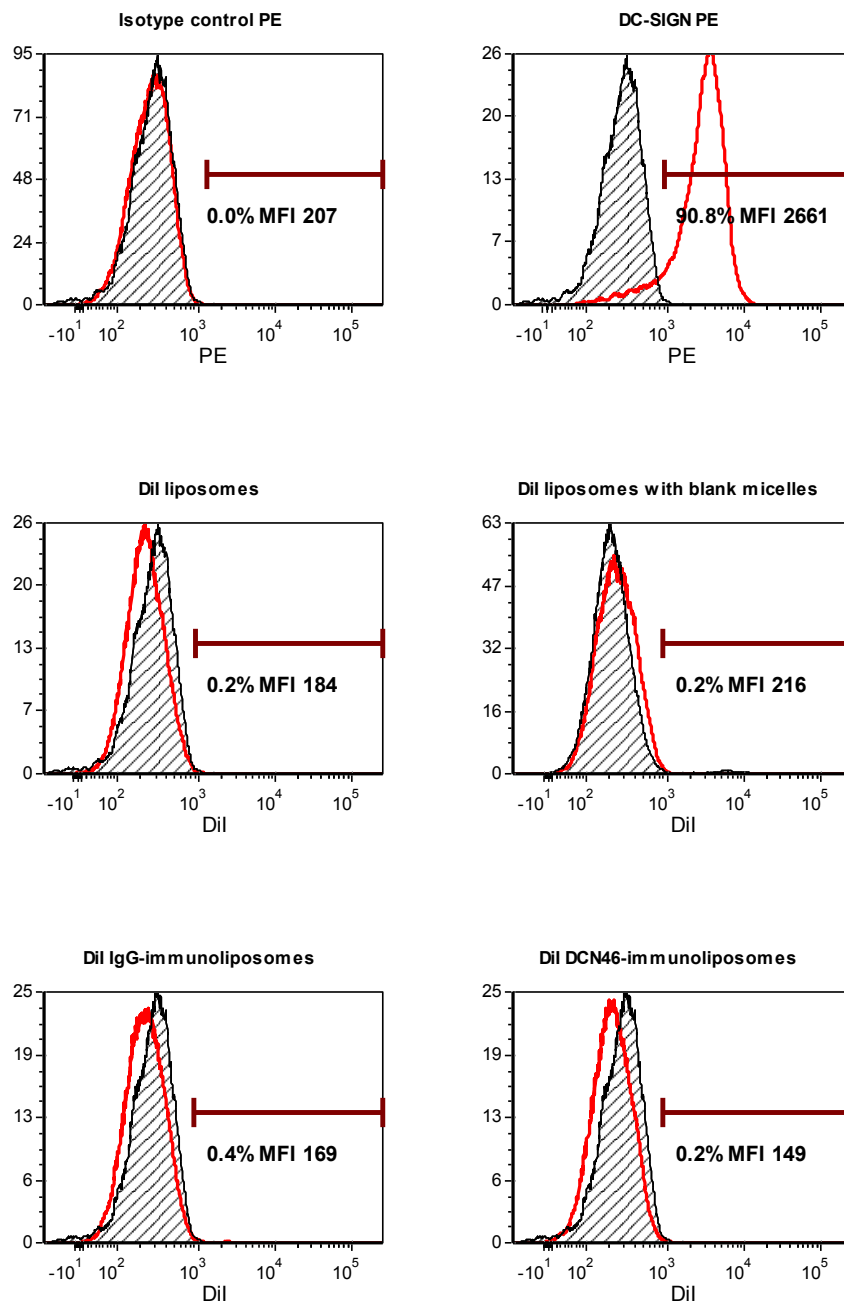


Figure 6.3.2. DiI immunoliposomes targeted to DC-SIGN incubated overnight with human MoDC do not show evidence of significant uptake.

Human immature MoDC (day 6 or 7 in culture with GM-CSF/IL-4) were incubated overnight at 37°C with different formulations of liposomes containing DiI, and liposome uptake was assessed by flow cytometry in the PE channel. All plots are normalised to control unstained cells, represented by shaded histograms. The numbers indicate the percentage of cells taking up liposomes. MoDC stained with isotype PE, or DC-SIGN PE, were used as negative and positive controls, respectively. MFI = mean fluorescence intensity; liposomes = non-conjugated liposomes; blank micelles = micelles in preparation had not been conjugated to antibody; IgG-immunoliposomes = liposomes conjugated to isotype IgG; DCN46-immunoliposomes = liposomes conjugated to clone DCN46 (targets DC-SIGN). Results shown are representative of three experiments.

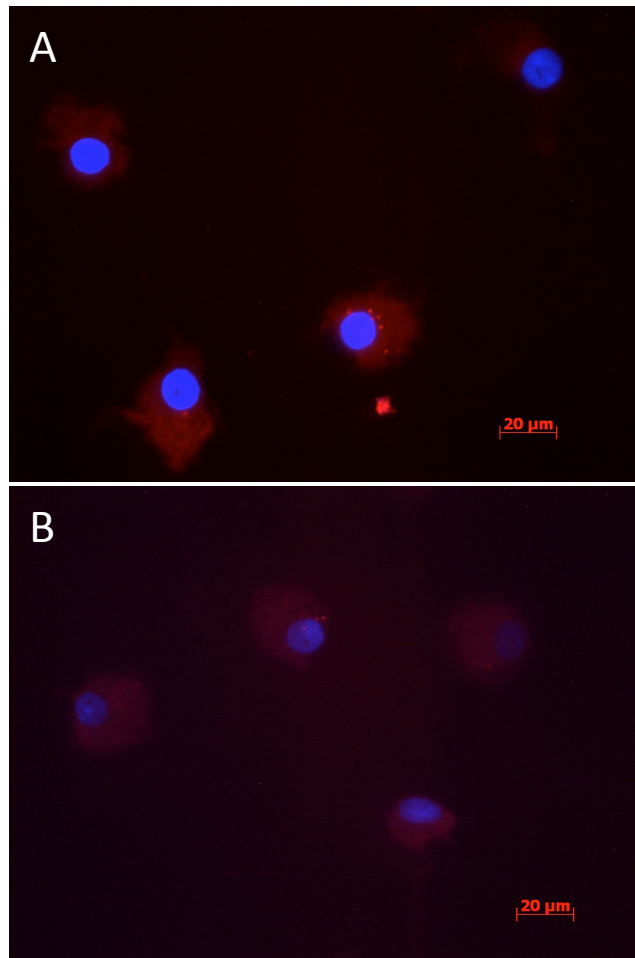


Figure 6.3.3. DiI immunoliposomes targeted to DC-SIGN incubated overnight with human MoDC do not show evidence of significant uptake.

Immunofluorescence microscopy of cytospin samples of human MoDC incubated overnight with immunoliposomes containing DiI. Cell nuclei are stained blue with DAPI counterstain. (A) MoDC incubated with media alone (negative control); (B) MoDC incubated with immunoliposomes conjugated to DCN46 antibody. Background autofluorescence detected in the rhodamine channel (shown in red; used to detect DiI) is seen, but no evidence of specific DiI uptake in the cytoplasm of MoDC is seen. MoDC incubated with IgG conjugated immunoliposomes or unconjugated liposomes showed similar findings (data not shown).

6.3.1.4 Protein quantitation assay

Liposome preparations (both unconjugated and immunoliposomes) were assayed for the presence of protein to determine the antibody yield of the conjugation process using a BCA assay (working range for protein detection 20-2000µg/ml; with enhanced protocol, sensitivity down to 5µg/ml). In some experiments, a micro BCA assay was used (working range 2-20 µg/ml). Initial experiments using DCN46 immunoliposomes dissolved in Triton X-100 indicated significant interference with the assay by lipids present in the preparation (data not shown). In subsequent experiments, human serum albumin (HSA) was used as an alternative to DCN46 antibody in immunoliposome preparations, to minimise inappropriate use of expensive antibody reagents.

A stepwise logical approach was subsequently followed to optimise the assay by (1) using sodium dodecyl sulphate (SDS) as an alternative to Triton X-100 to more effectively dissolve lipids, (2) using coumarin 6 rather than DiI as a liposome marker to avoid fluorescence interference, (3) extending the incubation time with SDS to maximise lipid dissolution, (4) increasing the amount of protein available for conjugation in the preparation, and (5) assaying liposome preparations spiked with known protein concentrations.

Figure 6.3.4 demonstrates that incubating liposomes with 2% SDS for 45 minutes rather than Triton X-100 reduced the extent of lipid interference, but did not fully reduce inappropriate 'protein' detection. A small difference was observed between DiI and coumarin 6 liposomes (reduced 'protein' detected in the latter), therefore coumarin 6 was used in subsequent liposome preparations for BCA analysis.

Figure 6.3.5 shows that when a longer incubation with 2% SDS was used (20 hours at room temperature, rather than 45 minutes at 37°C), there was evidence of persistent lipid interference in the assay. No significant differences were observed between blank and immunoliposome preparations, despite a higher amount of protein being used for conjugation to liposomes in one of the groups.

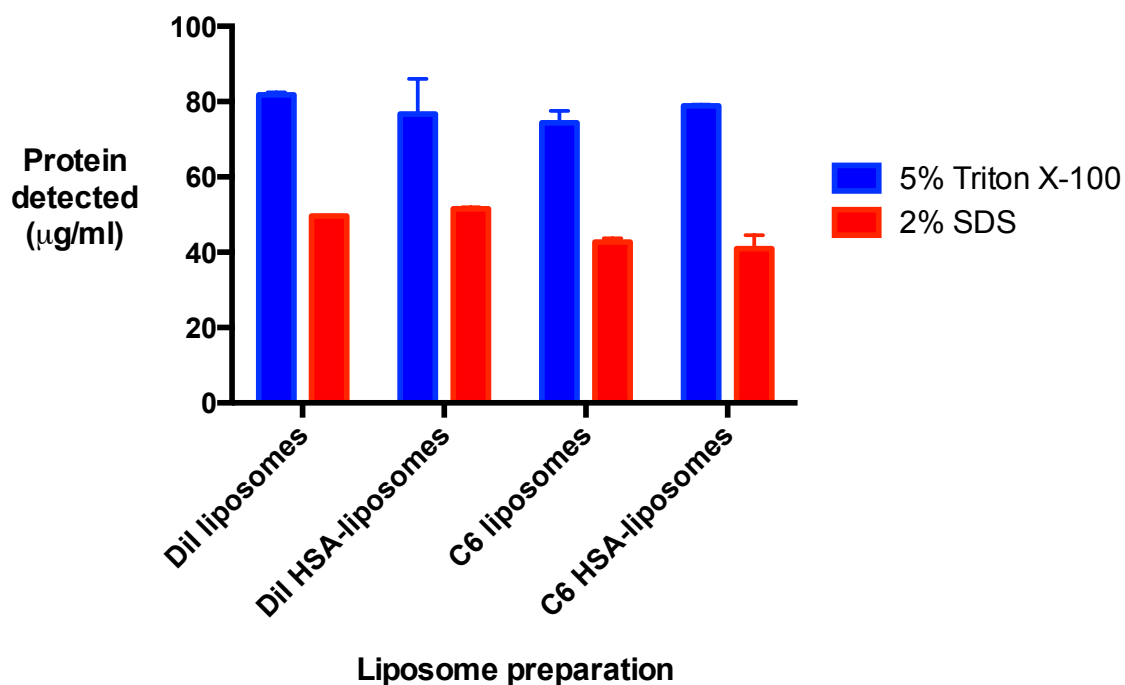


Figure 6.3.4. Protein quantitation assay: incubation of liposome preparations with Triton X-100 or SDS to remove phospholipid contamination.

Following incubation of liposome preparations with either 5% Triton X-100 or 2% SDS for 45 minutes at 37°C, there was evidence of significant interference with the BCA assay, with detection of significant amounts protein in 'blank' DiI or coumarin 6 (C6) liposomes. SDS was more effective than Triton X-100. There was no difference observed between 'blank' liposomes and protein (human serum albumin, HSA) conjugated liposomes. There was a small reduction in protein detected between coumarin 6 and DiI liposomes, indicating dye fluorescence was not the primary cause of observed interference. Liposome samples and standards were measured in duplicate and triplicate, respectively. Results shown are mean \pm standard deviation.

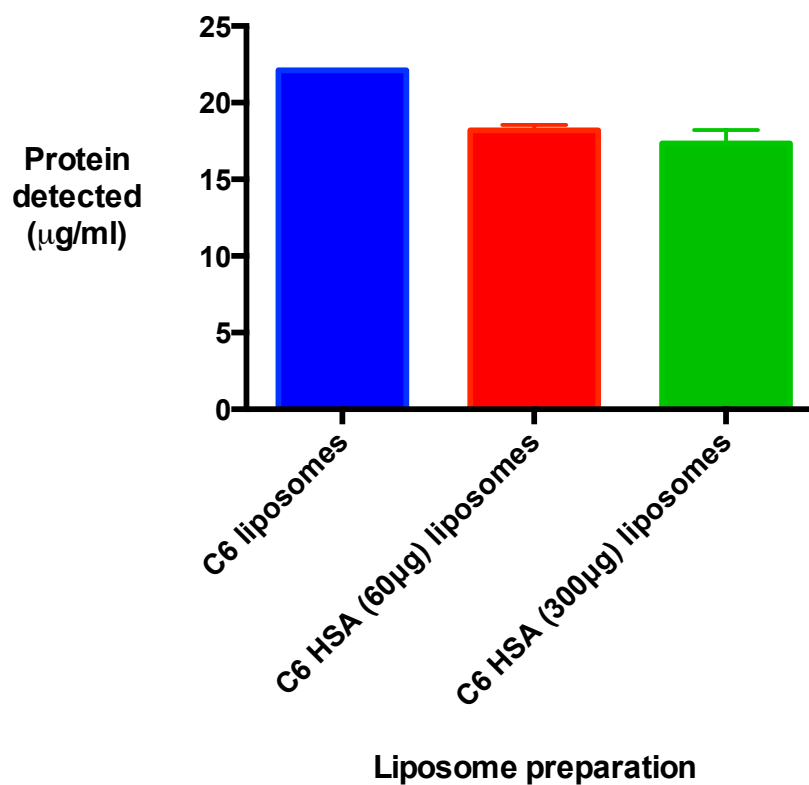


Figure 6.3.5. Protein quantitation assay: coumarin 6 liposome preparations with differing levels of protein conjugated to liposomes.

Preparations of coumarin 6 liposomes, either 'blank' or conjugated to human serum albumin (HSA), were assayed for the presence of protein using the BCA assay. Two different amounts of HSA were added preparations for conjugation, a standard dose (60µg) and a high dose (300µg). Preparations were incubated with 2% SDS for an extended period (20 hours) at room temperature to maximise lipid dissolution. Liposome samples and standards were measured in duplicate and triplicate, respectively. Results shown are mean \pm standard deviation.

Because of evidence of ongoing phospholipid interference, further assays were performed to determine whether the BCA assay was capable of detecting known amounts of protein in the presence of phospholipid, i.e. whether this interference could be eliminated in the presence of adequate amounts of protein. Using a range of HSA protein concentrations (to reflect different degrees of conjugation efficiency of HSA, representative of DCN46 antibody used in the immunoliposome preparations described in sections 6.3.1.2 and 6.3.1.3 above) liposome preparations spiked with known amounts of HSA protein were assayed using the protein quantitation assay. Results of this experiment are shown in Table 6.3.2.

Table 6.3.2 Protein quantitation assay: Coumarin 6 liposomes spiked with known concentrations of human serum albumin (HSA) to reflect 10%, 60% and 100% conjugation of DCN46 antibody used in immunoliposome preparations.

All liposome samples were incubated with 2% SDS for 20 hours prior to analysis. Results presented are mean \pm standard deviation; samples were assayed in duplicate.

Sample	Expected protein concentration ($\mu\text{g/ml}$)	Detected protein concentration ($\mu\text{g/ml}$)	Difference (%)
Blank liposome sample	0	15.5 ± 3.9	
Spiked liposome sample (10%)	5.9	33.0 ± 2.1	$+27.1 \pm 2.1$ (>100%)
Spiked liposome sample (60%)	35.5	45.7 ± 6.3	$+10.2 \pm 2.1$ (~30%)
Spiked liposome sample (100%)	59	52.7 ± 2.3	-6.3 ± 2.3 (~10%)

6.3.2. PLGA nanoparticles

6.3.2.1 Characterisation of PLGA nanoparticles

The size, polydispersity and zeta potential of PLGA nanoparticles were determined in triplicate using dynamic light scattering. For the characterisation experiments, coumarin 6 PLGA nanoparticles were conjugated to human serum albumin (HSA); in all subsequent experiments nanoparticles were conjugated to either DCN46 or IgG (as described in the relevant sections). Results are shown in Table 6.3.3.

Table 6.3.3 Physicochemical characteristics of PLGA nanoparticles

Sample	Size* (nm)	Polydispersity index	Zeta potential* (mV)
Unconjugated PLGA nanoparticles	119 ± 1.8	0.08 ± 0.03	-22.5 ± 0.1
HSA conjugated PLGA nanoparticles	138 ± 0.1 [†]	0.09 ± 0.01	-13.9 ± 1.1 [‡]

* Mean ± standard deviation

[†] p=0.0001 for size of HSA-conjugated versus unconjugated PLGA nanoparticles (unpaired t test)

[‡] p=0.0002 for zeta potential of HSA-conjugated vs unconjugated PLGA nanoparticles (unpaired t test)

Conjugation of HSA to PLGA nanoparticles via carbodiimide chemistry increased the size and reduced (made less negative) the zeta potential of nanoparticles compared with unconjugated PLGA nanoparticles. All PLGA nanoparticle preparations were monodispersed, as shown by polydispersity indices less than 0.3.

6.3.2.2 PLGA nanoparticles conjugated with DCN46 bind to DC-SIGN in an ELISA

Using a modified ELISA assay, the functionality of DCN46-conjugated PLGA nanoparticles was confirmed (Figure 6.3.6). Strong binding was observed, suggesting high levels of functional DCN46 on the surface of these PLGA nanoparticles, and thus that these nanoparticles would be a suitable drug delivery system to use for further in vitro studies of targeting to DC-SIGN on the surface of human or marmoset DC.

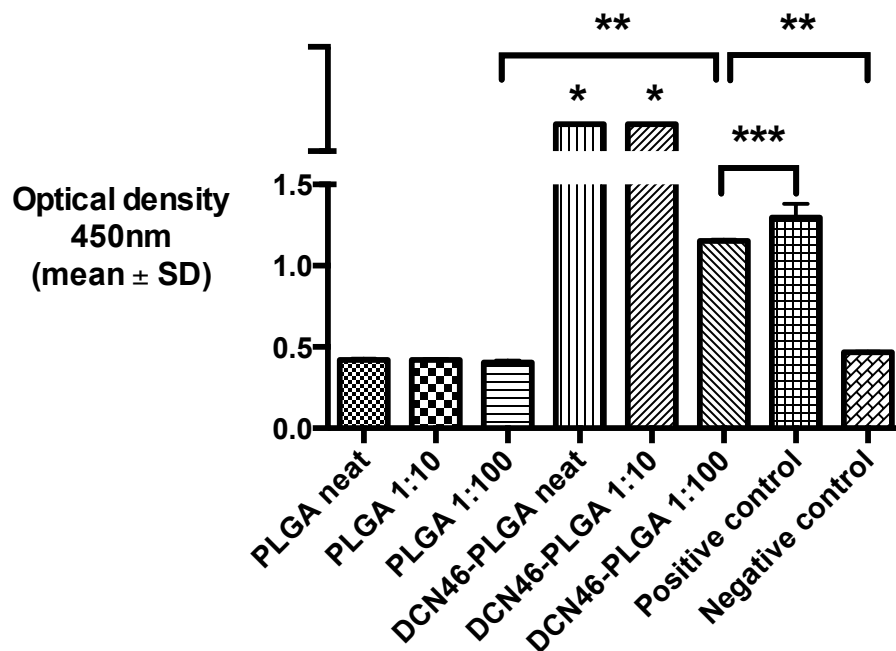


Figure 6.3.6. PLGA nanoparticles targeted to DC-SIGN show evidence of strong binding to DC-SIGN in a qualitative ELISA assay.

Serially diluted samples of unconjugated PLGA nanoparticles, or PLGA nanoparticles conjugated to DCN46 (DC-SIGN antibody) were assayed for binding in an ELISA plate coated with recombinant human DC-SIGN-Fc chimera. Purified DC-SIGN antibody (5µg/ml) was used as a positive control; PBS was used as a negative control. Results for neat and 1:10 dilution of PLGA-DCN46 showed strong binding that exceeded the limits of the assay (shown by the break in the X-axis); at 1:100 the reactivity was comparable to the positive control. Results are representative of two separate experiments.

* = Strong binding; exceeded limits of the assay

** = $p < 0.001$ for PLGA-DCN46 1:100 versus either PLGA 1:100 or negative control

*** = $p = NS$ for PLGA-DCN46 1:100 versus the positive control

NS = statistically non significant; SD = standard deviation

6.3.2.3 Coumarin-6 PLGA nanoparticles targeting DC-SIGN bind to and are taken up by human MoDC to a greater extent than non-targeted PLGA nanoparticles

PLGA nanoparticles containing the fluorescent hydrophobic molecule Coumarin 6 were cultured with human MoDC for 1 hour at either 4°C (Figure 6.3.7) or 37°C (Figure 6.3.8). Flow cytometry demonstrated that PLGA nanoparticles were taken up non-specifically by MoDC, particularly at 37°C. PLGA uptake was significantly enhanced by conjugation of PLGA with the DC-SIGN targeting antibody DCN46. In the presence of a competitive agonist (purified DC-SIGN antibody, also clone DCN46), this uptake was reduced, confirming the specificity of targeting.

Immunofluorescence microscopy confirmed that PLGA nanoparticles targeted to DC-SIGN had the highest degree of uptake into the cytoplasm of human MoDC (Figure 6.3.9).

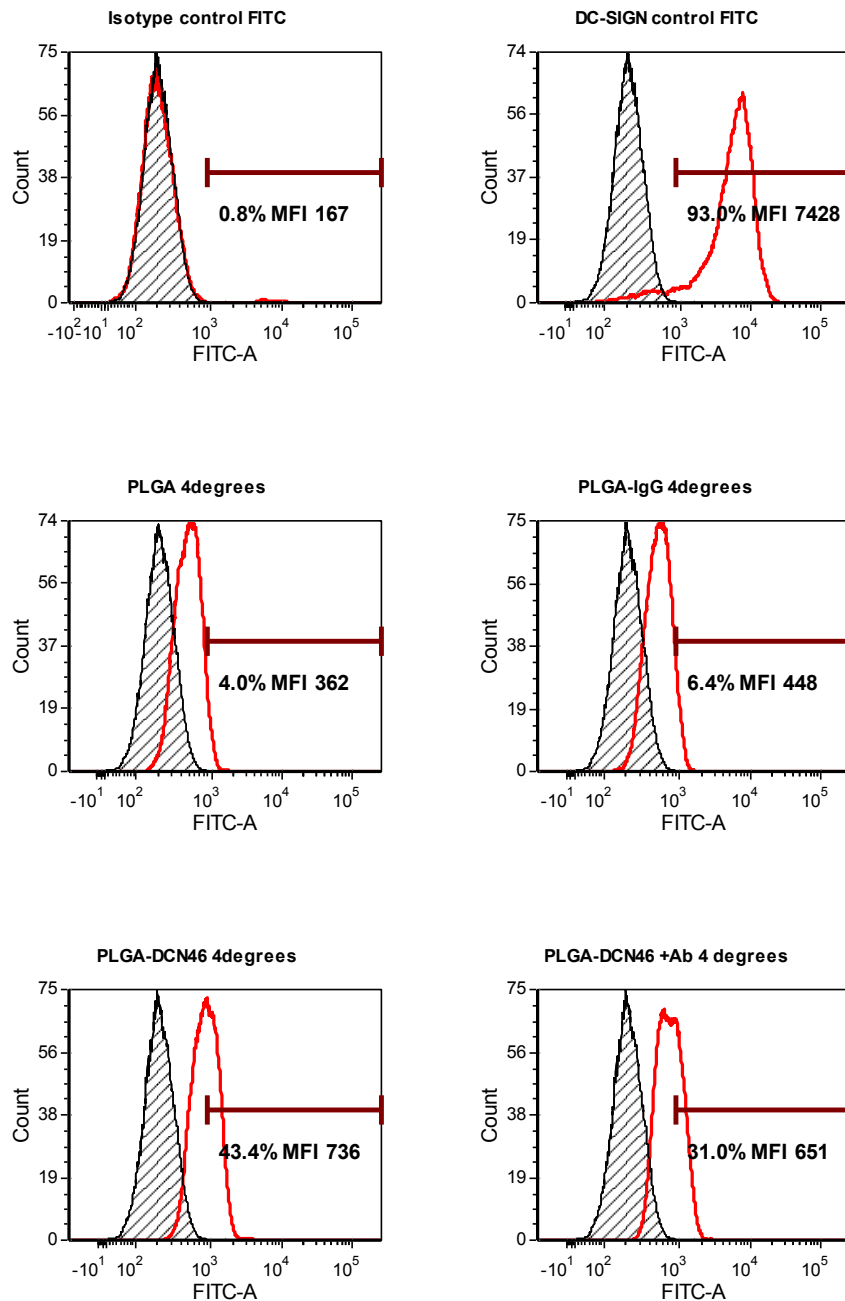


Figure 6.3.7. Coumarin 6-PLGA nanoparticles targeted to DC-SIGN incubated at 4°C with human MoDC are taken up to a greater extent than non-targeted nanoparticles.

Human MoDC (day 6 or 7 in culture with GM-CSF/IL-4) were incubated for 1 hour at 4 degrees with different formulations of PLGA nanoparticles containing Coumarin 6, and PLGA uptake was assessed by flow cytometry in the FL-1 channel (labelled FITC-A here). All plots are normalised to control unstained cells, represented by shaded histograms. The numbers indicate the percentage of cells taking up PLGA. MoDC stained with isotype FITC or DC-SIGN FITC were used as negative and positive controls, respectively. CTRL = control; MFI = mean fluorescence intensity; PLGA = non-conjugated PLGA nanoparticles; PLGA-IgG = PLGA nanoparticles conjugated to isotype IgG; PLGA-DCN46 = PLGA nanoparticles conjugated to clone DCN46 (targets DC-SIGN); +Ab – anti-DC-SIGN antibody added to culture prior to PLGA nanoparticles as a competitive agonist for DC-SIGN. Results are representative of two experiments.

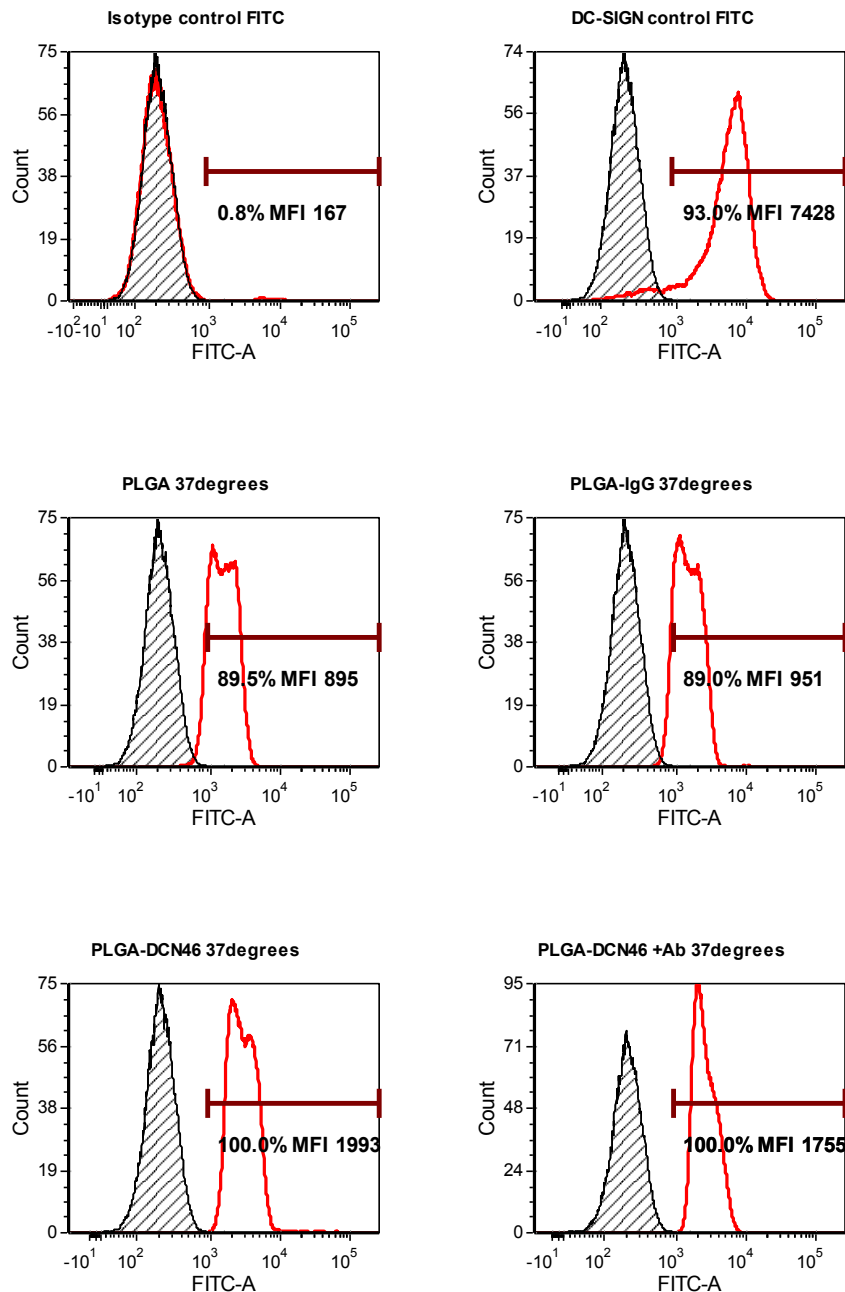


Figure 6.3.8. Coumarin 6-PLGA nanoparticles incubated at 37°C with human MoDC are taken up non-specifically by cells; targeting to DC-SIGN significantly improves this uptake.

Human MoDC (day 6 or 7 in culture with GM-CSF/IL-4) were incubated for 1 hour at 37 degrees with different formulations of PLGA nanoparticles containing Coumarin 6, and PLGA uptake was assessed by flow cytometry in the FL-1 channel (labelled FITC-A here). All plots are normalised to control unstained cells, represented by shaded histograms. The numbers indicate the percentage of cells taking up PLGA. MoDC stained with isotype FITC or DC-SIGN FITC were used as negative and positive controls, respectively. CTRL = control; MFI = mean fluorescence intensity; PLGA = non-conjugated PLGA nanoparticles; PLGA-IgG = PLGA nanoparticles conjugated to isotype IgG; PLGA-DCN46 = PLGA nanoparticles conjugated to clone DCN46 (targets DC-SIGN); +Ab – anti-DC-SIGN antibody added to culture prior to PLGA nanoparticles as a competitive agonist for DC-SIGN. Results are representative of two experiments.

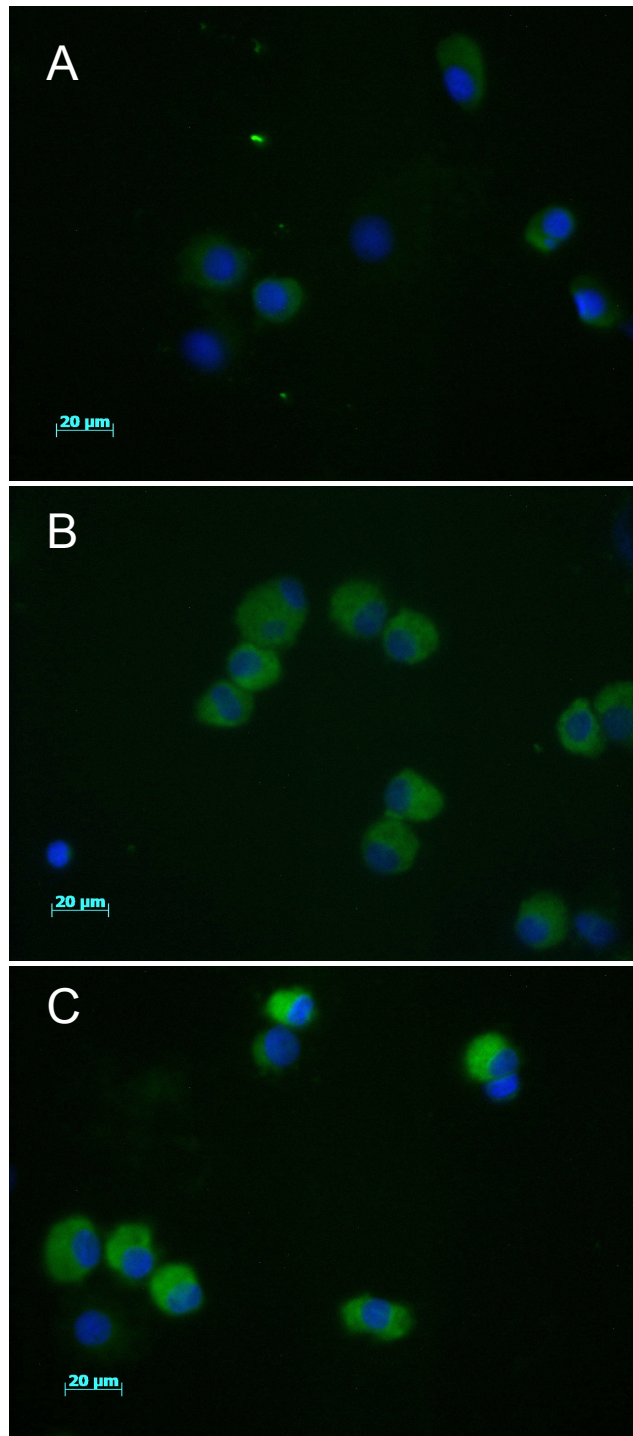


Figure 6.3.9. DC-SIGN targeted PLGA nanoparticles are taken up into the cytoplasm of human MoDC to a greater extent than non-targeted nanoparticles.

Immunofluorescence microscopy of cytospin samples of human MoDC incubated with PLGA nanoparticles containing Coumarin 6. PLGA nanoparticle uptake is shown via the green staining of cell cytoplasm with Coumarin 6. Cell nuclei are stained blue with DAPI counterstain. (A) MoDC incubated with unconjugated PLGA nanoparticles; (B) MoDC incubated with PLGA nanoparticles conjugated to irrelevant IgG; (C) MoDC incubated with PLGA nanoparticles conjugated with DCN46 antibody.

6.3.2.4 Coumarin-6 PLGA nanoparticles are taken up non-specifically by a small population of CD11c⁺Class II⁺ marmoset splenocytes

After overnight culture of fresh marmoset splenocytes with PLGA nanoparticles, there was minimal Coumarin-6 fluorescence observed in the whole spleen population (data not shown). However, a small population of CD11c⁺Class II⁺ cells demonstrated high intensity Coumarin-6 fluorescence (mean fluorescence intensity >100,000) with unconjugated, IgG and DCN46 conjugated PLGA nanoparticles (Figure 6.3.10).

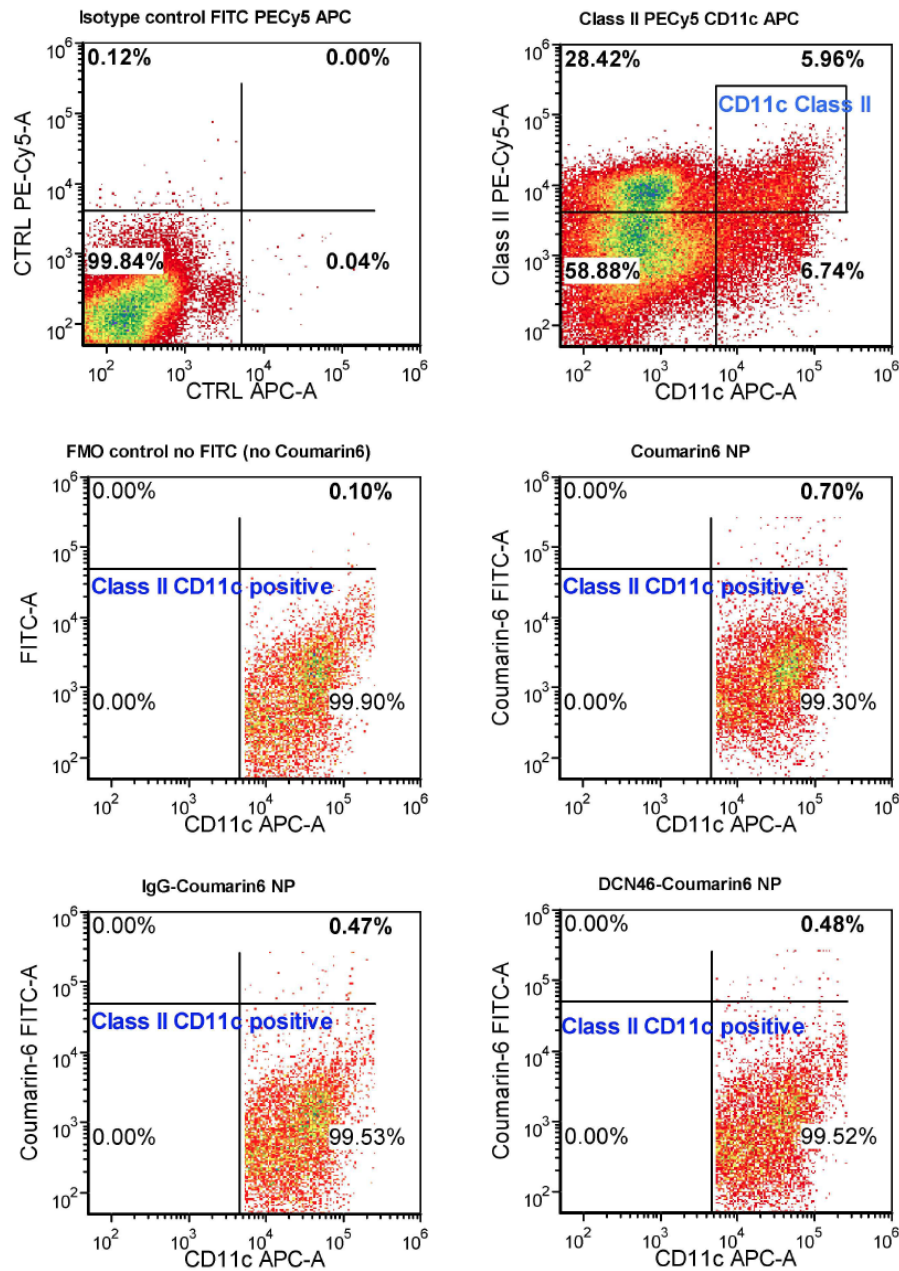


Figure 6.3.10 Coumarin 6-PLGA nanoparticles incubated overnight with marmoset splenocytes are taken up by a small population of Class II⁺ CD11c⁺ cells.

Marmoset spleen cells were incubated overnight with different formulations of PLGA nanoparticles containing Coumarin 6, and PLGA uptake (Coumarin-6 fluorescence) was assessed by multi-colour flow cytometry of likely DC (CD11c⁺ Class II⁺ cells) in the FITC channel. Density plots are shown. The top two panels show isotype control and Class II-CD11c stained cells respectively. The top right panel shows the gate used in subsequent panels. A FITC FMO control (gated at 0.1% positive) was used as the negative control for Coumarin-6 staining. A small population of highly fluorescent cells (MFI typically >100,000, range 0.47-0.70% of cells) were observed after incubation with PLGA nanoparticles conjugated to IgG, DCN46 or an unconjugated control, indicating that targeting with DC-SIGN specific antibody did not seem to have any effect on this non-specific uptake. Data are from one experiment.

6.3.2.5 Curcumin containing PLGA nanoparticles – effects on DC maturation and function

Flow cytometry analysis of human MoDC treated with curcumin-containing PLGA nanoparticles revealed non-significant alterations in the expression of some DC maturation markers, as shown in Figure 6.3.11. Compared with untreated mature DC, treatment with DCN46 targeted curcumin PLGA nanoparticles appeared to slightly reduce the expression of DC-SIGN, CD80 and CD83, and increase the expression of Class II and CD86. Non-targeted (IgG) curcumin PLGA nanoparticles had similar effects on Class II and CD86, but not on CD80 or CD83, suggesting a degree of specific effect via targeting to DC-SIGN. Overall, the effects were however modest, and were not suggestive of a significant resistance to the maturation effects of LPS.

When MoDC treated with curcumin containing PLGA nanoparticles were investigated for their stimulatory capacity in a dendritic cell MLR, no significant effects of the curcumin-nanoparticle treatment were observed (see Figure 6.3.12). However, when graded doses (with a five-fold higher neat concentration) of PLGA nanoparticles containing curcumin were added to a non-specific two-way MLR, there was evidence of significant suppression at the higher concentrations (see Figure 6.3.13).

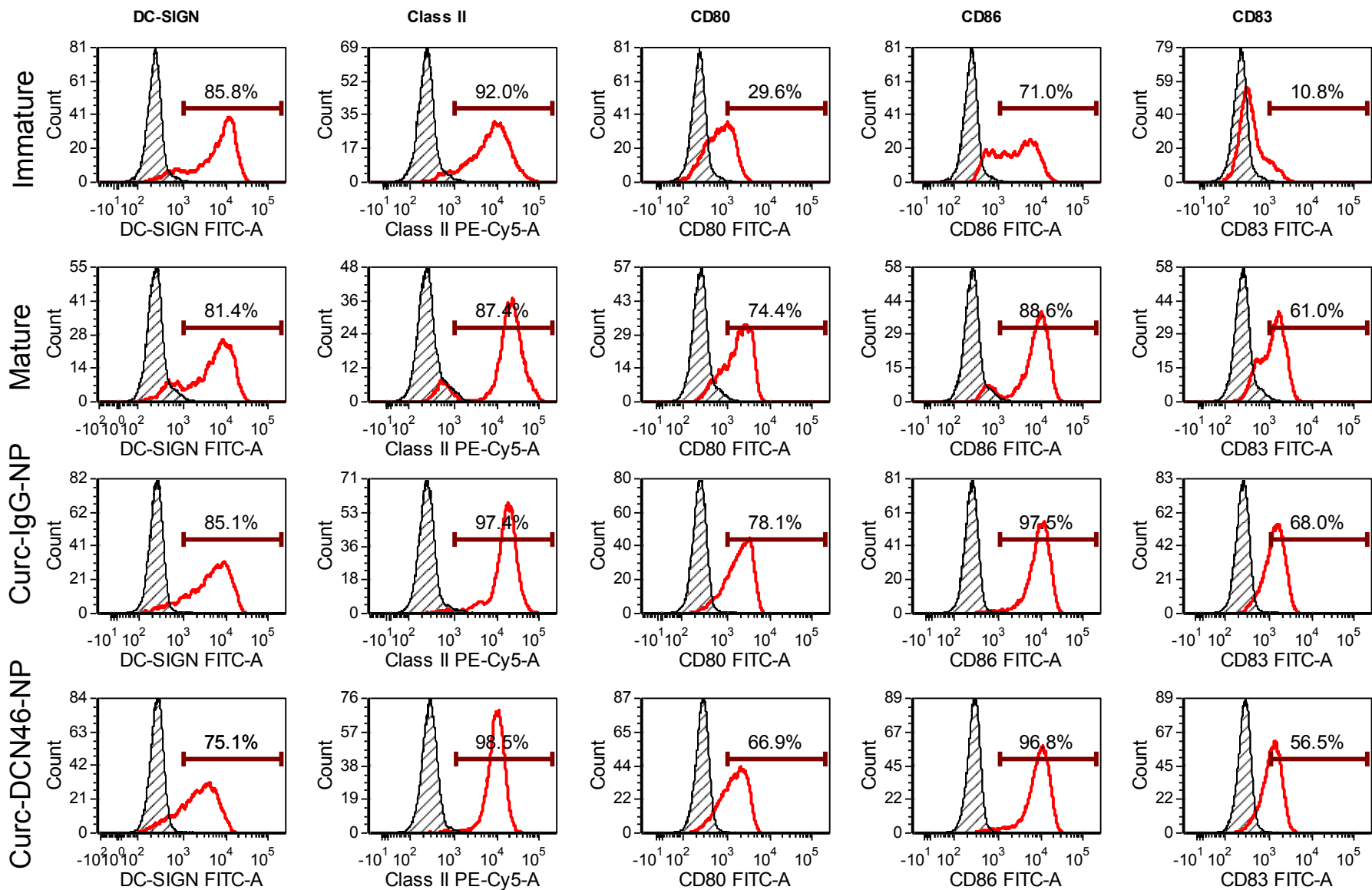


Figure 6.3.11. Human MoDC treated with curcumin containing PLGA nanoparticles targeted to DC-SIGN show alterations in DC maturation markers.

Human MoDC (day 5 in culture with GM-CSF/IL-4) were treated with different formulations of PLGA nanoparticles containing the immunomodulatory agent curcumin, given a maturation stimulus with lipopolysaccharide (LPS; 10ng/ml) on day 6, then stained on day 7 with monoclonal antibodies to the DC markers DC-SIGN, Class II, CD80, CD86 and CD83, prior to flow cytometry analysis. All plots are normalised to cells stained with the relevant isotype control antibodies, represented by shaded histograms. The numbers indicate the percentage of cells positive for the relevant DC marker. Untreated mature (given LPS) and immature (media only) MoDC were used as controls. Data reflect one experiment.

Immature = control MoDC untreated with either LPS or PLGA nanoparticles; Mature = control MoDC, treated with LPS only; Curc-IgG-NP = MoDC treated with curcumin PLGA nanoparticles conjugated to IgG, prior to LPS; Curc-DCN46-NP = MoDC treated with curcumin PLGA nanoparticles conjugated to DCN46 (targets DC-SIGN) prior to LPS.

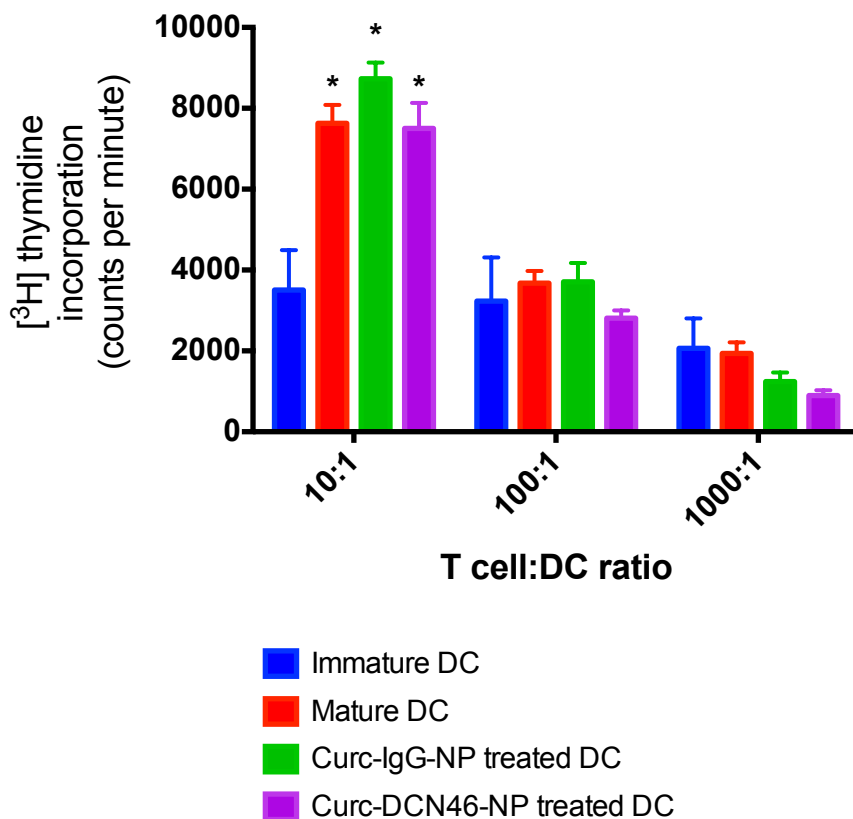


Figure 6.3.12. Human MoDC treated with curcumin containing PLGA nanoparticles targeted to DC-SIGN did not exhibit significant differences in allostimulatory capacity in a dendritic cell mixed leucocyte reaction (MLR).

Human MoDC (day 5 in culture with GM-CSF/IL-4) were treated with different formulations of PLGA nanoparticles containing curcumin (equivalent concentration of PLGA 14µg/ml), and matured with lipopolysaccharide (LPS; 10ng/ml) on day 6, and at day 7 were cultured to assess for allostimulatory capacity in a dendritic cell MLR. All stimulator MoDC were irradiated with 30Gy prior to co-culture with nylon wool T-cells (generated as per section 2.4.3.3) at various T-cell: DC ratios. T-cell proliferation was assessed by ³H-thymidine incorporation. Results shown are mean ± standard deviation and reflect one experiment. While maturation stimulation with LPS resulted in a significant increase in T-cell proliferation (at least at the 10:1 T-cell:DC ratio), this was not significantly affected by treatment with the curcumin containing PLGA nanoparticles. All samples were measured in quintuplicate.

DC = human MoDC; Curc-IgG-NP = curcumin PLGA nanoparticles conjugated to IgG; Curc-DCN46-NP = curcumin PLGA nanoparticles conjugated to DCN46 (targets DC-SIGN).

* = p<0.001 for T-cell proliferation versus immature DC

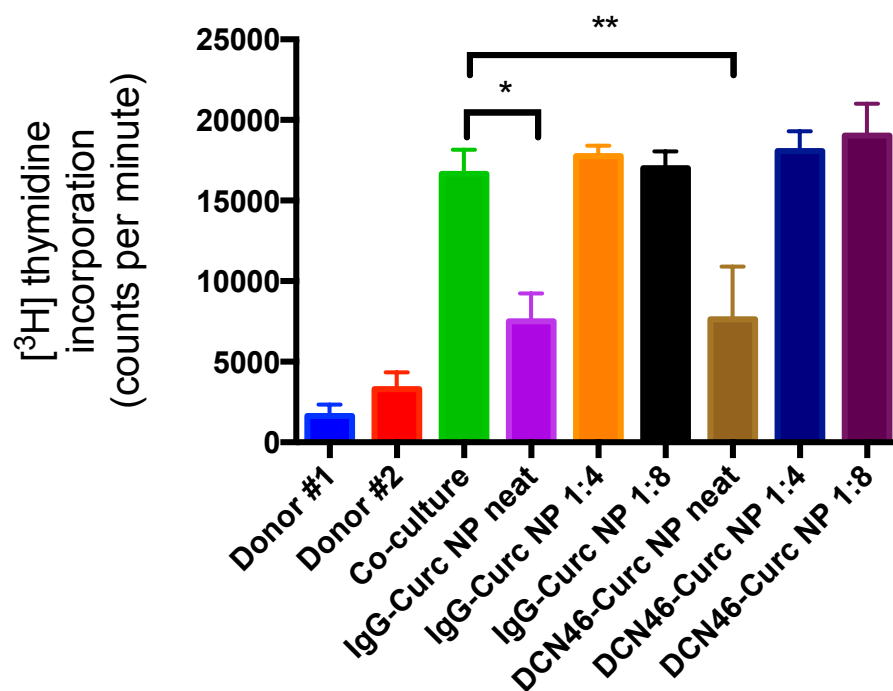


Figure 6.3.13. Curcumin containing PLGA nanoparticles cause dose-dependent suppression of alloproliferation in a two-way mixed leucocyte reaction (MLR).

PBMC isolated from two donors were co-cultured in a mixed two-way MLR; cells were not subjected to irradiation. Curcumin containing PLGA nanoparticles (conjugated to DCN46 to target DC-SIGN, or an irrelevant IgG) were added at graded concentrations (neat, 1:4 and 1:8 dilution) directly to the cells on the first day of culture. The equivalent concentration of PLGA nanoparticles (PEG-PLGA-COOH) was ~70µg/ml (a five-fold increase on the previous experiments) in the neat nanoparticle preparations. T-cell proliferation within the culture was assessed by ³H-thymidine incorporation. There was evidence of a significant suppression of proliferation with the highest dose of nanoparticles, but this was non-specific and not enhanced by specific targeting to DC-SIGN. Results shown are mean ± standard deviation, and reflect data from one experiment. All samples were measured in quintuplicate.

* = $p < 0.0001$ – co-culture versus IgG-Curc-NP treated PBMC (one way ANOVA); ** $p < 0.0001$ – co-culture versus DCN46-Curc-NP treated PBMC (one-way ANOVA); PBMC = peripheral blood mononuclear cells; Curc-IgG-NP = curcumin PLGA nanoparticles conjugated to IgG; Curc-DCN46-NP = curcumin PLGA nanoparticles conjugated to DCN46 (targets DC-SIGN).

6.4. Discussion

This chapter presents the results of two approaches to develop cell-specific therapy to target DC *in situ*; using firstly targeted immunoliposomes, and secondly targeted polymeric PLGA nanoparticles. In these studies, the monoclonal antibody DCN46 (BD Biosciences) was used as the means to target human or marmoset DC-SIGN via linking DCN46 to the surface of liposomes or nanoparticles. This antibody was chosen on the basis of demonstrated binding/cross-reactivity to both human and marmoset DC-SIGN, as outlined in the studies presented in Chapter 5. DC-SIGN expression and function shows considerably similarity between humans and non-human primates, and does not have a direct functional orthologue in mice⁶⁴³; thus therapy targeted to DC-SIGN is most appropriately evaluated *in vitro* with human cells and *in vivo* using a suitable NHP model.

6.4.1. Immunoliposomes targeting DC-SIGN

Immunoliposomes targeting DC-SIGN were developed using a post-insertion method, first described by Ishida et al,⁴⁷⁸ and subsequently utilised in a number of other studies of targeted immunoliposomes (see Chapter 1, section 1.7.1).^{477,479,646} This method involves the conjugation of antibodies to the distal end of a PEG-lipid in micellar phase via a covalent reaction between maleimide groups within the DSPE-PEG-mal lipid, and sulfhydryl groups on lysine residues within thiolated antibodies. Subsequently, antibody conjugated-micelles are added to pre-prepared drug-containing (in this case DiI) liposomes to facilitate incorporation into the lipid bilayer, and purified based on size using a Sepharose®CL-4B column. This method offers flexibility by enabling the generation of drug containing liposomes that can be conjugated at a later date to any desired antibody (or other protein ligand) via the use of different antibodies in the micelle preparations.⁴⁷⁷

Immunoliposomes incorporating DiI as a lipophilic fluorescent marker (within the lipid bilayer) and the monoclonal antibody DCN46 on their surface were successfully generated, and physicochemical characterisation demonstrated that these were of suitable size for optimal uptake by DC,⁶³⁹ and were of a generally uniform size (as measured by polydispersity index; Table 6.3.1). The presence of a net negative charge

on the surface would be expected to reduce the likelihood of non-specific uptake by DC,^{638,639} and thus increase the potential for effective targeting via antibody binding to DC-SIGN. There was a small increase in both the size and zeta potential observed for immunoliposomes (DCN46 or IgG) versus unconjugated liposomes, indicating the successful conjugation of positively charged antibody to the (negatively charged) PEG. Notably, there was also a small increase in polydispersity, which could be due to increased aggregation from reduced steric repulsion of negatively charged PEGylated liposomes,⁶⁴⁷ electrostatic interactions between net positive charge on DNC46 and the negatively charged PEG, as observed by Badiee et al,⁶⁴² or even as a consequence of the presence of free micelles in the formulation following purification.

Using a modified DC-SIGN ELISA, based on a method described by Badiee et al,⁶⁴² the presence of functional DCN46 binding to DC-SIGN in the DCN46 immunoliposome preparation was demonstrated (Figure 6.3.1). This was an important finding, as conjugating antibody to liposomes via the post insertion method may result in a random orientation of antibodies on the liposome surface,⁶⁴⁸ without necessarily having a high yield of functional F-ab regions available to interact with DC-SIGN. However, in this semi-quantitative assay, the level of functional DCN46 detected was low (mean 328pg/ml) compared with the amount of antibody added to the liposome preparations (~60µg/ml). Although conjugation efficiency cannot be directly estimated using this approach (due to the randomness of orientation of DCN46 and steric interference with the assay by liposomes), this difference suggests relatively low amounts of functional surface antibody post conjugation.

Despite evidence of functional DCN46 on the surface of immunoliposomes, following culture of targeted immunoliposomes with human MoDC expressing high levels of DC-SIGN, there was no evidence of uptake of fluorescent liposomes by these cells observed in either flow cytometry or immunofluorescence microscopy (Figure 6.3.2 and Figure 6.3.3). A number of factors may have contributed to this finding.

Firstly, it is possible that the DCN46 on the surface of immunoliposomes was not present in adequate amounts to facilitate binding to DC-SIGN in cell culture. Because of the semi-quantitative nature of the DC-SIGN ELISA assay, attempts were made to determine the antibody yield in the liposome preparations by assaying protein concentration using a BCA assay, as described by Badiee et al.⁶⁴² Although BCA assays

have been frequently used to determine the antibody yield in immunoliposome preparations,^{471,479,633,642} in this study it was not possible to eliminate interference with the assay despite using a number of methods of optimisation (outlined in section 6.3.1.4). The BCA assay detects a colour change when protein binds to the BCA reagent generating complexes with a strong absorbance at 562nm. The presence of phospholipid can result in artificially high values by interfering with the BCA reagent to generate a chromophore complex with an absorbance close to 562nm.^{649,650} It is therefore possible that if a low level of antibody/protein was present in the liposome formulations, and that this was inadequate to compete with residual lipid present even after prolonged incubation with 2% SDS (Figure 6.3.5).^{645,651} It was subsequently demonstrated that a conjugation efficiency of between 60 and 100% would have been needed to out-compete lipid effectively to detect levels of protein within ~10-30% of expected using the BCA assay (Table 6.3.2). It thus seems likely that the conjugation efficiency was lower than this level, despite the use of an appropriate, previously validated method of conjugation.⁴⁷⁸

In addition to a low level of antibody on the surface of immunoliposomes, it is possible that the Sepharose® CL-4B column chromatography purification step (which separates particles based on size) did not result in the complete removal of any remaining DCN46-micelles in the preparation. In a separate assay of micelles conjugated to 60µg of HSA (as a surrogate for antibody) using similar preparation methods, the mean size of micelles was ~171nm (unpublished results; Kitto LJ) substantially higher than that typically reported in literature of <100nm.⁶⁵² If this similarity in size had been the case with the studies presented here (where micelle size was not specifically assessed), it is possible that steric repulsion led to poor incorporation of micelles into liposomes and that subsequent separation by the purification column was incomplete. The reasons for such an unexpected increase in micelle size are not known, but could be due to the low volumes used and thus a lack of adequate dispersion of the lipid film during rehydration, which could be minimised in future by increasing the reagent amounts, or by additional vortexing and sonication.⁶⁵² If DCN46-micelles were present even at low concentration then it would be expected that the ELISA would detect the presence of these, and that if micelle binding to MoDC occurred in culture that no DiI fluorescence would be detected (due to the DiI being present only in liposomes).

The presence of DiI in the immunoliposome preparations should have resulted in detection of some degree of DiI fluorescence in the event of non-specific uptake by MoDC. That there was minimal fluorescence detected raises the possibility of the loss of DiI fluorescence during the process of purification of immunoliposomes. In this study, 0.3mol% of DiI (i.e. 0.3% of total phospholipid (mol)) was used in the initial preparation of liposomes; similar studies have reported using either 0.3mol%^{644,653} or 0.2mol%.⁶⁴² However, the purification process caused a five-fold reduction in concentration of immunoliposomes compared with unconjugated liposomes (section 6.3.1.1). This may have resulted in a relatively low concentration of DiI being present in the liposome preparations in buffer, despite DiI fluorescence being detected in the neat samples, prior to addition to cell culture. Although physicochemical characteristics such as size and zeta potential remained stable up to 97 days, it is also possible that DiI fluorescence was lost from liposomes during storage; this was not specifically assessed.

In conclusion, although immunoliposomes conjugated to DCN46 appeared to be successfully generated in these studies, there was no evidence of uptake by MoDC expressing DC-SIGN. This is most likely to be due to an inadequate amount of functional DCN46 to facilitate targeting. Future studies could address this by (1) increasing the amounts of reagents used to prepare the micelles, and ensuring these were of appropriate size by the inclusion of additional sonication and vortexing steps and subsequent physicochemical assessment⁶⁵²; (2) ensuring adequate amounts of DCN46 in micelles prior to their addition to liposomes and subsequent purification, either with the use of a BCA, or another protein quantification assay not subject to interference from lipid,⁶⁵⁴ such as a sandwich ELISA using a secondary anti-mouse-Ig antibody to detect antibody directly; (3) increasing the content of fluorescence (DiI or other similar agent) contained within liposomes and/or measuring DiI fluorescence immediately prior to cell culture to ensure adequate fluorescence remains present; or (4) using an alternative approach to conjugate DCN46 to liposomes, e.g. direct conjugation via maleimide groups contained within PEG-lipids in liposome formulations.⁶⁴⁴

Given the difficulties encountered in developing immunoliposomes targeted to DC-SIGN, an alternative approach utilising polymeric PLGA nanoparticles was undertaken for subsequent studies.

6.4.2. *PLGA nanoparticles targeting DC-SIGN*

PLGA nanoparticles were generated using nanoprecipitation⁴⁹⁶ and conjugated to DCN46 using a carbodiimide chemistry method (see Chapter 1, section 1.7.2).^{489,498} A major advantage of PLGA nanoparticles over liposomes is the ability to incorporate hydrophobic drugs at a higher concentration than their intrinsic water solubility within a hydrophobic core,⁶⁵⁵ and surround this with a hydrophilic shell to facilitate drug delivery to tissues. Nanoprecipitation, also known as the solvent displacement method, is a convenient and reproducible process for the preparation of monodisperse, polymeric nanoparticles in a size range of approximately 50-300nm.⁴⁹⁶ The approach adopted here involved using a commercially prepared amphiphilic PLGA-*b*-PEG co-polymer to encapsulate a high concentration of hydrophobic drug (in this case, coumarin 6, or curcumin) within the hydrophobic core of a polymeric nanoparticle with an exterior shell of hydrophilic PEG. By using PLGA-PEG-COOH as one of these copolymers (in combination with PLGA-mPEG), conjugation of amine groups on DCN46 (or IgG) to free carboxyl terminals of the PLGA polymer was achieved by activation of the carboxyl groups with EDC in the presence of NHS and the subsequent formation of covalent amide bonds.^{498,500,501,656} Any residual free antibody was then removed from the preparation by centrifugation, and nanoparticles were resuspended in buffer at the desired concentration for further studies.

Physicochemical characterisation (Table 6.3.3) of unconjugated PLGA nanoparticles containing coumarin 6 generated in these studies demonstrated that these were of a mean size of 119nm, were of uniform size (monodispersed), and had a net negative charge (mean -22.5mV). Conjugation of human serum albumin (HSA; used as a model protein in place of DCN46 antibody due to cost restraints) led to a significant increase in size (to a mean of 138nm) and a reduction of the negative charge to a mean of -13.9mV. These results are consistent with successful conjugation of positively charged HSA with an estimated size of 38x150Å (3.8x15nm)⁶⁵⁷ to the surface of the nanoparticles.

In contrast to the results observed for the immunoliposomes (discussed above), PLGA nanoparticles containing coumarin 6 and conjugated to DCN46 showed evidence of a high level of DCN46 functional activity in a qualitative (i.e. non quantitative) modified DC-SIGN ELISA.⁶⁴² BCA assays of the protein content of the preparations were not

performed, but could be used in future studies to assess the degree of conjugation efficiency,^{650,656} and would be unlikely to be subject to interference, an advantage of using polymeric nanoparticles rather than phospholipid containing liposomes.

After culture of the PLGA nanoparticles with human MoDC (expressing high levels of DC-SIGN), there was evidence of enhanced uptake by MoDC of nanoparticles conjugated to DCN46, compared to unconjugated or IgG-conjugated nanoparticles. In addition, specificity to DC-SIGN was demonstrated by adding a blocking antibody to the culture. Two different incubation temperatures – 4°C and 37°C – were used to investigate differences in binding to DC-SIGN, and uptake by metabolically active cells, respectively.⁶⁴⁰ These demonstrated that in addition to targeted uptake there was evidence of non-specific uptake of nanoparticles by MoDC, particularly at 37°C. This is an unsurprising finding, given the specialised antigen uptake capabilities of the immature human MoDC used in these studies,^{73,195} the size of these nanoparticles,⁶³⁹ and the lack of any competing cells or inhibitory factors in the culture. Given the functions of DC-SIGN, it is likely that uptake of DC-SIGN targeted PLGA nanoparticles occurs via receptor-mediated endocytosis, although the mechanism of uptake was not specifically examined here. Others have shown that PLGA nanoparticles targeted to DC surface receptors (e.g. via CD11c or DEC-205) can be taken up through receptor-mediated endocytosis, and also via phagocytosis.^{376,451} Future studies could thus be designed in this particular model to explore these mechanisms in detail via blockade of these pathways.

To investigate whether the DCN46 PLGA nanoparticles would have potential utility in an *in vivo* marmoset NHP model, it is important to determine whether marmoset DC expressing DC-SIGN would also be effectively targeted by the preparation. As propagated marmoset MoDC do not express high levels of DC-SIGN,^{403,621} a preliminary study of overnight culture of nanoparticles with marmoset spleen cells was undertaken. As shown in Chapter 5 (section 5.3.6), a population of DC-SIGN expressing DC can be identified in freshly isolated marmoset spleen that are negative for lineage markers, and express Class II and the myeloid DC marker CD11c. Results from this preliminary study suggested that the nanoparticles were taken up by a small population of marmoset CD11c⁺ Class II⁺ cells (Figure 6.3.10), albeit in a non-specific fashion, i.e. targeting had no discernable effect. Whether these represent DC-SIGN positive marmoset splenic DC is not certain, however, as it was not possible to include

lineage markers, due to the available marmoset cross reactive antibodies for lineage markers all being conjugated to FITC, which has similar excitation and emission spectra to coumarin 6. Ethical concerns regarding the inappropriate use of primates to obtain fresh tissue (without other indications for euthanasia), as well as the costs involved, limit the opportunities to obtain fresh marmoset splenocytes to use in these studies, and stored frozen marmoset spleen cells have been of variable quality in flow cytometry studies to identify rare populations of cells such as DC-SIGN⁺ cells (unpublished results; Collins MG and Jesudason S).

In order to explore the potential of DC-SIGN targeted PLGA nanoparticles to modify DC function, the hydrophobic immunomodulatory drug curcumin (see section 1.5.2) was incorporated as a model drug within the nanoparticles. In a preliminary study, MoDC treated with curcumin containing DC-SIGN targeted nanoparticles showed modest alterations in the expression of some maturation markers (CD80 and CD83) compared with non-targeted nanoparticles (Figure 6.3.11), however there was no evidence of any functional effects on allostimulation in a dendritic cell MLR (Figure 6.3.12). The lack of any functional effect may have been due to an inadequate dose of curcumin delivered to the MoDC, as increasing the dose of nanoparticles showed evidence of non-specific suppression of alloproliferation in a two-way MLR (Figure 6.3.13). Further studies need to be undertaken to determine the appropriate dose of curcumin nanoparticles required, whether higher doses would lead to more specific effects on DC function, and whether targeting via DC-SIGN enhances any such effects. In several other studies of curcumin loaded nanoparticles,^{658,659} a mass ratio of ~10% curcumin to PLGA has been used, twice the amount (5%) used in this study, a dose chosen on the basis of previous work done in this laboratory using liposomes loaded with curcumin.⁶⁶⁰ In addition, whether any leakage of curcumin from the nanoparticles occurred during storage is uncertain, but would be expected over time and could be specifically assessed.⁶⁶¹ The use of other, more potent immunosuppressive agents such as cyclosporine⁶⁶² or rapamycin⁶⁶³ within the nanoparticles might also enhance the effectiveness of targeted nanoparticle therapy on DC.

6.4.3. Conclusions

In the context of this thesis, these studies represent significant progress towards developing a nanocarrier-based DC targeted therapy in the common marmoset preclinical model of transplantation.

Although it was not possible to generate DCN46 immunoliposomes that showed evidence of targeting to DC-SIGN *in vitro*, there are a number of factors that might be addressed in future studies to achieve this. Optimisation of the preparation of DCN46 micelles and ascertainment of conjugation efficiency prior to adding these to drug containing liposomes is necessary. Alternatively, another approach could be taken to directly conjugate DCN46 to the surface of liposomes, rather than using the post-insertion method. If successful, the development of DC-SIGN targeted immunoliposomes offers the potential to deliver highly concentrated water-soluble drugs directly to DC to avoid systemic immunosuppressive toxicity, and further work to achieve this aim is warranted.

Solid PLGA nanoparticles – containing concentrated hydrophobic drugs and targeting DC-SIGN – were successfully generated in this study, and were shown to be taken up preferentially by monocyte-derived DC. It is now necessary to further develop these for use in the marmoset model by repeating the studies of targeting to marmoset splenic DC, and confirming that curcumin (or other suitable immunosuppressive drug) containing nanoparticles will modify DC function appropriately *in vitro* as well as *in vivo*. Ultimately, further testing of this therapy in a pre-clinical transplant NHP model to ascertain its effects on graft survival will be an important step towards the translation of this approach into the clinic.

Chapter 7: CONCLUSIONS AND FUTURE DIRECTIONS

7.1. Summary and Conclusions

Kidney transplantation represents the best treatment for end-stage kidney disease,^{9,10} but challenges remain because of the detrimental effects of immunosuppressive strategies on both patient and graft outcomes. Promoting tolerance in clinical transplantation, and thus avoiding or minimising immunosuppression, remains an important goal of investigators in this field. Current approaches to tolerance induction that have been the subject of clinical trials,^{60,61,64} while showing promising results, continue to have significant drawbacks, due to the need for heavy initial immunosuppression and the potential for immunodeficiency as a result.⁶⁵

DC play a pivotal role in the initiation and maintenance of immune responses *in vivo*, and the development of therapies utilising or targeting DC presents opportunities to manipulate the immune response in the setting of transplantation, and to promote tolerance induction. The use of cellular DC therapies, of both donor and recipient origin, and propagated *in vitro* with immature or semi-mature phenotypes has been shown to promote tolerogenic responses in small animal models,²²⁹ but to date there has been relatively limited translation of these findings into robust non-human primate models,^{350,351} and minimal investigation of the behaviour of these cells *in vivo* post infusion. As an alternative approach, targeting DC *in situ*, with the use of nanocarriers such as liposomes or nanoparticles,^{376,451-453} is a promising therapeutic strategy that could be utilised to promote tolerogenic responses, but to date has not been explored in transplant models.

The overall aim of the work undertaken for this thesis was to further develop the potential of DC based immunotherapies in a small and clinically relevant NHP model, the common marmoset monkey.

In order to establish the utility of marmosets as a suitable kidney transplant model, it is necessary to comprehensively characterise the nature of the spontaneous renal pathology that has been observed in these animals.^{541-548,550,551,565} The work described in Chapter 3 represents the only comprehensive study of marmoset renal histology, immunofluorescence and electron microscopy, correlated with blood and urine biochemistry findings, that has been reported to date. This work has established that marmosets develop a benign glomerulopathy characterised by mesangial expansion and

the presence of immunoglobulin deposits, which is associated with mild to moderate proteinuria. This glomerulopathy is not associated with renal dysfunction, does not progress with age, and does not appear to be related to the clinical occurrence of weight loss or the so-called wasting marmoset syndrome. The presence of this glomerulopathy would not present any barriers to the assessment of renal function or histology (e.g. to assess for the presence of acute rejection) in a marmoset kidney transplant model.

In Chapter 4, the trafficking behaviour of marmoset DC propagated *in vitro* from monocytes or haematopoietic progenitors in peripheral blood, given as cellular therapy and administered subcutaneously and intravenously, respectively, was explored using both autologous and allogeneic cells in marmoset monkeys. Prior work from this laboratory has established the stably immature and semi-mature phenotypes of these DC types, respectively,⁴⁰³ and established that intravenously injected marmoset allogeneic MoDC lead to non-specific suppression of recipient immune responses.³⁰³ Prior to the initiation of this study, the accepted paradigm established from small animal models was that injected donor-derived (allogeneic) DC exert therapeutic effects via trafficking to secondary lymphoid tissue and then direct interaction with recipient T-cells. The results of this study indicate however that allogeneic DC, whether administered intravenously or subcutaneously, are not present in secondary lymphoid tissues at 48 hours post administration. This finding is in contrast to results from this and other studies of both subcutaneously and intravenously administered autologous DC (see discussion, Chapter 4). These results suggest that allogeneic DC do not exhibit normal trafficking behaviour *in vivo*, at least in this NHP model. This leads to the speculation that these cells may be removed promptly by recipient NK cells,³⁶⁹ and that the observed effects of therapeutic donor DC on immune responses may in fact occur via the acquisition and reprocessing of donor antigen by recipient DC, as has been recently shown by others.^{331,602}

Given the findings of Chapter 4, and the logistical difficulties with cellular DC therapies in the setting of transplantation, the potential of targeting of marmoset DC *in vivo* via the DC-specific cell surface receptor DC-SIGN utilising monoclonal antibodies and drug-containing nanocarriers was investigated in Chapters 5 and 6. A strategy to develop a monoclonal antibody cross-reactive with both human and marmoset DC-SIGN was used and is outlined in the studies reported in Chapter 5. Marmoset DC-SIGN was successfully cloned and used both as a template for immunogenic peptides

used to generate monoclonal antibodies via mouse immunisations and the use of hybridoma technology, and also to successfully transfect a CHO cell line to express marmoset DC-SIGN. The latter was used to screen the generated monoclonal antibodies as well as a commercial anti-human DC-SIGN; binding was confirmed using immunofluorescence of marmoset lymphoid tissues. Although unforeseen problems with the produced monoclonal antibodies ultimately prevented their use in subsequent studies (see discussion, Chapter 5), a commercial anti-human DC-SIGN (DCN46) was identified as being cross-reactive with marmoset DC-SIGN. This antibody was used to confirm that although marmoset monocyte-derived DC do not express DC-SIGN, marmoset tissue resident DC-SIGN⁺ DC are present in spleen in the Lineage⁻ Class II⁺ CD11c⁺ fraction, a finding that has not previously been reported in this species.⁶²¹

Chapter 6 presents the results of a series of studies that were undertaken to develop a nanocarrier targeting human and marmoset DC-SIGN that might be suitable to evaluate as a cell-specific drug delivery strategy *in vivo* using a marmoset model of transplantation. Several approaches were undertaken using different methods of conjugation of the monoclonal antibody to two different nanocarrier types – liposomes and PLGA nanoparticles – respectively. Ultimately, PLGA nanoparticles conjugated to DCN46 were successfully developed that showed evidence of specific targeting to human DC-SIGN⁺ DC *in vitro*, appeared to be taken up (non-specifically) by marmoset splenic DC, and can be loaded with the immunomodulatory drug curcumin and demonstrate suppressive effects in a mixed leucocyte reaction, although the specificity of this approach via drug-targeting to DC has yet to be established. These findings represent a significant advance for this model, and establish the feasibility of continuing studies to established immunosuppressive drug loaded PLGA nanoparticles targeted specifically to DC.

In conclusion, this studies outlined in this thesis have significantly advanced the marmoset NHP model as a means to develop DC based immunotherapies to promote tolerance in kidney transplantation. In particular, the feasibility of DC targeted therapy in marmosets using anti-DC-SIGN monoclonal antibody-conjugated PLGA nanoparticles has been established, and this represents an exciting development towards the ability to target immunosuppressive or immunomodulatory drugs directly to DC *in vivo* in the setting of transplantation.

7.2. Future directions

The findings from this thesis provide a platform for ongoing studies that have the potential to establish the therapeutic efficacy of DC based immunotherapies in the marmoset NHP transplant model.

Further studies are needed to determine the best approach to tolerance induction in the marmoset model. Cellular DC therapy, either of donor or recipient origin, or therapies targeted specifically to DC *in vivo* offer considerable potential as novel therapies in transplantation, but which of these is optimal is unclear. Additional studies to optimise and further evaluate DC targeted PLGA nanoparticles as a drug delivery method for immunosuppression in a cell-specific fashion are needed, and it is important to determine the immunosuppressive effects of such an approach. Although this thesis examined the use of curcumin, it will be important to investigate other agents including cyclosporin, rapamycin, co-stimulation blockade, or anti-inflammatory cytokines for their effects on the immune response using this approach. Finally, whether targeting DC via DC-SIGN offers the best means to deliver immunosuppressive therapies without off-target effects remains to be determined, and there are a number of other cell-surface proteins that might have advantages over DC-SIGN as therapeutic targets.

Ultimately, this NHP model can be used to facilitate the translation of these novel therapies towards clinical trials in human subjects undergoing transplantation.

7.2.1. Proposed further studies evaluating allogeneic DC therapy in marmosets: allogeneic DC trafficking and effects on the immune response in vivo

Future studies are needed to determine whether donor or recipient derived marmoset DC have potential as cellular therapies to direct the immune response towards tolerance. The choice of donor or recipient origin of DC, the dose, route, frequency and timing of administration still need further evaluation in terms of the evoked immune responses *in vivo* prior to definitive testing in a marmoset model of transplantation. Further work on the trafficking of administered DC *in vivo* forms an important part of this, preferably through the development of non-invasive techniques. Specific studies that could be undertaken include:

- Evaluation of the migratory capacity of marmoset *in vitro* propagated DC (both MoDC and HPDC), with flow cytometry of DC for expression of chemokine receptors for which marmoset cross-reactive antibodies are now available; and the use of *in vitro* techniques to evaluate DC migration including Transwell® migration or a chemotaxis chamber.
- Use of alternative tracking methodologies for injected DC that do not involve killing the animal, and would be suitable to use in a small primate, such as bioluminescence, scintigraphy of radiolabelled DC, or MRI of magnetically labelled DC. Use of these techniques may allow more detailed imaging of DC trafficking and interaction with other cell types over time in a live animal.
- Assessment of the viability of remaining autologous and allogeneic DC at the site of subcutaneous injection, at various times after administration, e.g. with the use of immunofluorescence markers of apoptosis and necrosis. In addition staining for the presence of recipient cells that might be present and lead to the death of administered DC, e.g. T-cells, macrophages, NK cells (with the use of cross-reactive CD3, CD11b or CD56 markers).
- Further studies of the immunologic effects over time of allogeneic intravenously administered marmoset HPDC, including studies evaluating differing doses, frequency and duration/number of administered treatments, and comparison with previously observed effects of intravenously administered marmoset MoDC, e.g. with the use of MLR to assess donor specificity, and ELISPOT for interferon- γ production.
- Ultimately, the tolerogenic potential of marmoset allogeneic DC cellular therapy (HPDC or MoDC) should be tested for its effects on allograft survival in a kidney (or other solid organ) transplant model.

7.2.2. *Proposed further studies of monoclonal antibodies targeted to marmoset DC-SIGN, and the evaluation of marmoset DC-SIGN⁺ cells identified using DCN46 monoclonal antibody*

An important component of further development of the marmoset model and targeting to DC-SIGN is the generation of marmoset specific antibodies to this molecule, and

further characterisation of the nature of marmoset DC-SIGN expressing cells *in vivo*. Whether these cells actually represent DC from a morphologic, phenotypic or functional perspective remains to be confirmed. Specific studies that should be performed include:

- Generation of a stable cell-line expressing marmoset DC-SIGN, to facilitate the generation of additional monoclonal antibodies (e.g. using whole cells expressing marmoset DC-SIGN for mouse immunisations and hybridoma generation), and enable rapid and reproducible screening of such monoclonal antibodies for DC-SIGN binding.
- Replication of results described herein showing binding by DCN46 to a population of putative DC in the lineage⁻ CD11c⁺ Class II⁺ fraction marmoset spleen, and further evaluation of these cells for their functional and phenotypic characteristics. This could potentially be achieved via the use of FACS cell sorting isolation and subsequent flow cytometry analysis for surface marker expression, and RT-PCR or ELISA to assay the expression and secretion profile of DC cytokines (e.g. IL-12).
- Further detailed evaluation of the surface marker expression profiles (e.g. Lineage, myeloid and lymphoid marker expression) of DC-SIGN⁺ and DC-SIGN⁻ cells in marmoset spleen and other tissues (e.g. thymus, liver) utilising flow cytometry and known marmoset cross-reactive antibodies.

7.2.3. Proposed further studies of DC-SIGN targeted immunoliposomes

Although DC-SIGN targeted immunoliposomes were not successfully generated in this thesis, there are a number of approaches that could be taken to enable further studies of these nanocarriers as a means of manipulation of the immune response:

- Re-evaluate the methods utilised to generate DCN46 conjugated immunoliposomes, including further detailed physico-chemical and functional characterisation of liposomes, micelles and immunoliposomes at each step to ascertain where potential problems might have occurred leading to poor DCN46 yield in the final preparation. In particular, ensuring that DCN46-conjugated micelles were functionally active in the ELISA (i.e. bind DC-SIGN), were of appropriate size (<100nm), were incorporated effectively into liposomes, and were not retained inappropriately in the preparation (separately from liposomes) during the purification steps. Optimising

micelle preparation by ensuring adequate dispersion of the lipid film with higher reagent volumes, and the use of additional vortexing and sonication steps is an important component of this.

- Investigations for the continued presence of DiI within liposomes/immunoliposomes at all steps in the process, to ensure that immunoliposomes present in the final preparation are capable of being identified in cells utilising the techniques described here.
- Use of an alternative method of immunoliposome generation to the post-insertion method, e.g. direct linking of antibody to liposomes (rather than to micelles) via the use of a heterobifunctional cross-linking agent, or grafting antibodies directly to the PEG chains with the use of carbodiimide chemistry.

7.2.4. Proposed further studies of DC-SIGN targeted PLGA nanoparticles

Targeting therapies to DC via DC-SIGN using PLGA nanoparticles holds considerable potential as a novel approach to immunosuppression, although the efficacy of such an approach in transplantation is yet to be established. Specific studies to translate this therapy towards clinical application include:

- Further detailed characterisation of the DC-SIGN targeted nanoparticles, including determination of the yield of DCN46 in the final nanoparticle preparation, e.g. with the use of an optimised BCA assay, electron microscopy analysis of the morphology of the produced nanoparticles, and spectroscopy analysis to determine the drug content of generated nanoparticles.
- Investigation of the mechanisms of uptake of DC-SIGN targeted PLGA nanoparticles by DC, i.e. with the use of assays blocking receptor-mediated endocytosis or phagocytosis pathways.
- Confirmation of binding of DC-SIGN targeted nanoparticles to marmoset DC-SIGN, via flow cytometry analysis of a marmoset DC-SIGN expressing cell line incubated with nanoparticles (e.g. transfected CHO cells, or a stable marmoset DC-SIGN cell-line, as suggested above).

- Replication of the preliminary study and further investigation of uptake of DC-SIGN targeted nanoparticles by marmoset spleen cells, to confirm the effectiveness of targeting, and further characterise *in vitro* the surface marker profile and function of cells positive for nanoparticles.
- Replication of the preliminary study of the effects of curcumin-containing DC-SIGN targeted PLGA nanoparticles on human DC, with assays of both surface marker expression and stimulatory potential in an allogeneic DC MLR, using the appropriate (higher) dose of nanoparticles identified in the two-way MLR study.
- Development of DC-SIGN targeted PLGA nanoparticles loaded with other immunosuppressive drugs such as cyclosporin or rapamycin, in order to undertake studies of targeting of more potent immunosuppression direct to DC. It would be necessary to determine the appropriate drug dose to show effects *in vitro* before proceeding to studies *in vivo*.
- Administration of immunosuppressive drug-loaded DC-SIGN targeted PLGA nanoparticles versus non-targeted immunosuppressive drugs to marmoset monkeys to ascertain the effects on the immune response *in vivo*, and any differences in side effect profiles. Ultimately, it is planned that targeted immunosuppressive PLGA nanoparticles could be administered to marmoset recipients of an allograft (e.g. a kidney transplant) and allograft survival determined in comparison to allograft recipients receiving standard immunosuppression.

In conclusion, there is considerable scope for the further development of both cellular DC therapies, and DC-targeted nanocarrier based therapies in the marmoset NHP model. In particular, the ability to target immunosuppressive drugs to DC specifically and minimise toxic side effects holds considerable potential as a novel therapy in solid organ transplantation.

REFERENCES

1. McDonald SP, Excell L, Livingstone B. ANZDATA Registry Report 2008. Adelaide: Australia and New Zealand Dialysis and Transplant Registry 2008.
2. Collins AJ, Foley RN, Herzog C, Chavers B, Gilbertson D, Ishani A et al. United States Renal Data System 2008 Annual Data Report Abstract. *Am J Kidney Dis* 2009; **53**: vi-vii, S8-374.
3. Martin KJ, Gonzalez EA. Metabolic bone disease in chronic kidney disease. *J Am Soc Nephrol* 2007; **18**: 875-85.
4. Aparicio M, Cano N, Chauveau P, Azar R, Canaud B, Flory A et al. Nutritional status of haemodialysis patients: a French national cooperative study. French Study Group for Nutrition in Dialysis. *Nephrol Dial Transplant* 1999; **14**: 1679-86.
5. Young GA, Kopple JD, Lindholm B, Vonesh EF, De Vecchi A, Scalamogna A et al. Nutritional assessment of continuous ambulatory peritoneal dialysis patients: an international study. *Am J Kidney Dis* 1991; **17**: 462-71.
6. Kimmel PL, Thamer M, Richard CM, Ray NF. Psychiatric illness in patients with end-stage renal disease. *Am J Med* 1998; **105**: 214-21.
7. Abdel-Kader K, Unruh ML, Weisbord SD. Symptom burden, depression, and quality of life in chronic and end-stage kidney disease. *Clin J Am Soc Nephrol* 2009; **4**: 1057-64.
8. Howard K, Salkeld G, White S, McDonald S, Chadban S, Craig JC et al. The cost-effectiveness of increasing kidney transplantation and home-based dialysis. *Nephrology (Carlton)* 2009; **14**: 123-32.
9. McDonald SP, Russ GR. Survival of recipients of cadaveric kidney transplants compared with those receiving dialysis treatment in Australia and New Zealand, 1991-2001. *Nephrol Dial Transplant* 2002; **17**: 2212-9.
10. Wolfe RA, Ashby VB, Milford EL, Ojo AO, Ettenger RE, Agodoa LY et al. Comparison of mortality in all patients on dialysis, patients on dialysis awaiting transplantation, and recipients of a first cadaveric transplant. *N Engl J Med* 1999; **341**: 1725-30.

11. Laupacis A, Keown P, Pus N, Krueger H, Ferguson B, Wong C et al. A study of the quality of life and cost-utility of renal transplantation. *Kidney Int* 1996; **50**: 235-42.
12. Meier-Kriesche HU, Schold JD, Srinivas TR, Kaplan B. Lack of improvement in renal allograft survival despite a marked decrease in acute rejection rates over the most recent era. *Am J Transplant* 2004; **4**: 378-83.
13. Vajdic CM, McDonald SP, McCredie MR, van Leeuwen MT, Stewart JH, Law M et al. Cancer incidence before and after kidney transplantation. *JAMA* 2006; **296**: 2823-31.
14. Collins MG, Teo E, Cole SR, Chan CY, McDonald SP, Russ GR et al. Screening for colorectal cancer and advanced colorectal neoplasia in kidney transplant recipients: cross sectional prevalence and diagnostic accuracy study of faecal immunochemical testing for haemoglobin and colonoscopy. *BMJ* 2012; **345**: e4657.
15. Williams D, Haragsim L. Calcineurin nephrotoxicity. *Adv Chronic Kidney Dis* 2006; **13**: 47-55.
16. Ojo AO, Held PJ, Port FK, Wolfe RA, Leichtman AB, Young EW et al. Chronic renal failure after transplantation of a nonrenal organ. *N Engl J Med* 2003; **349**: 931-40.
17. Bishop GA, Ierino FL, Sharland AF, Hall BM, Alexander SI, Sandrin MS et al. Approaching the promise of operational tolerance in clinical transplantation. *Transplantation* 2011; **91**: 1065-74.
18. Kirk AD. Clinical tolerance 2008. *Transplantation* 2009; **87**: 953-5.
19. Billingham RE, Brent L, Medawar PB. Actively acquired tolerance of foreign cells. *Nature* 1953; **172**: 603-6.
20. Ashton-Chess J, Giral M, Brouard S, Souillou JP. Spontaneous operational tolerance after immunosuppressive drug withdrawal in clinical renal allotransplantation. *Transplantation* 2007; **84**: 1215-9.
21. Roussey-Kesler G, Giral M, Moreau A, Subra JF, Legendre C, Noel C et al. Clinical operational tolerance after kidney transplantation. *Am J Transplant* 2006; **6**: 736-46.
22. Devlin J, Doherty D, Thomson L, Wong T, Donaldson P, Portmann B et al. Defining the outcome of immunosuppression withdrawal after liver transplantation. *Hepatology* 1998; **27**: 926-33.

23. Takatsuki M, Uemoto S, Inomata Y, Egawa H, Kiuchi T, Fujita S et al. Weaning of immunosuppression in living donor liver transplant recipients. *Transplantation* 2001; **72**: 449-54.
24. Orlando G, Soker S, Wood K. Operational tolerance after liver transplantation. *J Hepatol* 2009; **50**: 1247-57.
25. Brouard S, Dupont A, Giral M, Louis S, Lair D, Braudeau C et al. Operationally tolerant and minimally immunosuppressed kidney recipients display strongly altered blood T-cell clonal regulation. *Am J Transplant* 2005; **5**: 330-40.
26. Burlingham WJ, Grailer AP, Fechner JH, Jr., Kusaka S, Trucco M, Kocova M et al. Microchimerism linked to cytotoxic T lymphocyte functional unresponsiveness (clonal anergy) in a tolerant renal transplant recipient. *Transplantation* 1995; **59**: 1147-55.
27. Christensen LL, Grunnet N, Rudiger N, Moller B, Birkeland SA. Indications of immunological tolerance in kidney transplantation. *Tissue Antigens* 1998; **51**: 637-44.
28. Fischer T, Schobel H, Barenbrock M. Specific immune tolerance during pregnancy after renal transplantation. *Eur J Obstet Gynecol Reprod Biol* 1996; **70**: 217-9.
29. Owens ML, Maxwell JG, Goodnight J, Wolcott MW. Discontinuance of immunosuppression in renal transplant patients. *Arch Surg* 1975; **110**: 1450-1.
30. Starzl TE, Murase N, Demetris AJ, Trucco M, Abu-Elmagd K, Gray EA et al. Lessons of organ-induced tolerance learned from historical clinical experience. *Transplantation* 2004; **77**: 926-9.
31. Strober S, Benike C, Krishnaswamy S, Engleman EG, Grumet FC. Clinical transplantation tolerance twelve years after prospective withdrawal of immunosuppressive drugs: studies of chimerism and anti-donor reactivity. *Transplantation* 2000; **69**: 1549-54.
32. Uehling DT, Hussey JL, Weinstein AB, Wank R, Bach FH. Cessation of immunosuppression after renal transplantation. *Surgery* 1976; **79**: 278-82.
33. VanBuskirk AM, Burlingham WJ, Jankowska-Gan E, Chin T, Kusaka S, Geissler F et al. Human allograft acceptance is associated with immune regulation. *J Clin Invest* 2000; **106**: 145-55.

34. Zoller KM, Cho SI, Cohen JJ, Harrington JT. Cessation of immunosuppressive therapy after successful transplantation: a national survey. *Kidney Int* 1980; **18**: 110-4.
35. Newell KA, Larsen CP. Tolerance assays: measuring the unknown. *Transplantation* 2006; **81**: 1503-9.
36. Calne RY. Prope tolerance--the future of organ transplantation from the laboratory to the clinic. *Int Immunopharmacol* 2005; **5**: 163-7.
37. Calne R, Friend P, Moffatt S, Bradley A, Hale G, Firth J et al. Prope tolerance, perioperative campath 1H, and low-dose cyclosporin monotherapy in renal allograft recipients. *Lancet* 1998; **351**: 1701-2.
38. Kean LS, Gangappa S, Pearson TC, Larsen CP. Transplant tolerance in non-human primates: progress, current challenges and unmet needs. *Am J Transplant* 2006; **6**: 884-93.
39. Knechtle SJ, Hamawy MM, Hu H, Fechner JH, Jr., Cho CS. Tolerance and near-tolerance strategies in monkeys and their application to human renal transplantation. *Immunol Rev* 2001; **183**: 205-13.
40. Hale DA, Dhanireddy K, Bruno D, Kirk AD. Induction of transplantation tolerance in non-human primate preclinical models. *Philos Trans R Soc Lond B Biol Sci* 2005; **360**: 1723-37.
41. Page EK, Dar WA, Knechtle SJ. Tolerogenic therapies in transplantation. *Front Immunol* 2012; **3**: 198.
42. Adams AB, Pearson TC, Larsen CP. Heterologous immunity: an overlooked barrier to tolerance. *Immunological Reviews* 2003; **196**: 147-60.
43. Adams AB, Williams MA, Jones TR, Shirasugi N, Durham MM, Kaech SM et al. Heterologous immunity provides a potent barrier to transplantation tolerance. *The Journal of Clinical Investigation* 2003; **111**: 1887-95.
44. Halloran PF. Immunosuppressive drugs for kidney transplantation. *N Engl J Med* 2004; **351**: 2715-29.
45. Vincenti F, Larsen C, Durrbach A, Wekerle T, Nashan B, Blancho G et al. Costimulation blockade with belatacept in renal transplantation. *N Engl J Med* 2005; **353**: 770-81.
46. Knechtle SJ, Burlingham WJ. Metastable tolerance in nonhuman primates and humans. *Transplantation* 2004; **77**: 936-9.

47. Kirk AD, Mannon RB, Kleiner DE, Swanson JS, Kampen RL, Cendales LK et al. Results from a human renal allograft tolerance trial evaluating T-cell depletion with alemtuzumab combined with deoxyspergualin. *Transplantation* 2005; **80**: 1051-9.
48. Barth RN, Janus CA, Lillesand CA, Radke NA, Pirsch JD, Becker BN et al. Outcomes at 3 years of a prospective pilot study of Campath-1H and sirolimus immunosuppression for renal transplantation. *Transpl Int* 2006; **19**: 885-92.
49. Knechtle SJ, Pirsch JD, H. Fechner J J, Becker BN, Friedl A, Colvin RB et al. Campath-1H induction plus rapamycin monotherapy for renal transplantation: results of a pilot study. *Am J Transplant* 2003; **3**: 722-30.
50. Kirk AD, Hale DA, Mannon RB, Kleiner DE, Hoffmann SC, Kampen RL et al. Results from a human renal allograft tolerance trial evaluating the humanized CD52-specific monoclonal antibody alemtuzumab (CAMPATH-1H). *Transplantation* 2003; **76**: 120-9.
51. Sykes M. Immune tolerance: Mechanisms and application in clinical transplantation. *Journal of Internal Medicine* 2007; **262**: 288-310.
52. Wekerle T, Sayegh MH, Ito H, Hill J, Chandraker A, Pearson DA et al. Anti-CD154 or CTLA4Ig obviates the need for thymic irradiation in a non-myeloablative conditioning regimen for the induction of mixed hematopoietic chimerism and tolerance. *Transplantation* 1999; **68**: 1348-55.
53. Kawai T, Cosimi AB, Colvin RB, Powelson J, Eason J, Kozlowski T et al. Mixed allogeneic chimerism and renal allograft tolerance in cynomolgus monkeys. *Transplantation* 1995; **59**: 256-62.
54. Kawai T, Poncelet A, Sachs DH, Mauiyyedi S, Boskovic S, Wee SL et al. Long-term outcome and alloantibody production in a non-myeloablative regimen for induction of renal allograft tolerance. *Transplantation* 1999; **68**: 1767-75.
55. Kawai T, Sogawa H, Boskovic S, Abrahamian G, Smith RN, Wee SL et al. CD154 blockade for induction of mixed chimerism and prolonged renal allograft survival in nonhuman primates. *Am J Transplant* 2004; **4**: 1391-8.
56. Kean LS, Adams AB, Strobert E, Hendrix R, Gangappa S, Jones TR et al. Induction of chimerism in rhesus macaques through stem cell transplant and costimulation blockade-based immunosuppression. *Am J Transplant* 2007; **7**: 320-35.

57. Buhler LH, Spitzer TR, Sykes M, Sachs DH, Delmonico FL, Tolkoff-Rubin N et al. Induction of kidney allograft tolerance after transient lymphohematopoietic chimerism in patients with multiple myeloma and end-stage renal disease. *Transplantation* 2002; **74**: 1405-9.
58. Fudaba Y, Spitzer TR, Shaffer J, Kawai T, Fehr T, Delmonico F et al. Myeloma responses and tolerance following combined kidney and nonmyeloablative marrow transplantation: in vivo and in vitro analyses. *Am J Transplant* 2006; **6**: 2121-33.
59. Kawai T, Cosimi AB, Spitzer TR, Tolkoff-Rubin N, Suthanthiran M, Saidman SL et al. HLA-mismatched renal transplantation without maintenance immunosuppression. *N Engl J Med* 2008; **358**: 353-61.
60. Kawai T, Sachs DH, Sykes M, Cosimi AB. HLA-mismatched renal transplantation without maintenance immunosuppression. *N Engl J Med* 2013; **368**: 1850-2.
61. Scandling JD, Busque S, Dejbakhsh-Jones S, Benike C, Millan MT, Shizuru JA et al. Tolerance and chimerism after renal and hematopoietic-cell transplantation. *N Engl J Med* 2008; **358**: 362-8.
62. Fugier-Vivier IJ, Rezzoug F, Huang Y, Graul-Layman AJ, Schanie CL, Xu H et al. Plasmacytoid precursor dendritic cells facilitate allogeneic hematopoietic stem cell engraftment. *J Exp Med* 2005; **201**: 373-83.
63. Leventhal J, Abecassis M, Miller J, Gallon L, Ravindra K, Tollerud DJ et al. Chimerism and tolerance without GVHD or engraftment syndrome in HLA-mismatched combined kidney and hematopoietic stem cell transplantation. *Sci Transl Med* 2012; **4**: 124ra28.
64. Leventhal J, Abecassis M, Miller J, Gallon L, Tollerud D, Elliott MJ et al. Tolerance induction in HLA disparate living donor kidney transplantation by donor stem cell infusion: durable chimerism predicts outcome. *Transplantation* 2013; **95**: 169-76.
65. Halloran PF, Bromberg J, Kaplan B, Vincenti F. Tolerance versus immunosuppression: a perspective. *Am J Transplant* 2008; **8**: 1365-6.
66. Steinman RM, Cohn ZA. Identification of a novel cell type in peripheral lymphoid organs of mice. I. Morphology, quantitation, tissue distribution. *J Exp Med* 1973; **137**: 1142-62.

67. Steinman RM, Cohn ZA. Identification of a novel cell type in peripheral lymphoid organs of mice. II. Functional properties in vitro. *J Exp Med* 1974; **139**: 380-97.
68. Steinman RM, Lustig DS, Cohn ZA. Identification of a novel cell type in peripheral lymphoid organs of mice. 3. Functional properties in vivo. *J Exp Med* 1974; **139**: 1431-45.
69. Steinman RM, Banchereau J. Taking dendritic cells into medicine. *Nature* 2007; **449**: 419-26.
70. Steinman RM. The dendritic cell system and its role in immunogenicity. *Annu Rev Immunol* 1991; **9**: 271-96.
71. Hart DN. Dendritic cells: unique leukocyte populations which control the primary immune response. *Blood* 1997; **90**: 3245-87.
72. Banchereau J, Steinman RM. Dendritic cells and the control of immunity. *Nature* 1998; **392**: 245-52.
73. Banchereau J, Briere F, Caux C, Davoust J, Lebecque S, Liu YJ et al. Immunobiology of dendritic cells. *Annu Rev Immunol* 2000; **18**: 767-811.
74. Lotze MT, Thomson AW, editors. Dendritic cells: Biology and clinical applications. 2 ed. London, San Diego: *Academic Press*; 2001.
75. Shortman K, Naik SH. Steady-state and inflammatory dendritic-cell development. *Nat Rev Immunol* 2007; **7**: 19-30.
76. Steinman RM. Dendritic cells: Understanding immunogenicity. *Eur J Immunol* 2007; **37**: S53-60.
77. Wu L, Liu YJ. Development of dendritic-cell lineages. *Immunity* 2007; **26**: 741-50.
78. Coquerelle C, Moser M. DC subsets in positive and negative regulation of immunity. *Immunol Rev* 2010; **234**: 317-34.
79. Liu K, Nussenzweig MC. Origin and development of dendritic cells. *Immunol Rev* 2010; **234**: 45-54.
80. Steinman RM, Idoyaga J. Features of the dendritic cell lineage. *Immunol Rev* 2010; **234**: 5-17.
81. Ziegler-Heitbrock L, Ancuta P, Crowe S, Dalod M, Grau V, Hart DN et al. Nomenclature of monocytes and dendritic cells in blood. *Blood* 2010; **116**: e74-80.

82. Cunningham AL, Harman A, Kim M, Nasr N, Lai J. Immunobiology of dendritic cells and the influence of HIV infection. *Adv Exp Med Biol* 2013; **762**: 1-44.
83. Belz GT, Nutt SL. Transcriptional programming of the dendritic cell network. *Nat Rev Immunol* 2012; **12**: 101-13.
84. Collin M, McGovern N, Haniffa M. Human dendritic cell subsets. *Immunology* 2013.
85. Coates PT, Barratt-Boyes SM, Zhang L, Donnenberg VS, O'Connell PJ, Logar AJ et al. Dendritic cell subsets in blood and lymphoid tissue of rhesus monkeys and their mobilization with Flt3 ligand. *Blood* 2003; **102**: 2513-21.
86. Shortman K, Liu YJ. Mouse and human dendritic cell subtypes. *Nat Rev Immunol* 2002; **2**: 151-61.
87. Caux C, Dezutter-Dambuyant C, Schmitt D, Banchereau J. GM-CSF and TNF-alpha cooperate in the generation of dendritic Langerhans cells. *Nature* 1992; **360**: 258-61.
88. Caux C, Vanbervliet B, Massacrier C, Dezutter-Dambuyant C, de Saint-Vis B, Jacquet C et al. CD34+ hematopoietic progenitors from human cord blood differentiate along two independent dendritic cell pathways in response to GM-CSF+TNF alpha. *J Exp Med* 1996; **184**: 695-706.
89. Inaba K, Inaba M, Deguchi M, Hagi K, Yasumizu R, Ikehara S et al. Granulocytes, macrophages, and dendritic cells arise from a common major histocompatibility complex class II-negative progenitor in mouse bone marrow. *Proc Natl Acad Sci U S A* 1993; **90**: 3038-42.
90. Reid CD, Stackpoole A, Meager A, Tikerpae J. Interactions of tumor necrosis factor with granulocyte-macrophage colony-stimulating factor and other cytokines in the regulation of dendritic cell growth in vitro from early bipotent CD34+ progenitors in human bone marrow. *J Immunol* 1992; **149**: 2681-8.
91. Szabolcs P, Avigan D, Gezelter S, Ciocon DH, Moore MA, Steinman RM et al. Dendritic cells and macrophages can mature independently from a human bone marrow-derived, post-colony-forming unit intermediate. *Blood* 1996; **87**: 4520-30.
92. Romani N, Gruner S, Brang D, Kampgen E, Lenz A, Trockenbacher B et al. Proliferating dendritic cell progenitors in human blood. *J Exp Med* 1994; **180**: 83-93.

93. Sallusto F, Lanzavecchia A. Efficient presentation of soluble antigen by cultured human dendritic cells is maintained by granulocyte/macrophage colony-stimulating factor plus interleukin 4 and downregulated by tumor necrosis factor alpha. *J Exp Med* 1994; **179**: 1109-18.
94. Zhou LJ, Tedder TF. CD14+ blood monocytes can differentiate into functionally mature CD83+ dendritic cells. *Proc Natl Acad Sci U S A* 1996; **93**: 2588-92.
95. Grouard G, Risoan MC, Filgueira L, Durand I, Banchereau J, Liu YJ. The enigmatic plasmacytoid T cells develop into dendritic cells with interleukin (IL)-3 and CD40-ligand. *J Exp Med* 1997; **185**: 1101-11.
96. Risoan MC, Soumelis V, Kadowaki N, Grouard G, Briere F, de Waal Malefyt R et al. Reciprocal control of T helper cell and dendritic cell differentiation. *Science* 1999; **283**: 1183-6.
97. Vremec D, Zorbas M, Scollay R, Saunders DJ, Ardavin CF, Wu L et al. The surface phenotype of dendritic cells purified from mouse thymus and spleen: investigation of the CD8 expression by a subpopulation of dendritic cells. *J Exp Med* 1992; **176**: 47-58.
98. Wu L, Li CL, Shortman K. Thymic dendritic cell precursors: relationship to the T lymphocyte lineage and phenotype of the dendritic cell progeny. *J Exp Med* 1996; **184**: 903-11.
99. Wu L, Vremec D, Ardavin C, Winkel K, Suss G, Georgiou H et al. Mouse thymus dendritic cells: kinetics of development and changes in surface markers during maturation. *Eur J Immunol* 1995; **25**: 418-25.
100. Manz MG, Traver D, Akashi K, Merad M, Miyamoto T, Engleman EG et al. Dendritic cell development from common myeloid progenitors. *Ann N Y Acad Sci* 2001; **938**: 167-73; discussion 73-4.
101. Manz MG, Traver D, Miyamoto T, Weissman IL, Akashi K. Dendritic cell potentials of early lymphoid and myeloid progenitors. *Blood* 2001; **97**: 3333-41.
102. Wu L, D'Amico A, Hochrein H, O'Keeffe M, Shortman K, Lucas K. Development of thymic and splenic dendritic cell populations from different hemopoietic precursors. *Blood* 2001; **98**: 3376-82.
103. Naik SH, Sathe P, Park HY, Metcalf D, Proietto AI, Dakic A et al. Development of plasmacytoid and conventional dendritic cell subtypes from single precursor cells derived in vitro and in vivo. *Nat Immunol* 2007; **8**: 1217-26.

104. D'Amico A, Wu L. The early progenitors of mouse dendritic cells and plasmacytoid predendritic cells are within the bone marrow hemopoietic precursors expressing Flt3. *J Exp Med* 2003; **198**: 293-303.
105. Onai N, Obata-Onai A, Schmid MA, Ohteki T, Jarrossay D, Manz MG. Identification of clonogenic common Flt3+M-CSFR+ plasmacytoid and conventional dendritic cell progenitors in mouse bone marrow. *Nat Immunol* 2007; **8**: 1207-16.
106. Serbina NV, Salazar-Mather TP, Biron CA, Kuziel WA, Pamer EG. TNF/iNOS-producing dendritic cells mediate innate immune defense against bacterial infection. *Immunity* 2003; **19**: 59-70.
107. Varol C, Landsman L, Fogg DK, Greenshtein L, Gildor B, Margalit R et al. Monocytes give rise to mucosal, but not splenic, conventional dendritic cells. *J Exp Med* 2007; **204**: 171-80.
108. Cheong C, Matos I, Choi JH, Dandamudi DB, Shrestha E, Longhi MP et al. Microbial stimulation fully differentiates monocytes to DC-SIGN/CD209(+) dendritic cells for immune T cell areas. *Cell* 2010; **143**: 416-29.
109. Liu K, Victora GD, Schwickert TA, Guermonprez P, Meredith MM, Yao K et al. In vivo analysis of dendritic cell development and homeostasis. *Science* 2009; **324**: 392-7.
110. Diao J, Mikhailova A, Tang M, Gu H, Zhao J, Catral MS. Immunostimulatory conventional dendritic cells evolve into regulatory macrophage-like cells. *Blood* 2012; **119**: 4919-27.
111. McKenna HJ, Stocking KL, Miller RE, Brasel K, De Smedt T, Maraskovsky E et al. Mice lacking flt3 ligand have deficient hematopoiesis affecting hematopoietic progenitor cells, dendritic cells, and natural killer cells. *Blood* 2000; **95**: 3489-97.
112. Maraskovsky E, Brasel K, Teepe M, Roux ER, Lyman SD, Shortman K et al. Dramatic increase in the numbers of functionally mature dendritic cells in Flt3 ligand-treated mice: multiple dendritic cell subpopulations identified. *J Exp Med* 1996; **184**: 1953-62.
113. Maraskovsky E, Daro E, Roux E, Teepe M, Maliszewski CR, Hoek J et al. In vivo generation of human dendritic cell subsets by Flt3 ligand. *Blood* 2000; **96**: 878-84.

114. Caux C, Massacrier C, Dubois B, Valladeau J, Dezutter-Dambuyant C, Durand I et al. Respective involvement of TGF-beta and IL-4 in the development of Langerhans cells and non-Langerhans dendritic cells from CD34+ progenitors. *J Leukoc Biol* 1999; **66**: 781-91.
115. Arpinati M, Green CL, Heimfeld S, Heuser JE, Anasetti C. Granulocyte-colony stimulating factor mobilizes T helper 2-inducing dendritic cells. *Blood* 2000; **95**: 2484-90.
116. Pulendran B, Banchereau J, Burkeholder S, Kraus E, Guinet E, Chalouni C et al. Flt3-ligand and granulocyte colony-stimulating factor mobilize distinct human dendritic cell subsets in vivo. *J Immunol* 2000; **165**: 566-72.
117. Ammon C, Mondal K, Andreesen R, Krause SW. Differential expression of the transcription factor NF-kappaB during human mononuclear phagocyte differentiation to macrophages and dendritic cells. *Biochem Biophys Res Commun* 2000; **268**: 99-105.
118. Clark GJ, Gunningham S, Troy A, Vuckovic S, Hart DN. Expression of the RelB transcription factor correlates with the activation of human dendritic cells. *Immunology* 1999; **98**: 189-96.
119. Neumann M, Fries H, Scheicher C, Keikavoussi P, Kolb-Maurer A, Brocker E et al. Differential expression of Rel/NF-kappaB and octamer factors is a hallmark of the generation and maturation of dendritic cells. *Blood* 2000; **95**: 277-85.
120. Pettit AR, Quinn C, MacDonald KP, Cavanagh LL, Thomas G, Townsend W et al. Nuclear localization of RelB is associated with effective antigen-presenting cell function. *J Immunol* 1997; **159**: 3681-91.
121. Crozat K, Guiton R, Guilliams M, Henri S, Baranek T, Schwartz-Cornil I et al. Comparative genomics as a tool to reveal functional equivalences between human and mouse dendritic cell subsets. *Immunol Rev* 2010; **234**: 177-98.
122. Guilliams M, Henri S, Tamoutounour S, Ardouin L, Schwartz-Cornil I, Dalod M et al. From skin dendritic cells to a simplified classification of human and mouse dendritic cell subsets. *Eur J Immunol* 2010; **40**: 2089-94.
123. Haniffa M, Shin A, Bigley V, McGovern N, Teo P, See P et al. Human tissues contain CD141hi cross-presenting dendritic cells with functional homology to mouse CD103+ nonlymphoid dendritic cells. *Immunity* 2012; **37**: 60-73.

124. Harman AN, Bye CR, Nasr N, Sandgren KJ, Kim M, Mercier SK et al. Identification of lineage relationships and novel markers of blood and skin human dendritic cells. *J Immunol* 2013; **190**: 66-79.
125. Lindstedt M, Lundberg K, Borrebaeck CA. Gene family clustering identifies functionally associated subsets of human in vivo blood and tonsillar dendritic cells. *J Immunol* 2005; **175**: 4839-46.
126. Lundberg K, Albrekt AS, Nelissen I, Santegoets S, de Gruijl TD, Gibbs S et al. Transcriptional profiling of human dendritic cell populations and models--unique profiles of in vitro dendritic cells and implications on functionality and applicability. *PLoS One* 2013; **8**: e52875.
127. Robbins SH, Walzer T, Dembele D, Thibault C, Defays A, Bessou G et al. Novel insights into the relationships between dendritic cell subsets in human and mouse revealed by genome-wide expression profiling. *Genome Biol* 2008; **9**: R17.
128. Segura E, Touzot M, Bohineust A, Cappuccio A, Chiochia G, Hosmalin A et al. Human inflammatory dendritic cells induce Th17 cell differentiation. *Immunity* 2013; **38**: 336-48.
129. Gautier EL, Shay T, Miller J, Greter M, Jakubzick C, Ivanov S et al. Gene-expression profiles and transcriptional regulatory pathways that underlie the identity and diversity of mouse tissue macrophages. *Nat Immunol* 2012; **13**: 1118-28.
130. Miller JC, Brown BD, Shay T, Gautier EL, Jojic V, Cohain A et al. Deciphering the transcriptional network of the dendritic cell lineage. *Nat Immunol* 2012; **13**: 888-99.
131. Larsen CP, Steinman RM, Witmer-Pack M, Hankins DF, Morris PJ, Austyn JM. Migration and maturation of Langerhans cells in skin transplants and explants. *J Exp Med* 1990; **172**: 1483-93.
132. John R, Nelson PJ. Dendritic cells in the kidney. *J Am Soc Nephrol* 2007; **18**: 2628-35.
133. Rogers NM, Matthews TJ, Kausman JY, Kitching RA, Coates PT. Review article: Kidney dendritic cells: their role in homeostasis, inflammation and transplantation. *Nephrology (Carlton)* 2009; **14**: 625-35.
134. Lambrecht BN, Hammad H. Biology of lung dendritic cells at the origin of asthma. *Immunity* 2009; **31**: 412-24.

135. Thomson AW, Drakes ML, Zahorchak AF, O'Connell PJ, Steptoe RJ, Qian S et al. Hepatic dendritic cells: immunobiology and role in liver transplantation. *J Leukoc Biol* 1999; **66**: 322-30.
136. Thomson AW, Lu L. Are dendritic cells the key to liver transplant tolerance? *Immunol Today* 1999; **20**: 27-32.
137. Bedoui S, Whitney PG, Waithman J, Eidsmo L, Wakim L, Caminschi I et al. Cross-presentation of viral and self antigens by skin-derived CD103⁺ dendritic cells. *Nat Immunol* 2009; **10**: 488-95.
138. Belz GT, Smith CM, Kleinert L, Reading P, Brooks A, Shortman K et al. Distinct migrating and nonmigrating dendritic cell populations are involved in MHC class I-restricted antigen presentation after lung infection with virus. *Proc Natl Acad Sci U S A* 2004; **101**: 8670-5.
139. Villadangos JA, Heath WR. Life cycle, migration and antigen presenting functions of spleen and lymph node dendritic cells: limitations of the Langerhans cells paradigm. *Semin Immunol* 2005; **17**: 262-72.
140. Naik SH, Metcalf D, van Nieuwenhuijze A, Wicks I, Wu L, O'Keeffe M et al. Intrasplenic steady-state dendritic cell precursors that are distinct from monocytes. *Nat Immunol* 2006; **7**: 663-71.
141. den Haan JM, Lehar SM, Bevan MJ. CD8(+) but not CD8(-) dendritic cells cross-prime cytotoxic T cells in vivo. *J Exp Med* 2000; **192**: 1685-96.
142. Smith CM, Belz GT, Wilson NS, Villadangos JA, Shortman K, Carbone FR et al. Cutting edge: conventional CD8 alpha⁺ dendritic cells are preferentially involved in CTL priming after footpad infection with herpes simplex virus-1. *J Immunol* 2003; **170**: 4437-40.
143. Pooley JL, Heath WR, Shortman K. Cutting edge: intravenous soluble antigen is presented to CD4 T cells by CD8⁻ dendritic cells, but cross-presented to CD8 T cells by CD8⁺ dendritic cells. *J Immunol* 2001; **166**: 5327-30.
144. Schuler G, Steinman RM. Murine epidermal Langerhans cells mature into potent immunostimulatory dendritic cells in vitro. *J Exp Med* 1985; **161**: 526-46.
145. Merad M, Manz MG, Karsunky H, Wagers A, Peters W, Charo I et al. Langerhans cells renew in the skin throughout life under steady-state conditions. *Nat Immunol* 2002; **3**: 1135-41.
146. Douillard P, Stoitzner P, Tripp CH, Clair-Moninot V, Ait-Yahia S, McLellan AD et al. Mouse lymphoid tissue contains distinct subsets of langerin/CD207

- dendritic cells, only one of which represents epidermal-derived Langerhans cells. *J Invest Dermatol* 2005; **125**: 983-94.
147. Chorro L, Sarde A, Li M, Woollard KJ, Chambon P, Malissen B et al. Langerhans cell (LC) proliferation mediates neonatal development, homeostasis, and inflammation-associated expansion of the epidermal LC network. *J Exp Med* 2009; **206**: 3089-100.
148. Cella M, Jarrossay D, Facchetti F, Alebardi O, Nakajima H, Lanzavecchia A et al. Plasmacytoid monocytes migrate to inflamed lymph nodes and produce large amounts of type I interferon. *Nat Med* 1999; **5**: 919-23.
149. Siegal FP, Kadowaki N, Shodell M, Fitzgerald-Bocarsly PA, Shah K, Ho S et al. The nature of the principal type 1 interferon-producing cells in human blood. *Science* 1999; **284**: 1835-7.
150. Liu YJ. IPC: professional type 1 interferon-producing cells and plasmacytoid dendritic cell precursors. *Annu Rev Immunol* 2005; **23**: 275-306.
151. Yoneyama H, Matsuno K, Zhang Y, Nishiwaki T, Kitabatake M, Ueha S et al. Evidence for recruitment of plasmacytoid dendritic cell precursors to inflamed lymph nodes through high endothelial venules. *Int Immunol* 2004; **16**: 915-28.
152. Mosca PJ, Hobeika AC, Colling K, Clay TM, Thomas EK, Caron D et al. Multiple signals are required for maturation of human dendritic cells mobilized in vivo with Flt3 ligand. *J Leukoc Biol* 2002; **72**: 546-53.
153. Ochando JC, Homma C, Yang Y, Hidalgo A, Garin A, Tacke F et al. Alloantigen-presenting plasmacytoid dendritic cells mediate tolerance to vascularized grafts. *Nat Immunol* 2006; **7**: 652-62.
154. Kool M, Soullie T, van Nimwegen M, Willart MA, Muskens F, Jung S et al. Alum adjuvant boosts adaptive immunity by inducing uric acid and activating inflammatory dendritic cells. *J Exp Med* 2008; **205**: 869-82.
155. Leon B, Lopez-Bravo M, Ardavin C. Monocyte-derived dendritic cells formed at the infection site control the induction of protective T helper 1 responses against *Leishmania*. *Immunity* 2007; **26**: 519-31.
156. Dzionek A, Fuchs A, Schmidt P, Cremer S, Zysk M, Miltenyi S et al. BDCA-2, BDCA-3, and BDCA-4: three markers for distinct subsets of dendritic cells in human peripheral blood. *J Immunol* 2000; **165**: 6037-46.

157. MacDonald KP, Munster DJ, Clark GJ, Dzionek A, Schmitz J, Hart DN. Characterization of human blood dendritic cell subsets. *Blood* 2002; **100**: 4512-20.
158. Mittag D, Proietto AI, Loudovaris T, Mannering SI, Vremec D, Shortman K et al. Human dendritic cell subsets from spleen and blood are similar in phenotype and function but modified by donor health status. *J Immunol* 2011; **186**: 6207-17.
159. Bachem A, Guttler S, Hartung E, Ebstein F, Schaefer M, Tannert A et al. Superior antigen cross-presentation and XCR1 expression define human CD11c+CD141+ cells as homologues of mouse CD8+ dendritic cells. *J Exp Med* 2010; **207**: 1273-81.
160. Angel CE, George E, Brooks AE, Ostrovsky LL, Brown TL, Dunbar PR. Cutting edge: CD1a+ antigen-presenting cells in human dermis respond rapidly to CCR7 ligands. *J Immunol* 2006; **176**: 5730-4.
161. Lenz A, Heine M, Schuler G, Romani N. Human and murine dermis contain dendritic cells. Isolation by means of a novel method and phenotypical and functional characterization. *J Clin Invest* 1993; **92**: 2587-96.
162. Nestle FO, Zheng XG, Thompson CB, Turka LA, Nickoloff BJ. Characterization of dermal dendritic cells obtained from normal human skin reveals phenotypic and functionally distinctive subsets. *J Immunol* 1993; **151**: 6535-45.
163. Angel CE, Chen CJ, Horlacher OC, Winkler S, John T, Browning J et al. Distinctive localization of antigen-presenting cells in human lymph nodes. *Blood* 2009; **113**: 1257-67.
164. Takahashi K, Asagoe K, Zaishun J, Yanai H, Yoshino T, Hayashi K et al. Heterogeneity of dendritic cells in human superficial lymph node: in vitro maturation of immature dendritic cells into mature or activated interdigitating reticulum cells. *Am J Pathol* 1998; **153**: 745-55.
165. Segura E, Valladeau-Guilemond J, Donnadieu MH, Sastre-Garau X, Soumelis V, Amigorena S. Characterization of resident and migratory dendritic cells in human lymph nodes. *J Exp Med* 2012; **209**: 653-60.
166. Summers KL, Hock BD, McKenzie JL, Hart DN. Phenotypic characterization of five dendritic cell subsets in human tonsils. *Am J Pathol* 2001; **159**: 285-95.

167. Jongbloed SL, Kassianos AJ, McDonald KJ, Clark GJ, Ju X, Angel CE et al. Human CD141+ (BDCA-3)+ dendritic cells (DCs) represent a unique myeloid DC subset that cross-presents necrotic cell antigens. *J Exp Med* 2010; **207**: 1247-60.
168. Poulin LF, Salio M, Griessinger E, Anjos-Afonso F, Craciun L, Chen JL et al. Characterization of human DNGR-1+ BDCA3+ leukocytes as putative equivalents of mouse CD8alpha+ dendritic cells. *J Exp Med* 2010; **207**: 1261-71.
169. Dorner BG, Dorner MB, Zhou X, Opitz C, Mora A, Guttler S et al. Selective expression of the chemokine receptor XCR1 on cross-presenting dendritic cells determines cooperation with CD8+ T cells. *Immunity* 2009; **31**: 823-33.
170. Poulin LF, Reyat Y, Uronen-Hansson H, Schraml BU, Sancho D, Murphy KM et al. DNGR-1 is a specific and universal marker of mouse and human Batf3-dependent dendritic cells in lymphoid and nonlymphoid tissues. *Blood* 2012; **119**: 6052-62.
171. Reizis B, Bunin A, Ghosh HS, Lewis KL, Sisirak V. Plasmacytoid dendritic cells: recent progress and open questions. *Annu Rev Immunol* 2011; **29**: 163-83.
172. Rogers NM, Isenberg JS, Thomson AW. Plasmacytoid dendritic cells: no longer an enigma and now key to transplant tolerance? *Am J Transplant* 2013; **13**: 1125-33.
173. Cox K, North M, Burke M, Singhal H, Renton S, Aqel N et al. Plasmacytoid dendritic cells (PDC) are the major DC subset innately producing cytokines in human lymph nodes. *J Leukoc Biol* 2005; **78**: 1142-52.
174. Klechevsky E, Morita R, Liu M, Cao Y, Coquery S, Thompson-Snipes L et al. Functional specializations of human epidermal Langerhans cells and CD14+ dermal dendritic cells. *Immunity* 2008; **29**: 497-510.
175. Haniffa M, Ginhoux F, Wang XN, Bigley V, Abel M, Dimmick I et al. Differential rates of replacement of human dermal dendritic cells and macrophages during hematopoietic stem cell transplantation. *J Exp Med* 2009; **206**: 371-85.
176. Ochoa MT, Loncaric A, Krutzik SR, Becker TC, Modlin RL. "Dermal dendritic cells" comprise two distinct populations: CD1+ dendritic cells and CD209+ macrophages. *J Invest Dermatol* 2008; **128**: 2225-31.

177. Matthews K, Chung NP, Klasse PJ, Moore JP, Sanders RW. Potent induction of antibody-secreting B cells by human dermal-derived CD14⁺ dendritic cells triggered by dual TLR ligation. *J Immunol* 2012; **189**: 5729-44.
178. Langlet C, Tamoutounour S, Henri S, Luche H, Ardouin L, Gregoire C et al. CD64 expression distinguishes monocyte-derived and conventional dendritic cells and reveals their distinct role during intramuscular immunization. *J Immunol* 2012; **188**: 1751-60.
179. Plantinga M, Guilliams M, Vanheerswynghels M, Deswarte K, Branco-Madeira F, Toussaint W et al. Conventional and monocyte-derived CD11b(+) dendritic cells initiate and maintain T helper 2 cell-mediated immunity to house dust mite allergen. *Immunity* 2013; **38**: 322-35.
180. Romani N, Lenz A, Glassel H, Stossel H, Stanzl U, Majdic O et al. Cultured human Langerhans cells resemble lymphoid dendritic cells in phenotype and function. *J Invest Dermatol* 1989; **93**: 600-9.
181. Hunger RE, Sieling PA, Ochoa MT, Sugaya M, Burdick AE, Rea TH et al. Langerhans cells utilize CD1a and langerin to efficiently present nonpeptide antigens to T cells. *J Clin Invest* 2004; **113**: 701-8.
182. Iwasaki A. Mucosal dendritic cells. *Annu Rev Immunol* 2007; **25**: 381-418.
183. Valladeau J, Dezutter-Dambuyant C, Saeland S. Langerin/CD207 sheds light on formation of birbeck granules and their possible function in Langerhans cells. *Immunol Res* 2003; **28**: 93-107.
184. Romani N, Clausen BE, Stoitzner P. Langerhans cells and more: langerin-expressing dendritic cell subsets in the skin. *Immunol Rev* 2010; **234**: 120-41.
185. Valladeau J, Ravel O, Dezutter-Dambuyant C, Moore K, Kleijmeer M, Liu Y et al. Langerin, a novel C-type lectin specific to Langerhans cells, is an endocytic receptor that induces the formation of Birbeck granules. *Immunity* 2000; **12**: 71-81.
186. Wollenberg A, Mommaas M, Oppel T, Schottdorf EM, Gunther S, Moderer M. Expression and function of the mannose receptor CD206 on epidermal dendritic cells in inflammatory skin diseases. *J Invest Dermatol* 2002; **118**: 327-34.
187. Hansel A, Gunther C, Ingwersen J, Starke J, Schmitz M, Bachmann M et al. Human slan (6-sulfo LacNAc) dendritic cells are inflammatory dermal dendritic cells in psoriasis and drive strong TH17/TH1 T-cell responses. *J Allergy Clin Immunol* 2011; **127**: 787-94 e1-9.

188. Cros J, Cagnard N, Woollard K, Patey N, Zhang SY, Senechal B et al. Human CD14dim monocytes patrol and sense nucleic acids and viruses via TLR7 and TLR8 receptors. *Immunity* 2010; **33**: 375-86.
189. Buzzeo MP, Yang J, Casella G, Reddy V. Hematopoietic stem cell mobilization with G-CSF induces innate inflammation yet suppresses adaptive immune gene expression as revealed by microarray analysis. *Exp Hematol* 2007; **35**: 1456-65.
190. Sunami K, Teshima T, Nawa Y, Hiramatsu Y, Maeda Y, Takenaka K et al. Administration of granulocyte colony-stimulating factor induces hyporesponsiveness to lipopolysaccharide and impairs antigen-presenting function of peripheral blood monocytes. *Exp Hematol* 2001; **29**: 1117-24.
191. Ueda Y, Itoh T, Fuji N, Harada S, Fujiki H, Shimizu K et al. Successful induction of clinically competent dendritic cells from granulocyte colony-stimulating factor-mobilized monocytes for cancer vaccine therapy. *Cancer Immunol Immunother* 2007; **56**: 381-9.
192. Jeras M, Bergant M, Repnik U. In vitro preparation and functional assessment of human monocyte-derived dendritic cells - Potential antigen-specific modulators of in vivo immune responses. *Transplant Immunology* 2005; **14**: 231-44.
193. Baribaud F, Pohlmann S, Leslie G, Mortari F, Doms RW. Quantitative expression and virus transmission analysis of DC-SIGN on monocyte-derived dendritic cells. *J Virol* 2002; **76**: 9135-42.
194. Kiertscher SM, Roth MD. Human CD14+ leukocytes acquire the phenotype and function of antigen-presenting dendritic cells when cultured in GM-CSF and IL-4. *J Leukoc Biol* 1996; **59**: 208-18.
195. Romani N, Reider D, Heuer M, Ebner S, Kampgen E, Eibl B et al. Generation of mature dendritic cells from human blood. An improved method with special regard to clinical applicability. *J Immunol Methods* 1996; **196**: 137-51.
196. Arrighi JF, Hauser C, Chapuis B, Zubler RH, Kindler V. Long-term culture of human CD34(+) progenitors with FLT3-ligand, thrombopoietin, and stem cell factor induces extensive amplification of a CD34(-)CD14(-) and a CD34(-)CD14(+) dendritic cell precursor. *Blood* 1999; **93**: 2244-52.
197. Paczesny S, Li YP, Li N, Latger-Cannard V, Marchal L, Ou-Yang JP et al. Efficient generation of CD34+ progenitor-derived dendritic cells from G-CSF-mobilized peripheral mononuclear cells does not require hematopoietic stem cell enrichment. *J Leukoc Biol* 2007; **81**: 957-67.

198. Chen W, Antonenko S, Sederstrom JM, Liang X, Chan AS, Kanzler H et al. Thrombopoietin cooperates with FLT3-ligand in the generation of plasmacytoid dendritic cell precursors from human hematopoietic progenitors. *Blood* 2004; **103**: 2547-53.
199. Geijtenbeek TB, Gringhuis SI. Signalling through C-type lectin receptors: shaping immune responses. *Nat Rev Immunol* 2009; **9**: 465-79.
200. Ebner S, Ehammer Z, Holzmann S, Schwingshackl P, Forstner M, Stoitzner P et al. Expression of C-type lectin receptors by subsets of dendritic cells in human skin. *Int Immunol* 2004; **16**: 877-87.
201. Figdor CG, van Kooyk Y, Adema GJ. C-type lectin receptors on dendritic cells and Langerhans cells. *Nat Rev Immunol* 2002; **2**: 77-84.
202. Valladeau J, Duvert-Frances V, Pin JJ, Dezutter-Dambuyant C, Vincent C, Massacrier C et al. The monoclonal antibody DCGM4 recognizes Langerin, a protein specific of Langerhans cells, and is rapidly internalized from the cell surface. *Eur J Immunol* 1999; **29**: 2695-704.
203. Flacher V, Bouschbacher M, Verronese E, Massacrier C, Sisirak V, Berthier-Vergnes O et al. Human Langerhans cells express a specific TLR profile and differentially respond to viruses and Gram-positive bacteria. *J Immunol* 2006; **177**: 7959-67.
204. Ito T, Amakawa R, Kaisho T, Hemmi H, Tajima K, Uehira K et al. Interferon-alpha and interleukin-12 are induced differentially by Toll-like receptor 7 ligands in human blood dendritic cell subsets. *J Exp Med* 2002; **195**: 1507-12.
205. Jarrossay D, Napolitani G, Colonna M, Sallusto F, Lanzavecchia A. Specialization and complementarity in microbial molecule recognition by human myeloid and plasmacytoid dendritic cells. *Eur J Immunol* 2001; **31**: 3388-93.
206. Kadowaki N, Ho S, Antonenko S, Malefyt RW, Kastelein RA, Bazan F et al. Subsets of human dendritic cell precursors express different toll-like receptors and respond to different microbial antigens. *J Exp Med* 2001; **194**: 863-9.
207. Krug A, Towarowski A, Britsch S, Rothenfusser S, Hornung V, Bals R et al. Toll-like receptor expression reveals CpG DNA as a unique microbial stimulus for plasmacytoid dendritic cells which synergizes with CD40 ligand to induce high amounts of IL-12. *Eur J Immunol* 2001; **31**: 3026-37.

208. van Kooyk Y, Rabinovich GA. Protein-glycan interactions in the control of innate and adaptive immune responses. *Nat Immunol* 2008; **9**: 593-601.
209. Wintergerst E, Manz-Keinke H, Plattner H, Schlepper-Schafer J. The interaction of a lung surfactant protein (SP-A) with macrophages is mannose dependent. *Eur J Cell Biol* 1989; **50**: 291-8.
210. Sallusto F, Cella M, Danieli C, Lanzavecchia A. Dendritic cells use macropinocytosis and the mannose receptor to concentrate macromolecules in the major histocompatibility complex class II compartment: downregulation by cytokines and bacterial products. *J Exp Med* 1995; **182**: 389-400.
211. Stahl PD, Ezekowitz RA. The mannose receptor is a pattern recognition receptor involved in host defense. *Curr Opin Immunol* 1998; **10**: 50-5.
212. Lahoud MH, Ahmet F, Zhang JG, Meuter S, Policheni AN, Kitsoulis S et al. DEC-205 is a cell surface receptor for CpG oligonucleotides. *Proc Natl Acad Sci U S A* 2012; **109**: 16270-5.
213. Mahnke K, Guo M, Lee S, Sepulveda H, Swain SL, Nussenzweig M et al. The dendritic cell receptor for endocytosis, DEC-205, can recycle and enhance antigen presentation via major histocompatibility complex class II-positive lysosomal compartments. *J Cell Biol* 2000; **151**: 673-84.
214. Inaba K, Swiggard WJ, Inaba M, Meltzer J, Mirza A, Sasagawa T et al. Tissue distribution of the DEC-205 protein that is detected by the monoclonal antibody NLDC-145. I. Expression on dendritic cells and other subsets of mouse leukocytes. *Cell Immunol* 1995; **163**: 148-56.
215. Jiang W, Swiggard WJ, Heufler C, Peng M, Mirza A, Steinman RM et al. The receptor DEC-205 expressed by dendritic cells and thymic epithelial cells is involved in antigen processing. *Nature* 1995; **375**: 151-5.
216. Bonifaz L, Bonnyay D, Mahnke K, Rivera M, Nussenzweig MC, Steinman RM. Efficient targeting of protein antigen to the dendritic cell receptor DEC-205 in the steady state leads to antigen presentation on major histocompatibility complex class I products and peripheral CD8⁺ T cell tolerance. *J Exp Med* 2002; **196**: 1627-38.
217. Geijtenbeek TB, Kwon DS, Torensma R, van Vliet SJ, van Duijnhoven GC, Middel J et al. DC-SIGN, a dendritic cell-specific HIV-1-binding protein that enhances trans-infection of T cells. *Cell* 2000; **100**: 587-97.

218. Geijtenbeek TB, Torensma R, van Vliet SJ, van Duijnhoven GC, Adema GJ, van Kooyk Y et al. Identification of DC-SIGN, a novel dendritic cell-specific ICAM-3 receptor that supports primary immune responses. *Cell* 2000; **100**: 575-85.
219. Bernhard OK, Lai J, Wilkinson J, Sheil MM, Cunningham AL. Proteomic analysis of DC-SIGN on dendritic cells detects tetramers required for ligand binding but no association with CD4. *J Biol Chem* 2004; **279**: 51828-35.
220. Svajger U, Anderluh M, Jeras M, Obermajer N. C-type lectin DC-SIGN: an adhesion, signalling and antigen-uptake molecule that guides dendritic cells in immunity. *Cell Signal* 2010; **22**: 1397-405.
221. Gallegos AM, Bevan MJ. Central tolerance: good but imperfect. *Immunol Rev* 2006; **209**: 290-6.
222. Nossal GJ. Negative selection of lymphocytes. *Cell* 1994; **76**: 229-39.
223. Bonasio R, Scimone ML, Schaerli P, Grabie N, Lichtman AH, von Andrian UH. Clonal deletion of thymocytes by circulating dendritic cells homing to the thymus. *Nat Immunol* 2006; **7**: 1092-100.
224. Proietto AI, van Dommelen S, Zhou P, Rizzitelli A, D'Amico A, Steptoe RJ et al. Dendritic cells in the thymus contribute to T-regulatory cell induction. *Proc Natl Acad Sci U S A* 2008; **105**: 19869-74.
225. Watanabe N, Wang YH, Lee HK, Ito T, Cao W, Liu YJ. Hassall's corpuscles instruct dendritic cells to induce CD4⁺CD25⁺ regulatory T cells in human thymus. *Nature* 2005; **436**: 1181-5.
226. Martin-Gayo E, Sierra-Filardi E, Corbi AL, Toribio ML. Plasmacytoid dendritic cells resident in human thymus drive natural Treg cell development. *Blood* 2010; **115**: 5366-75.
227. Ohnmacht C, Pullner A, King SB, Drexler I, Meier S, Brocker T et al. Constitutive ablation of dendritic cells breaks self-tolerance of CD4 T cells and results in spontaneous fatal autoimmunity. *J Exp Med* 2009; **206**: 549-59.
228. Guermonprez P, Valladeau J, Zitvogel L, Thery C, Amigorena S. Antigen presentation and T cell stimulation by dendritic cells. *Annu Rev Immunol* 2002; **20**: 621-67.
229. Morelli AE, Thomson AW. Tolerogenic dendritic cells and the quest for transplant tolerance. *Nature Reviews Immunology* 2007; **7**: 610-21.

230. Steinman RM, Hawiger D, Nussenzweig MC. Tolerogenic dendritic cells. *Annu Rev Immunol* 2003; **21**: 685-711.
231. Tanaka K, Albin MJ, Yuan X, Yamaura K, Habicht A, Murayama T et al. PDL1 is required for peripheral transplantation tolerance and protection from chronic allograft rejection. *J Immunol* 2007; **179**: 5204-10.
232. Zhang Y, Chung Y, Bishop C, Daugherty B, Chute H, Holst P et al. Regulation of T cell activation and tolerance by PDL2. *Proc Natl Acad Sci U S A* 2006; **103**: 11695-700.
233. Flatekval GF, Sioud M. Modulation of dendritic cell maturation and function with mono- and bifunctional small interfering RNAs targeting indoleamine 2,3-dioxygenase. *Immunology* 2009; **128**: e837-48.
234. Gregori S, Tomasoni D, Pacciani V, Scirpoli M, Battaglia M, Magnani CF et al. Differentiation of type 1 T regulatory cells (Tr1) by tolerogenic DC-10 requires the IL-10-dependent ILT4/HLA-G pathway. *Blood* 2010; **116**: 935-44.
235. Chauveau C, Remy S, Royer PJ, Hill M, Tanguy-Royer S, Hubert FX et al. Heme oxygenase-1 expression inhibits dendritic cell maturation and proinflammatory function but conserves IL-10 expression. *Blood* 2005; **106**: 1694-702.
236. Yolcu ES, Gu X, Lacelle C, Zhao H, Bandura-Morgan L, Askenasy N et al. Induction of tolerance to cardiac allografts using donor splenocytes engineered to display on their surface an exogenous fas ligand protein. *J Immunol* 2008; **181**: 931-9.
237. Ilarregui JM, Croci DO, Bianco GA, Toscano MA, Salatino M, Vermeulen ME et al. Tolerogenic signals delivered by dendritic cells to T cells through a galectin-1-driven immunoregulatory circuit involving interleukin 27 and interleukin 10. *Nat Immunol* 2009; **10**: 981-91.
238. Jenkins MK, Chen CA, Jung G, Mueller DL, Schwartz RH. Inhibition of antigen-specific proliferation of type 1 murine T cell clones after stimulation with immobilized anti-CD3 monoclonal antibody. *J Immunol* 1990; **144**: 16-22.
239. Jonuleit H, Schmitt E, Schuler G, Knop J, Enk AH. Induction of interleukin 10-producing, nonproliferating CD4(+) T cells with regulatory properties by repetitive stimulation with allogeneic immature human dendritic cells. *J Exp Med* 2000; **192**: 1213-22.

240. Matzinger P. The danger model: a renewed sense of self. *Science* 2002; **296**: 301-5.
241. Albert ML, Pearce SF, Francisco LM, Sauter B, Roy P, Silverstein RL et al. Immature dendritic cells phagocytose apoptotic cells via alphavbeta5 and CD36, and cross-present antigens to cytotoxic T lymphocytes. *J Exp Med* 1998; **188**: 1359-68.
242. Albert ML, Sauter B, Bhardwaj N. Dendritic cells acquire antigen from apoptotic cells and induce class I-restricted CTLs. *Nature* 1998; **392**: 86-9.
243. Rubartelli A, Poggi A, Zocchi MR. The selective engulfment of apoptotic bodies by dendritic cells is mediated by the alpha(v)beta3 integrin and requires intracellular and extracellular calcium. *Eur J Immunol* 1997; **27**: 1893-900.
244. Inaba K, Turley S, Yamaide F, Iyoda T, Mahnke K, Inaba M et al. Efficient presentation of phagocytosed cellular fragments on the major histocompatibility complex class II products of dendritic cells. *J Exp Med* 1998; **188**: 2163-73.
245. Morelli AE, Larregina AT, Shufesky WJ, Zahorchak AF, Logar AJ, Papworth GD et al. Internalization of circulating apoptotic cells by splenic marginal zone dendritic cells: dependence on complement receptors and effect on cytokine production. *Blood* 2003; **101**: 611-20.
246. Harshyne LA, Watkins SC, Gambotto A, Barratt-Boyes SM. Dendritic cells acquire antigens from live cells for cross-presentation to CTL. *J Immunol* 2001; **166**: 3717-23.
247. They C, Duban L, Segura E, Veron P, Lantz O, Amigorena S. Indirect activation of naive CD4+ T cells by dendritic cell-derived exosomes. *Nat Immunol* 2002; **3**: 1156-62.
248. Scheinecker C, McHugh R, Shevach EM, Germain RN. Constitutive presentation of a natural tissue autoantigen exclusively by dendritic cells in the draining lymph node. *J Exp Med* 2002; **196**: 1079-90.
249. Bujdoso R, Hopkins J, Dutia BM, Young P, McConnell I. Characterization of sheep afferent lymph dendritic cells and their role in antigen carriage. *J Exp Med* 1989; **170**: 1285-301.
250. Liu L, Zhang M, Jenkins C, MacPherson GG. Dendritic cell heterogeneity in vivo: two functionally different dendritic cell populations in rat intestinal lymph can be distinguished by CD4 expression. *J Immunol* 1998; **161**: 1146-55.

251. Matsuno K, Ezaki T, Kudo S, Uehara Y. A life stage of particle-laden rat dendritic cells in vivo: their terminal division, active phagocytosis, and translocation from the liver to the draining lymph. *J Exp Med* 1996; **183**: 1865-78.
252. Lutz MB, Schuler G. Immature, semi-mature and fully mature dendritic cells: which signals induce tolerance or immunity? *Trends Immunol* 2002; **23**: 445-9.
253. Reis e Sousa C. Dendritic cells in a mature age. *Nat Rev Immunol* 2006; **6**: 476-83.
254. Morelli AE, Thomson AW. Dendritic cells: Regulators of alloimmunity and opportunities for tolerance induction. *Immunological Reviews* 2003; **196**: 125-46.
255. Inaba K, Pack M, Inaba M, Sakuta H, Isdell F, Steinman RM. High levels of a major histocompatibility complex II-self peptide complex on dendritic cells from the T cell areas of lymph nodes. *J Exp Med* 1997; **186**: 665-72.
256. Lu L, Li W, Zhong C, Qian S, Fung JJ, Thomson AW et al. Increased apoptosis of immunoreactive host cells and augmented donor leukocyte chimerism, not sustained inhibition of B7 molecule expression are associated with prolonged cardiac allograft survival in mice preconditioned with immature donor dendritic cells plus anti-CD40L mAb. *Transplantation* 1999; **68**: 747-57.
257. Lu L, McCaslin D, Starzl TE, Thomson AW. Bone marrow-derived dendritic cell progenitors (NLDC 145+, MHC class II+, B7-1dim, B7-2-) induce alloantigen-specific hyporesponsiveness in murine T lymphocytes. *Transplantation* 1995; **60**: 1539-45.
258. Dhodapkar MV, Steinman RM, Krasovsky J, Munz C, Bhardwaj N. Antigen-specific inhibition of effector T cell function in humans after injection of immature dendritic cells. *J Exp Med* 2001; **193**: 233-8.
259. Fehervari Z, Sakaguchi S. Control of Foxp3+ CD25+CD4+ regulatory cell activation and function by dendritic cells. *Int Immunol* 2004; **16**: 1769-80.
260. Darrasse-Jeze G, Deroubaix S, Mouquet H, Victora GD, Eisenreich T, Yao KH et al. Feedback control of regulatory T cell homeostasis by dendritic cells in vivo. *J Exp Med* 2009; **206**: 1853-62.
261. Levings MK, Gregori S, Tresoldi E, Cazzaniga S, Bonini C, Roncarolo MG. Differentiation of Tr1 cells by immature dendritic cells requires IL-10 but not CD25+CD4+ Tr cells. *Blood* 2005; **105**: 1162-9.

262. Ito T, Yang M, Wang YH, Lande R, Gregorio J, Perng OA et al. Plasmacytoid dendritic cells prime IL-10-producing T regulatory cells by inducible costimulator ligand. *J Exp Med* 2007; **204**: 105-15.
263. Moseman EA, Liang X, Dawson AJ, Panoskaltsis-Mortari A, Krieg AM, Liu YJ et al. Human plasmacytoid dendritic cells activated by CpG oligodeoxynucleotides induce the generation of CD4+CD25+ regulatory T cells. *J Immunol* 2004; **173**: 4433-42.
264. Ezzelarab M, Thomson AW. Tolerogenic dendritic cells and their role in transplantation. *Semin Immunol* 2011; **23**: 252-63.
265. Manicassamy S, Pulendran B. Dendritic cell control of tolerogenic responses. *Immunol Rev* 2011; **241**: 206-27.
266. Coates PTH, Thomson AW. Dendritic cells, tolerance induction and transplant outcome. *American Journal of Transplantation* 2002; **2**: 299-307.
267. Larsen CP, Morris PJ, Austyn JM. Migration of dendritic leukocytes from cardiac allografts into host spleens. A novel pathway for initiation of rejection. *J Exp Med* 1990; **171**: 307-14.
268. Gould DS, Auchincloss Jr H. Direct and indirect recognition: the role of MHC antigens in graft rejection. *Immunology Today* 1999; **20**: 77-82.
269. Herrera OB, Golshayan D, Tibbott R, Ochoa FS, James MJ, Marelli-Berg FM et al. A Novel Pathway of Alloantigen Presentation by Dendritic Cells. *J Immunol* 2004; **173**: 4828-37.
270. Harshyne LA, Watkins SC, Gambotto A, Barratt-Boyes SM. Dendritic Cells Acquire Antigens from Live Cells for Cross-Presentation to CTL. *J Immunol* 2001; **166**: 3717-23.
271. Babcock SK, Gill RG, Bellgrau D, Lafferty KJ. Studies on the two-signal model for T cell activation in vivo. *Transplant Proc* 1987; **19**: 303-6.
272. Bromley SK, Iaboni A, Davis SJ, Whitty A, Green JM, Shaw AS et al. The immunological synapse and CD28-CD80 interactions. *Nat Immunol* 2001; **2**: 1159-66.
273. Lechler RI, Batchelor JR. Restoration of immunogenicity to passenger cell-depleted kidney allografts by the addition of donor strain dendritic cells. *J Exp Med* 1982; **155**: 31-41.
274. Starzl TE, Demetris AJ, Murase N, Ildstad S, Ricordi C, Trucco M. Cell migration, chimerism, and graft acceptance. *Lancet* 1992; **339**: 1579-82.

275. Starzl TE, Demetris AJ, Trucco M, Zeevi A, Ramos H, Terasaki P et al. Chimerism and donor-specific nonreactivity 27 to 29 years after kidney allotransplantation. *Transplantation* 1993; **55**: 1272-7.
276. Thomson AW, Lu L, Murase N, Demetris AJ, Rao AS, Starzl TE. Microchimerism, dendritic cell progenitors and transplantation tolerance. *Stem Cells* 1995; **13**: 622-39.
277. Benichou G, Valujskikh A, Heeger PS. Contributions of Direct and Indirect T Cell Alloreactivity During Allograft Rejection in Mice. *J Immunol* 1999; **162**: 352-8.
278. Auchincloss H, Jr., Lee R, Shea S, Markowitz JS, Grusby MJ, Glimcher LH. The role of "indirect" recognition in initiating rejection of skin grafts from major histocompatibility complex class II-deficient mice. *Proc Natl Acad Sci U S A* 1993; **90**: 3373-7.
279. Brennan TV, Jaigirdar A, Hoang V, Hayden T, Liu F-C, Zaid H et al. Preferential Priming of Alloreactive T Cells with Indirect Reactivity. *American Journal of Transplantation* 2009; **9**: 709-18.
280. Jiang S, Herrera O, Lechler RI. New spectrum of allorecognition pathways: Implications for graft rejection and transplantation tolerance. *Current Opinion in Immunology* 2004; **16**: 550-7.
281. Gallucci S, Lolkema M, Matzinger P. Natural adjuvants: endogenous activators of dendritic cells. *Nat Med* 1999; **5**: 1249-55.
282. Huppa JB, Davis MM. T-cell-antigen recognition and the immunological synapse. *Nat Rev Immunol* 2003; **3**: 973-83.
283. Lu W, Arraes LC, Ferreira WT, Andrieu JM. Therapeutic dendritic-cell vaccine for chronic HIV-1 infection. *Nat Med* 2004; **10**: 1359-65.
284. Rinaldo CR. Dendritic cell-based human immunodeficiency virus vaccine. *J Intern Med* 2009; **265**: 138-58.
285. Engell-Noerregaard L, Hansen TH, Andersen MH, Thor Straten P, Svane IM. Review of clinical studies on dendritic cell-based vaccination of patients with malignant melanoma: assessment of correlation between clinical response and vaccine parameters. *Cancer Immunol Immunother* 2009; **58**: 1-14.
286. Lopez MN, Pereda C, Segal G, Munoz L, Aguilera R, Gonzalez FE et al. Prolonged survival of dendritic cell-vaccinated melanoma patients correlates

- with tumor-specific delayed type IV hypersensitivity response and reduction of tumor growth factor beta-expressing T cells. *J Clin Oncol* 2009; **27**: 945-52.
287. Mayordomo JI, Andres R, Isla MD, Murillo L, Cajal R, Yubero A et al. Results of a pilot trial of immunotherapy with dendritic cells pulsed with autologous tumor lysates in patients with advanced cancer. *Tumori* 2007; **93**: 26-30.
288. Berntsen A, Geertsen PF, Svane IM. Therapeutic dendritic cell vaccination of patients with renal cell carcinoma. *Eur Urol* 2006; **50**: 34-43.
289. Fujii S, Shimizu K, Fujimoto K, Kiyokawa T, Tsukamoto A, Sanada I et al. Treatment of post-transplanted, relapsed patients with hematological malignancies by infusion of HLA-matched, allogeneic-dendritic cells (DCs) pulsed with irradiated tumor cells and primed T cells. *Leuk Lymphoma* 2001; **42**: 357-69.
290. Murphy GP, Tjoa BA, Simmons SJ, Jarisch J, Bowes VA, Ragde H et al. Infusion of dendritic cells pulsed with HLA-A2-specific prostate-specific membrane antigen peptides: a phase II prostate cancer vaccine trial involving patients with hormone-refractory metastatic disease. *Prostate* 1999; **38**: 73-8.
291. Murphy GP, Tjoa BA, Simmons SJ, Ragde H, Rogers M, Elgamal A et al. Phase II prostate cancer vaccine trial: report of a study involving 37 patients with disease recurrence following primary treatment. *Prostate* 1999; **39**: 54-9.
292. Tjoa BA, Simmons SJ, Elgamal A, Rogers M, Ragde H, Kenny GM et al. Follow-up evaluation of a phase II prostate cancer vaccine trial. *Prostate* 1999; **40**: 125-9.
293. Abe M, Wang Z, de Creus A, Thomson AW. Plasmacytoid dendritic cell precursors induce allogeneic T-cell hyporesponsiveness and prolong heart graft survival. *Am J Transplant* 2005; **5**: 1808-19.
294. Fu F, Li Y, Qian S, Lu L, Chambers F, Starzl TE et al. Costimulatory molecule-deficient dendritic cell progenitors (MHC class II+, CD80dim, CD86-) prolong cardiac allograft survival in nonimmunosuppressed recipients. *Transplantation* 1996; **62**: 659-65.
295. Hawiger D, Inaba K, Dorsett Y, Guo M, Mahnke K, Rivera M et al. Dendritic cells induce peripheral T cell unresponsiveness under steady state conditions in vivo. *J Exp Med* 2001; **194**: 769-79.
296. Kusuhara M, Matsue K, Edelbaum D, Loftus J, Takashima A, Matsue H. Killing of naive T cells by CD95L-transfected dendritic cells (DC): in vivo study using

- killer DC-DC hybrids and CD4(+) T cells from DO11.10 mice. *Eur J Immunol* 2002; **32**: 1035-43.
297. Lutz MB, Suri RM, Niimi M, Ogilvie AL, Kukutsch NA, Rossner S et al. Immature dendritic cells generated with low doses of GM-CSF in the absence of IL-4 are maturation resistant and prolong allograft survival in vivo. *Eur J Immunol* 2000; **30**: 1813-22.
298. Tan PH, Yates JB, Xue SA, Chan C, Jordan WJ, Harper JE et al. Creation of tolerogenic human dendritic cells via intracellular CTLA4: a novel strategy with potential in clinical immunosuppression. *Blood* 2005; **106**: 2936-43.
299. Turnquist HR, Raimondi G, Zahorchak AF, Fischer RT, Wang Z, Thomson AW. Rapamycin-conditioned dendritic cells are poor stimulators of allogeneic CD4+ T cells, but enrich for antigen-specific Foxp3+ T regulatory cells and promote organ transplant tolerance. *Journal of Immunology* 2007; **178**: 7018-31.
300. Fu CL, Chuang YH, Huang HY, Chiang BL. Induction of IL-10 producing CD4+ T cells with regulatory activities by stimulation with IL-10 gene-modified bone marrow derived dendritic cells. *Clin Exp Immunol* 2008; **153**: 258-68.
301. Gilliet M, Liu YJ. Generation of human CD8 T regulatory cells by CD40 ligand-activated plasmacytoid dendritic cells. *J Exp Med* 2002; **195**: 695-704.
302. Kuo YR, Huang CW, Goto S, Wang CT, Hsu LW, Lin YC et al. Alloantigen-pulsed host dendritic cells induce T-cell regulation and prolong allograft survival in a rat model of hindlimb allotransplantation. *J Surg Res* 2009; **153**: 317-25.
303. Prasad S. Studies of immune biology of the common marmoset: a novel non-human primate transplant model. Adelaide: University of Adelaide; 2009.
304. Probst HC, Lagnel J, Kollias G, van den Broek M. Inducible transgenic mice reveal resting dendritic cells as potent inducers of CD8+ T cell tolerance. *Immunity* 2003; **18**: 713-20.
305. Moreau A, Varey E, Beriou G, Hill M, Bouchet-Delbos L, Segovia M et al. Tolerogenic dendritic cells and negative vaccination in transplantation: from rodents to clinical trials. *Front Immunol* 2012; **3**: 218.
306. DePaz HA, Oluwole OO, Adeyeri AO, Witkowski P, Jin MX, Hardy MA et al. Immature rat myeloid dendritic cells generated in low-dose granulocyte macrophage-colony stimulating factor prolong donor-specific rat cardiac allograft survival. *Transplantation* 2003; **75**: 521-8.

307. Steinbrink K, Wolf M, Jonuleit H, Knop J, Enk AH. Induction of tolerance by IL-10-treated dendritic cells. *J Immunol* 1997; **159**: 4772-80.
308. Lu L, Li W, Fu F, Chambers FG, Qian S, Fung JJ et al. Blockade of the CD40-CD40 ligand pathway potentiates the capacity of donor-derived dendritic cell progenitors to induce long-term cardiac allograft survival. *Transplantation* 1997; **64**: 1808-15.
309. Lan YY, Wang Z, Raimondi G, Wu W, Colvin BL, de Creus A et al. "Alternatively activated" dendritic cells preferentially secrete IL-10, expand Foxp3+CD4+ T cells, and induce long-term organ allograft survival in combination with CTLA4-Ig. *J Immunol* 2006; **177**: 5868-77.
310. Yamano T, Watanabe S, Hasegawa H, Suzuki T, Abe R, Tahara H et al. Ex vivo-expanded DCs induce donor-specific central and peripheral tolerance and prolong the acceptance of donor skin grafts. *Blood* 2011; **117**: 2640-8.
311. Giannoukakis N, Bonham CA, Qian S, Chen Z, Peng L, Harnaha J et al. Prolongation of cardiac allograft survival using dendritic cells treated with NF- κ B decoy oligodeoxyribonucleotides. *Mol Ther* 2000; **1**: 430-7.
312. Bonham CA, Peng L, Liang X, Chen Z, Wang L, Ma L et al. Marked prolongation of cardiac allograft survival by dendritic cells genetically engineered with NF- κ B oligodeoxyribonucleotide decoys and adenoviral vectors encoding CTLA4-Ig. *J Immunol* 2002; **169**: 3382-91.
313. Min WP, Gorczynski R, Huang XY, Kushida M, Kim P, Obataki M et al. Dendritic cells genetically engineered to express Fas ligand induce donor-specific hyporesponsiveness and prolong allograft survival. *Journal of Immunology* 2000; **164**: 161-7.
314. Li M, Zhang X, Zheng X, Lian D, Zhang ZX, Ge W et al. Immune modulation and tolerance induction by RelB-silenced dendritic cells through RNA interference. *J Immunol* 2007; **178**: 5480-7.
315. Hackstein H, Thomson AW. Dendritic cells: Emerging pharmacological targets of immunosuppressive drugs. *Nature Reviews Immunology* 2004; **4**: 24-34.
316. Leishman AJ, Silk KM, Fairchild PJ. Pharmacological manipulation of dendritic cells in the pursuit of transplantation tolerance. *Curr Opin Organ Transplant* 2011; **16**: 372-8.

317. Matyszak MK, Citterio S, Rescigno M, Ricciardi-Castagnoli P. Differential effects of corticosteroids during different stages of dendritic cell maturation. *Eur J Immunol* 2000; **30**: 1233-42.
318. Lee JI, Ganster RW, Geller DA, Burckart GJ, Thomson AW, Lu L. Cyclosporine A inhibits the expression of costimulatory molecules on in vitro-generated dendritic cells: association with reduced nuclear translocation of nuclear factor kappa B. *Transplantation* 1999; **68**: 1255-63.
319. Hackstein H, Taner T, Zahorchak AF, Morelli AE, Logar AJ, Gessner A et al. Rapamycin inhibits IL-4--induced dendritic cell maturation in vitro and dendritic cell mobilization and function in vivo. *Blood* 2003; **101**: 4457-63.
320. Hackstein H, Morelli AE, Larregina AT, Ganster RW, Papworth GD, Logar AJ et al. Aspirin inhibits in vitro maturation and in vivo immunostimulatory function of murine myeloid dendritic cells. *J Immunol* 2001; **166**: 7053-62.
321. Gregori S, Casorati M, Amuchastegui S, Smiroldo S, Davalli AM, Adorini L. Regulatory T cells induced by 1 alpha,25-dihydroxyvitamin D3 and mycophenolate mofetil treatment mediate transplantation tolerance. *J Immunol* 2001; **167**: 1945-53.
322. Penna G, Adorini L. 1 Alpha,25-dihydroxyvitamin D3 inhibits differentiation, maturation, activation, and survival of dendritic cells leading to impaired alloreactive T cell activation. *J Immunol* 2000; **164**: 2405-11.
323. Rogers NM, Kireta S, Coates PT. Curcumin induces maturation-arrested dendritic cells that expand regulatory T cells in vitro and in vivo. *Clin Exp Immunol* 2010; **162**: 460-73.
324. Singh S, Aggarwal BB. Activation of transcription factor NF-kappa B is suppressed by curcumin (diferuloylmethane) [corrected]. *J Biol Chem* 1995; **270**: 24995-5000.
325. Reichardt W, DÄ¼rr C, von Elverfeldt D, JÄ¼ttner E, Gerlach UV, Yamada M et al. Impact of mammalian target of rapamycin inhibition on lymphoid homing and tolerogenic function of nanoparticle-labeled dendritic cells following allogeneic hematopoietic cell transplantation. *Journal of immunology (Baltimore, Md : 1950)* 2008; **181**: 4770-9.
326. Li Y, Li XC, Zheng XX, Wells AD, Turka LA, Strom TB. Blocking both signal 1 and signal 2 of T-cell activation prevents apoptosis of alloreactive T cells and induction of peripheral allograft tolerance. *Nat Med* 1999; **5**: 1298-302.

327. Bestard O, Cruzado JM, Grinyo JM. Inhibitors of the mammalian target of rapamycin and transplant tolerance. *Transplantation* 2009; **87**: S27-9.
328. Thomson AW, Turnquist HR, Raimondi G. Immunoregulatory functions of mTOR inhibition. *Nat Rev Immunol* 2009; **9**: 324-37.
329. Griffin MD, Lutz WH, Phan VA, Bachman LA, McKean DJ, Kumar R. Potent inhibition of dendritic cell differentiation and maturation by vitamin D analogs. *Biochem Biophys Res Commun* 2000; **270**: 701-8.
330. Griffin MD, Lutz W, Phan VA, Bachman LA, McKean DJ, Kumar R. Dendritic cell modulation by 1alpha,25 dihydroxyvitamin D3 and its analogs: a vitamin D receptor-dependent pathway that promotes a persistent state of immaturity in vitro and in vivo. *Proc Natl Acad Sci U S A* 2001; **98**: 6800-5.
331. Divito SJ, Wang Z, Shufesky WJ, Liu Q, Tkacheva OA, Montecalvo A et al. Endogenous dendritic cells mediate the effects of intravenously injected therapeutic immunosuppressive dendritic cells in transplantation. *Blood* 2010; **116**: 2694-705.
332. Anderson AE, Sayers BL, Haniffa MA, Swan DJ, Diboll J, Wang XN et al. Differential regulation of naive and memory CD4+ T cells by alternatively activated dendritic cells. *J Leukoc Biol* 2008; **84**: 124-33.
333. Rastellini C, Lu L, Ricordi C, Starzl TE, Rao AS, Thomson AW. Granulocyte/macrophage colony-stimulating factor-stimulated hepatic dendritic cell progenitors prolong pancreatic islet allograft survival. *Transplantation* 1995; **60**: 1366-70.
334. Gao JX, Madrenas J, Zeng W, Cameron MJ, Zhang Z, Wang JJ et al. CD40-deficient dendritic cells producing interleukin-10, but not interleukin-12, induce T-cell hyporesponsiveness in vitro and prevent acute allograft rejection. *Immunology* 1999; **98**: 159-70.
335. Niimi M, Shirasugi N, Ikeda Y, Kan S, Takami H, Hamano K. Operational tolerance induced by pretreatment with donor dendritic cells under blockade of CD40 pathway. *Transplantation* 2001; **72**: 1556-62.
336. O'Connell PJ, Li W, Wang Z, Specht SM, Logar AJ, Thomson AW. Immature and mature CD8alpha+ dendritic cells prolong the survival of vascularized heart allografts. *J Immunol* 2002; **168**: 143-54.
337. Sun W, Wang Q, Zhang L, Liu Y, Zhang M, Wang C et al. Blockade of CD40 pathway enhances the induction of immune tolerance by immature dendritic

- cells genetically modified to express cytotoxic T lymphocyte antigen 4 immunoglobulin. *Transplantation* 2003; **76**: 1351-9.
338. Coates PTH, Duncan FJ, Colvin BL, Wang Z, Zahorchak AF, Shufesky WJ et al. In vivo-mobilized kidney dendritic cells are functionally immature, subvert alloreactive t-cell responses, and prolong organ allograft survival. *Transplantation* 2004; **77**: 1080-9.
339. Bjorck P, Coates PT, Wang Z, Duncan FJ, Thomson AW. Promotion of long-term heart allograft survival by combination of mobilized donor plasmacytoid dendritic cells and anti-CD154 monoclonal antibody. *J Heart Lung Transplant* 2005; **24**: 1118-20.
340. Garrod KR, Chang CK, Liu FC, Brennan TV, Foster RD, Kang SM. Targeted lymphoid homing of dendritic cells is required for prolongation of allograft survival. *J Immunol* 2006; **177**: 863-8.
341. Wang Q, Liu Y, Wang J, Ding G, Zhang W, Chen G et al. Induction of allospecific tolerance by immature dendritic cells genetically modified to express soluble TNF receptor. *Journal of Immunology* 2006; **177**: 2175-85.
342. Garroville M, Ali A, Oluwole SF. Indirect allorecognition in acquired thymic tolerance: induction of donor-specific tolerance to rat cardiac allografts by allopeptide-pulsed host dendritic cells. *Transplantation* 1999; **68**: 1827-34.
343. Garroville M, Ali A, Depaz HA, Gopinathan R, Oluwole OO, Hardy MA et al. Induction of transplant tolerance with immunodominant allopeptide-pulsed host lymphoid and myeloid dendritic cells. *Am J Transplant* 2001; **1**: 129-37.
344. Miranda V, Berton I, Read J, Cook T, Smith J, Dorling A et al. Modified dendritic cells coexpressing self and allogeneic major histocompatibility complex molecules: an efficient way to induce indirect pathway regulation. *J Am Soc Nephrol* 2004; **15**: 987-97.
345. Taner T, Hackstein H, Wang Z, Morelli AE, Thomson AW. Rapamycin-treated, alloantigen-pulsed host dendritic cells induce ag-specific T cell regulation and prolong graft survival. *Am J Transplant* 2005; **5**: 228-36.
346. Peche H, Trinite B, Martinet B, Cuturi MC. Prolongation of heart allograft survival by immature dendritic cells generated from recipient type bone marrow progenitors. *Am J Transplant* 2005; **5**: 255-67.

347. Beriou G, Peche H, Guillonnet C, Merieau E, Cuturi MC. Donor-specific allograft tolerance by administration of recipient-derived immature dendritic cells and suboptimal immunosuppression. *Transplantation* 2005; **79**: 969-72.
348. Horibe EK, Sacks J, Unadkat J, Raimondi G, Wang Z, Ikeguchi R et al. Rapamycin-conditioned, alloantigen-pulsed dendritic cells promote indefinite survival of vascularized skin allografts in association with T regulatory cell expansion. *Transpl Immunol* 2008; **18**: 307-18.
349. Hill M, Thebault P, Segovia M, Louvet C, Beriou G, Tilly G et al. Cell therapy with autologous tolerogenic dendritic cells induces allograft tolerance through interferon-gamma and epstein-barr virus-induced gene 3. *Am J Transplant* 2011; **11**: 2036-45.
350. Zahorchak AF, Kean LS, Tokita D, Turnquist HR, Abe M, Finke J et al. Infusion of stably immature monocyte-derived dendritic cells plus CTLA4Ig modulates alloimmune reactivity in rhesus macaques. *Transplantation* 2007; **84**: 196-206.
351. Ezzelarab MB, Zahorchak AF, Lu L, Morelli AE, Chalasani G, Demetris AJ et al. Regulatory Dendritic Cell Infusion Prolongs Kidney Allograft Survival in Nonhuman Primates. *Am J Transplant* 2013; **13**: 1989-2005.
352. Coates PT, Duncan FJ, Colvin BL, Wang Z, Zahorchak AF, Shufesky WJ et al. In vivo-mobilized kidney dendritic cells are functionally immature, subvert alloreactive T-cell responses, and prolong organ allograft survival. *Transplantation* 2004; **77**: 1080-9.
353. Wang Q, Liu Y, Wang J, Ding G, Zhang W, Chen G et al. Induction of allospecific tolerance by immature dendritic cells genetically modified to express soluble TNF receptor. *J Immunol* 2006; **177**: 2175-85.
354. Kuo YR, Huang CW, Goto S, Wang CT, Hsu LW, Lin YC et al. Alloantigen-Pulsed Host Dendritic Cells Induce T-Cell Regulation and Prolong Allograft Survival in a Rat Model of Hindlimb Allotransplantation. *J Surg Res* 2008; **in press; Jun 25 (online publication)**.
355. Giannoukakis N, Phillips B, Finegold D, Harnaha J, Trucco M. Phase I (safety) study of autologous tolerogenic dendritic cells in type 1 diabetic patients. *Diabetes Care* 2011; **34**: 2026-32.
356. Machen J, Harnaha J, Lakomy R, Styche A, Trucco M, Giannoukakis N. Antisense oligonucleotides down-regulating costimulation confer diabetes-

- preventive properties to nonobese diabetic mouse dendritic cells. *J Immunol* 2004; **173**: 4331-41.
357. Hilkens CM, Isaacs JD, Thomson AW. Development of dendritic cell-based immunotherapy for autoimmunity. *Int Rev Immunol* 2010; **29**: 156-83.
358. Geissler EK. The ONE Study compares cell therapy products in organ transplantation: introduction to a review series on suppressive monocyte-derived cells. *Transplant Res* 2012; **1**: 11.
359. Boros P, Bromberg JS. Human FOXP3⁺ regulatory T cells in transplantation. *Am J Transplant* 2009; **9**: 1719-24.
360. Jiang S, Lechler RI, He XS, Huang JF. Regulatory T cells and transplantation tolerance. *Hum Immunol* 2006; **67**: 765-76.
361. Wood KJ, Sakaguchi S. Regulatory T cells in transplantation tolerance. *Nat Rev Immunol* 2003; **3**: 199-210.
362. Banerjee DK, Dhodapkar MV, Matayeva E, Steinman RM, Dhodapkar KM. Expansion of FOXP3^{high} regulatory T cells by human dendritic cells (DCs) in vitro and after injection of cytokine-matured DCs in myeloma patients. *Blood* 2006; **108**: 2655-61.
363. Jiang S, Golshayan D, Tsang J, Lombardi G, Lechler RI. In vitro expanded alloantigen-specific CD4⁺CD25⁺ regulatory T cell treatment for the induction of donor-specific transplantation tolerance. *Int Immunopharmacol* 2006; **6**: 1879-82.
364. Moreau A, Chiffolleau E, Beriou G, Deschamps JY, Heslan M, Ashton-Chess J et al. Superiority of bone marrow-derived dendritic cells over monocyte-derived ones for the expansion of regulatory T cells in the macaque. *Transplantation* 2008; **85**: 1351-6.
365. Thomson CW, Mossoba ME, Siatskas C, Chen W, Sung A, Medin JA et al. Lentivirally transduced recipient-derived dendritic cells serve to ex vivo expand functional FcR γ -sufficient double-negative regulatory T cells. *Mol Ther* 2007; **15**: 818-24.
366. Wang Z, Larregina AT, Shufesky WJ, Perone MJ, Montecalvo A, Zahorchak AF et al. Use of the inhibitory effect of apoptotic cells on dendritic cells for graft survival via T-cell deletion and regulatory T cells. *American Journal of Transplantation* 2006; **6**: 1297-311.

367. Xia G, He J, Leventhal JR. Ex vivo-expanded natural CD4⁺CD25⁺ regulatory T cells synergize with host T-cell depletion to promote long-term survival of allografts. *Am J Transplant* 2008; **8**: 298-306.
368. Yamazaki S, Dudziak D, Heidkamp GF, Fiorese C, Bonito AJ, Inaba K et al. CD8⁺ CD205⁺ splenic dendritic cells are specialized to induce Foxp3⁺ regulatory T cells. *J Immunol* 2008; **181**: 6923-33.
369. Yu G, Xu X, Vu MD, Kilpatrick ED, Li XC. NK cells promote transplant tolerance by killing donor antigen-presenting cells. *J Exp Med* 2006; **203**: 1851-8.
370. Sen P, Wallet MA, Yi Z, Huang Y, Henderson M, Mathews CE et al. Apoptotic cells induce Mer tyrosine kinase-dependent blockade of NF-kappaB activation in dendritic cells. *Blood* 2007; **109**: 653-60.
371. Palucka K, Banchereau J. Cancer immunotherapy via dendritic cells. *Nat Rev Cancer* 2012; **12**: 265-77.
372. Bonifaz LC, Bonnyay DP, Charalambous A, Darguste DI, Fujii S, Soares H et al. In vivo targeting of antigens to maturing dendritic cells via the DEC-205 receptor improves T cell vaccination. *J Exp Med* 2004; **199**: 815-24.
373. Dudziak D, Kamphorst AO, Heidkamp GF, Buchholz VR, Trumfheller C, Yamazaki S et al. Differential antigen processing by dendritic cell subsets in vivo. *Science* 2007; **315**: 107-11.
374. Li D, Romain G, Flamar AL, Duluc D, Dullaers M, Li XH et al. Targeting self- and foreign antigens to dendritic cells via DC-ASGPR generates IL-10-producing suppressive CD4⁺ T cells. *J Exp Med* 2012; **209**: 109-21.
375. Jung KC, Park CG, Jeon YK, Park HJ, Ban YL, Min HS et al. In situ induction of dendritic cell-based T cell tolerance in humanized mice and nonhuman primates. *J Exp Med* 2011; **208**: 2477-88.
376. Reddy ST, Swartz MA, Hubbell JA. Targeting dendritic cells with biomaterials: developing the next generation of vaccines. *Trends in Immunology* 2006; **27**: 573-9.
377. Bontrop RE. Non-human primates: essential partners in biomedical research. *Immunol Rev* 2001; **183**: 5-9.
378. Wang J, Xing F. A novel cell subset: interferon-producing killer dendritic cells. *Sci China C Life Sci* 2008; **51**: 671-5.

379. Barratt-Boyes SM, Henderson RA, Finn OJ. Chimpanzee dendritic cells with potent immunostimulatory function can be propagated from peripheral blood. *Immunology* 1996; **87**: 528-34.
380. O'Doherty U, Ignatius R, Bhardwaj N, Pope M. Generation of monocyte-derived dendritic cells from precursors in rhesus macaque blood. *J Immunol Methods* 1997; **207**: 185-94.
381. Pinchuk LM, Grouard-Vogel G, Magaletti DM, Doty RT, Andrews RG, Clark EA. Isolation and characterization of macaque dendritic cells from CD34(+) bone marrow progenitors. *Cell Immunol* 1999; **196**: 34-40.
382. Pichyangkul S, Saengkrai P, Yongvanitchit K, Limsomwong C, Gettayacamin M, Walsh DS et al. Isolation and characterization of rhesus blood dendritic cells using flow cytometry. *J Immunol Methods* 2001; **252**: 15-23.
383. Lore K. Isolation and immunophenotyping of human and rhesus macaque dendritic cells. *Methods Cell Biol* 2004; **75**: 623-42.
384. Teleshova N, Jones J, Kenney J, Purcell J, Bohm R, Gettie A et al. Short-term Flt3L treatment effectively mobilizes functional macaque dendritic cells. *J Leukoc Biol* 2004; **75**: 1102-10.
385. Zahorchak AF, Raimondi G, Thomson AW. Rhesus monkey immature monocyte-derived dendritic cells generate alloantigen-specific regulatory T cells from circulating CD4+CD127-/lo T cells. *Transplantation* 2009; **88**: 1057-64.
386. Moreau A, Hill M, Thebault P, Deschamps JY, Chiffolleau E, Chauveau C et al. Tolerogenic dendritic cells actively inhibit T cells through heme oxygenase-1 in rodents and in nonhuman primates. *Faseb J* 2009; **23**: 3070-7.
387. Brown KN, Barratt-Boyes SM. Surface phenotype and rapid quantification of blood dendritic cell subsets in the rhesus macaque. *J Med Primatol* 2009; **38**: 272-8.
388. Autissier P, Soulas C, Burdo TH, Williams KC. Immunophenotyping of lymphocyte, monocyte and dendritic cell subsets in normal rhesus macaques by 12-color flow cytometry: clarification on DC heterogeneity. *J Immunol Methods* 2010; **360**: 119-28.
389. Malleret B, Karlsson I, Maneglier B, Brochard P, Delache B, Andrieu T et al. Effect of SIVmac infection on plasmacytoid and CD1c+ myeloid dendritic cells in cynomolgus macaques. *Immunology* 2008; **124**: 223-33.

390. Barratt-Boyes SM, Zimmer MI, Harshyne LA, Meyer EM, Watkins SC, Capuano S, 3rd et al. Maturation and trafficking of monocyte-derived dendritic cells in monkeys: implications for dendritic cell-based vaccines. *J Immunol* 2000; **164**: 2487-95.
391. Soderlund J, Nilsson C, Ekman M, Walther L, Gaines H, Biberfeld G et al. Recruitment of monocyte derived dendritic cells ex vivo from SIV infected and non-infected cynomolgus monkeys. *Scand J Immunol* 2000; **51**: 186-94.
392. Mehlhop E, Villamide LA, Frank I, Gettie A, Santisteban C, Messmer D et al. Enhanced in vitro stimulation of rhesus macaque dendritic cells for activation of SIV-specific T cell responses. *J Immunol Methods* 2002; **260**: 219-34.
393. Koopman G, Niphuis H, Haaksma AG, Farese AM, Casey DB, Kahn LE et al. Increase in plasmacytoid and myeloid dendritic cells by progenipoiectin-1, a chimeric Flt-3 and G-CSF receptor agonist, in SIV-Infected rhesus macaques. *Hum Immunol* 2004; **65**: 303-16.
394. Xia H, Liu H, Zhang G, Zheng Y. Phenotype and function of monocyte-derived dendritic cells from chinese rhesus macaques. *Cell Mol Immunol* 2009; **6**: 159-65.
395. Mortara L, Ploquin MJ, Faye A, Scott-Algara D, Vaslin B, Butor C et al. Phenotype and function of myeloid dendritic cells derived from African green monkey blood monocytes. *J Immunol Methods* 2006; **308**: 138-55.
396. Ashton-Chess J, Blanco G. An in vitro evaluation of the potential suitability of peripheral blood CD14(+) and bone marrow CD34(+)-derived dendritic cells for a tolerance inducing regimen in the primate. *J Immunol Methods* 2005; **297**: 237-52.
397. Awasthi S, Cropper J. Immunophenotype and functions of fetal baboon bone-marrow derived dendritic cells. *Cell Immunol* 2006; **240**: 31-40.
398. Gabriela D, Carlos PL, Clara S, Elkin PM. Phenotypical and functional characterization of non-human primate Aotus spp. dendritic cells and their use as a tool for characterizing immune response to protein antigens. *Vaccine* 2005; **23**: 3386-95.
399. Ohta S, Ueda Y, Yaguchi M, Matsuzaki Y, Nakamura M, Toyama Y et al. Isolation and characterization of dendritic cells from common marmosets for preclinical cell therapy studies. *Immunology* 2008; **123**: 566-74.

400. Prasad S, Kireta S, Leedham E, Russ GR, Coates PT. Propagation and characterisation of dendritic cells from G-CSF mobilised peripheral blood monocytes and stem cells in common marmoset monkeys. *J Immunol Methods* 2009; **352**: 59-70.
401. Prasad S, Humphreys I, Kireta S, Gilchrist RB, Bardy P, Russ GR et al. MHC Class II DRB genotyping is highly predictive of in-vitro alloreactivity in the common marmoset. *J Immunol Methods* 2006; **314**: 153-63.
402. Prasad S, Humphreys I, Kireta S, Gilchrist RB, Bardy P, Russ GR et al. The common marmoset as a novel preclinical transplant model: identification of new MHC class II DRB alleles and prediction of in vitro alloreactivity. *Tissue Antigens* 2007; **69 Suppl 1**: 72-5.
403. Prasad S, Kireta S, Leedham E, Russ GR, Coates PT. Propagation and characterisation of dendritic cells from G-CSF mobilised peripheral blood monocytes and stem cells in common marmoset monkeys. *J Immunol Methods* 2010; **352**: 59-70.
404. Ohta S, Ueda Y, Yaguchi M, Matsuzaki Y, Nakamura M, Toyama Y et al. Isolation and characterization of dendritic cells from common marmosets for preclinical cell therapy studies. *Immunology* 2007.
405. Rosenzweig M, Canque B, Gluckman JC. Human dendritic cell differentiation pathway from CD34+ hematopoietic precursor cells. *Blood* 1996; **87**: 535-44.
406. Brasel K, De Smedt T, Smith JL, Maliszewski CR. Generation of murine dendritic cells from flt3-ligand-supplemented bone marrow cultures. *Blood* 2000; **96**: 3029-39.
407. Ward KA, Stewart LA, Schwarzer AP. CD34+ -derived CD11c+ + + BDCA-1+ + CD123+ + DC: expansion of a phenotypically undescribed myeloid DC1 population for use in adoptive immunotherapy. *Cytotherapy* 2006; **8**: 130-40.
408. Papayannopoulou T, Nakamoto B, Andrews RG, Lyman SD, Lee MY. In vivo effects of Flt3/Flk2 ligand on mobilization of hematopoietic progenitors in primates and potent synergistic enhancement with granulocyte colony-stimulating factor. *Blood* 1997; **90**: 620-9.
409. Donahue RE, Kirby MR, Metzger ME, Agricola BA, Sellers SE, Cullis HM. Peripheral blood CD34+ cells differ from bone marrow CD34+ cells in Thy-1 expression and cell cycle status in nonhuman primates mobilized or not

- mobilized with granulocyte colony-stimulating factor and/or stem cell factor. *Blood* 1996; **87**: 1644-53.
410. Hillyer CD, Swenson RB, Hart KK, Lackey DA, 3rd, Winton EF. Peripheral blood stem cell acquisition by large-volume leukapheresis in growth factor-stimulated and unstimulated rhesus monkeys: development of an animal model. *Exp Hematol* 1993; **21**: 1455-9.
411. Ageyama N, Kimikawa M, Eguchi K, Ono F, Shibata H, Yoshikawa Y et al. Modification of the leukapheresis procedure for use in rhesus monkeys (*Macaca mulata*). *J Clin Apher* 2003; **18**: 26-31.
412. MacVittie TJ, Farese AM, Davis TA, Lind LB, McKearn JP. Myelopoietin, a chimeric agonist of human interleukin 3 and granulocyte colony-stimulating factor receptors, mobilizes CD34+ cells that rapidly engraft lethally x-irradiated nonhuman primates. *Exp Hematol* 1999; **27**: 1557-68.
413. Hibino H, Tani K, Ikebuchi K, Wu MS, Sugiyama H, Nakazaki Y et al. The common marmoset as a target preclinical primate model for cytokine and gene therapy studies. *Blood* 1999; **93**: 2839-48.
414. Osugi Y, Vuckovic S, Hart DN. Myeloid blood CD11c(+) dendritic cells and monocyte-derived dendritic cells differ in their ability to stimulate T lymphocytes. *Blood* 2002; **100**: 2858-66.
415. Soilleux EJ. DC-SIGN (dendritic cell-specific ICAM-grabbing non-integrin) and DC-SIGN-related (DC-SIGNR): friend or foe? *Clin Sci (Lond)* 2003; **104**: 437-46.
416. Schwartz AJ, Alvarez X, Lackner AA. Distribution and immunophenotype of DC-SIGN-expressing cells in SIV-infected and uninfected macaques. *AIDS Res Hum Retroviruses* 2002; **18**: 1021-9.
417. Jameson B, Baribaud F, Pohlmann S, Ghavimi D, Mortari F, Doms RW et al. Expression of DC-SIGN by dendritic cells of intestinal and genital mucosae in humans and rhesus macaques. *J Virol* 2002; **76**: 1866-75.
418. Wu L, Bashirova AA, Martin TD, Villamide L, Mehlhop E, Chertov AO et al. Rhesus macaque dendritic cells efficiently transmit primate lentiviruses independently of DC-SIGN. *Proc Natl Acad Sci U S A* 2002; **99**: 1568-73.
419. Ploquin MJ, Diop OM, Sol-Foulon N, Mortara L, Faye A, Soares MA et al. DC-SIGN from African green monkeys is expressed in lymph nodes and mediates

- infection in trans of simian immunodeficiency virus SIVagm. *J Virol* 2004; **78**: 798-810.
420. Pereira CF, Torensma R, Hebeda K, Kretz-Rommel A, Faas SJ, Figdor CG et al. In vivo targeting of DC-SIGN-positive antigen-presenting cells in a nonhuman primate model. *J Immunother* 2007; **30**: 705-14.
421. Ketloy C, Engering A, Srichairatanakul U, Limsalakpetch A, Yongvanitchit K, Pichyangkul S et al. Expression and function of Toll-like receptors on dendritic cells and other antigen presenting cells from non-human primates. *Vet Immunol Immunopathol* 2008; **125**: 18-30.
422. Kubsch S, Graulich E, Knop J, Steinbrink K. Suppressor activity of anergic T cells induced by IL-10-treated human dendritic cells: association with IL-2- and CTLA-4-dependent G1 arrest of the cell cycle regulated by p27Kip1. *Eur J Immunol* 2003; **33**: 1988-97.
423. Koski GK, Lyakh LA, Cohen PA, Rice NR. CD14+ monocytes as dendritic cell precursors: diverse maturation-inducing pathways lead to common activation of NF-kappaB/RelB. *Crit Rev Immunol* 2001; **21**: 179-89.
424. Clement A, Pereboev A, Curiel DT, Dong SS, Hutchings A, Thomas JM. Converting nonhuman primate dendritic cells into potent antigen-specific cellular immunosuppressants by genetic modification. *Immunol Res* 2002; **26**: 297-302.
425. Asiedu C, Dong SS, Pereboev A, Wang W, Navarro J, Curiel DT et al. Rhesus monocyte-derived dendritic cells modified to over-express TGF-beta1 exhibit potent veto activity. *Transplantation* 2002; **74**: 629-37.
426. Koopman G, Mortier D, Niphuis H, Farese AM, Kahn LE, Mann D et al. Systemic mobilization of antigen presenting cells, with a chimeric Flt-3 and G-CSF receptor agonist, during immunization of *Macaca mulatta* with HIV-1 antigens is insufficient to modulate immune responses or vaccine efficacy. *Vaccine* 2005; **23**: 4195-202.
427. Reeves RK, Fultz PN. Disparate effects of acute and chronic infection with SIVmac239 or SHIV-89.6P on macaque plasmacytoid dendritic cells. *Virology* 2007; **365**: 356-68.
428. Brown KN, Trichel A, Barratt-Boyes SM. Parallel loss of myeloid and plasmacytoid dendritic cells from blood and lymphoid tissue in simian AIDS. *J Immunol* 2007; **178**: 6958-67.

429. Chung E, Amrute SB, Abel K, Gupta G, Wang Y, Miller CJ et al. Characterization of virus-responsive plasmacytoid dendritic cells in the rhesus macaque. *Clin Diagn Lab Immunol* 2005; **12**: 426-35.
430. Mandl JN, Barry AP, Vanderford TH, Kozyr N, Chavan R, Klucking S et al. Divergent TLR7 and TLR9 signaling and type I interferon production distinguish pathogenic and nonpathogenic AIDS virus infections. *Nat Med* 2008; **14**: 1077-87.
431. Diop OM, Ploquin MJ, Mortara L, Faye A, Jacquelin B, Kunkel D et al. Plasmacytoid dendritic cell dynamics and alpha interferon production during Simian immunodeficiency virus infection with a nonpathogenic outcome. *J Virol* 2008; **82**: 5145-52.
432. Vuckovic S, Gardiner D, Field K, Chapman GV, Khalil D, Gill D et al. Monitoring dendritic cells in clinical practice using a new whole blood single-platform TruCOUNT assay. *J Immunol Methods* 2004; **284**: 73-87.
433. Brown KN, Wijewardana V, Liu X, Barratt-Boyes SM. Rapid influx and death of plasmacytoid dendritic cells in lymph nodes mediate depletion in acute simian immunodeficiency virus infection. *PLoS Pathog* 2009; **5**: e1000413.
434. Carter DL, Shieh TM, Blosser RL, Chadwick KR, Margolick JB, Hildreth JE et al. CD56 identifies monocytes and not natural killer cells in rhesus macaques. *Cytometry* 1999; **37**: 41-50.
435. Autissier P, Soulas C, Burdo TH, Williams KC. Evaluation of a 12-color flow cytometry panel to study lymphocyte, monocyte, and dendritic cell subsets in humans. *Cytometry A* 2010; **77**: 410-9.
436. Teleshova N, Kenney J, Jones J, Marshall J, Van Nest G, Dufour J et al. CpG-C immunostimulatory oligodeoxyribonucleotide activation of plasmacytoid dendritic cells in rhesus macaques to augment the activation of IFN-gamma-secreting simian immunodeficiency virus-specific T cells. *J Immunol* 2004; **173**: 1647-57.
437. O'Keeffe M, Hochrein H, Vremec D, Pooley J, Evans R, Woulfe S et al. Effects of administration of progenipoiectin 1, Flt-3 ligand, granulocyte colony-stimulating factor, and pegylated granulocyte-macrophage colony-stimulating factor on dendritic cell subsets in mice. *Blood* 2002; **99**: 2122-30.
438. Morelli AE, Coates PT, Shufesky WJ, Barratt-Boyes SM, Fung JJ, Demetris AJ et al. Growth factor-induced mobilization of dendritic cells in kidney and liver

- of rhesus macaques: implications for transplantation. *Transplantation* 2007; **83**: 656-62.
439. Rosenzweig M, MacVittie TJ, Harper D, Hempel D, Glickman RL, Johnson RP et al. Efficient and durable gene marking of hematopoietic progenitor cells in nonhuman primates after nonablative conditioning. *Blood* 1999; **94**: 2271-86.
440. Taweechaisupapong S, Sriurairatana S, Angsubhakorn S, Yoksan S, Bhamarapavati N. In vivo and in vitro studies on the morphological change in the monkey epidermal Langerhans cells following exposure to dengue 2 (16681) virus. *Southeast Asian J Trop Med Public Health* 1996; **27**: 664-72.
441. Hu J, Pope M, Brown C, O'Doherty U, Miller CJ. Immunophenotypic characterization of simian immunodeficiency virus-infected dendritic cells in cervix, vagina, and draining lymph nodes of rhesus monkeys. *Lab Invest* 1998; **78**: 435-51.
442. Barratt-Boyes SM, Zimmer MI, Harshyne L. Changes in dendritic cell migration and activation during SIV infection suggest a role in initial viral spread and eventual immunosuppression. *J Med Primatol* 2002; **31**: 186-93.
443. Soderlund J, Nilsson C, Lore K, Castanos-Velez E, Ekman M, Heiden T et al. Dichotomy between CD1a⁺ and CD83⁺ dendritic cells in lymph nodes during SIV infection of macaques. *J Med Primatol* 2004; **33**: 16-24.
444. Kaaya E, Li SL, Feichtinger H, Stahmer I, Putkonen P, Mandache E et al. Accessory cells and macrophages in the histopathology of SIVsm-infected cynomolgus monkeys. *Res Virol* 1993; **144**: 81-92.
445. Reeves RK, Fultz PN. Characterization of plasmacytoid dendritic cells in bone marrow of pig-tailed macaques. *Clin Vaccine Immunol* 2008; **15**: 35-41.
446. Pereira LE, Ansari AA. A case for innate immune effector mechanisms as contributors to disease resistance in SIV-infected sooty mangabeys. *Curr HIV Res* 2009; **7**: 12-22.
447. Buffa V, Negri DR, Leone P, Borghi M, Bona R, Michelini Z et al. Evaluation of a self-inactivating lentiviral vector expressing simian immunodeficiency virus gag for induction of specific immune responses in vitro and in vivo. *Viral Immunol* 2006; **19**: 690-701.
448. Brown K, Gao W, Alber S, Trichel A, Murphey-Corb M, Watkins SC et al. Adenovirus-transduced dendritic cells injected into skin or lymph node prime

- potent simian immunodeficiency virus-specific T cell immunity in monkeys. *J Immunol* 2003; **171**: 6875-82.
449. Lu W, Wu X, Lu Y, Guo W, Andrieu JM. Therapeutic dendritic-cell vaccine for simian AIDS. *Nat Med* 2003; **9**: 27-32.
450. Kwissa M, Amara RR, Robinson HL, Moss B, Alkan S, Jabbar A et al. Adjuvanting a DNA vaccine with a TLR9 ligand plus Flt3 ligand results in enhanced cellular immunity against the simian immunodeficiency virus. *J Exp Med* 2007; **204**: 2733-46.
451. Hamdy S, Haddadi A, Hung RW, Lavasanifar A. Targeting dendritic cells with nano-particulate PLGA cancer vaccine formulations. *Adv Drug Deliv Rev* 2011; **63**: 943-55.
452. Altin JG, Parish CR. Liposomal vaccines--targeting the delivery of antigen. *Methods* 2006; **40**: 39-52.
453. Cruz LJ, Tacke PJ, Rueda F, Domingo JC, Albericio F, Figdor CG. Targeting nanoparticles to dendritic cells for immunotherapy. *Methods Enzymol* 2012; **509**: 143-63.
454. Bangham AD, Standish MM, Watkins JC. Diffusion of univalent ions across the lamellae of swollen phospholipids. *J Mol Biol* 1965; **13**: 238-52.
455. Paszko E, Senge MO. Immunoliposomes. *Curr Med Chem* 2012; **19**: 5239-77.
456. Bitounis D, Fanciullino R, Iliadis A, Ciccolini J. Optimizing Druggability through Liposomal Formulations: New Approaches to an Old Concept. *ISRN Pharm* 2012; **2012**: 738432.
457. Torchilin VP. Recent advances with liposomes as pharmaceutical carriers. *Nat Rev Drug Discov* 2005; **4**: 145-60.
458. Rogers NM. Modulation of antigen presenting cell function to affect innate and adaptive immune responses: implications for organ transplantation. Adelaide, Australia: University of Adelaide; 2011.
459. Senior JH. Fate and behavior of liposomes in vivo: a review of controlling factors. *Crit Rev Ther Drug Carrier Syst* 1987; **3**: 123-93.
460. Yan X, Scherphof GL, Kamps JA. Liposome opsonization. *J Liposome Res* 2005; **15**: 109-39.
461. Gabizon A, Papahadjopoulos D. The role of surface charge and hydrophilic groups on liposome clearance in vivo. *Biochim Biophys Acta* 1992; **1103**: 94-100.

462. Lee KD, Hong K, Papahadjopoulos D. Recognition of liposomes by cells: in vitro binding and endocytosis mediated by specific lipid headgroups and surface charge density. *Biochim Biophys Acta* 1992; **1103**: 185-97.
463. Fang J, Nakamura H, Maeda H. The EPR effect: Unique features of tumor blood vessels for drug delivery, factors involved, and limitations and augmentation of the effect. *Adv Drug Deliv Rev* 2011; **63**: 136-51.
464. Maruyama K, Kennel SJ, Huang L. Lipid composition is important for highly efficient target binding and retention of immunoliposomes. *Proc Natl Acad Sci U S A* 1990; **87**: 5744-8.
465. Papahadjopoulos D, Allen TM, Gabizon A, Mayhew E, Matthay K, Huang SK et al. Sterically stabilized liposomes: improvements in pharmacokinetics and antitumor therapeutic efficacy. *Proc Natl Acad Sci U S A* 1991; **88**: 11460-4.
466. Allen TM, Hansen C, Martin F, Redemann C, Yau-Young A. Liposomes containing synthetic lipid derivatives of poly(ethylene glycol) show prolonged circulation half-lives in vivo. *Biochim Biophys Acta* 1991; **1066**: 29-36.
467. Lasic DD, Martin FJ, Gabizon A, Huang SK, Papahadjopoulos D. Sterically stabilized liposomes: a hypothesis on the molecular origin of the extended circulation times. *Biochim Biophys Acta* 1991; **1070**: 187-92.
468. Torchilin VP, Khaw BA, Smirnov VN, Haber E. Preservation of antimitotic antibody activity after covalent coupling to liposomes. *Biochem Biophys Res Commun* 1979; **89**: 1114-9.
469. Kirpotin DB, Noble CO, Hayes ME, Huang Z, Kornaga T, Zhou Y et al. Building and characterizing antibody-targeted lipidic nanotherapeutics. *Methods Enzymol* 2012; **502**: 139-66.
470. Manjappa AS, Chaudhari KR, Venkataraju MP, Dantuluri P, Nanda B, Sidda C et al. Antibody derivatization and conjugation strategies: application in preparation of stealth immunoliposome to target chemotherapeutics to tumor. *J Control Release* 2011; **150**: 2-22.
471. Ansell SM, Harasym TO, Tardi PG, Buchkowsky SS, Bally MB, Cullis PR. Antibody conjugation methods for active targeting of liposomes. *Methods Mol Med* 2000; **25**: 51-68.
472. Jue R, Lambert JM, Pierce LR, Traut RR. Addition of sulfhydryl groups to Escherichia coli ribosomes by protein modification with 2-iminothiolane (methyl 4-mercaptobutyrimidate). *Biochemistry* 1978; **17**: 5399-406.

473. Traut RR, Bollen A, Sun TT, Hershey JW, Sundberg J, Pierce LR. Methyl 4-mercaptobutyrimidate as a cleavable cross-linking reagent and its application to the Escherichia coli 30S ribosome. *Biochemistry* 1973; **12**: 3266-73.
474. Kirpotin D, Park JW, Hong K, Zalipsky S, Li WL, Carter P et al. Sterically stabilized anti-HER2 immunoliposomes: design and targeting to human breast cancer cells in vitro. *Biochemistry* 1997; **36**: 66-75.
475. Cheng WW, Allen TM. Targeted delivery of anti-CD19 liposomal doxorubicin in B-cell lymphoma: a comparison of whole monoclonal antibody, Fab' fragments and single chain Fv. *J Control Release* 2008; **126**: 50-8.
476. Volkel T, Holig P, Merdan T, Muller R, Kontermann RE. Targeting of immunoliposomes to endothelial cells using a single-chain Fv fragment directed against human endoglin (CD105). *Biochim Biophys Acta* 2004; **1663**: 158-66.
477. Iden DL, Allen TM. In vitro and in vivo comparison of immunoliposomes made by conventional coupling techniques with those made by a new post-insertion approach. *Biochim Biophys Acta* 2001; **1513**: 207-16.
478. Ishida T, Iden DL, Allen TM. A combinatorial approach to producing sterically stabilized (Stealth) immunoliposomal drugs. *FEBS Lett* 1999; **460**: 129-33.
479. Tuscano JM, Martin SM, Ma Y, Zamboni W, O'Donnell RT. Efficacy, biodistribution, and pharmacokinetics of CD22-targeted pegylated liposomal doxorubicin in a B-cell non-Hodgkin's lymphoma xenograft mouse model. *Clin Cancer Res* 2010; **16**: 2760-8.
480. Uster PS, Allen TM, Daniel BE, Mendez CJ, Newman MS, Zhu GZ. Insertion of poly(ethylene glycol) derivatized phospholipid into pre-formed liposomes results in prolonged in vivo circulation time. *FEBS Lett* 1996; **386**: 243-6.
481. Sawant RR, Jhaveri AM, Torchilin VP. Immunomicelles for advancing personalized therapy. *Adv Drug Deliv Rev* 2012; **64**: 1436-46.
482. Langer R, Folkman J. Polymers for the sustained release of proteins and other macromolecules. *Nature* 1976; **263**: 797-800.
483. Dinarvand R, Sepehri N, Manoochehri S, Rouhani H, Atyabi F. Polylactide-co-glycolide nanoparticles for controlled delivery of anticancer agents. *Int J Nanomedicine* 2011; **6**: 877-95.
484. Nicolas J, Mura S, Brambilla D, Mackiewicz N, Couvreur P. Design, functionalization strategies and biomedical applications of targeted

- biodegradable/biocompatible polymer-based nanocarriers for drug delivery. *Chem Soc Rev* 2013; **42**: 1147-235.
485. Silva JM, Videira M, Gaspar R, Preat V, Florindo HF. Immune system targeting by biodegradable nanoparticles for cancer vaccines. *J Control Release* 2013; **168**: 179-99.
486. Kim TY, Kim DW, Chung JY, Shin SG, Kim SC, Heo DS et al. Phase I and pharmacokinetic study of Genexol-PM, a cremophor-free, polymeric micelle-formulated paclitaxel, in patients with advanced malignancies. *Clin Cancer Res* 2004; **10**: 3708-16.
487. Athanasiou KA, Niederauer GG, Agrawal CM. Sterilization, toxicity, biocompatibility and clinical applications of polylactic acid/polyglycolic acid copolymers. *Biomaterials* 1996; **17**: 93-102.
488. Gref R, Luck M, Quellec P, Marchand M, Dellacherie E, Harnisch S et al. 'Stealth' corona-core nanoparticles surface modified by polyethylene glycol (PEG): influences of the corona (PEG chain length and surface density) and of the core composition on phagocytic uptake and plasma protein adsorption. *Colloids Surf B Biointerfaces* 2000; **18**: 301-13.
489. Chan JM, Valencia PM, Zhang L, Langer R, Farokhzad OC. Polymeric nanoparticles for drug delivery. *Methods Mol Biol* 2010; **624**: 163-75.
490. Anton N, Benoit JP, Saulnier P. Design and production of nanoparticles formulated from nano-emulsion templates-a review. *J Control Release* 2008; **128**: 185-99.
491. Lamprecht A, Ubrich N, Hombreiro Perez M, Lehr C, Hoffman M, Maincent P. Influences of process parameters on nanoparticle preparation performed by a double emulsion pressure homogenization technique. *Int J Pharm* 2000; **196**: 177-82.
492. Murakami H, Kobayashi M, Takeuchi H, Kawashima Y. Preparation of poly(DL-lactide-co-glycolide) nanoparticles by modified spontaneous emulsification solvent diffusion method. *Int J Pharm* 1999; **187**: 143-52.
493. Yoo HS, Lee KH, Oh JE, Park TG. In vitro and in vivo anti-tumor activities of nanoparticles based on doxorubicin-PLGA conjugates. *J Control Release* 2000; **68**: 419-31.

494. Ibrahim H, Bindschaedler C, Doelker E, Buri P, Gurny R. Aqueous nanodispersions prepared by a salting-out process. *Int J Pharm* 1992; **87**: 239-46.
495. Nah JW, Paek YW, Jeong YI, Kim DW, Cho CS, Kim SH et al. Clonazepam release from poly(DL-lactide-co-glycolide) nanoparticles prepared by dialysis method. *Arch Pharm Res* 1998; **21**: 418-22.
496. Fessi H, Puisieux F, Devissaguet JP, Ammoury N, Benita S. Nanocapsule formation by interfacial polymer deposition following solvent displacement. *International Journal of Pharmaceutics* 1989; **55**: R1-R4.
497. Betancourt T, Brown B, Brannon-Peppas L. Doxorubicin-loaded PLGA nanoparticles by nanoprecipitation: preparation, characterization and in vitro evaluation. *Nanomedicine (Lond)* 2007; **2**: 219-32.
498. Farokhzad OC, Cheng J, Teply BA, Sherifi I, Jon S, Kantoff PW et al. Targeted nanoparticle-aptamer bioconjugates for cancer chemotherapy in vivo. *Proc Natl Acad Sci U S A* 2006; **103**: 6315-20.
499. Farokhzad OC, Jon S, Khademhosseini A, Tran TN, Lavan DA, Langer R. Nanoparticle-aptamer bioconjugates: a new approach for targeting prostate cancer cells. *Cancer Res* 2004; **64**: 7668-72.
500. Kocbek P, Obermajer N, Cegnar M, Kos J, Kristl J. Targeting cancer cells using PLGA nanoparticles surface modified with monoclonal antibody. *J Control Release* 2007; **120**: 18-26.
501. Betancourt T, Byrne JD, Sunaryo N, Crowder SW, Kadapakkam M, Patel S et al. PEGylation strategies for active targeting of PLA/PLGA nanoparticles. *J Biomed Mater Res A* 2009; **91**: 263-76.
502. Cheng J, Teply BA, Sherifi I, Sung J, Luther G, Gu FX et al. Formulation of functionalized PLGA-PEG nanoparticles for in vivo targeted drug delivery. *Biomaterials* 2007; **28**: 869-76.
503. Milane L, Duan Z, Amiji M. Development of EGFR-targeted polymer blend nanocarriers for combination paclitaxel/lonidamine delivery to treat multi-drug resistance in human breast and ovarian tumor cells. *Mol Pharm* 2011; **8**: 185-203.
504. Luo G, Yu X, Jin C, Yang F, Fu D, Long J et al. LyP-1-conjugated nanoparticles for targeting drug delivery to lymphatic metastatic tumors. *Int J Pharm* 2010; **385**: 150-6.

505. Sakhalkar HS, Dalal MK, Salem AK, Ansari R, Fu J, Kiani MF et al. Leukocyte-inspired biodegradable particles that selectively and avidly adhere to inflamed endothelium in vitro and in vivo. *Proc Natl Acad Sci U S A* 2003; **100**: 15895-900.
506. Montgomery SP, Hale DA, Hirshberg B, Harlan DM, Kirk AD. Preclinical evaluation of tolerance induction protocols and islet transplantation in non-human primates. *Immunol Rev* 2001; **183**: 214-22.
507. Abbott DH, Barnett DK, Colman RJ, Yamamoto ME, Schultz-Darken NJ. Aspects of common marmoset basic biology and life history important for biomedical research. *Comp Med* 2003; **53**: 339-50.
508. Benirschke K, Anderson JM, Brownhill LE. Marrow Chimerism in Marmosets. *Science* 1962; **138**: 513-5.
509. Benirschke K, Brownhill LE. Heterosexual Cells in Testes of Chimeric Marmoset Monkeys. *Cytogenetics* 1963; **24**: 331-40.
510. Gengozian N. Immunology and blood chimerism of the marmoset. *Primates Med* 1978; **10**: 173-83.
511. Ross CN, French JA, Orti G. Germ-line chimerism and paternal care in marmosets (*Callithrix kuhlii*). *Proc Natl Acad Sci U S A* 2007; **104**: 6278-82.
512. Niblack GD, Kateley JR, Gengozian N. T-and B-lymphocyte chimerism in the marmoset. *Immunology* 1977; **32**: 257-63.
513. Picus J, Aldrich WR, Letvin NL. A naturally occurring bone-marrow-chimeric primate. I. Integrity of its immune system. *Transplantation* 1985; **39**: 297-303.
514. Watkins DI, Chen ZW, Hughes AL, Hodi FS, Letvin NL. Genetically distinct cell populations in naturally occurring bone marrow-chimeric primates express similar MHC class I gene products. *J Immunol* 1990; **144**: 3726-35.
515. Kohu K, Yamabe E, Matsuzawa A, Onda D, Suemizu H, Sasaki E et al. Comparison of 30 immunity-related genes from the common marmoset with orthologues from human and mouse. *Tohoku J Exp Med* 2008; **215**: 167-80.
516. Villinger F, Bostik P, Mayne A, King CL, Genain CP, Weiss WR et al. Cloning, sequencing, and homology analysis of nonhuman primate Fas/Fas-ligand and co-stimulatory molecules. *Immunogenetics* 2001; **53**: 315-28.
517. Brok HP, Hornby RJ, Griffiths GD, Scott LA, Hart BA. An extensive monoclonal antibody panel for the phenotyping of leukocyte subsets in the common marmoset and the cotton-top tamarin. *Cytometry* 2001; **45**: 294-303.

518. Foerster M, Delgado I, Abraham K, Gerstmayr S, Neubert R. Comparative study on age-dependent development of surface receptors on peripheral blood lymphocytes in children and young nonhuman primates (marmosets). *Life Sci* 1997; **60**: 773-85.
519. Hibino H, Tani K, Sugiyama H, Suzuki S, Wu MS, Izawa K et al. Haematopoietic progenitor cells from the common marmoset as targets of gene transduction by retroviral and adenoviral vectors. *Eur J Haematol* 2001; **66**: 272-80.
520. Kireta S, Zola H, Gilchrist RB, Coates PT. Cross-reactivity of anti-human chemokine receptor and anti-TNF family antibodies with common marmoset (*Callithrix jacchus*) leukocytes. *Cell Immunol* 2005; **236**: 115-22.
521. Riecke K, Nogueira AC, Alexi-Meskishvili V, Stahlmann R. Cross-reactivity of antibodies on thymic epithelial cells from humans and marmosets by flow-cytometry. *J Med Primatol* 2000; **29**: 343-9.
522. Genain CP, Hauser SL. Experimental allergic encephalomyelitis in the New World monkey *Callithrix jacchus*. *Immunol Rev* 2001; **183**: 159-72.
523. Laman JD, van Meurs M, Schellekens MM, de Boer M, Melchers B, Massacesi L et al. Expression of accessory molecules and cytokines in acute EAE in marmoset monkeys (*Callithrix jacchus*). *J Neuroimmunol* 1998; **86**: 30-45.
524. t Hart BA, Hintzen RQ, Laman JD. Preclinical assessment of therapeutic antibodies against human CD40 and human interleukin-12/23p40 in a nonhuman primate model of multiple sclerosis. *Neurodegener Dis* 2008; **5**: 38-52.
525. t Hart BA, van Meurs M, Brok HP, Massacesi L, Bauer J, Boon L et al. A new primate model for multiple sclerosis in the common marmoset. *Immunol Today* 2000; **21**: 290-7.
526. van Vliet SA, Blezer EL, Jongasma MJ, Vanwersch RA, Olivier B, Philippens IH. Exploring the neuroprotective effects of modafinil in a marmoset Parkinson model with immunohistochemistry, magnetic resonance imaging and spectroscopy. *Brain Res* 2008; **1189**: 219-28.
527. Soars MG, Riley RJ, Burchell B. Evaluation of the marmoset as a model species for drug glucuronidation. *Xenobiotica* 2001; **31**: 849-60.
528. Siddall RA. The use of marmosets (*Callithrix jacchus*) in teratological and toxicological research. *Primates Med* 1978; **10**: 215-24.

529. Seltzer LJ, Ziegler TE. Non-invasive measurement of small peptides in the common marmoset (*Callithrix jacchus*): a radiolabeled clearance study and endogenous excretion under varying social conditions. *Horm Behav* 2007; **51**: 436-42.
530. Bagi CM, Volberg M, Moalli M, Shen V, Olson E, Hanson N et al. Age-related changes in marmoset trabecular and cortical bone and response to alendronate therapy resemble human bone physiology and architecture. *Anat Rec (Hoboken)* 2007; **290**: 1005-16.
531. Suda T, Takahashi N, Shinki T, Yamaguchi A, Tanioka Y. The common marmoset as an animal model for vitamin D-dependent rickets, type II. *Adv Exp Med Biol* 1986; **196**: 423-35.
532. Wood JM, Gulati N, Michel JB, Hofbauer KG. Two-kidney, one clip renal hypertension in the marmoset. *J Hypertens* 1986; **4**: 251-4.
533. Abb J, Rodt H, Thierfelder S, Deinhardt F. Specific anti-marmoset T-cell globulin: cytotoxic and mitogenic properties. *Blut* 1980; **41**: 11-8.
534. Deisboeck TS, Wakimoto H, Nestler U, Louis DN, Sehgal PK, Simon M et al. Development of a novel non-human primate model for preclinical gene vector safety studies. Determining the effects of intracerebral HSV-1 inoculation in the common marmoset: a comparative study. *Gene Ther* 2003; **10**: 1225-33.
535. Gilchrist RB, Wicherek M, Heistermann M, Nayudu PL, Hodges JK. Changes in follicle-stimulating hormone and follicle populations during the ovarian cycle of the common marmoset. *Biol Reprod* 2001; **64**: 127-35.
536. Grupen CG, Gilchrist RB, Nayudu PL, Barry MF, Schulz SJ, Ritter LJ et al. Effects of ovarian stimulation, with and without human chorionic gonadotrophin, on oocyte meiotic and developmental competence in the marmoset monkey (*Callithrix jacchus*). *Theriogenology* 2007; **68**: 861-72.
537. Kurita R, Sasaki E, Yokoo T, Hiroyama T, Takasugi K, Imoto H et al. Tal1/Scl gene transduction using a lentiviral vector stimulates highly efficient hematopoietic cell differentiation from common marmoset (*Callithrix jacchus*) embryonic stem cells. *Stem Cells* 2006; **24**: 2014-22.
538. Sasaki E, Hanazawa K, Kurita R, Akatsuka A, Yoshizaki T, Ishii H et al. Establishment of novel embryonic stem cell lines derived from the common marmoset (*Callithrix jacchus*). *Stem Cells* 2005; **23**: 1304-13.

539. Yaguchi M, Tabuse M, Ohta S, Ohkusu-Tsukada K, Takeuchi T, Yamane J et al. Transplantation of dendritic cells promotes functional recovery from spinal cord injury in common marmoset. *Neurosci Res* 2009.
540. Blom D, Orloff MS. A more versatile and reliable method for renal transplantation in the rat. *Microsurgery* 1998; **18**: 267-9.
541. Brack M. IgM-mesangial nephropathy in callithricids. *Vet Pathol* 1988; **25**: 270-6.
542. Brack M. Callitrichid IgM-nephropathy--an old age-related disease? *Lab Anim* 1995; **29**: 54-8.
543. Brack M, Fooke M. Circulating IgM in Callitrichid IgM-nephropathy. *Prim Rep* 1991; **30**: 9-15.
544. Brack M, Rothe H. Chronic tubulointerstitial nephritis and wasting disease in marmosets (*Callithrix jacchus*). *Vet Pathol* 1981; **18**: 45-54.
545. Brack M, Schroeder C, Fooke M, Schlumberger W. IgM/IgA nephropathy in callitrichids: antigen studies. *Nephron* 1999; **82**: 221-31.
546. Brack M, Weber M. Ultrastructural and immunohistochemical studies in callitrichid renal glomeruli. *J Med Primatol* 1994; **23**: 325-32.
547. Brack M, Weber M. Ultrastructural and histochemical mesangial alterations in Callitrichid IgM nephropathy (primates: platyrrhina). *Nephron* 1995; **69**: 286-92.
548. Isobe K, Adachi K, Hayashi S, Ito T, Miyoshi A, Kato A et al. Spontaneous Glomerular and Tubulointerstitial Lesions in Common Marmosets (*Callithrix jacchus*). *Vet Pathol* 2011.
549. Ross Cn Fau - Davis K, Davis K Fau - Dobek G, Dobek G Fau - Tardif SD, Tardif SD. Aging Phenotypes of Common Marmosets (*Callithrix jacchus*). *J Aging Res* 2012; **2012**: 567143.
550. Schroeder C, Osman AA, Roggenbuck D, Mothes T. IgA-gliadin antibodies, IgA-containing circulating immune complexes, and IgA glomerular deposits in wasting marmoset syndrome. *Nephrol Dial Transplant* 1999; **14**: 1875-80.
551. Tucker MJ. A survey of the pathology of marmosets (*Callithrix jacchus*) under experiment. *Lab Anim* 1984; **18**: 351-8.
552. Augustine JJ, Siu DS, Clemente MJ, Schulak JA, Heeger PS, Hricik DE. Pre-transplant IFN-gamma ELISPOTs are associated with post-transplant renal

- function in African American renal transplant recipients. *Am J Transplant* 2005; **5**: 1971-5.
553. van der Mast BJ, Rischen-Vos J, de Kuiper P, Vaessen LM, van Besouw NM, Weimar W. Calcineurin inhibitor withdrawal in stable kidney transplant patients decreases the donor-specific cytotoxic T lymphocyte precursor frequency. *Transplantation* 2005; **80**: 1220-5.
554. NHMRC. Policy on the care and use of non-human primates for scientific purposes. : National Health and Medical Research Council of Australia; 2003. Available from: http://www.nhmrc.gov.au/_files_nhmrc/publications/attachments/ea14.pdf. Accessed:31 May 2013
555. Zuhlke U, Weinbauer G. The common marmoset (*Callithrix jacchus*) as a model in toxicology. *Toxicol Pathol* 2003; **31 Suppl**: 123-7.
556. Tabo M, Hara T, Sone S, Shishido N, Kuramoto S, Nakano K et al. Prediction of drug-induced QT interval prolongation in telemetered common marmosets. *J Toxicol Sci* 2008; **33**: 315-25.
557. Sasaki E, Suemizu H, Shimada A, Hanazawa K, Oiwa R, Kamioka M et al. Generation of transgenic non-human primates with germline transmission. *Nature* 2009; **459**: 523-7.
558. Giddens WE, Jr., Boyce JT, Blakley GA, Morton WR. Renal disease in the pigtailed macaque (*Macaca nemestrina*). *Vet Pathol* 1981; **18**: 70-81.
559. Heidel JR, Giddens WE, Jr., Boyce JT. Renal pathology of catheterized baboons (*Papio cynocephalus*). *Vet Pathol* 1981; **18**: 59-69.
560. Skelton-Stroud P, Glaister J. Naturally occurring renal disease in non-human primates. In: Bach P, Lock E, editors. Nephrotoxicity in the Experimental and Clinical Situation. New York, NY: *Martinus Nijhoff Publishers*; 1987. p. 189-210.
561. Borda JT, Idiart JR, Negrette MS. Glomerular lesions in renal biopsies of *Saimiri boliviensis* (primate) examined by light and electron microscopy and immunohistochemistry. *Vet Pathol* 2000; **37**: 409-14.
562. Gozalo A, Dagle GE, Montoya E, Weller RE, Malaga CA. Spontaneous cardiomyopathy and nephropathy in the owl monkey (*Aotus* sp.) in captivity. *J Med Primatol* 1992; **21**: 279-84.

563. Potkay S. Diseases of the Callitrichidae: a review. *J Med Primatol* 1992; **21**: 189-236.
564. Stills HF, Jr., Bullock BC. Renal disease in squirrel monkeys (*Saimiri sciureus*). *Vet Pathol* 1981; **18**: 38-44.
565. Ross CN, Davis K, Dobek G, Tardif SD. Aging Phenotypes of Common Marmosets (*Callithrix jacchus*). *J Aging Res* 2012; **2012**: 567143.
566. Ludlage E, Mansfield K. Clinical care and diseases of the common marmoset (*Callithrix jacchus*). *Comp Med* 2003; **53**: 369-82.
567. Mahoney J. Chapter 16 - Medical Care. In: Wolfe-Coote S, editor. *The Laboratory Primate*. London: *Academic Press*; 2005. p. 241-57.
568. Kambham N, Markowitz GS, Valeri AM, Lin J, D'Agati VD. Obesity-related glomerulopathy: an emerging epidemic. *Kidney Int* 2001; **59**: 1498-509.
569. Cheng H, Dong HR, Lin RQ, Sun LJ, Chen YP. Determination of normal value of glomerular size in Chinese adults by different measurement methods. *Nephrology (Carlton)* 2012; **17**: 488-92.
570. Osawa G, Kimmelstiel P, Seiling V. Thickness of glomerular basement membranes. *Am J Clin Pathol* 1966; **45**: 7-20.
571. Caramori ML, Basgen JM, Mauer M. Glomerular structure in the normal human kidney: differences between living and cadaver donors. *J Am Soc Nephrol* 2003; **14**: 1901-3.
572. Nossent H, Berden J, Swaak T. Renal immunofluorescence and the prediction of renal outcome in patients with proliferative lupus nephritis. *Lupus* 2000; **9**: 504-10.
573. Moriyama T, Shimizu A, Takei T, Uchida K, Honda K, Nitta K. Characteristics of immunoglobulin A nephropathy with mesangial immunoglobulin G and immunoglobulin M deposition. *Nephrology (Carlton)* 2010; **15**: 747-54.
574. Bloom PM, Filo RS, Smith EJ. Immunofluorescent deposits in normal kidneys. *Kidney International* [Abstract] 1976; **10**: 539.
575. Larsen S. Glomerular immune deposits in kidneys from patients with no clinical or light microscopic evidence of glomerulonephritis. Assessment of the influence of autolysis on identification of immunoglobulins and complement. *Acta Pathol Microbiol Scand A* 1979; **87A**: 313-9.
576. Lane PH, Steffes MW, Mauer SM. Estimation of glomerular volume: a comparison of four methods. *Kidney Int* 1992; **41**: 1085-9.

577. Pagtalunan ME, Drachman JA, Meyer TW. Methods for estimating the volume of individual glomeruli. *Kidney Int* 2000; **57**: 2644-9.
578. Solez K, Colvin RB, Racusen LC, Haas M, Sis B, Mengel M et al. Banff 07 classification of renal allograft pathology: updates and future directions. *Am J Transplant* 2008; **8**: 753-60.
579. van Kooten C, Lombardi G, Gelderman KA, Sagoo P, Buckland M, Lechler R et al. Dendritic cells as a tool to induce transplantation tolerance: obstacles and opportunities. *Transplantation* 2011; **91**: 2-7.
580. Quah BJ, Warren HS, Parish CR. Monitoring lymphocyte proliferation in vitro and in vivo with the intracellular fluorescent dye carboxyfluorescein diacetate succinimidyl ester. *Nat Protoc* 2007; **2**: 2049-56.
581. Last'ovicka J, Budinsky V, Spisek R, Bartunkova J. Assessment of lymphocyte proliferation: CFSE kills dividing cells and modulates expression of activation markers. *Cell Immunol* 2009; **256**: 79-85.
582. Ahrens ET, Flores R, Xu H, Morel PA. In vivo imaging platform for tracking immunotherapeutic cells. *Nat Biotechnol* 2005; **23**: 983-7.
583. Baumjohann D, Lutz MB. Non-invasive imaging of dendritic cell migration in vivo. *Immunobiology* 2006; **211**: 587-97.
584. Eggert AA, Schreurs MW, Boerman OC, Oyen WJ, de Boer AJ, Punt CJ et al. Biodistribution and vaccine efficiency of murine dendritic cells are dependent on the route of administration. *Cancer Res* 1999; **59**: 3340-5.
585. Kim SH, Kim S, Evans CH, Ghivizzani SC, Oligino T, Robbins PD. Effective treatment of established murine collagen-induced arthritis by systemic administration of dendritic cells genetically modified to express IL-4. *J Immunol* 2001; **166**: 3499-505.
586. Kupiec-Weglinski JW, Austyn JM, Morris PJ. Migration patterns of dendritic cells in the mouse. Traffic from the blood, and T cell-dependent and -independent entry to lymphoid tissues. *J Exp Med* 1988; **167**: 632-45.
587. Olasz EB, Lang L, Seidel J, Green MV, Eckelman WC, Katz SI. Fluorine-18 labeled mouse bone marrow-derived dendritic cells can be detected in vivo by high resolution projection imaging. *J Immunol Methods* 2002; **260**: 137-48.
588. Barratt-Boyes SM, Watkins SC, Finn OJ. In vivo migration of dendritic cells differentiated in vitro: a chimpanzee model. *J Immunol* 1997; **158**: 4543-7.

589. Coates PT, Colvin BL, Ranganathan A, Duncan FJ, Lan YY, Shufesky WJ et al. CCR and CC chemokine expression in relation to Flt3 ligand-induced renal dendritic cell mobilization. *Kidney Int* 2004; **66**: 1907-17.
590. Takayama T, Morelli AE, Onai N, Hirao M, Matsushima K, Tahara H et al. Mammalian and viral IL-10 enhance C-C chemokine receptor 5 but down-regulate C-C chemokine receptor 7 expression by myeloid dendritic cells: impact on chemotactic responses and in vivo homing ability. *J Immunol* 2001; **166**: 7136-43.
591. Mou Y, Hou Y, Chen B, Hua Z, Zhang Y, Xie H et al. In vivo migration of dendritic cells labeled with synthetic superparamagnetic iron oxide. *Int J Nanomedicine* 2011; **6**: 2633-40.
592. Barratt-Boyes SM, Watkins SC, Finn OJ. Migration of cultured chimpanzee dendritic cells following intravenous and subcutaneous injection. *Adv Exp Med Biol* 1997; **417**: 71-5.
593. Morse MA, Coleman RE, Akabani G, Niehaus N, Coleman D, Lysterly HK. Migration of human dendritic cells after injection in patients with metastatic malignancies. *Cancer Res* 1999; **59**: 56-8.
594. Ridolfi R, Riccobon A, Galassi R, Giorgetti G, Petrini M, Fiammenghi L et al. Evaluation of in vivo labelled dendritic cell migration in cancer patients. *J Transl Med* 2004; **2**: 27.
595. Verdijk P, Aarntzen EH, Lesterhuis WJ, Boullart AC, Kok E, van Rossum MM et al. Limited amounts of dendritic cells migrate into the T-cell area of lymph nodes but have high immune activating potential in melanoma patients. *Clin Cancer Res* 2009; **15**: 2531-40.
596. Mackensen A, Krause T, Blum U, Uhrmeister P, Mertelsmann R, Lindemann A. Homing of intravenously and intralymphatically injected human dendritic cells generated in vitro from CD34+ hematopoietic progenitor cells. *Cancer Immunol Immunother* 1999; **48**: 118-22.
597. Prince HM, Wall DM, Ritchie D, Honemann D, Harrison S, Quach H et al. In vivo tracking of dendritic cells in patients with multiple myeloma. *J Immunother* 2008; **31**: 166-79.
598. Creusot RJ, Yaghoubi SS, Chang P, Chia J, Contag CH, Gambhir SS et al. Lymphoid-tissue-specific homing of bone-marrow-derived dendritic cells. *Blood* 2009; **113**: 6638-47.

599. Quillien V, Moisan A, Carsin A, Lesimple T, Lefeuvre C, Adamski H et al. Biodistribution of radiolabelled human dendritic cells injected by various routes. *Eur J Nucl Med Mol Imaging* 2005; **32**: 731-41.
600. de Vries IJ, Lesterhuis WJ, Barentsz JO, Verdijk P, van Krieken JH, Boerman OC et al. Magnetic resonance tracking of dendritic cells in melanoma patients for monitoring of cellular therapy. *Nat Biotechnol* 2005; **23**: 1407-13.
601. Prins RM, Craft N, Bruhn KW, Khan-Farooqi H, Koya RC, Stripecke R et al. The TLR-7 agonist, imiquimod, enhances dendritic cell survival and promotes tumor antigen-specific T cell priming: relation to central nervous system antitumor immunity. *J Immunol* 2006; **176**: 157-64.
602. Wang Z, Divito SJ, Shufesky WJ, Sumpter T, Wang H, Tkacheva OA et al. Dendritic cell therapies in transplantation revisited: deletion of recipient DCs deters the effect of therapeutic DCs. *Am J Transplant* 2012; **12**: 1398-408.
603. Yewdall AW, Drutman SB, Jinwala F, Bahjat KS, Bhardwaj N. CD8+ T cell priming by dendritic cell vaccines requires antigen transfer to endogenous antigen presenting cells. *PLoS One* 2010; **5**: e11144.
604. Marti HP, Henschkowski J, Laux G, Vogt B, Seiler C, Opelz G et al. Effect of donor-specific transfusions on the outcome of renal allografts in the cyclosporine era. *Transpl Int* 2006; **19**: 19-26.
605. Sharma RK, Rai PK, Kumar A, Kumar P, Gupta A, Kher V et al. Role of preoperative donor-specific transfusion and cyclosporine in haplo-identical living related renal transplant recipients. *Nephron* 1997; **75**: 20-4.
606. Kushwah R, Oliver JR, Zhang J, Siminovitch KA, Hu J. Apoptotic dendritic cells induce tolerance in mice through suppression of dendritic cell maturation and induction of antigen-specific regulatory T cells. *J Immunol* 2009; **183**: 7104-18.
607. Smyth LA, Ratnasothy K, Moreau A, Alcock S, Sagoo P, Meader L et al. Tolerogenic Donor-Derived Dendritic Cells Risk Sensitization In Vivo owing to Processing and Presentation by Recipient APCs. *J Immunol* 2013; **190**: 4848-60.
608. Morse MA, Niedzwiecki D, Marshall JL, Garrett C, Chang DZ, Aklilu M et al. A Randomized Phase II Study of Immunization With Dendritic Cells Modified With Poxvectors Encoding CEA and MUC1 Compared With the Same Poxvectors Plus GM-CSF for Resected Metastatic Colorectal Cancer. *Ann Surg* 2013.

609. Oshita C, Takikawa M, Kume A, Miyata H, Ashizawa T, Iizuka A et al. Dendritic cell-based vaccination in metastatic melanoma patients: phase II clinical trial. *Oncol Rep* 2012; **28**: 1131-8.
610. Beare A, Stockinger H, Zola H, Nicholson I. Monoclonal antibodies to human cell surface antigens. *Curr Protoc Immunol* 2008; **Appendix 4**: 4A.
611. Egri G, Takats A. The immunodiagnosis of lung cancer with monoclonal antibodies. *Med Sci Monit* 2005; **11**: RA296-300.
612. Bauer K, Rancea M, Roloff V, Elter T, Hallek M, Engert A et al. Rituximab, ofatumumab and other monoclonal anti-CD20 antibodies for chronic lymphocytic leukaemia. *Cochrane Database Syst Rev* 2012; **11**: CD008079.
613. Kohler G, Milstein C. Continuous cultures of fused cells secreting antibody of predefined specificity. *Nature* 1975; **256**: 495-7.
614. Yokoyama WM. Production of monoclonal antibodies. *Curr Protoc Cytom* 2006; **Appendix 3**: Appendix 3J.
615. Yokoyama WM. Production of monoclonal antibody supernatant and ascites fluid. *Curr Protoc Mol Biol* 2008; **Chapter 11**: Unit 11 0.
616. Lonberg N, Taylor LD, Harding FA, Trounstein M, Higgins KM, Schramm SR et al. Antigen-specific human antibodies from mice comprising four distinct genetic modifications. *Nature* 1994; **368**: 856-9.
617. Kimball JA, Norman DJ, Shield CF, Schroeder TJ, Lisi P, Garovoy M et al. The OKT3 Antibody Response Study: a multicentre study of human anti-mouse antibody (HAMA) production following OKT3 use in solid organ transplantation. *Transpl Immunol* 1995; **3**: 212-21.
618. Geijtenbeek TB, Engering A, Van Kooyk Y. DC-SIGN, a C-type lectin on dendritic cells that unveils many aspects of dendritic cell biology. *J Leukoc Biol* 2002; **71**: 921-31.
619. Ortiz M, Kaessmann H, Zhang K, Bashirova A, Carrington M, Quintana-Murci L et al. The evolutionary history of the CD209 (DC-SIGN) family in humans and non-human primates. *Genes Immun* 2008; **9**: 483-92.
620. Zhu Y, Jin B, Sun C, Huang C, Liu X. The effects of hybridoma growth factor in conditioned media upon the growth, cloning, and antibody production of heterohybridoma cell lines. *Hum Antibodies Hybridomas* 1993; **4**: 31-5.
621. Jesudason S, Collins MG, Rogers NM, Kireta S, Coates PT. Non-human primate dendritic cells. *J Leukoc Biol* 2012; **91**: 217-28.

622. Relloso M, Puig-Kroger A, Pello OM, Rodriguez-Fernandez JL, de la Rosa G, Longo N et al. DC-SIGN (CD209) expression is IL-4 dependent and is negatively regulated by IFN, TGF-beta, and anti-inflammatory agents. *J Immunol* 2002; **168**: 2634-43.
623. Mitchell DA, Fadden AJ, Drickamer K. A novel mechanism of carbohydrate recognition by the C-type lectins DC-SIGN and DC-SIGNR. Subunit organization and binding to multivalent ligands. *J Biol Chem* 2001; **276**: 28939-45.
624. Granelli-Piperno A, Pritsker A, Pack M, Shimeliovich I, Arrighi JF, Park CG et al. Dendritic cell-specific intercellular adhesion molecule 3-grabbing nonintegrin/CD209 is abundant on macrophages in the normal human lymph node and is not required for dendritic cell stimulation of the mixed leukocyte reaction. *J Immunol* 2005; **175**: 4265-73.
625. Gruber A, Chalmers AS, Popov S, Ruprecht RM. Functional aspects of binding of monoclonal antibody DCN46 to DC-SIGN on dendritic cells. *Immunol Lett* 2002; **84**: 103-8.
626. Hodges A, Sharrocks K, Edelmann M, Baban D, Moris A, Schwartz O et al. Activation of the lectin DC-SIGN induces an immature dendritic cell phenotype triggering Rho-GTPase activity required for HIV-1 replication. *Nat Immunol* 2007; **8**: 569-77.
627. Sierra-Filardi E, Estechea A, Samaniego R, Fernandez-Ruiz E, Colmenares M, Sanchez-Mateos P et al. Epitope mapping on the dendritic cell-specific ICAM-3-grabbing non-integrin (DC-SIGN) pathogen-attachment factor. *Mol Immunol* 2010; **47**: 840-8.
628. Tacke PJ, Ginter W, Berod L, Cruz LJ, Joosten B, Sparwasser T et al. Targeting DC-SIGN via its neck region leads to prolonged antigen residence in early endosomes, delayed lysosomal degradation, and cross-presentation. *Blood* 2011; **118**: 4111-9.
629. Dalby B, Cates S, Harris A, Ohki EC, Tilkins ML, Price PJ et al. Advanced transfection with Lipofectamine 2000 reagent: primary neurons, siRNA, and high-throughput applications. *Methods* 2004; **33**: 95-103.
630. Hartley JL. Why proteins in mammalian cells? *Methods Mol Biol* 2012; **801**: 1-12.

631. Lagaraine C, Lebranchu Y. Effects of immunosuppressive drugs on dendritic cells and tolerance induction. *Transplantation* 2003; **75**.
632. Barratt-Boyes SM, Thomson AW. Dendritic cells: Tools and targets for transplant tolerance. *American Journal of Transplantation* 2005; **5**: 2807-13.
633. Gao J, Zhong W, He J, Li H, Zhang H, Zhou G et al. Tumor-targeted PE38KDEL delivery via PEGylated anti-HER2 immunoliposomes. *Int J Pharm* 2009; **374**: 145-52.
634. Li S, Goins B, Hrycushko BA, Phillips WT, Bao A. Feasibility of eradication of breast cancer cells remaining in postlumpectomy cavity and draining lymph nodes following intracavitary injection of radioactive immunoliposomes. *Mol Pharm* 2012; **9**: 2513-22.
635. Ma Y, Zheng Y, Liu K, Tian G, Tian Y, Xu L et al. Nanoparticles of Poly(Lactide-Co-Glycolide)-d- α -Tocopheryl Polyethylene Glycol 1000 Succinate Random Copolymer for Cancer Treatment. *Nanoscale Res Lett* 2010; **5**: 1161-9.
636. Mamot C, Ritschard R, Wicki A, Stehle G, Dieterle T, Bubendorf L et al. Tolerability, safety, pharmacokinetics, and efficacy of doxorubicin-loaded anti-EGFR immunoliposomes in advanced solid tumours: a phase 1 dose-escalation study. *Lancet Oncol* 2012; **13**: 1234-41.
637. Kwon YJ, James E, Shastri N, Frechet JM. In vivo targeting of dendritic cells for activation of cellular immunity using vaccine carriers based on pH-responsive microparticles. *Proc Natl Acad Sci U S A* 2005; **102**: 18264-8.
638. Foged C, Arigita C, Sundblad A, Jiskoot W, Storm G, Frokjaer S. Interaction of dendritic cells with antigen-containing liposomes: effect of bilayer composition. *Vaccine* 2004; **22**: 1903-13.
639. Foged C, Brodin B, Frokjaer S, Sundblad A. Particle size and surface charge affect particle uptake by human dendritic cells in an in vitro model. *Int J Pharm* 2005; **298**: 315-22.
640. Cruz LJ, Tacke PJ, Fokkink R, Figdor CG. The influence of PEG chain length and targeting moiety on antibody-mediated delivery of nanoparticle vaccines to human dendritic cells. *Biomaterials* 2011; **32**: 6791-803.
641. Cruz LJ, Tacke PJ, Fokkink R, Joosten B, Stuart MC, Albericio F et al. Targeted PLGA nano- but not microparticles specifically deliver antigen to

- human dendritic cells via DC-SIGN in vitro. *J Control Release* 2010; **144**: 118-26.
642. Badiee A, Davies N, McDonald K, Radford K, Michiue H, Hart D et al. Enhanced delivery of immunoliposomes to human dendritic cells by targeting the multilectin receptor DEC-205. *Vaccine* 2007; **25**: 4757-66.
643. Caminschi I, Corbett AJ, Zahra C, Lahoud M, Lucas KM, Sofi M et al. Functional comparison of mouse CIRE/mouse DC-SIGN and human DC-SIGN. *Int Immunol* 2006; **18**: 741-53.
644. Wicki A, Rochlitz C, Orleth A, Ritschard R, Albrecht I, Herrmann R et al. Targeting tumor-associated endothelial cells: anti-VEGFR2 immunoliposomes mediate tumor vessel disruption and inhibit tumor growth. *Clin Cancer Res* 2012; **18**: 454-64.
645. Deo N, Somasundaran P. Mechanism of mixed liposome solubilization in the presence of sodium dodecyl sulfate. *Colloids and Surfaces A: Physicochemical and Engineering Aspects* 2001; **186**: 33-41.
646. O'Donnell RT, Martin SM, Ma Y, Zamboni WC, Tuscano JM. Development and characterization of CD22-targeted pegylated-liposomal doxorubicin (IL-PLD). *Invest New Drugs* 2010; **28**: 260-7.
647. Woodle MC, Newman MS, Cohen JA. Sterically stabilized liposomes: physical and biological properties. *J Drug Target* 1994; **2**: 397-403.
648. Allen TM, Sapra P, Moase E, Moreira J, Iden D. Adventures in targeting. *J Liposome Res* 2002; **12**: 5-12.
649. Kessler RJ, Fanestil DD. Interference by lipids in the determination of protein using bicinchoninic acid. *Anal Biochem* 1986; **159**: 138-42.
650. Sapan CV, Lundblad RL, Price NC. Colorimetric protein assay techniques. *Biotechnol Appl Biochem* 1999; **29 (Pt 2)**: 99-108.
651. Morton RE, Evans TA. Modification of the bicinchoninic acid protein assay to eliminate lipid interference in determining lipoprotein protein content. *Anal Biochem* 1992; **204**: 332-4.
652. Ashok B, Arleth L, Hjelm RP, Rubinstein I, Onyuksel H. In vitro characterization of PEGylated phospholipid micelles for improved drug solubilization: effects of PEG chain length and PC incorporation. *J Pharm Sci* 2004; **93**: 2476-87.

653. Ruger R, Muller D, Fahr A, Kontermann RE. Generation of immunoliposomes using recombinant single-chain Fv fragments bound to Ni-NTA-liposomes. *J Drug Target* 2005; **13**: 399-406.
654. Noble JE, Bailey MJ. Quantitation of protein. *Methods Enzymol* 2009; **463**: 73-95.
655. Liu J, Xiao Y, Allen C. Polymer-drug compatibility: a guide to the development of delivery systems for the anticancer agent, ellipticine. *J Pharm Sci* 2004; **93**: 132-43.
656. McCarron PA, Marouf WM, Donnelly RF, Scott C. Enhanced surface attachment of protein-type targeting ligands to poly(lactide-co-glycolide) nanoparticles using variable expression of polymeric acid functionality. *J Biomed Mater Res A* 2008; **87**: 873-84.
657. Sigma-Aldrich. Albumin, human - product information sheet. [cited 2013 29 April 2013]; Available from: http://www.sigmaaldrich.com/etc/medialib/docs/Sigma/Product_Information_Sheet/a9511pis.Par.0001.File.tmp/a9511pis.pdf.
658. Mathew A, Fukuda T, Nagaoka Y, Hasumura T, Morimoto H, Yoshida Y et al. Curcumin loaded-PLGA nanoparticles conjugated with Tet-1 peptide for potential use in Alzheimer's disease. *PLoS One* 2012; **7**: e32616.
659. Yallapu MM, Gupta BK, Jaggi M, Chauhan SC. Fabrication of curcumin encapsulated PLGA nanoparticles for improved therapeutic effects in metastatic cancer cells. *J Colloid Interface Sci* 2010; **351**: 19-29.
660. Rogers NM, Stephenson MD, Kitching AR, Horowitz JD, Coates PT. Amelioration of renal ischaemia-reperfusion injury by liposomal delivery of curcumin to renal tubular epithelial and antigen-presenting cells. *Br J Pharmacol* 2012; **166**: 194-209.
661. Fredenberg S, Wahlgren M, Reslow M, Axelsson A. The mechanisms of drug release in poly(lactic-co-glycolic acid)-based drug delivery systems--a review. *Int J Pharm* 2011; **415**: 34-52.
662. Tang L, Azzi J, Kwon M, Mounayar M, Tong R, Yin Q et al. Immunosuppressive Activity of Size-Controlled PEG-PLGA Nanoparticles Containing Encapsulated Cyclosporine A. *J Transplant* 2012; **2012**: 896141.

663. Woo HN, Chung HK, Ju EJ, Jung J, Kang HW, Lee SW et al. Preclinical evaluation of injectable sirolimus formulated with polymeric nanoparticle for cancer therapy. *Int J Nanomedicine* 2012; 7: 2197-208.

APPENDIX

Jesudason, S., Collins, M.G., Rogers, N.M., Kireta, S. & Coates, P.T. (2012) Non-human primate dendritic cells.

Journal of Leukocyte Biology, v. 91(2), pp. 217-228

NOTE:

This publication is included on pages 333-344 in the print copy of the thesis held in the University of Adelaide Library.

It is also available online to authorised users at:

<http://dx.doi.org/10.1189/jlb.0711355>